



Hay, Jake James (2018) *Utilising non-pathogenic bacteria as a substrate for mesenchymal stem cell adhesion and differentiation*. PhD thesis.

<https://theses.gla.ac.uk/8961/>

Copyright and moral rights for this work are retained by the author

A copy can be downloaded for personal non-commercial research or study, without prior permission or charge

This work cannot be reproduced or quoted extensively from without first obtaining permission in writing from the author

The content must not be changed in any way or sold commercially in any format or medium without the formal permission of the author

When referring to this work, full bibliographic details including the author, title, awarding institution and date of the thesis must be given

Enlighten: Theses

<https://theses.gla.ac.uk/>  
[research-enlighten@glasgow.ac.uk](mailto:research-enlighten@glasgow.ac.uk)



University  
of Glasgow

**Utilising non-pathogenic bacteria as a substrate for  
mesenchymal stem cell adhesion and  
differentiation.**

**Jake James Hay**

(BSc Hons, MRes)

Submitted in fulfilment of the requirements for the Degree of  
Doctor of Philosophy (PhD)



University  
of Glasgow

**MiMe Research Group**

Microenvironments for Medicine

**MiMe Research Group**  
**College of Science and Engineering**  
**University of Glasgow**  
**G12 8LT**

## Abstract

Tissue engineering and regenerative medicine is a constantly evolving field of science that directs the use of cells to repair damaged or diseased tissue. Currently, stem cells are the most widely used source of cells due to their inherent characteristics of self-renewal and differentiation. However, stem cell regenerative therapies are still lacking, upon removal from the body, stem cells grow dysplastically towards unwanted lineages, compounded by their limited number makes the therapeutic potential of these cells difficult to obtain. These problems are due to the lack of knowledge of the underlying systems and mechanisms of phenotypical commitment through differentiation.

In an attempt to circumvent these problems, scientists have begun the construction of dynamic surfaces, that is, surfaces that mimic the constantly evolving and changing environment in which stem cells reside in the body, known as the niche. These biomimetic strategies aim to reproduce the physical architecture, chemical composition and plasticity of the *in vivo* environment *in vitro*. This physical architecture can provide the cells with behavioural cues, mainly through transmembrane receptors known as integrins which link the extracellular matrix to the cytoskeleton; and therefore convey physical architecture of the environment to the cell. Scientists consciously design biomimetic systems to incorporate integrin binding ligands such as the adhesive tripeptide arginine-glycine-aspartic acid (RGD). The chemical composition of the niche depends on the *in vivo* milieu, and the needs of the body at this specified time. More specifically, mesenchymal stem cells reside in a variety of niches, with the bone marrow being a prime example. Upon osteogenesis, many chemical signals are delivered to this niche, with arguably the strongest osteogenic signal from bone morphogenetic protein 2 (BMP-2). This growth factor can activate osteogenic genes within the mesenchymal stem cell and predetermine differentiation of the cell towards an osteoblastic fate.

In this work, we have developed a genetically engineered non-pathogenic bacteria, *Lactococcus lactis* to display the III<sub>7-10</sub> fragment of fibronectin to allow mammalian cell integrin adhesion. This fragment contains two important sequences, the RGD adhesive tripeptide and the synergy sequence proline-histidine-serine-arginine-asparagine (PHSRN). RGD allows the mammalian cells to interact with the bacteria through promiscuous integrin attachment. The PHSRN sequence binds synergistically with RGD to some integrins, such as  $\alpha 5\beta 1$ . These bacteria have also been modified to express the osteogenic growth factor, BMP-2 to direct mesenchymal stem cell differentiation towards an osteoblastic fate.

These bacteria readily form spontaneous two-dimensional biofilms on a variety of surfaces, and can therefore act as a *living interface* between the synthetic surface below and the mammalian cells seeded above. The results of this thesis demonstrate that *Lactococcus lactis* can be used as a successful dynamic surface to control the adhesion, proliferation and differentiation of mesenchymal stem cells.

Mesenchymal stem cells seeded over BMP-2 secreting *Lactococcus lactis* demonstrate decreased cell proliferation at short time points and increased osteoblastic markers at longer time points. Further to this, the interface has been made dynamic by making the bacteria inducible, that is, BMP-2 can be expressed in a temporal manner, and at different concentrations to finely tailor specific protein production.

In the future, this system can be further exploited to express or deliver almost any protein or small molecule that can aid in the development of new tissues from their progenitor cells. As demonstrated, these proteins can both be secreted into the medium or displayed as cell wall bound proteins; and can also be constitutively or inducibly expressed. This interface, based on non-pathogenic bacteria establishes a new paradigm in surface functionalisation for regenerative medicine applications.

# Contents

1. Introduction .....	1
1.1 Tissue Engineering and Implantable Devices .....	1
1.2 Dynamic Surfaces and the Extracellular Matrix .....	2
1.3 Cell Adhesion and integrins .....	4
1.4 Stem cells .....	7
1.5 Bone Morphogenetic Protein 2 (BMP-2) .....	9
1.6 MAPK signalling pathway .....	13
1.7 Genetic Engineering .....	17
1.8 Gibson assembly .....	19
1.9 Why <i>Lactococcus lactis</i> ? .....	21
1.10 <i>L. lactis</i> phylogeny .....	26
1.11 <i>L. lactis</i> metabolism .....	27
1.12 Aims of the project .....	30
2. Materials and methods .....	31
2.1 Bacterial culture .....	31
2.2 <i>L. lactis</i> biofilm production .....	32
2.3 Sample preparation .....	32
2.4 Mammalian cell culture .....	33
2.4.1 C2C12 murine myoblasts .....	33
2.4.2 Human bone marrow derived mesenchymal stem cells (MSCs) .....	34
2.5 Immunofluorescence assays .....	34
2.5.1 Cell adhesion .....	34
2.5.2 Osteogenic differentiation .....	35
2.6 von Kossa staining .....	36
2.7 Bacterial viability .....	36
2.8 Image analysis .....	37
2.9 Statistical analysis .....	37
3. Cell-bacteria co-cultures and initial differentiation studies .....	38
3.1 Introduction .....	39
3.2 Materials and methods .....	42
3.2.1 Scanning electron microscopy (SEM) .....	42
3.2.2 Quantitative real-time PCR (qPCR) .....	42
3.3 Results .....	45
3.3.1 Bacterial viability and metabolism .....	45
3.3.2 Cell adhesion and morphology .....	48
3.3.3 Mesenchymal stem cell differentiation .....	57

3.4 Discussion .....	64
3.5 Conclusion.....	67
4. <i>Lactococcus lactis</i> cloning and characterisation .....	68
4.1 Introduction .....	69
4.2 Materials and Methods .....	72
4.2.1 Cloning.....	72
4.2.2 Transformation of chemically competent <i>Escherichia coli</i> ( <i>E.coli</i> ) .....	73
4.2.3 <i>E. coli</i> culture .....	74
4.2.4 Plasmid isolation from <i>E.coli</i> .....	74
4.2.5 Plasmid purification .....	74
4.2.6 Preparation of <i>L. lactis</i> electrocompetent cells .....	75
4.2.7 Polymerase chain reaction (PCR) .....	75
4.2.8 Gibson Assembly .....	78
4.2.9 Electroporation of <i>L. lactis</i> .....	79
4.2.10 Plasmid isolation from <i>L. lactis</i> .....	79
4.2.11 Sequencing.....	79
4.2.12 Agarose gel preparation .....	80
4.2.13 Preparation of the nisin stock.....	80
4.2.14 GFP Assay .....	80
4.2.15 Western blot .....	81
4.2.16 Enzyme Linked Immunosorbent Assay (ELISA) .....	81
4.3 Results .....	83
4.3.1 NZ9000 FNIII <sub>7-10</sub> -GFP and BMP-2 strains .....	83
4.3.2 Bacterial viability.....	91
4.3.3 Mammalian cell viability on NZ9000.....	92
4.3.4 NZ9020 FNIII <sub>7-10</sub> fragment and BMP-2 expressing bacteria.....	97
4.3.5 Mammalian cell viability on NZ9020.....	104
4.4 Discussion .....	105
4.5 Conclusion.....	108
5. Cell-bacteria interaction dynamics.....	109
5.1 Introduction .....	110
5.2 Materials and methods.....	112
5.2.1 Nisin induction for cell adhesion .....	112
5.2.2 Cell proliferation.....	112
5.2.3 Bacterial internalisation .....	112
5.3 Results .....	114
5.3.1 Cell adhesion.....	114
5.3.2 Cell proliferation.....	116

5.3.3 Cell-bacteria dynamics.....	119
5.4 Discussion .....	123
5.5 Conclusion.....	125
6. Mammalian cell differentiation on BMP-2 expressing bacteria .....	126
6.1 Introduction .....	127
6.2 Materials and Methods .....	129
6.2.1 Collagen sponges .....	129
6.2.2 Cell adhesion to collagen sponges .....	129
6.2.3 Alkaline phosphatase (ALP) assay .....	129
6.2.4 Animals .....	130
6.2.5 Surgical protocol.....	130
6.2.6 Sponge implantation .....	130
6.2.7 Micro computed tomography ( $\mu$ CT).....	130
6.2.8 Implant removal and histology .....	131
6.3 Results .....	132
6.3.1 Mesenchymal stem cell differentiation .....	132
6.3.2 <i>In vivo</i> mouse study.....	140
6.4 Discussion .....	146
6.5 Conclusion.....	149
7. Discussion and conclusion .....	150
7.1 Summary .....	150
7.2 General discussion.....	152
7.3 Cell adhesion and proof of concept.....	153
7.4 <i>L. lactis</i> characterisation.....	154
7.5 Initial mammalian cell studies.....	154
7.6 <i>L. lactis</i> derived osteogenesis .....	155
7.7 Future work .....	155
7.8 General conclusion .....	156
8. Annex .....	158
9. References .....	161

## Abbreviations

ANOVA	Analysis of variance
ATP	Adenosine triphosphate
BMP	Bone morphogenetic protein
BMP-2	Bone morphogenetic protein 2
BMPR	Bone morphogenetic protein receptor
BrdU	5-bromo-2-deoxyuridine
BSA	Bovine Serum Albumin
CCR	Carbon catabolite repression
cDNA	Complementary DNA
CWAP	Cell-wall anchored protein
DAPI	4',6-diamino-2-phenylindole
DMEM	Dulbecco's Modified Eagle Medium
DNA	Deoxyribonucleic acid
dNTP	deoxynucleotide phosphate
DLVO	Derjaguin-Landau-Verwey-Overbeek theory
DPBS	Dulbecco's Phosphate Buffered Saline
ECM	Extracellular matrix
EFSA	European Food Safety Authority
ELISA	Enzyme Linked Immunosorbent Assay
EPS	Exopolysaccharide
ERK	Extracellular regulated kinase
ESC	Embryonic stem cell
FA	Focal adhesion
FAK	Focal adhesion kinase
FBS	Foetal bovine serum
FDA	US Food and Drug Administration
FGF	Fibroblast growth factor
FN	Fibronectin
GAP	Glyceraldehyde 3-phosphate
GE	Genetic engineering

GFP	Green fluorescent protein
GM-CSF	Granulocyte-macrophage colony-stimulating factor
GRAS	Generally regarded as safe
H&E	Haematoxylin and eosin
IL-3	Interleukin-3
IMAC	Immobilised metal-affinity chromatography
JNK	c-Jun N-terminal kinase
MSC	Mesenchymal stem cell
iPSC	induced pluripotent stem cell
LAB	Lactic acid bacteria
LB	Luria-Bertani broth
LPS	Lipopolysaccharide
MCS	Multiple cloning site
MAPK	Mitogen-activated protein kinase
NADH	Reduced nicotinamide adenine dinucleotide
NAD <sup>+</sup>	Oxidized nicotinamide adenine dinucleotide
OCN	Osteocalcin
OD	Optical density
OPN	Osteopontin
OSX	Osterix
MAPK	Mitogen-activated protein kinase
PAGE	Polyacrylamide gel electrophoresis
PCR	Polymerase chain reaction
PDB	Protein Data Bank
PEA	Poly (ethyl acrylate)
PDGF	Platelet-derived growth factor
P/S	Penicillin streptomycin
PTS	Phosphotransferase system
qPCR	Quantitative real-time polymerase chain reaction
QPS	Qualified presumption of safety
RGD	Arginine-glycine-aspartic acid
RNA	Ribonucleic acid

RUNX2	Runt-related transcription factor 2
SB	Synthetic Biology
SCF	Stem cell factor
SMAD	Sma and mothers against decapentaplegic protein
SEM	Scanning electron microscopy
SMX	Sulfamethoxazole
SSC	Somatic stem cell
tRNA	Transfer ribonucleic acid
TC	Tetracycline
TE	Tissue engineering
TGF- $\beta$	Transforming growth factor-beta
SDS	Sodium dodecyl sulfate
VEGF	Vascular endothelial growth factors
WB	Western blot
XDLVO	Extended Derjaguin-Landau-Verwey-Overbeek theory

## List of Tables

<b>Table 1.1</b>	Biological functions of the BMPs
<b>Table 1.2</b>	Recombinant proteins produced by <i>L. lactis</i> for biomedical purposes
<b>Table 2.1</b>	Antibodies and suppliers used in this thesis
<b>Table 3.1</b>	Primers used in the qPCR gene expression analysis
<b>Table 4.1</b>	Isolation of BMP-2 from pGEM-T-BMP2
<b>Table 4.2</b>	Primers for constitutively secreted biologically active BMP-2 (Usp45-BMP-2)
<b>Table 4.3</b>	Primers for constitutively secreted BMP-2-GFP (Usp45-BMP-2-GFP)
<b>Table 4.4</b>	Primers for constitutively cell wall bound BMP-2 (Usp45-BMP-2-spaX)
<b>Table 4.5</b>	Primers for constitutively cell wall bound BMP-2-GFP (Usp45-GFP-BMP-2-spaX)
<b>Table 4.6</b>	Primers for inducible secreted BMP-2-6xHis (Usp45-6xHis-BMP-2).
<b>Table 4.7</b>	Primers for inducible cell wall bound BMP-2-6xHis (Usp45-6xHis-BMP-2-spaX)
<b>Table 4.8</b>	Primers for inducible cell wall FNIII <sub>7-10</sub> -GFP (Usp45-GFP-FNIII <sub>7-10</sub> -spaX)
<b>Table 4.9</b>	Primers for inserting chloramphenicol into pT1NX for the creation of pT2NX
<b>Table 4.10</b>	Primers for sequencing
<b>Table 4.11</b>	<i>L. lactis</i> metabolism under different conditions
<b>Table 6.1</b>	Calculated bone volume (mm <sup>3</sup> ) in collagen sponges after 2 weeks
<b>Table 6.2</b>	Calculated bone volume (mm <sup>3</sup> ) in collagen sponges after 4 weeks

## List of Figures

- Figure 1.1** Cells in tissue engineering
- Figure 1.2** Integrin conformation
- Figure 1.3** BMP-2 and its receptors
- Figure 1.4** BMP-2 dependent osteogenesis
- Figure 1.5** MAPK signalling cascades
- Figure 1.6** BMP-2 can activate MAPK
- Figure 1.7** p38 implication in osteoblast differentiation
- Figure 1.8** Gibson Assembly
- Figure 1.9** Gibson Assembly primer overlap
- Figure 1.10** *L. lactis* plasmids
- Figure 1.11** *L. lactis* anchoring mechanism
- Figure 1.12** *L. lactis* nisin controlled gene expression system
- Figure 1.13** Phylogenetic tree of the lactic acid bacteria (LAB) clade
- Figure 1.14** Homolactic fermentation process in *L. lactis*
- 
- Figure 3.1** Conceptual overview of the system
- Figure 3.2** *L. lactis* biofilm viability
- Figure 3.3** Biofilm coverage after one, two, three and four weeks
- Figure 3.4** High magnification SEM images of C2C12 murine myoblasts seeded over *L. lactis*-empty after three hours
- Figure 3.5** Low and high magnification SEM images of C2C12 murine myoblasts interacting with *L. lactis*-FN after three hours
- Figure 3.6** Low magnification SEM images of C2C12 murine myoblasts seeded over FN coated glass after three hours
- Figure 3.7** Low and high magnification SEM images of C2C12 murine myoblasts under alcian blue fixative after three hours
- Figure 3.8** Morphological study of the MSCs by SEM

- Figure 3.9** Adhesion assessment of MSCs cultured on *L. lactis*-empty, *L. lactis*-FN and FN-coated surface
- Figure 3.10** Long term focal adhesion analysis
- Figure 3.11** Immunofluorescent images of MSCs stained for integrin  $\alpha 5$ ,  $\beta 1$  and  $\alpha V\beta 3$
- Figure 3.12** Graphs detailing integrin adhesion after 75 minutes
- Figure 3.13** Osteocalcin and cell count after three weeks of culture
- Figure 3.14** Osteopontin production by cells
- Figure 3.15** Bacterial coverage after three weeks
- Figure 3.16** Extracellular matrix mineralisation
- Figure 3.17** Gene expression analysis of MSCs after 14 days
- 
- Figure 4.1** Schematic representation of the commercially available pGEM-T-BMP-2 used in this thesis
- Figure 4.2** Western blot against constitutive NZ9000 cell wall bound GFP-BMP-2
- Figure 4.3** GFP fluorescence assay to confirm the presence of constitutive BMP-2-GFP from NZ9000
- Figure 4.4** Western blot against constitutive NZ9000 cell wall bound FNIII<sub>7-10</sub>-GFP
- Figure 4.5** Western blot against inducible NZ9000 cell wall bound BMP-2
- Figure 4.6** ELISA data for inducible NZ9000 secreted BMP-2
- Figure 4.7** Western blot against inducible NZ9000 cell wall bound FNIII<sub>7-10</sub>-GFP under different concentrations of inducer
- Figure 4.8** Bacterial viability
- Figure 4.9** Mesenchymal stem cell viability on NZ9000 *L. lactis* clones
- Figure 4.10** MSC and C2C12 viability on *L. lactis*
- Figure 4.11** Simplified representation of glycolysis, homolactic, and mixed-acid fermentations and heme-dependent respiration in *L. lactis*
- Figure 4.12** pH of M17 after one day of *L. lactis* growth
- Figure 4.13** Western blot against constitutive NZ9020 cell wall bound GFP-BMP-2

- Figure 4.14** GFP fluorescence assay to confirm the presence of constitutive NZ9020 BMP-2-GFP
- Figure 4.15** Western blot against constitutive NZ9020 cell wall bound FNIII<sub>7-10</sub>-GFP
- Figure 4.16** Western blot against inducible NZ9020 cell wall bound BMP-2
- Figure 4.17** ELISA data for inducible NZ9020 secreted BMP-2
- Figure 4.18** Western blot against inducible NZ9020 cell wall bound FNIII<sub>7-10</sub>-GFP under different concentrations of inducer
- Figure 4.19** Mesenchymal stem cell viability on NZ9020 *L. lactis* clones
- 
- Figure 5.1** MSC cell cycle schematic
- Figure 5.2** MSC adhesion to inducibly expressed FNIII<sub>7-10</sub> from *L. lactis*
- Figure 5.3** Graphical representation of cell area after nisin induction
- Figure 5.4** Cell proliferation on differing constitutive *L. lactis* clones
- Figure 5.5** Cell proliferation on inducible *L. lactis* clones
- Figure 5.6** Bacterial internalisation by C2C12 murine myoblasts
- Figure 5.7** Bacterial internalisation by RAW macrophages
- Figure 5.8** Graphs detailing bacterial internalisation
- 
- Figure 6.1** ALP activity of MSCs after 10 days
- Figure 6.2** ALP activity of MSCs after 12 days
- Figure 6.3** Nisin induction profiles
- Figure 6.4** Osteogenic differentiation of MSCs through osteocalcin
- Figure 6.5** Osteocalcin quantitation
- Figure 6.6** Osteogenic differentiation of MSCs through von Kossa
- Figure 6.7** Phosphate deposition quantitation
- Figure 6.8** Overall osteogenic differentiation
- Figure 6.9** MSC adhesion to functionalised collagen sponges after one day

- Figure 6.10** ALP activity of MSCs after 10 days on collagen sponges
- Figure 6.11** ALP activity of MSCs after 15 days on collagen sponges
- Figure 6.12** Haematoxylin and eosin staining of sliced collagen sponges after 4 weeks
- 
- Figure 7.1** 3D schematic representation of the interaction between *L. lactis* and MSCs
- 
- Figure 8.1** C2C12 murine myoblasts seeded over *L. lactis*-FN under alcian blue fixative for three hours
- Figure 8.2**  $\mu$ CT images of functionalised collagen sponges after two weeks
- Figure 8.3**  $\mu$ CT images of functionalised collagen sponges after four weeks

## **Acknowledgements**

I would first like to dedicate my appreciation and sincerest apologies to the animals that gave their lives for the completion of this thesis. I will always have that on my conscious and I hope the sacrifice is not wasted.

Next, I would like to show my deepest appreciation to my supervisors, Professors Manuel Salmerón-Sánchez and Matthew Dalby, who have shown me great guidance and directed me along the right routes throughout the last 3/4 years. Thank you for the patience and guidance, I appreciate it more than I can put into words.

I couldn't have completed this thesis without the help of my colleague, now great friend, Alexandre Rodrigo-Navarro. I bet at first I came across as some guy who had no idea what I was doing (because it's true) but you stuck with me and gave me the help and guidance, above and beyond anything that was asked of you. Thank you for never giving up on me and I hope I never let you down. Along with the ridiculously good help given to me, you have been an amazing friend and I have thoroughly enjoyed working with you, I will miss the endless jokes about chicken and the crazy photoshopped images, at which you have an uncanny, slightly weird skill for. THANK YOU!!!!

I would also like to thank my girlfriend Hilary Anderson, who has made my time in Glasgow amazing, it is now like a second home to me (I'm not quite sure where my first home is to be fair). The PhD is not all about work, my mental state was kept sane due to you and the fun we have had, well I can't quite fit it all on one page. From spending our masters project together, the fun has never stopped (crab dancing, high pitch chats and holidays just to name a few).

Lastly, I would like to show my everlasting gratitude to the people I have met up here. Particularly those from MiMe and CCE, but I could not forget Mark Bennett and Ricky Unadkat, whom I have shared a flat with (somewhat illegally) for the last 3 years. Flanter, great friends and good times have been on point and I wouldn't have changed a thing, except for Ricky's ineptitude at keeping things tidy. Overall, everything and everyone has been awesome and I will always look back on this as one of the best times of my life. Except for the write up, that was well boring.

## **Author's Declaration**

I hereby declare that the research presented within this thesis is my own work unless otherwise stated, and has not been submitted elsewhere for any other academic degree.

Jake Hay, October 2017

# 1. Introduction

## 1.1 Tissue Engineering and Implantable Devices

Tissue engineering (TE) combines the methods and practises of the life sciences and engineering to overcome the problems understanding the structure-function relationship of tissues and their disease states. The answers aid in the assembly of materials and techniques to begin the construction of artificial organs and/or tissues. Irrespective of clinical feasibility, the potential of TE is innumerable; its uses can range from *ex vivo* construction, to autologous grafts or complete organ replacements (Bianco and Robey 2001). Cells must be isolated and cultured in order to synthetically grow new tissues where biomaterials play a crucial role. Biomaterials aim to recapitulate the critical aspects of the extracellular matrix (ECM), which is to facilitate the interaction of the cells with the material and the surrounding microenvironment. These materials must display some kind of biocompatibility, usually characterised by the material's ability to coexist in the body without causing harm (Williams 2008). However, there are many issues that must be overcome to ensure the creation of a successful biomaterial. Biomimetic synthetic polymers and naturally occurring polymers have been fashioned to overcome initial problems with biocompatibility, yet issues with biomimicry still exist. Artificial scaffolds are still designed on the macroscale to support cell growth and these do not recapitulate the nanoscale detail observed in real organs (Ratner and Bryant 2004, Lenas, Luyten et al. 2011, Ding, Fan et al. 2016, Yousefi, James et al. 2016). All approaches to TE require a source of cells. Stem cells are typically used as they possess inherent differentiation capabilities and can thus have myriad uses (Duscher, Barrera et al. 2016, Muzzarelli, El Mehtedi et al. 2016). Furthermore, many appropriate sources of stem cells as well as culture techniques have been established. The potential of stem cell therapies is however, limited. Upon removal from the body uncontrollable differentiation to undesired lineages occurs and thus, the creation of a synthetic tissue is severely hindered. This issue also poses clinical complications, for example, this can lead to the improper formation of tissue surrounding implantable devices, a leading cause of implant failure. Figure 1.1 highlights the current workflow for tissue engineering organs.

To combat this problem, the use of dynamic surfaces, which aim to better emulate the extracellular matrix have come to the forefront of TE (Dhowre, Rajput et al. 2015, Anderson, Sahoo et al. 2016). These surfaces react to externally derived stimuli and ultimately alter the phenotype of the cells through alterations in the ECM. Fundamentally, these surfaces

presently provide the best user controlled mechanism for studying spatiotemporal alterations to the niche in a reductionist manner.

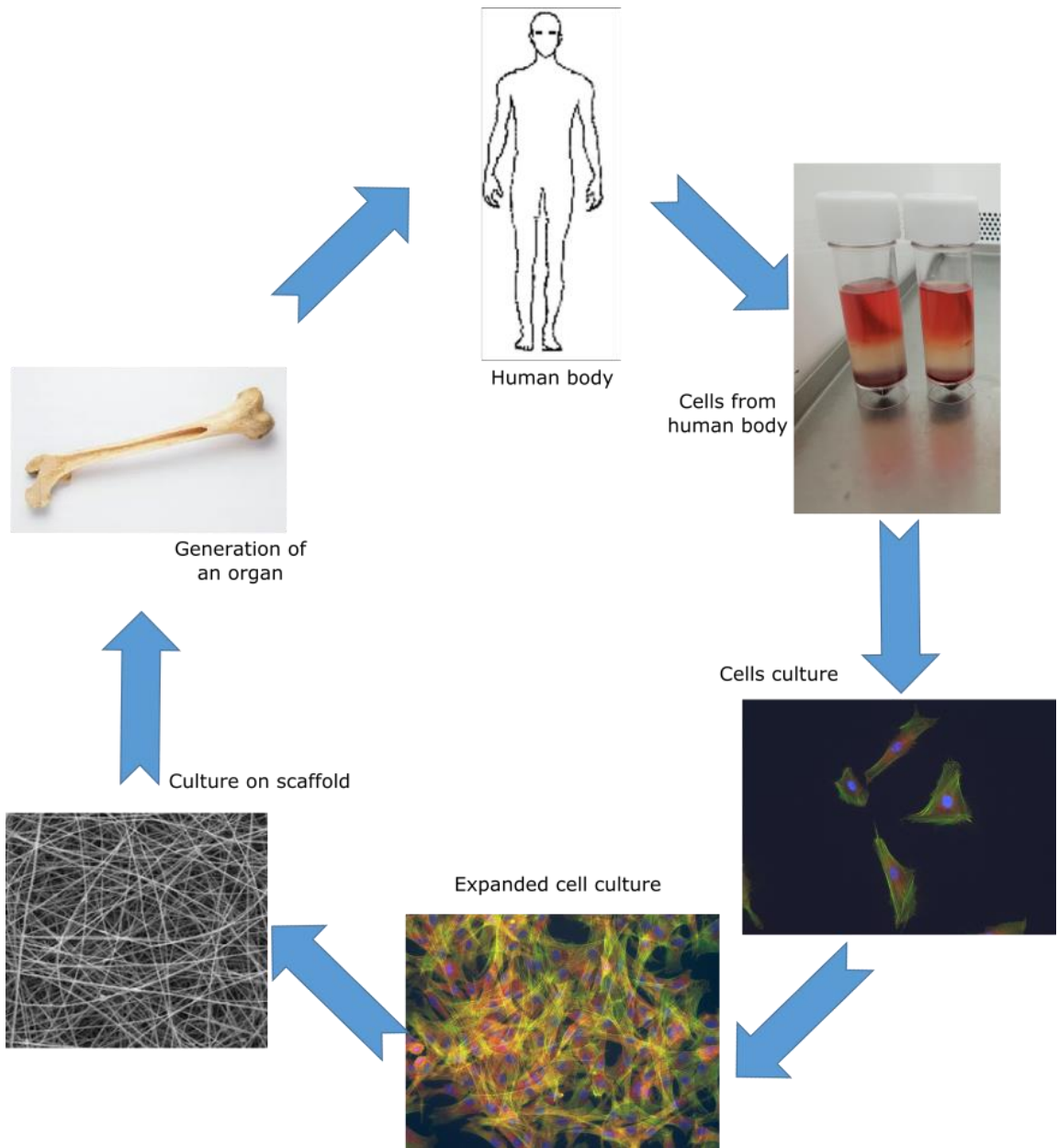


**Figure 1.1 Cells in tissue engineering.** Cells are isolated from the body before expansion in culture. The cells are usually then cultured on a scaffold to aid in the generation of organs before being implanted. Jake Hay unpublished work.

## 1.2 Dynamic Surfaces and the Extracellular Matrix

Cells are innately sensitive to their extracellular environment on the macro, micro and nanoscale and thus, both chemistry and topography play a vital role in cellular development and behaviour (Dalby, Gadegaard et al. 2007, McMurray, Gadegaard et al. 2011, Nikukar, Reid et al. 2013). Understanding how cells interact with materials is of utmost importance

to engineer microenvironments. Genes must be activated in the correct sequence and synchrony in order to express the numerous proteins needed for proliferation and differentiation to hierarchical organisation within organs; extrinsic signals from the ECM are mandatory to direct distinct development (Stevens and George 2005). *In vivo*, the ECM is a heterogeneous setting and comprises an elaborate natural web of proteins and growth factors; this instructive background ultimately guides cell behaviour (Scott 1995, Aumailley and Gayraud 1998, Wallner, Yang et al. 1998). This complex array of nanofibers, proteins, growth factors and chemicals reveals a level of detail unmatched outside the biological world. However, the ability to synthesise these materials is rapidly becoming a reality (Hench and Polak 2002, Shin, Jo et al. 2003, Zhang 2003, Ratner and Bryant 2004, Lutolf and Hubbell 2005, Rosso, Marino et al. 2006, Zisch, Ehrbar et al. 2006, Chen and Hunt 2007, Ma 2008, Liu, Smith et al. 2009, Zheng, Zhang et al. 2010, Cordonnier, Sohier et al. 2011, Lendlein 2011, Ebara, Kotsuchibashi et al. 2014). There have been many attempts at synthetic replication of the niche, and recently, dynamic user controlled surfaces have been developed in which the surface is spatially and temporally controlled. These surfaces react to externally derived stimuli and ultimately alter the phenotype of the cells through alterations in the ECM. Previously, different types of triggering mechanisms have been utilised including light (Wirkner, Weis et al. 2011, Lee, Garcia et al. 2015), temperature (Ebara, Yamato et al. 2004) and enzymes (Todd, Scurr et al. 2009, Zelzer, Scurr et al. 2012). The requirement for synthetic materials that mimic the characteristics of the ECM is essential in biomedical engineering to comprehend the complex and dynamic behaviour of cells.

Recent studies have advanced the theory that inherent material properties can encourage, or even induce lineage specific cell differentiation through innate characteristics such as stiffness (Engler, Sen et al. 2006, Lee, Abdeen et al. 2013), nanotopography (Dalby, Gadegaard et al. 2007, Yim, Darling et al. 2010, McMurray, Gadegaard et al. 2011) chemical functionality (Benoit, Schwartz et al. 2008, Saha, Mei et al. 2011) and enzyme responsive surfaces (Roberts, Sahoo et al. 2016). These studies clearly show that these synthetic materials can produce a milieu from which stem cell fate can be user controlled. The addition of other co-factors or biochemical supplements further compounds the results. To ensure increased control over stem cell behaviour, it is necessary to ascertain a deeper understanding of how inherent material properties under defined chemical conditions influence stem cell fate. For effective control of stem cells, libraries of material properties that influence cell fate will have to be produced. Presently, for control of cells through biochemical means, specific and time controlled addition of supplements are added in a particular sequence; the same will be needed for exact material control. The availability of the material to change therefore

directly affects cellular behaviour, compounded with biochemical cocktails can create a synthetic surface with the potential to mimic the stem cell niche (Murphy, McDevitt et al. 2014). In the future, we can expect a material which can be altered upon external demand in a temporal sequence that relates material properties to gene activation.

We hypothesise that biofilms formed by non-pathogenic bacteria can be utilised to accomplish a successful dynamic surface. They can be genetically modified to express or secrete different proteins which can be used to direct cell behaviour and ultimately control stem cell fate. In that case, bacterial cell to mammalian cell communication can be facilitated on the level of the bacterial biofilm interface due to bacterial capability to colonise many different biomaterials to form a monolayer.

### **1.3 Cell Adhesion and integrins**

Many molecules are involved in ECM construction. The organisation and assembled structure of collagens, proteoglycans, laminins and fibronectin (FN) all play a crucial role in the finalised ECM. Furthermore, different cells require different behavioural cues and thus all ECMs vary from each other, this multiplicity arises from the amalgamation of unambiguous molecular interactions and countless number of protein isoforms. In addition, the ratios, geometrical arrangements, intercellular interactions, nanotopography and molecular mechanisms create an environment with abounding informational cues (Stevens and George 2005). Individually, ECM components have evolved specific biological functions and together form highly particular hierarchical structures. A major constituent of the ECM is the protein FN. FN size ranges from 230-270 kDa and binds into dimers via two disulfide bonds at the C-termini of the proteins. The structure of FN is composed of three types of repeating modules, I, II and III. Both type I and II contain intramolecular disulfide bonds to stabilize the folded structure, while type III lacks these disulfide bonds. Type I and II modules are structured in beta-sheets enclosing a hydrophobic core that contains highly conserved aromatic amino acids (Mao and Schwarzbauer 2005, Singh, Carraher et al. 2010). The type III repeats hold the well characterised arginine-glycine-aspartic acid tri-peptide (RGD) in the III<sub>10</sub> repeat and the proline-histidine-serine-arginine-asparagine (PHSRN) in the III<sub>9</sub> repeat which are required for interactions with mammalian cell surface receptors known as integrins (Mouw 2014). In this thesis, we use the FN repeats III<sub>7-10</sub> (FNIII<sub>7-10</sub>) as it houses the RGD domain and has been previously shown to induce mammalian cell integrin attachment (Saadeddin, Rodrigo-Navarro et al. 2013, Rodrigo-Navarro, Rico et al. 2014). The rationale for using FNIII<sub>7-10</sub> as opposed to the whole FN molecule is based mainly on

the size of the protein. FN is 220-270 kDa and the largest protein known to be able to be synthesised using the bacterial secretion system is 160 kDa (Le Loir, Azevedo et al. 2005). It would therefore be impossible to synthesise the whole FN molecule. Moreover, it has been previously shown that short RGD containing peptides can induce a similar level of mammalian cell attachment as native FN through mammalian transmembrane receptors known as integrins (Pierschbacher and Ruoslahti 1984, Dsouza, Ginsberg et al. 1991, Rico, Gonzalez-Garcia et al. 2010).

Integrins are a diverse family of heterodimeric integral membrane glycoproteins comprised of an  $\alpha$  and  $\beta$  subunit which anchor cells to the ECM through focal adhesions. In humans there are 18  $\alpha$  subunits and 8  $\beta$  subunits that can combine to form 24  $\alpha\beta$  combinations. Integrins are the principal mediators of cell-ECM focal adhesions and recognise integrin binding motifs, such as the RGD sequence. Focal adhesion formation serves to both anchor cells to their surrounding matrix, and to transmit signals between the ECM and the cell. Integrins are associated with focal adhesions via cytoplasmic anchor proteins talin, tensin, paxillin and vinculin, amongst others which can then alter tension on the actin cytoskeleton (Hynes 2009) resulting in biochemical signaling cascades utilising various signal transduction molecules including focal adhesion kinase (FAK) (Hanks and Polte 1997, Sieg, Hauck et al. 1999, Mitra, Hanson et al. 2005). Focal adhesions form in protrusive parts of cells, such as filopodia and lamellipodia and during this initial stage of attachment, transient focal complexes (<1  $\mu\text{m}$  in length) begin to establish allowing primary migration (Nobes and Hall 1995). Focal complexes (1-5  $\mu\text{m}$  in length) quickly form and dissociate as the leading edge of the cell advances (Ridley and Hall 1992). Maturation of focal complexes into fully developed focal adhesions corresponds to their recruitment of additional proteins such as RhoA and  $\alpha$  actinin (Ridley and Hall 1992). Focal adhesions can in turn, further mature into fibrillary adhesions, which are large collectives of integrin rich focal complexes (Friedland, Lee et al. 2009).

The loss of integrin mediated cell contact leads to apoptosis through anoikis (cell 'homelessness') (Frisch and Francis 1994) in a majority of cell types, this includes mesenchymal stem cells (MSCs) (Benoit, Tripodi et al. 2007). Anoikis is triggered by inappropriate or inadequate cell-matrix contacts and demonstrates an evolutionary safeguard mechanism *in vivo* as it prevents detached cells from reattaching to a new matrix and growing dysplastically (Frisch and Ruoslahti 1997). It has been proven that integrins play a vital role in anoikis inhibition as demonstrated by many authors (Giancotti and Ruoslahti

1999, Giancotti 2000, Bissell and Radisky 2001, Alahari, Reddig et al. 2002, Guo and Giancotti 2004, Ramsay, Marshall et al. 2007). The detachment of integrins from ECM proteins leads to the absence of apoptotic inhibitory signals ultimately resulting in caspase activity and cell anoikis (Frisch and Screaton 2001). This proves that adhesion is of utmost importance for cell survival and that integrin attachment leads to the synthesis of a diverse array of genetic products to ensure cell survival. Moreover, this validates the importance of integrins ability to influence cellular fate and thus, cell-ECM interactions are tightly regulated as misguided adhesion often result in pathological conditions which can vary from wound healing deficiencies to tumourigenesis (Hynes 2002, Kumar and Weaver 2009, Schiller and Fassler 2013, Wolfenson, Lavelin et al. 2013).

Integrin-ligand binding is regulated through their interaction with divalent metal cations ( $Mg^{2+}$ ,  $Mn^{2+}$  and  $Ca^{2+}$ ) (Valdramidou, Humphries et al. 2008, Raborn and Luo 2012). Crystallography and electron microscopy have highlighted the regions of cation binding to specific areas on the  $\beta$  subunit known as the metal ion dependent adhesion site. Cation occupancy then directs the coupling of the subunits followed by the subsequent unfolding of the integrins during their transition from inactive to an active confirmation, highlighted in Figure 1.2 (Luo and Springer 2006).

Further studies into integrin structure have highlighted three divergent conformations, which directly relate to their function and activation state shown in Figure 1.2. In the 'closed' configuration, integrins exist in a bent shape with the head directed towards the membrane; but can adopt an 'open' state to bind a ligand. This rearrangement occurs when divalent metal ions bind and cause a change in the tertiary and quaternary structure. For example, studies involving the binding of the RGD tripeptide highlighted the importance of this structural change where the arginine residue coordinates into a cleft within the  $\alpha$  subunit while the aspartic acid is drawn toward the  $Mg^{2+}$  ion within the  $\beta$  subunit (Xiong, Stehle et al. 2002, Takagi 2007, Wang, Fu et al. 2010, Nagae, Re et al. 2012).

In addition to their roles in anchorage to the ECM, integrins play a fundamental role in dictating cellular behaviour, by transmitting chemical signals into the cell (outside-in signalling) (Hynes 2002). These signals detail location, local environment, adhesive state and the surrounding matrix which in turn determines the cellular response (Miranti and Brugge 2002). Behaviours such as migration, differentiation and motility are all partially controlled through integrin signalling. Integrins can also regulate their affinity for ECM ligands by enduring conformational changes. Their extracellular domain is modified in response to signals that alter their cytoplasmic tail, a process termed inside-out signalling (Calderwood 2004).

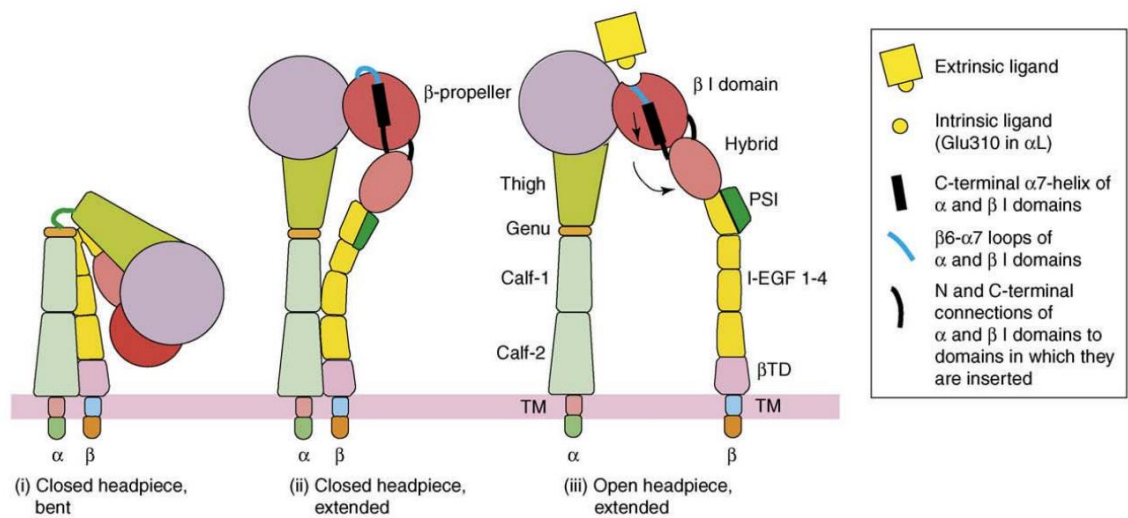


**Figure 1.2. Integrin conformation.** In their low affinity state integrins adopt a bent conformation concealing the ligand binding site. Extension of the subunits reveals the ligand binding domain resulting in a 'primed' state. Further changes to the structure enable ligand binding. Figure shows the low-affinity, high-affinity and ligand-bound structures for "I-less integrins (Luo and Springer, 2006).

Upon cellular migration, focal adhesions are recycled and transported to the leading edge of the cell. This disassembly is of significant importance for cells, as it assures their mobility and recycling of integrin receptors and adapter proteins. This turnover of focal adhesions is primarily controlled from within the cell by intracellular signalling (Bretscher 1984, Bretscher 1992).

## 1.4 Stem cells

Stem cells are widely regarded as the future of regenerative medicine due to their inherent capability to differentiate into a variety of cell types; as well as their ability to self-renew (Duscher, Barrera et al. 2016). This sets them apart from other cell types in that they can

replenish their reserves, and then commit to a specific cell type on demand. There are three widely accepted varieties of stem cells, embryonic stem cells (ESCs), somatic stem cells (SSCs) and induced-pluripotent stem cells (iPSCs). ESCs are derived from the inner cell mass of blastocyst stage embryos and are pluripotent, that is, they can form any cell type. They were first made accessible from mice in 1981 by Evans and Kaufman (Evans and Kaufman 1981), and 17 years later in 1998, human ESCs were isolated by Thomson (Thomson, Itskovitz-Eldor et al. 1998). The use of ESCs in research is complex due to the nature of their isolation; from fertilised human embryos and therefore ethical approval is needed before use.

In context, SSCs are present in adult tissues, within dedicated niches. These niches exist in order to control the proliferative and differentiation potential of the stem cells and include tissues such as brain tissue, adipose tissue and bone marrow, amongst many others (Gronthos, Graves et al. 1994, Watt and Hogan 2000, Alvarez-Buylla, Seri et al. 2002, Zuk, Zhu et al. 2002, Mendez-Ferrer, Michurina et al. 2010). Their main purpose is to serve as a bank of readily available cells to replenish dead cells or to help in wound healing and remodelling. SSCs are multipotent, and can only form a specific set of cell types. SSCs do not have the same ability as ESCs to form every cell type.

There are many types of SSCs and each can be found in specific areas in the body. For example, MSCs were first identified in 1963 in the bone marrow (Becker, Mc et al. 1963) but have been found in other niches since (Campagnoli, Roberts et al. 2001, Tan, Zheng et al. 2017). They strongly resemble fibroblasts in morphology but can become very large well spread cells if space is available. Since their discovery, they have become a very popular cell type to work with due to their ease of use and relatively simple isolation from the body. As they are taken from adult patients, the ethical dispute surrounding ESCs is avoided and MSCs are not subject to the same constrictions of use (de Wert and Mummery 2003).

iPSCs are somatic cells that have been reprogrammed to display ESC like qualities. The original method for the generation of iPSCs was developed by Yamanaka in 2006 and utilised the retroviral transduction of the four key transcription factors Oct4, Sox2, Klf4, and c-myc into the nucleus of a mouse cell (Takahashi and Yamanaka 2006). iPSCs display a higher plasticity than SSCs and are not surrounded by the same ethical disputes as ESCs. However, a major drawback in iPSC work is the fact that they tend to cause tumour growth due to the oncogenic nature of some of the transcription factors (Knoepfler 2009, Kooreman and Wu 2010).

More specifically, MSCs, a subset of SSCs will be used in this thesis, due to their comparative ease of use and their differentiation characteristics fit the work to be completed. MSCs are stromal cells that are capable of differentiating into and replenishing cells of the mesenchymal germ layer, such as bone, cartilage, muscle, adipose, ligaments and tendons. They have the ability to expand in culture whilst maintaining their multipotency and were first described as a subpopulation of bone marrow cells which were found to be plastic adherent. Friedenstein and colleagues placed whole bone marrow in plastic dishes and removed the non-adherent fraction after 4 hours, thus discarding most of the hematopoietic stem cells. The adherent cells were found to be fibroblast like, and had a high capacity for proliferation after 2-4 days of culture (Friedenstein, Petrakova et al. 1968, Friedenstein, Deriglasova et al. 1974). Further studies demonstrated the potential for these cells to begin differentiation towards cellular deposits that resembled bone or cartilage (Owen and Friedenstein 1988, Benayahu, Kletter et al. 1989). Friedenstein's observations were further tested by other groups throughout the 80s; and it was concluded that the cells isolated by his methods were multipotent and could differentiate into cells of the mesenchymal germ layer (Osdoby and Caplan 1981, Sparks and Scott 1986, Filipak, Estervig et al. 1989). Newer, faster methods for MSC isolation have been implemented and these rely on the expression of specific molecules; such as STRO-1, CD29, CD73, CD105 and CD146 amongst many others, and are negative for CD14, CD34 and CD45 (Arvidson, Abdallah et al. 2011).

## **1.5 Bone Morphogenetic Protein 2 (BMP-2)**

Bone Morphogenetic proteins (BMPs) were discovered in 1965 and are multifunctional cytokines belonging to the larger transforming growth factor-beta (TGF- $\beta$ ) family (Urist 1965, Urist 1997). As well as being a regulator in bone induction, maintenance and repair, BMPs play a vital role in mammalian embryonic development with defects in BMP production leading to various diseases including cancer and cardiovascular diseases. More than 20 homo and heterodimeric BMP ligands are encoded in the human genome and these can be divided into four discrete groups based primarily on their function, amino acid homology and structures: (i) BMP-2 and 4; (ii) BMP-5, 6, 7, 8a and 8b; (iii) BMP-8 and 10; and (iv) BMP12, 13 and 14. Of these, only BMP-2, BMP-4 through to 7 and BMP-9 have shown the potential to induce bone formation whereas the others have not displayed osteogenic capability (Carreira, Lojudice et al. 2014). Table 1.1 displays BMP subtypes and their biological functions (Rahman, Akhtar et al. 2015).

BMPs are synthesised by osteoblasts as a mature 400-500 amino acid preprotein before cleavage reveals the biologically active protein. The preprotein consists of a hydrophobic N-terminal secretory leader signal and a non-conserved domain attached to the biologically active mature C-terminal. This active C-terminal comprises 100-140 amino acids and has a region of conserved cysteine amino acids which form part of a cysteine knot with two finger like double stranded sheets (Bessa, Casal et al. 2008). Generally, the C-terminal is cleaved at a consensus sequence Arg-x-x-Arg site and is released from the preprotein to form dimers by means of a disulphide bond, a precondition for bone induction (Sopory, Nelsen et al. 2006). More specifically, BMP-2 shown in Figure 1.3 is a multifunctional growth factor comprising two 114 amino acid subunits. Two receptor binding sites have been identified in the dimer, a wrist epitope which utilises motifs from both subunits and has a high affinity for the receptor BMPRIA while the knuckle epitope consists of one subunit and binds weakly to the receptor BMPRII (Miyazono, Kamiya et al. 2010). BMPs have sites for N and O glycosylation which has been shown to increase the stability of the protein, however, it has been proven that this modification has no effect on the osteogenic capability of the growth factor (Bessho, Konishi et al. 2000, Schmoekel, Schense et al. 2004, Lee, Kim et al. 2010, Kim, Lee et al. 2011, van de Watering, van den Beucken et al. 2012).

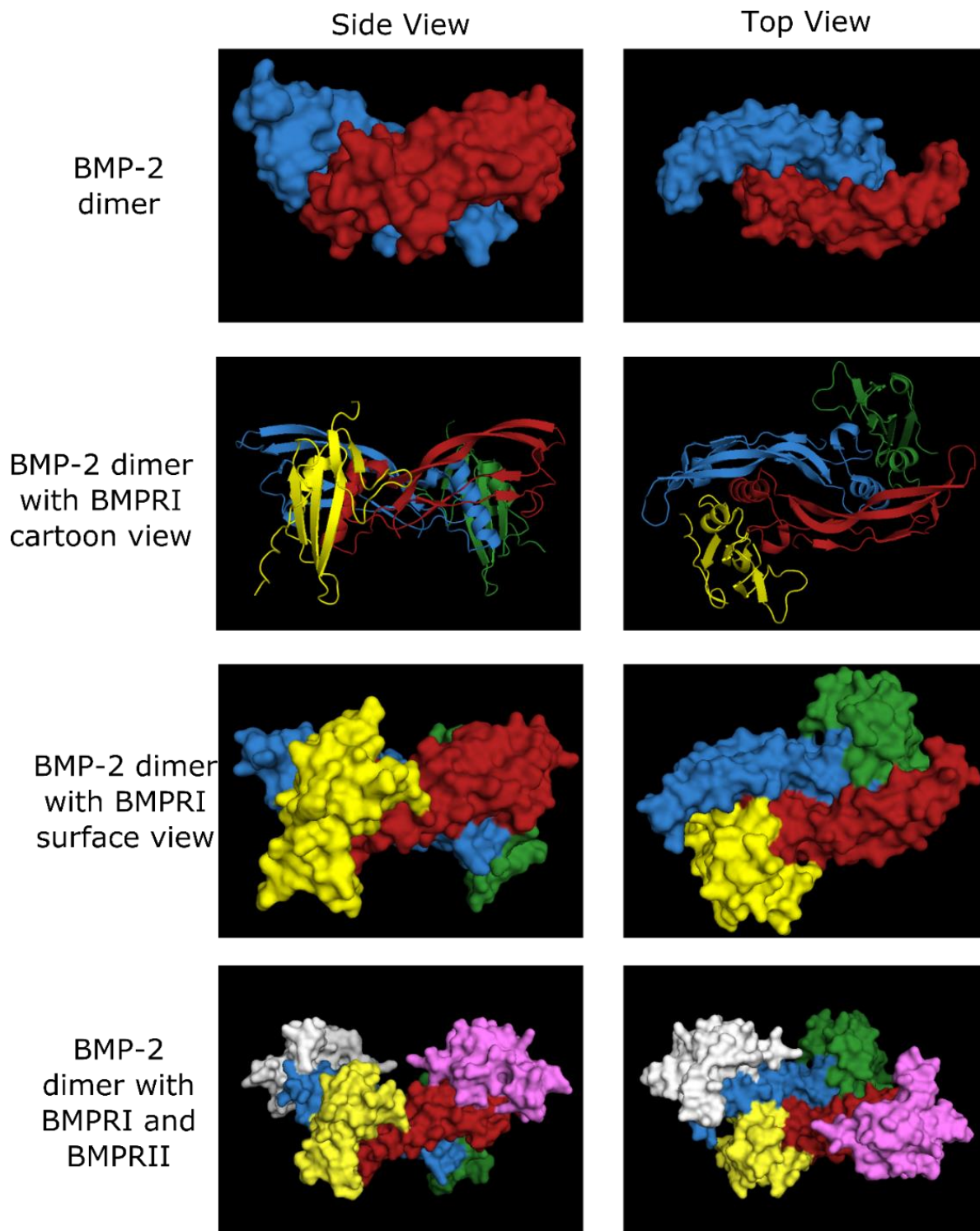
BMPs react with BMPRs (bone morphogenetic protein receptors) which comprise three parts: a short extracellular domain, a membrane spanning membrane domain and an intracellular domain which houses the active serine/threonine kinase region (Rao, Ugale et al. 2013). There are many different BMPRs, but they can be categorised into two families. Three BMPRI (BMPRIA or ALK3, BMPRIIB or ALK6 and ALK2: IA activin receptors) and three BMPRII (BMPRIIB, ACTRIIA and ACTRIIB) are known to bind BMP. Of the three BMPRI, BMPRIA and B are highly similar with ALK2 showing some sequence divergence. However, they all possess a highly conserved TTSGSGSG motif which is necessary for kinase activity (Lin and Hankenson 2011). BMPRIIs have a constitutively active kinase domain which when brought into contact with BMPRI leads to the activation of downstream effectors and ultimately leads to an alteration of phenotype. Normally, signalling is initiated by the binding of BMP-2 to a BMPRI which begins the recruitment of the other receptors. Once two of each type of receptor has been recruited to form a ternary holocomplex signalling can occur (Allendorph, Vale et al. 2006). From the current understanding, heteromeric complexes of BMPRI and BMPRII are essential for signal propagation. It is believed that the specificity of signals and binding is largely determined by BMPRI whereas BMPRII is used to stabilise the complex and initiate downstream signalling.

**Table 1.1. Biological functions of the BMPs (Rahman, Akhtar et al. 2015).**

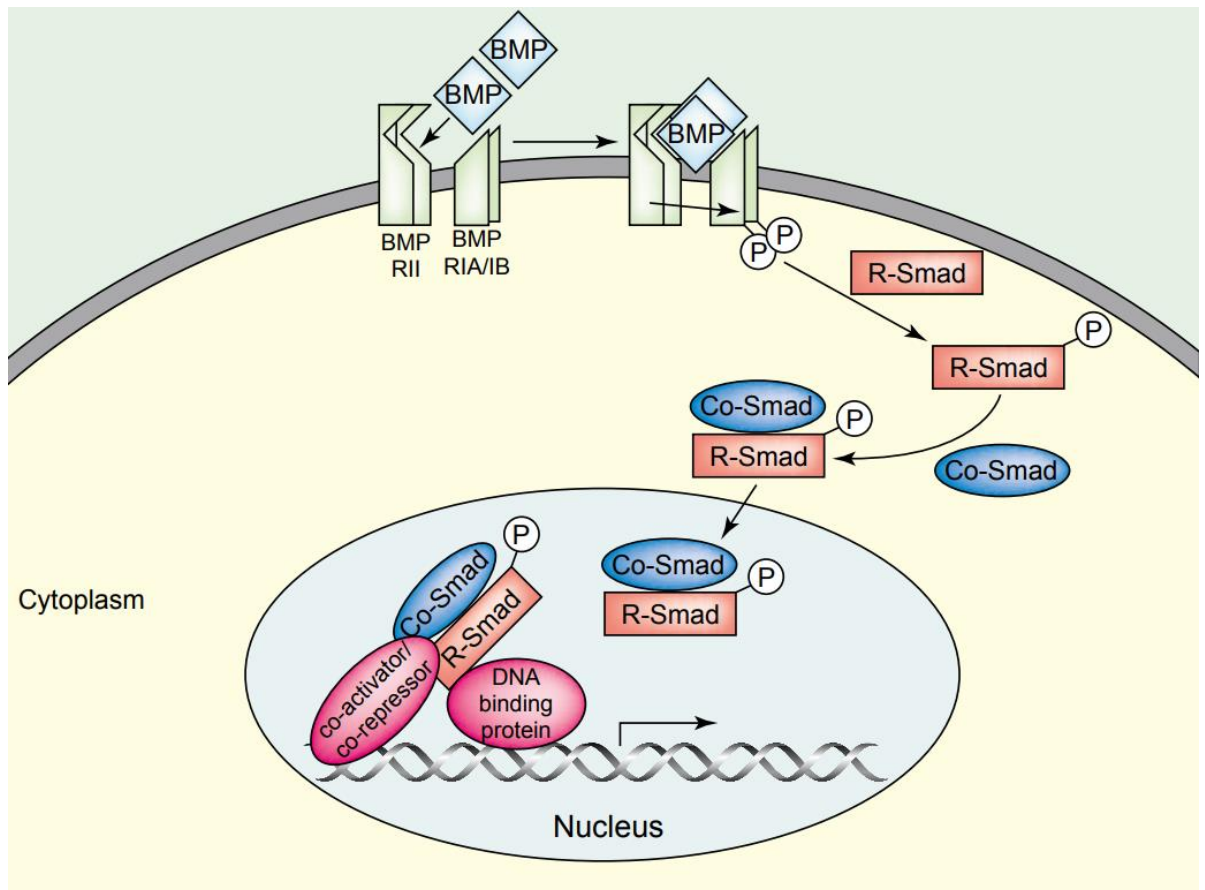
Subtype(s)	Biological Function(s)
BMP1	Cleaves procollagens to produce fragments that self-associate for cartilage formation
BMP2/BMP2a	Induced bone morphogenesis and involved in heart formation
BMP3A/Osteogenin	Negative regulator of bone morphogenesis, induces synthesis and secretion of TGF- $\beta$ 1
BMP3B	Negative regulator of bone morphogenesis in embryonic stage, with opposite effect in mature animals
BMP4/BMP2B	Involved in bone induction, cartilage, limb and kidney formation, tooth development and fracture repair
BMP5	Role in early developmental skeleton patterning, limb development and bone morphogenesis
BMP6	Active role in osteoblast lineage specific differentiation
BMP7	Role in bone homeostasis and calcium regulation
BMP8A	Role in bone morphogenesis
BMP8B	Found only in mice spermatogenesis
BMP9	Active role in osteogenesis and in mature osteoblasts
BMP10	Heart morphogenesis
BMP11	Role during embryogenesis and skeletal patterning
BMP12	Involved in tendon and ligament formation
BMP13	Involved in chondrogenesis and hypertrophy
BMP14	Survival promoting molecule for neurons and enhances tendon healing and bone formation
BMP15	Role in ovarian development and function
BMP16	Embryonic patterning
BMP17	Embryonic patterning
BMP18	Embryonic patterning

Figure 1.3 (created with PyMol (DeLano 2009) using data from the Protein Data Bank (PDB)) shows how BMP-2 monomers dimerise to form the biologically active molecule; and how this osteogenic factor binds to its receptors in the membrane. BMP binding to the membrane leads to the recruitment of the pathway restricted SMADs (R-SMADs 1, 5 and 8) shown in Figure 1.4 (Itoh, Itoh et al. 2000, Moustakas, Souchelnytskyi et al. 2001, Derynck and Zhang 2003). These are then released from the receptor and recruit the common mediator SMAD (SMAD 4) and then this complex migrates to the nucleus and induces expression of osteogenic transcription factors (Watanabe, Masuyama et al. 2000, Xiao, Watson et al. 2001, Inman, Nicolas et al. 2002). Two main routes for osteogenic induction have been discovered after BMP extracellular binding. Either through activating the transcription factors RUNX2 (runt- related transcription factor 2) and/or osterix (OSX) through the SMAD proteins (canonical BMP signalling) (Shi and Massague 2003, Afzal, Pratap et al. 2005, Massague, Seoane et al. 2005). Or through p38MAPK (mitogen-activated protein kinase) and JNK (c-Jun N-terminal kinase) cascades (non-canonical BMP signalling) which is similar to the

pathways induced by integrin binding (Guicheux, Lemonnier et al. 2003). There are strict genetic commitments necessary to predispose MSCs to the osteoblastic phenotype, these genes are activated by numerous transcription factors which are ultimately guided by regulatory pathways governed by cell receptors such as those for growth hormones and integrins (Chamberlain, Fox et al. 2007, Shih, Tseng et al. 2011).



**Figure 1.3. BMP-2 and its receptors.** Images constructed in PyMol using structures from the Protein Data Bank (PDB). Red and blue show BMP-2 monomers (PDB reference 3BMP), yellow and green show BMPRI and white and pink show BMPRII (PDB reference 3EVS). It is believed that a ternary homocomplex of two of each receptor is needed to bind BMP-2 in order to propagate osteogenic signalling. Accessed December 2016 using PyMol 1.7.x.



**Figure 1.4. BMP-2 dependent osteogenesis.** BMP-2 signalling begins with the binding of BMP-2 to its receptors in the membrane. Then the phosphorylation of the recruiter Smad leads to the recruitment of Co-Smads and subsequent translocation to the nucleus. Here, the induction of osteogenic genes take place.

## 1.6 MAPK signalling pathway

The transmission of extracellular events into the cell are largely mediated by a network of interacting proteins that propagate a diverse range of intracellular changes. Many efforts have led to the discovery of a highly complex signalling mechanism, collectively involving the activation of many membrane signalling molecules, and their subsequent intracellular induction. This is known as the MAPK signalling cascade (Seger and Krebs 1995). Classical MAPK pathways utilise the extracellular signal-regulated kinases 1 and 2 (ERK1/2), c-Jun N-terminal kinases 1-3 (JNK 1-3) and p38 ( $\alpha$ ,  $\beta$ ,  $\gamma$  and  $\delta$ ) amongst many others (Cargnello and Roux 2011). Extracellular signals are amplified and transmitted along a series of regulatory molecules in the cytoplasm towards the nucleus, where cellular processes such as proliferation and differentiation are controlled.

MAPK signalling can be initiated in a variety of ways, from stress (Aikawa, Komuro et al. 1997, Xia, Makris et al. 2000, Xu, Wang et al. 2013), growth factors (such as BMP-2) (Kao, Jaiswal et al. 2001, von Kriegsheim, Baiocchi et al. 2009), G protein coupled receptors (Crespo, Xu et al. 1994, Koch, Hawes et al. 1994) and integrins (Aplin and Juliano 1999,

Fincham, James et al. 2000). Activation by these means leads to stimulation of MAP3Ks, a group of kinases which in turn phosphorylate and activate MAP2Ks, which again, activate MAPKs (Plotnikov, Zehorai et al. 2011, Humphreys, Piala et al. 2013). MAPKs can then either translocate to the nucleus or activate additional kinases (Roux et al., 2007), this cascade can be viewed in Figure 1.5 (Escos, Risco et al. 2016) (Nagai, Urushihara et al. 2016).

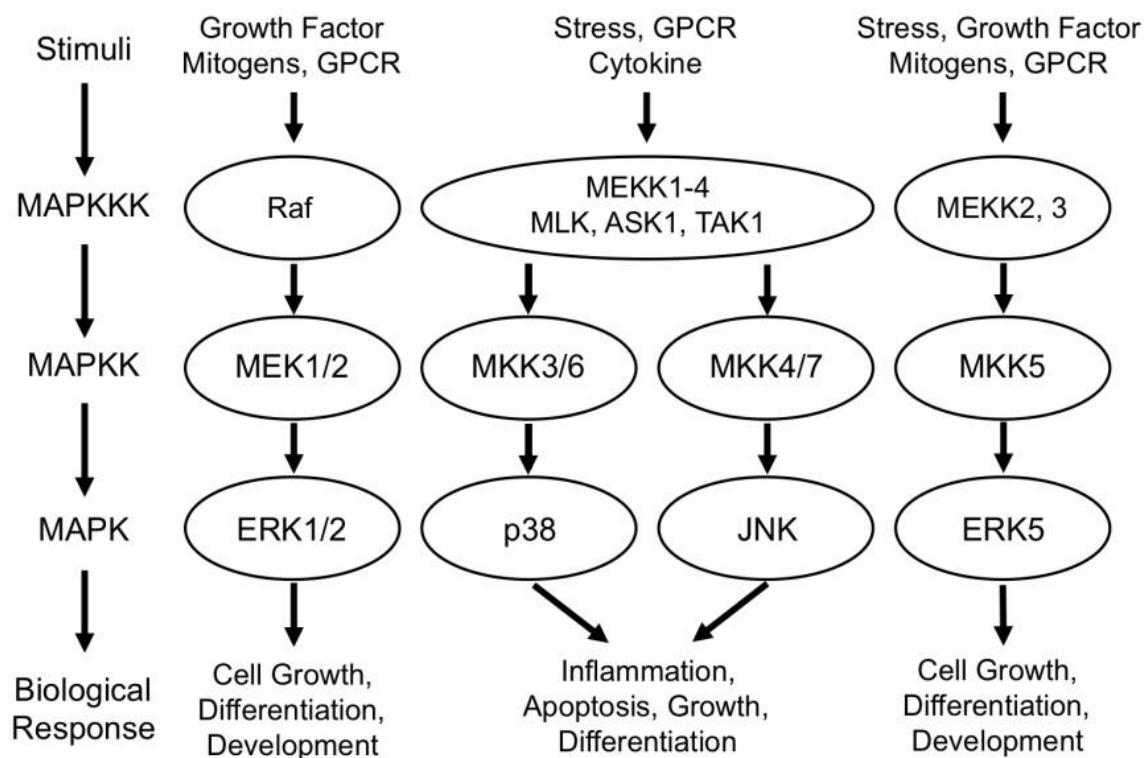


**Figure 1.5. MAPK signalling cascades.** Classical MAPK signalling pathways can be divided into four cascades (ERK1/2, p38, JNK and ERK5). The MAP3Ks are activated in response to numerous extracellular stimuli and propagate via MAP2Ks and MAPKs. MAPKs can engage with target transcription factors within the nucleus altering gene expression and functional output.

The main pathways contain few constituents, with the core mediators being used in most pathways. However, the number of proteins that feed in and out of the network exponentially increase as you extend out of the pathways. Computational analysis was used to ascertain the amount of proteins with a direct physical link to the MAPK pathway and assembled a list of 2000 proteins (Bandyopadhyay, Tsuji et al. 2006). Figure 1.6 summarises the effect of BMP-2 through both canonical (smad 1/5/8) and non-canonical (p38, ERK1/2 and JNK1/2).

Two decades ago, MAPK pathways were identified as major components in skeletal development and bone homeostasis. Although the MAPK pathways are vast with far reaching effects, the activities of p38 and ERK are predominantly involved in shaping osteoblast commitment and differentiation. Many hundreds of publications detail both *in vivo* and *in*

*in vitro* analysis of p38 and ERK through the osteoblastic differentiation process, from a mesenchymal progenitor into a fully functional anabolic bone cell (Ehrlich and Lanyon 2002, Bai, Lu et al. 2004). Most work completed highlights the use of genetic knockouts and inhibitors on MAPK activity which aid in the determination of ERK and p38 on specific processes within the cell (Aouadi, Binetruy et al. 2006, Chang, Sonoyama et al. 2007).

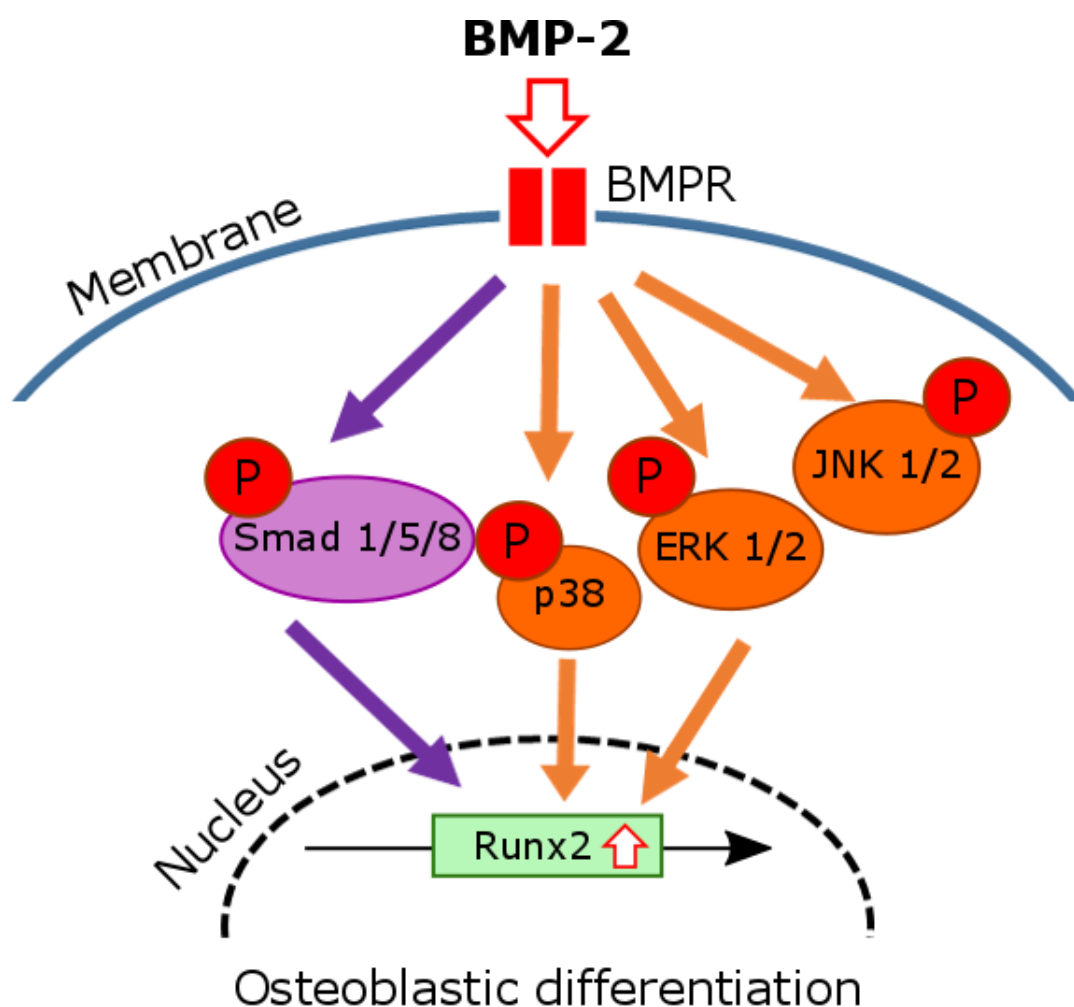


**Figure 1.6. BMP-2 can activate MAPK.** MAPK cascades can be activated by growth factors. They can activate additional downstream kinases and also interact with transcription factors within the nucleus altering gene expression.

ERK induction in terms of MSC differentiation occurs primarily through integrin signalling through tension and mechanical stress (Kanno, Takahashi et al. 2007, Ward, Salaszyk et al. 2007, Zhang, Wu et al. 2012). It has been shown that tensile stress plays a vital role in osteoblastic differentiation, in that externally applied tension alone can induce differentiation (Engler, Sen et al. 2006, Kilian, Bugarija et al. 2010). Integrin signalling through ERK leads to the activation of RUNX2, a transcription factor that is essential for bone growth *in vivo*. It has been proved that RUNX2 knockouts develop many skeletal irregularities with death the

final outcome due to a lack of ossification (Komori, Yagi et al. 1997). Similarly, RUNX2 inhibits the adipogenic transcription factor PPAR $\gamma$  (Hu, Kim et al. 1996).

p38 can be activated through the methods listed above, but again, is primarily through integrin binding and BMP-2 activation. The osteogenic potential of p38 is due to its ability to phosphorylate and activate key transcription factors, like ERK, p38 can activate RUNX2 (Ge, Xiao et al. 2009, Greenblatt, Shim et al. 2010). BMP-2 signalling and p38 work together to induce osteogenesis, BMP-2 can increase DLX5 activation of the osterix promoter, but first DLX5 must be phosphorylated by p38 (Ulsamer, Ortuno et al. 2008). Additionally, DLX3, another DLX member is induced by BMP-2 by cooperation through SMAD5 and p38 which ultimately leads to osterix activation (Yang, Yuan et al. 2014). These pathways are simplified in Figure 1.7 (Rodriguez-Carballo, Gamez et al. 2016). MAPK pathways play vital roles in many aspects of osteoblastic differentiation. These have been proven by both ERK and p38 deletion hampering osteoblast differentiation *in vivo*.

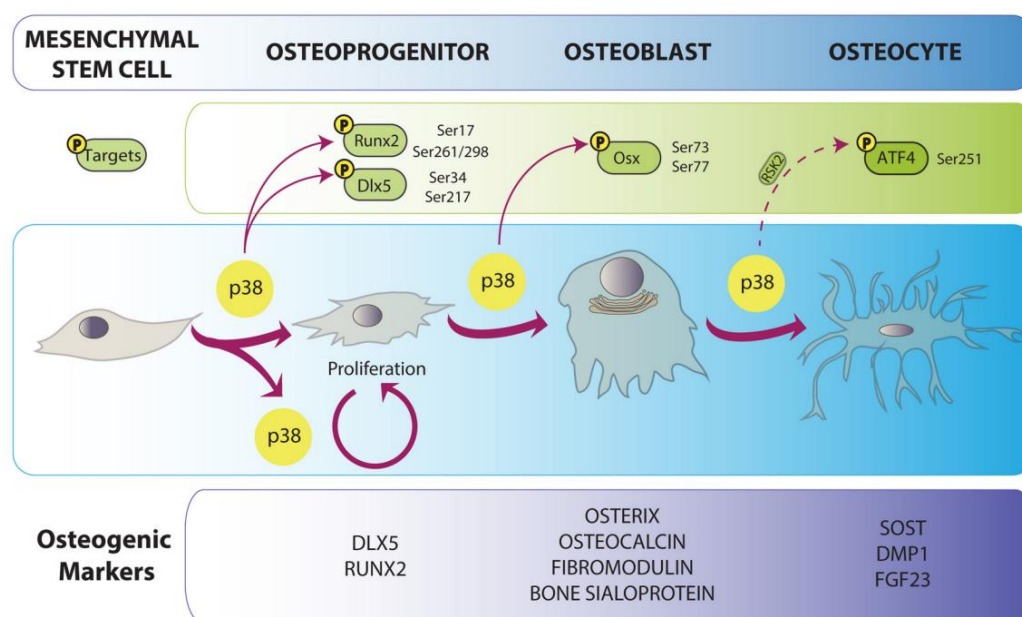


**Figure 1.7. p38 implication in osteoblast differentiation.** p38-mediated phosphorylation promotes progression in osteogenesis by the enhancement of the activity or expression of osteoblast-specific transcription factors genes such as RUNX2, DLX5 and osterix. Direct arrows indicate direct phosphorylation whole dashed arrows indicate indirect action of p38. Image courtesy of (Rodriguez-Carballo, Gamez et al. 2016).

It is apparent that BMP-2 can directly affect osteogenic differentiation of MSCs, through both smad (canonical) and p38/ERK1/2 (non-canonical) mechanisms. The MAPK pathways are thus important in healthy bone development and are a necessary constituent of differentiation.

## 1.7 Genetic Engineering

The field of genetic engineering (GE) utilises techniques to directly manipulate an organism's genome. These techniques involve insertion, deletion or modification of the existing genetic material. IUPAC defines GE as '*the process of inserting new genetic information into existing cells to modify a specific organism for the purpose of changing its characteristics*' (Vert, Doi et al. 2012). There are many examples and types of manipulation possible, the most common being the insertion of a foreign gene from one species into another. Others involve altering a specific gene (mutagenesis), activating, silencing or changing the expression levels of one or more multiple genes. These can be accomplished through multiple techniques, such as RNA interference, antisense oligonucleotides, ribozymes, catalytic RNA molecules that possess the ability cut RNA strands at desired locations amongst many more (Tollefsbol 2007, Kole, Krainer et al. 2012, Wilson and Doudna 2013). In this thesis, we are using the technique known as Gibson Assembly (Gibson, Young et al. 2009) which will be covered in more detail later. Genetic engineering encompasses the use of recombinant nucleic acid techniques, either DNA or RNA, to synthesise new genetic sequences. These are then inserted into living organisms, transiently or permanently, via direct modification of the genome using vectors.

Many strains of bacteria have undergone serious research as a host of genetic manipulation, the most important of these is the gram negative bacteria *Escherichia coli* (*E. coli*) (Boyer and Roulland-Dussoix 1969, Chong 2001, Sawitzke, Thomason et al. 2007). This strain has been extensively studied and used in plasmid engineering, however, there are also many other bacteria with commercially available tools for genetic manipulation, including gram positive strains. The choice of bacteria will be explained in the next section. Of these bacteria, the lactic acid bacteria clade, especially *Lactococcus lactis* (*L. lactis*) displayed the greatest amount of potential due to the current availability of genetic manipulation tools, combined with its ability to form 2D biofilms.

Once a suitable host organism has been chosen, it is also important to select an appropriate genetic vector. These can range from plasmids to artificial chromosomes. Plasmids usually contain promoters, either constitutive or inducible, several selectable genetic markers and multiple cloning sites where restriction sites are readily available. The use of promoters depends on the outcome of the application, e.g., bacterial kill-switches cannot be constitutively expressed and must be controlled by an inducer. In contrast, constitutive promoters are always 'on'. Inducible promoters can be controlled in a stimulus derived fashion, with the use of chemicals, pH, temperature and light, among many others (de Vos

1999, Mierau and Kleerebezem 2005, Siren, Salonen et al. 2009). Upon choosing the correct organism and vector, the sequence of DNA to be cloned needs to be obtained and amplified using the polymerase chain reaction (PCR). This allows biologists to obtain more than suitable amounts of DNA. PCR is a highly specific and extremely versatile technique that can add specific DNA sequences to either 5' or 3' ends of sequences, induce single nucleotide polymorphisms, create deletions and mutate DNA. Upon the completion of a PCR reaction, the mixture comprises many proteins, including the polymerase, nucleic acids including the sequence and primers and dNTPs. Usually, this mixture needs purifying before further steps can be completed.

Next, the chosen DNA and vector need to be ligated. Conventional cloning techniques utilise restriction enzymes in order to linearise the destination vector generating blunt or sticky ends where the foreign DNA fragment can be inserted. DNA ligase is also added to the mixture which leads to the ligation of the vector and the chosen DNA sequence. DNA ligase works by creating a phosphodiester bond in the sugar backbone between the two DNA sequences resulting in the insertion of the chosen DNA sequence at the exact desired point.

More recently, the use of restriction endonucleases have been made more redundant. Techniques such as TOPO, Gateway, overlap extension PCR or Gibson assembly use the power of PCR to generate fragments with overlapping sequences that can be partially digested with exonuclease, repaired and joined together again (Xu and Li 2008, Gibson, Young et al. 2009, Bryksin and Matsumura 2010, Petersen and Stowers 2011). Once the DNA is constructed, it must be inserted into the host cell. In bacterial cells, electroporation and heat-shock transformation are most widely used.

For gram positive cells, such as *L. lactis*, electroporation is used due to the structure of the cell wall. Firstly, the bacteria of choice need to be made electrocompetent, usually by growing the cells in a glycine rich medium which leads to the weakening of the cell wall. Upon the addition of an electric pulse to the system, the bacteria becomes porous and if plasmid has been added to the mixture, DNA can enter the cells. Heat-shock works by altering the bacterial membrane fluidity creating a number of small pores. Cells are kept at 0 °C with calcium chloride as this creates a positive charge on the bacterial membrane allowing the negatively charged DNA to stick to the bacteria. By increasing the temperature to 42 °C, the membrane fluidity changes creating pores allowing the plasmid to enter the cell. The temperature is then decreased to 0 °C again returning the membrane fluidity to normal.

After the transformation step, the transformed cell, that is the ones with the new plasmid inside needs to be separated from the wild type cells. Generally, engineered plasmid vectors contain at least one antibiotic resistance gene, so that if a cell has been transformed with the plasmid, it will be able to grow on an agar plate supplemented with that antibiotic. This is not only limited to bacteria, for instance, mammalian cell vectors usually contain a geneticin-resistance gene. Geneticin is largely toxic to all cell types and therefore correctly transformed cells will display a resistance. A further method to screen for positively transformed cells is to look for marker proteins, such as GFP (Tsien 1998). GFP is fluorescent under normal conditions; that is room temperature and a neutral pH and can therefore be detected non-destructively in real time with UV light excitation (395 nm). Correctly transformed cells would display GFP fluorescence at 509 nm once excited with light of 395 nm.

Genetic engineering has evolved over the last few decades and has given rise to synthetic biology. Genetic engineering approaches are usually ad hoc, whereas synthetic biology aims to apply engineering principles such as standardisation, modularisation, and reusability. This allows the creation of new genes, and in the long term, the potential to tailor new organisms for a desired application. For example, pT1NX, one of the plasmids used in this thesis which will be described later is comprised of DNA from different species including phage T7, *Enterococcus faecalis* and *Staphylococcus aureus*. These convey specific functionality, and have been joined together to create a useful tool for both cell wall bound and secreted heterologous protein expression in *Lactococcus*.

## 1.8 Gibson assembly

In 2009, Dr Gibson at the J. Craig Venter Institute developed an easy method to enable the assembly of multiple linear fragments of DNA (Gibson, Young et al. 2009). Multiple overlapping fragments can be joined in a single isothermal reaction utilising the power of three different enzymes, T5 exonuclease, Phusion polymerase and Taq ligase. This can result in the creation of a fully ligated double stranded DNA molecule. It is primarily used by molecular biologists in the creation of synthetic plasmids and has rapidly overtaken more conventional cloning techniques due to its ease of use, ability to join almost any two fragments regardless of sequence (due to lack of restriction sites). There are no ‘scars’ between ligated sites and the technique has been shown to combine up to six fragments at a time in a single tube. A simple schematic of the system can be visualised in Figure 1.8.

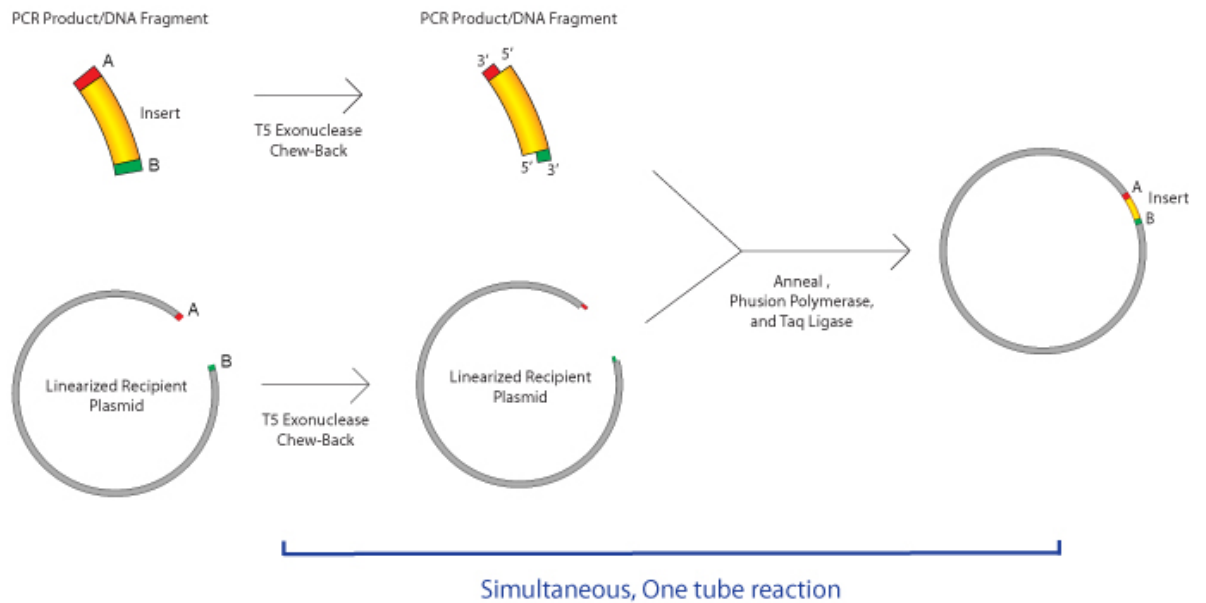


**Figure 1.8. Gibson Assembly.** Gibson Assembly details a method for the easy assembly of multiple linear DNA fragments in a single isothermal reaction. By using overlapping primers, the enzymes T5 exonuclease, Phusion DNA polymerase and TAQ DNA ligase can form a fully ligated double-stranded DNA molecule. Image courtesy of Addgene (<https://www.addgene.org/protocols/gibson-assembly/>).

Complementary termini of PCR products determine the order in which the fragments will be assembled and can be seen in Figure 1.9. In order for these PCR products to assemble, the three enzymes mentioned above play a pivotal role.

T5 exonuclease creates single stranded 3' overhangs by chewing back from the 5' end. This allows the complementary DNA fragments to subsequently anneal to each other.

Phusion DNA polymerase integrates new nucleotides to fill in the gaps in the annealed DNA fragments.

Taq DNA ligase covalently links the newly annealed DNA fragments, removing any nicks and creating a continuous DNA fragment, thus eliminating any scars left in the construct.

Upon designing primers with overlapping complimentary regions (see coloured regions in Figure 1.9), the PCR products are added to a Gibson Master Mix which contains the 3 enzymes and dNTPs. This single tube is left at 50 °C for 15-60 minutes and the resulting plasmid is then to be transformed into a host bacteria.

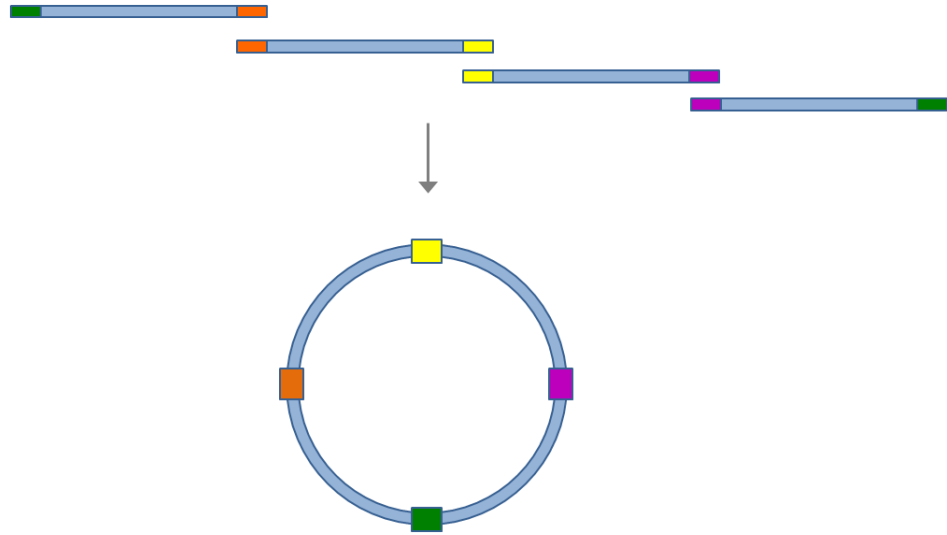


**Figure 1.9. Gibson Assembly primer overlap.** By creating primers with overlapping regions (yellow, purple, green and orange regions), a fully ligated DNA molecule can be assembled in a single reaction vessel.

## 1.9 Why *Lactococcus lactis*?

Lactic acid bacteria (LAB) have a long history of safe use in humans, being used for hundreds of years in the food industry and more recently, use as probiotics in human health. Of late, there has been an increased effort to use LAB as microbial cell factories for the production of proteins of interest. So far, these bacteria have been used as vectors for the delivery of functional proteins to mucosal tissues amongst others shown in Table 1.2 (Cano-Garrido, Seras-Franzoso et al. 2015). *L. lactis*, amongst other LAB have GRAS (Generally Regarded As Safe) status by the US Food and Drug Administration (FDA) and fulfil criteria of the qualified presumption of safety (QPS) according to the European Food Safety Authority (EFSA) (Cano-Garrido, Seras-Franzoso et al. 2015).

This bacteria was chosen as LAB are gram-positive, in contrast to gram negative bacteria such as *E. coli*, and therefore do not contain lipopolysaccharide (LPS). LPS is known to cause anaphylactic shock in humans and so the use of gram positive bacteria is of utmost importance when trying to create synergistic environments for mammalian cells and bacteria (Rueda, Cano-Garrido et al. 2014).

Furthermore, this strain features a very low production of exopolysaccharide (EPS) (Le Loir, Azevedo et al. 2005), a mandatory requirement to ensure the interaction of the mammalian cell integrins with the exposed fibronectin fragment in the cell wall and allowing ease of secretion of BMP-2.

Another important characteristic of this strain is it has the ability to spontaneously develop biofilms (Mercier, Durrieu et al. 2002, Habimana, Le Goff et al. 2007). Despite its low EPS production, *L. lactis* has the potential to colonise a vast array of surfaces, including the widely used tissue culture substrates. These biofilms have been shown to remain stable for at least four weeks (Hay, Rodrigo-Navarro et al. 2016) and support MSC adhesion and differentiation.

Lastly, *L. lactis* has been widely used and has been deeply characterised, being the first LAB to have its genome sequenced. In addition, it is an expression system that can be easily manipulated and has a vast array of commercial cloning and expression systems already in place.

In this work we are using the pT1NX plasmid designed by Dr L Steidler which features the P1 lactococcal promoter and erythromycin resistance gene (Waterfield, Lepage et al. 1995, Steidler, Viaene et al. 1998). mRNA synthesis is controlled by the T7g10 terminator from phage T7 (Schotte, Steidler et al. 2000). The replicon is from the *Enterococcus faecalis* plasmid pAM $\beta$ 1 origin and the plasmid also includes repD and repE. It has been used for the constitutive expression of both anchored and secreted proteins and is commercially available with the tools to accomplish these protein types. pT1NX has many features and the important sections will be discussed, a basic map can be seen in Figure 1.10.

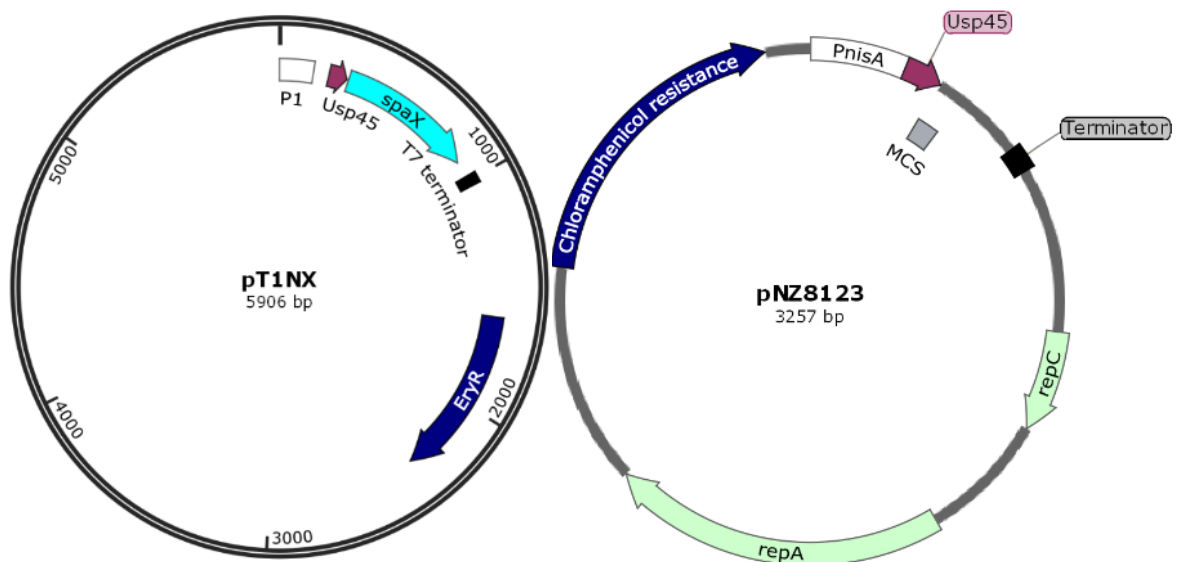


**Figure 1.10.** *L. lactis* plasmids. pT1NX and pNZ8123 vector maps showing the P1 lactococcal promoter (pT1NX), PnisA nisin A promoter (pNZ8123), *usp45* secretion signal, *spaX* protein A anchor (pT1NX), the *ermAM* erythromycin resistance gene (pT1NX) and chloramphenicol resistance gene (pNZ123).

A further plasmid designed by Mobitec known as pNZ8123 also features in this work. This harbours the PnisA promoter which is under the control of the inducer nisin controlled by the terminator T. It also contains a chloramphenicol resistance gene as well as repC and repA and pSH71 origin of replication. A basic map can be seen in Figure 1.10.

**Table 1.2. Recombinant proteins produced by *L. lactis* for biomedical purposes (Cano-Garrido, Seras-Franzoso et al. 2015).**

<b>Bacteria</b>	<b>Application</b>	<b>Recombinant protein</b>	<b>Expression vector</b>	<b>Protein display</b>
<i>Lactococcus lactis</i>	Intestinal disease	Anti TNF alpha antibodies	pTREX	Secreted
<i>Lactococcus lactis</i>	Intestinal disease	Trefoil factors	pTREX	Secreted
<i>Lactococcus lactis</i>	Intestinal disease	Low calcium response	pNZYR	Secreted
<i>Lactococcus lactis</i>	Intestinal disease	Superoxide dismutase	pSodA	Secreted
<i>Lactococcus lactis</i>	Intestinal disease	IL-10	Chromosome integrated	Secreted
<i>Lactococcus lactis</i>	Intestinal disease	IL-27	pT1NX	Secreted
<i>Lactococcus lactis</i>	Intestinal disease	Murine IL-10	pLB263	Cytoplasmic
<i>Lactococcus lactis</i>	Colorectal cancer	Catalase	pSEC:KatE	Secreted
<i>Lactococcus lactis</i>	Type 1 diabetes	Pro-insulin	pT1NX	Secreted/cytoplasmic
<i>Lactococcus lactis</i>	Type 1 diabetes	HSP65	pCYT:HSP65	Secreted
<i>Lactococcus lactis</i>	Type 1 diabetes	GAD65	pCYT:HSP66	Secreted
<i>Lactococcus lactis</i>	Diabetes	Single chain insulin	pNZPnisA	Secreted
<i>Lactococcus lactis</i>	Type 2 diabetes	Glucagon like peptide 1	pUBGLP	Secreted
<i>Lactococcus lactis</i>	Cancer	HPV-16 E7 antigen	pLB263	Cytoplasmic
<i>Lactococcus lactis</i>	Cervical cancer	HPV-16 E7	pMG36e	Anchored
<i>Lactococcus lactis</i>	Cervical cancer	HPV-16 E7	pMG36e	Cytoplasmic
<i>Lactococcus lactis</i>	Cervical cancer	HPV-16 E7	pMG36e	Anchored
<i>Lactococcus lactis</i>	Staphylococcal infection	Staphylococcal nuclease	pLB263	Secreted

The genes found in pT1NX and pNZ8123 can be utilised in the creation of either cell wall bound or secreted proteins. Protein A (SpA) is a 42 kDa protein found in the cell wall of *Staphylococcus aureus* (known as spaX) (Steidler, Viaene et al. 1998). To allow anchorage, a C-terminal 35 residue sorting sequence is essential, which contains the conserved peptide LPXTG followed by a tail mainly composed of positively charged amino acids which prevents the full secretion of the protein. The C-terminal is cleaved by a signal peptidase which leads to the translocation of the protein. After translocation, a sortase with proteolytic activity (Mazmanian, Hung et al. 2001, Mercier, Durrieu et al. 2002) that modifies surface proteins by recognising the LPETF motif in the C-terminal cleaves between a threonine and glycine residue and leaves the C-terminal end anchored to the cell wall. The C-terminal of the threonine is covalently linked to the free amino groups of the peptidoglycan cross bridge via an amide bond which allows the final crosslinking to be completed. This mechanism is not always 100 % accurate and sometimes these molecules can be found in the extracellular space, mainly due to the physical turnover and release of peptidoglycan fragments linked with surface proteins. Figure 1.11 displays a schematic of the anchoring mechanism.

The Usp45 signal peptide used is part of Usp45 (unknown secreted protein 45) found in many LAB (Vanasseldonk, Rutten et al. 1990). This protein has no known biological activity but can be exploited by biologists to allow the secretion of desired proteins. This secretion peptide comprises the first 27 residues of the native N-terminal region of Usp45 (Vanasseldonk, Rutten et al. 1990). The largest protein known to be secreted using this protein is 160 kDa and therefore, will not affect the proteins planned to be secreted in this thesis.

The use of the Usp45 secretion peptide is mandatory for both cell wall bound and secreted proteins as this protein tells the bacteria to transport the cargo to the outside of the cell, however, spaX is only necessary for cell wall bound expression. By utilising the powers of these proteins, we can tailor specific protein design and their localisation.

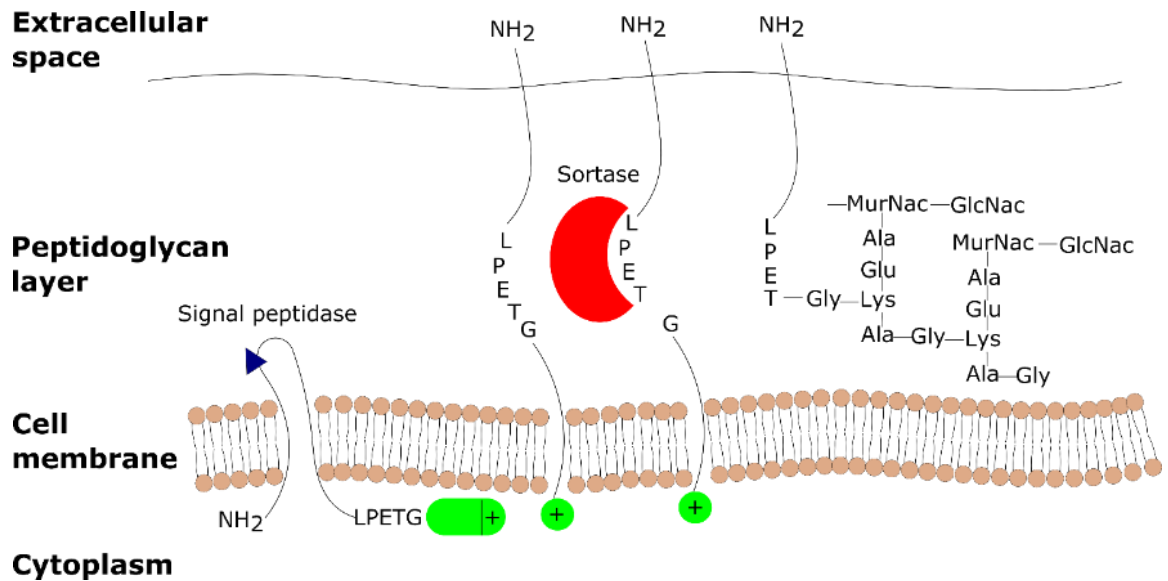


**Figure 1.11. *L. lactis* anchoring mechanism.** Anchoring mechanism of the LPETG motif onto the peptidoglycan layer. A signal peptidase cleaves near the N-termini of the protein, which is translocated to the outer part of the cell wall. Then, a sortase cleaves the polypeptide chain between the threonine and glycine and anchors the threonine to the tetrapeptide motif that crosslinks the peptidoglycan layer.

In contrast to the constitutive expression of pT1NX, many inducible plasmids have been constructed for effective secretion in *L. lactis*. pNZ8123 provides the Usp45 secretion peptide under control of the PnisA promoter. The most commonly used regulated expression system in *L. lactis* is the Nisin Controlled Gene Expression System (NICE) (deRuyter, Kuipers et al. 1996). This utilises sub-toxic amounts of the bacteriocin nisin (ng/mL) which is enough to fully activate the normally tightly controlled promoter (Kuipers, de Ruyter et al. 1998). Naturally, extracellular nisin can bind to the nisin receptor NisK, which activates NisR by phosphorylation. This in turn induces the nisin operon at the PnisA promoter. This system and operon have been exploited by synthetic biologists in order to create a gram positive inducible protein expression system. The genes of the receptor (*NisK*) and response regulator (*NisR*) have been isolated and placed on the chromosome of a suitable host strain (NZ9000 and NZ9020 in this work). In addition to this, PnisA has been isolated and placed on many plasmids, including pNZ8123. Upon downstream gene placement at PnisA, and insertion of this plasmid into a *nisRK* strain, expression of this protein can be controlled by the addition of nisin (deRuyter, Kuipers et al. 1996). Localisation of the protein is determined by the presence of Usp45 and spaX (discussed above). Figure 1.12 displays a schematic of the NICE system (Mierau, Olieman et al. 2005)

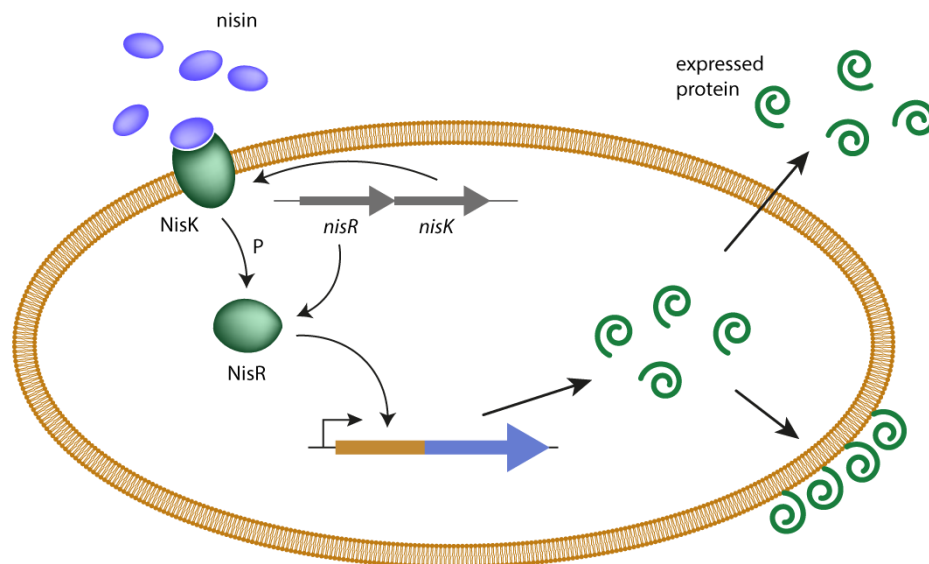


**Figure 1.12. *L. lactis* nisin-controlled gene expression system.** After binding of nisin to the specific receptor NisK autophosphorylates and transfers the phosphate group to NisR. Activated NisR induces transcription from the target gene placed under the control of the promoter. Depending on the presence of the spaX anchor, proteins are either secreted or cell wall bound.

## 1.10 *L. lactis* phylogeny

LAB are classified using a variety of characteristics, which have evolved over time. Traditionally, mode of glucose metabolism, morphology, growth rates (both temperature, pH and salt concentrations), type of lactic acid produced, cell wall constituents and alkaline tolerance. However, due to the advent of DNA sequencing, the 16S and 23S ribosomal RNA (rRNA) as well as G + C content (percentage moles of guanosine and cytosine content in the genomic DNA) are used to classify the organism. Eubacteria are subdivided into gram negative and gram positive phyla. LAB can be found in the gram positive low G + C content tree of eubacteria.

Based on 16S and 23S rRNA data, gram positive bacteria form two major lines of descent shown in Figure 1.13 (Schleifer and Ludwig 1996). One phylum consists of bacteria with a high G + C content (actinomycetes) and one with a low G + C content (clostridium). LAB are considered as a super cluster, located between the facultative aerobic species staphylococci and bacilli and the anaerobic species clostridia. As such, *Lactococcus* has its own cluster within the clostridium branch. It is difficult to form an exact definition of what a typical LAB should be. However, they could be described as gram positive, catalase deficient (some have catalase activity), largely anaerobic (can tolerate oxygen), acid tolerant, no cytochromes, non-spore forming and having lactic acid as the end product of metabolism.

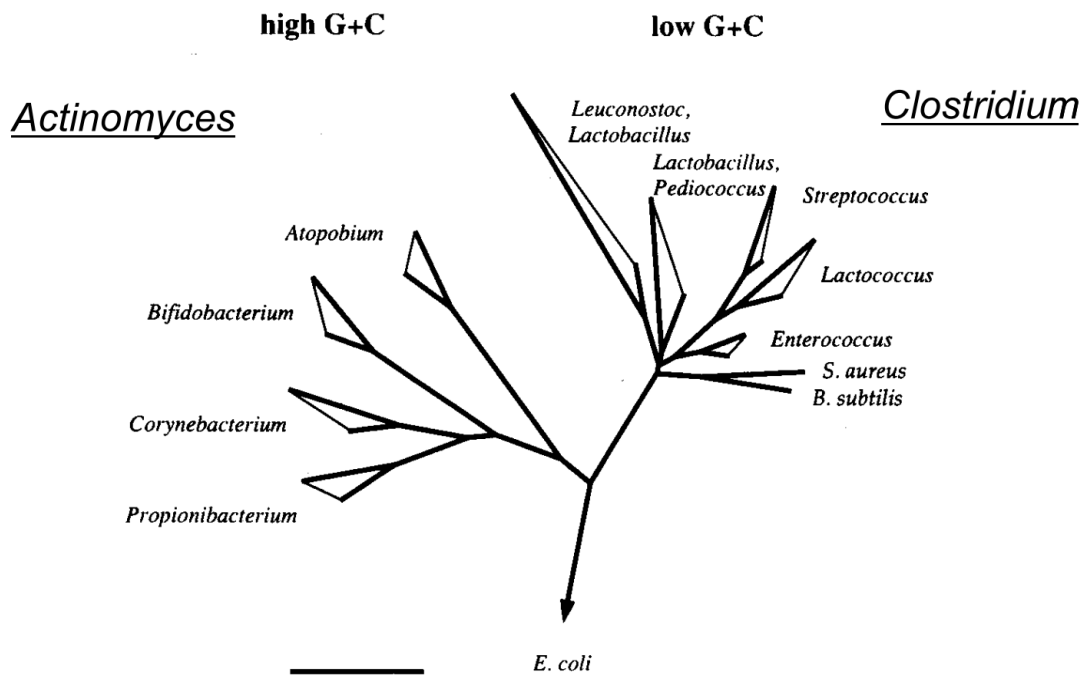
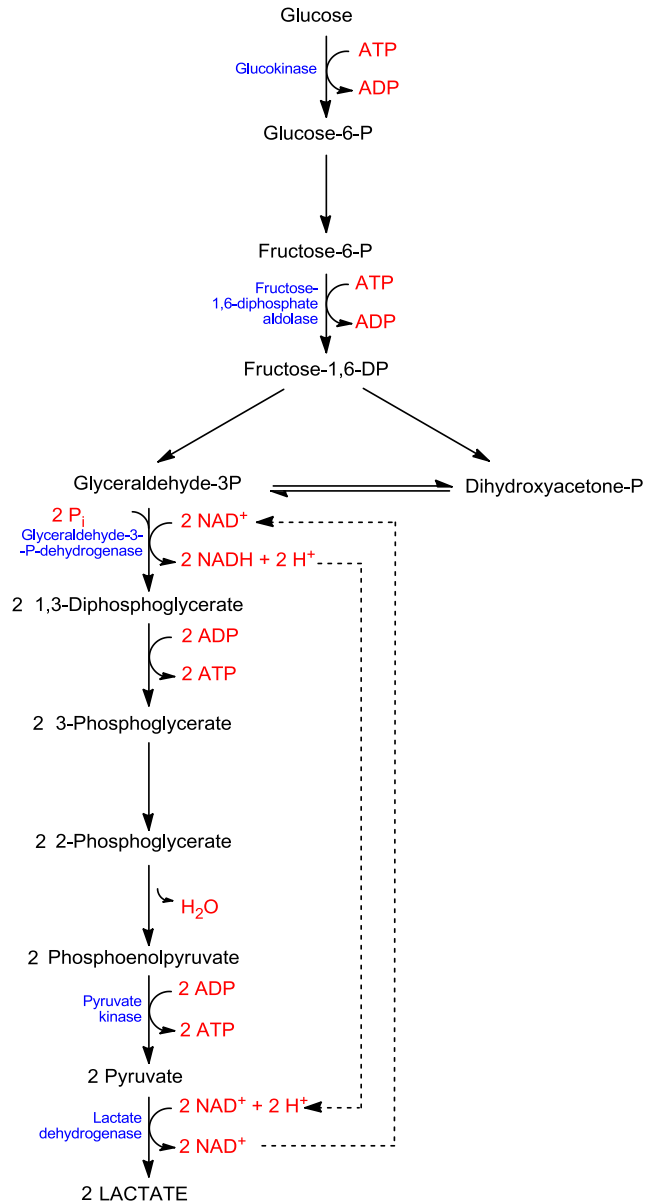


Figure 1.12. Phylogenetic tree of the lactic acid bacteria (LAB) clade.

### 1.11 *L. lactis* metabolism

*L. lactis*, as well as other bacteria in the LAB clade primarily metabolise glucose to lactic acid (Cocaign-Bousquet, Garrigues et al. 1996, Bolotin, Wincker et al. 2001, Rezaiki, Cesselin et al. 2004). This high carbohydrate fermentation coupled with substrate level phosphorylation activity is used for the synthesis of ATP. ATPase is membrane bound and utilises a H<sup>+</sup> gradient to generate a proton motive force that drives the transport of ions and metabolites into the cell. *L. lactis* uses the glycolytic Embden-Meyerhor-Parnas pathway, which is also known as homolactic fermentation to produce ATP from glucose. This pathway is almost exclusively used and results in almost all of the glucose available to the bacteria transformed into L-(+)-lactic acid, through the formation of fructose 1,6-diphosphate, which is then converted into dihydroxyacetonephosphate and glyceraldehyde-3-phosphate which are then both further transformed into pyruvate. Under laboratory conditions, that is cell culture medium where oxygen access is restricted and glucose is in high excess, the pyruvate is reduced to lactic acid by a NAD<sup>+</sup>- lactate dehydrogenase, reoxidising the NADH to NAD<sup>+</sup>. Usually, the only product of this reaction is lactic acid, however, in some cases where more complex ingredients are found in the growth medium, the formation of other molecules such as acetic acid can be found (Stahl, Molin et al. 1990). Pyruvate can be utilised in many different ways by *L. lactis*. Pyruvate can be converted by pyruvate formate lyase, giving acetyl-CoA and formate. Pyruvate dehydrogenase can also produce acetyl-CoA, and results

in the production of NADH and CO<sub>2</sub> when oxygen is present. Moreover, acetyl-CoA can either be converted into ethanol via alcohol dehydrogenase, resulting in the generation of two molecules of NAD<sup>+</sup>, or into acetate via phosphotransacetylase and acetylkinase with a net gain of one ATP molecule. These pathways are used less frequently but there are other routes for ATP genesis such as when pyruvate is converted into 2,3-butanediol. One ATP molecule and two CO<sub>2</sub> molecules are formed from one 2,3-butanediol molecule. Although this pathway is very rarely used in normal laboratory conditions, improved production of 2,3-butanediol can be easily achieved by metabolic and genetic engineering strategies (Gaspar, Neves et al. 2011). The production of 2,3-butanediol, acetate, ethanol and formate is called mixed-acid fermentation, mainly taking place under sub-optimal conditions of growth, which is not usually found in the high glucose rich laboratory growth conditions (Thomas, Ellwood et al. 1979). *L. lactis* almost exclusively grows homofermentatively, meaning that most of the pyruvate formed in glycolysis is converted into lactate with recovery of NAD<sup>+</sup>. Figure 1.14 highlights the homolactic fermentation process in *L. lactis*. The glycolytic pathway can be explained best by carbon catabolite repression (CCR). When extracellular glucose is present, the uptake and metabolic pathways of less favoured sugars are downregulated (Warner and Lolkema 2003). CCR is caused by an array of proteins that systematically phosphorylate specific protein products. A complex of the proteins CcpA and HPr phosphorylate at its serine on position 46 (Gunnewijk and Poolman 2000, Bolotin, Wincker et al. 2001). This complex then binds to CcpA binding motifs (*cre*-sites) which are located upstream of many central metabolism genes (Zomer, Buist et al. 2007). The phosphorylation state of HPr is completely reliant on a phosphotransferase system which allows phosphorylation transfer between different enzymes (EI, EIIA, EIIB and HPr). A glycolytic intermediate molecule PEP donates its phosphoryl group to EI, transfers it to HPr, which phosphorylates EIIA and EIIB. EIIB then phosphorylates intracellular glucose, forming glucose-6-phosphate. At low extracellular glucose concentrations the cell accumulates phosphorylated EI and HPr His-15 (Deutscher 2008). Conversely, at high glucose concentrations, HPr His-15P gets dephosphorylated and then HprK/P, HPr can be phosphorylated at Ser-46 (Reizer, Hoischen et al. 1998). HPr Ser46-P can form a complex with CcpA that results in CCR. Additionally, as well as acting as a repressor, CcpA-HPr Ser46-P is also capable of binding to *cre*-sites upstream of the *las*-operon, which results in the activation of the highly important glycolytic enzymes, namely *pfk*, *pyk* and *ldh* (Luesink, van Herpen et al. 1998).



**Figure 1.14. Homolactic fermentation process in *L. lactis*.** Glycolytic pathway of *L. lactis*, yielding lactate as final product.

In addition to glucose, *L. lactis* can metabolise other sugars such as mannose, fructose and galactose. For mannose and fructose, a permease transport system allows these sugars to enter the cell cytoplasm. Galactose metabolism depends on the strain and the presence of a sugar phosphotransferase system (PTS). If the galactose PTS is present in the cell, galactose is converted into galactose-6-P entering the glycolytic pathway at the glyceraldehyde-3-P level (Figure 1.14 left) (White and Kennedy 1979). In the absence of such a system, galactose follows a different pathway, the Leloir pathway (Figure 1.14 right) (White and Kennedy 1979).

How *L. lactis* controls its carbohydrate metabolism has been a major driver of investigation into the bacterium due to its industrial applications and all the answers are still not present.

## 1.12 Aims of the project

Current strategies for controlled stem cell differentiation are limited and provide a major challenge to stem cell based regenerative medicine. *In vivo*, stem cells reside in an area defined as a niche, which is a specialised milieu of cells, ECM and growth factors that maintains stem cells in a quiescent state and also plays a role in their activation.

One way of implementing existing technology to mimic this niche, is to use genetically modified, non-pathogenic bacteria to control cell behaviour. These bacteria can be tailored to synthesise proteins in a constitutive or inducible manner and thus, creating a living, dynamic interface for stem cell differentiation.

It had been shown by this laboratory that FN null fibroblasts (FN -/-) adhered to our modified *L. lactis* monolayer displaying the FN fragment FNIII<sub>7-10</sub> leads to the development of focal adhesions and promoted FAK based signaling (Rodrigo-Navarro, Rico et al. 2014). This FNIII<sub>7-10</sub> fragment comprises the RGD adhesion motif (FNIII<sub>10</sub>) and the PHSRN synergy site (FNIII<sub>9</sub>). The RGD and PHSRN sequence are both essential to promote  $\alpha_5\beta_1$  integrin mediated adhesion as well as promiscuous integrin adhesion (Aumailley, Gurrath et al. 1991). It has been shown that short RGD containing peptides can mimic a number of the properties of cell adhesive proteins and allow integrin attachment, therefore promoting adhesion of cells to the surface (Pierschbacher and Ruoslahti 1984, Dsouza, Ginsberg et al. 1991).

The goal of this thesis is to utilise this platform of bacteria harnessing the FNIII<sub>7-10</sub> fragment to sustain long-term MSC adhesion, whilst simultaneously, the induced production of BMP-2 can begin to initiate the differentiation of MSCs to osteoblasts. It has also been shown that  $\alpha_5\beta_1$  integrins and BMP-2 can act synergistically to create strong osteogenic differentiation (Salmeron-Sanchez and Dalby 2016).

The specific aims have been broken down and are thus:

1. Explore the effect of the FNIII<sub>7-10</sub> fragment coupled with the addition of exogenous BMP-2 on MSCs.
2. Engineer the secretion and cell wall bound expression of BMP-2 into *L. lactis* in a constitutive and inducible manner.
3. Deduce MSC behaviour in response to bacterially expressed BMP-2 *in vitro* and *in vivo*.

## 2. Materials and methods

This chapter details a general methods section with specific details highlighted in the individual results chapters.

### 2.1 Bacterial culture

*L. lactis* was cultured in M17 medium (Oxoid Microbiology Products) to allow growth in standing cultures. The composition of M17 is (Terzaghi and Sandine 1975):

- Tryptone (5 g/L)
- Soya-peptone (5 g/L)
- “Lab-lemco” (5 g/L)
- Yeast extract (2.5 g/L)
- Ascorbic acid (0.5 g/L)
- Magnesium sulphate (250 mg/L)
- Di-sodium glycerophosphate (19 g/L)

When dissolved, the media has a pH of  $6.9 \pm 0.2$  at 25 °C. The medium is bought as a powder that has to be reconstituted at 37.25 g/L in ultrapure water before sterilisation at 126 °C for 20 minutes. Upon cooling, 0.5 % v/v sterile glucose and any appropriate antibiotic was added. This prevents the caramelisation of the glucose and degradation of the antibiotic. *L. lactis* was then grown at 30 °C in anaerobic conditions (unless stated otherwise) in standing cultures. The stationary phase of growth is usually met within 8 hours and the bacteria slowly begin to form a pellet at the bottom of the culture.

To allow for unimpeded protein expression and characterisation, bacteria were grown in M9 minimal medium. This again allows growth but does not include as many ingredients as M17 and therefore allows much easier downstream experimentation. The composition of M9 is (Steidler, Wells et al. 1995):

- 25.6 g/L  $\text{Na}_2\text{H}_2\text{PO}_4$
- 6 g/L  $\text{KH}_2\text{PO}_4$
- 1 g/L NaCl
- 2 g/L  $\text{NH}_4\text{Cl}$

The following was added to complete the media for *L. lactis*:

- 20 mM MgSO<sub>4</sub>
- 2 mM CaCl<sub>2</sub>
- 50 nM NaHCO<sub>3</sub> / Na<sub>2</sub>CO<sub>3</sub>
- 0.5 % w/v glucose

## **2.2 *L. lactis* biofilm production**

The method to develop an *L. lactis* biofilm was adapted from other authors (Burmolle, Webb et al. 2006). A frozen stock of *L. lactis* was kept at -80 °C and used to streak a fresh M17 1 % agar plate supplemented with 0.5 % glucose and appropriate antibiotic. The plate was kept at 30 °C for 24 hours until 1-2 mm colonies had grown. A single colony was picked and inoculated in 10 mL fresh M17 with 0.5 % glucose v/v until an optical density of 0.3-0.5 at 600 nm was measured. The bacterial culture was then poured over an appropriate surface in a multiwell plate and sealed with parafilm and grown at 30 °C for 24 hours.

After 24 hours, the media was removed along with the planktonic phase, and the adhered portion of the bacteria were washed 3 times with sterile ultrapure water. These wash steps ensure that all planktonic phase bacteria are removed and the only bacteria that remain are those attached to the surface. This results in a bacterial monolayer adhered to the material surface and are ready for further experimentation.

## **2.3 Sample preparation**

Glass coverslips were spin coated with 4% w/v poly (ethyl acrylate) (PEA) in toluene prior to coating with fibronectin (FN) or *L. lactis*. PEA sheets were dissolved in toluene to a final 4 % w/v concentration. The solution was stirred for two days until all the polymer was properly dissolved, obtaining a viscous solution as a result. Spin-coating was performed over 12 or 25 mm glass coverslips at 2000 rpm for 30 seconds. Samples were dried in vacuum at 60 °C to remove solvent traces before biofilm preparation. For FN functionalisation, 200 µL of a solution of 20 µg/mL FN was used to coat the PEA surface for an hour at room temperature. The methods used to develop a biofilm on surfaces has been previously published (Burmolle, Webb et al. 2006, Zaidi, Bakkes et al. 2011). In these experiments *L. lactis* were grown as standing cultures in M17 broth with the appropriate antibiotic at 30 °C

for 24 hours. The cells were then harvested at 3000 g for 10 minutes and resuspended in 500  $\mu$ L of the same medium and streaked on M17 agar plates supplemented with 0.5 % w/v glucose and the appropriate antibiotic and left to grow at 30 °C overnight. Colonies were taken from the plates and transferred into sterile M17 broth until OD 660 was 0.3. 4.8 mL of suspension was used for the glass coverslips in the 6 well plates and 1 mL for 24 well plates. These were then sealed and left at 30 °C for 24 hours. After 24 hours the non-adherent planktonic phase bacteria were removed by shaking and washing. The wells were shaken by hand and the planktonic phase bacteria were removed via pipette followed by 3 washes with sterile water.

PEA coated coverslips were only used for long term cell culture (more than 4 days) as it was found that the bacteria were able to adhere to this surface for longer periods than on glass alone.

## **2.4 Mammalian cell culture**

Two cell types have been used in this work, human bone marrow-derived mesenchymal stem cells (MSCs) and murine C2C12 myoblasts. The first experiments were completed with the C2C12s as these are a well-documented model for osteogenic differentiation. These were used in preliminary studies to ensure both the interaction of the cells with the FNIII<sub>7-10</sub> subunit and the differentiation capabilities of BMP-2 in short term cultures. Finally, MSCs were used to assess the differentiation capabilities of BMP-2 in long term cultures.

### **2.4.1 C2C12 murine myoblasts**

This is a murine myoblastic cell line that can be used a model system for osteoblastic differentiation. The cells were purchased from ATCC (USA) and a stock was created. Cells were used before passage 10. This cell type can differentiate into myotubes and under the correct circumstances, be induced down the osteogenic pathway. It is not advised to allow this cell type to reach confluence as the myoblastic population rapidly depletes due to paracrine interactions (Katagiri, Yamaguchi et al. 1995, Watt, Judson et al. 2010, Velica and Bunce 2011). These cells were grown in DMEM (Dulbecco's modified eagle medium) with 4.5 g/L glucose, 20 % FBS (foetal bovine serum) and 1 % P/S (penicillin-streptomycin).

## 2.4.2 Human bone marrow derived mesenchymal stem cells (MSCs)

These cells were obtained from PromoCell and show great therapeutic potential due to their inherent differentiation capabilities. The PromoCells used in this thesis are harvested from normal human bone marrow and are vigorously tested for their ability to differentiate *in vitro* into adipocytes, chondrocytes, osteoblasts and neuronal cells (Pittenger, Mackay et al. 1999). These cells are verified through marker selection CD73<sup>+</sup>/CD90<sup>+</sup>/CD105<sup>+</sup> and CD14<sup>-</sup>/CD19<sup>-</sup>/CD34<sup>-</sup>/CD45<sup>-</sup>/HLA-DR<sup>-</sup> and adhere to the expression profile compiled by the International Society for Cellular Therapy (Dominici, Le Blanc et al. 2006). Under the right conditions, these cells can differentiate to osteoblasts, adipose cells, nerve cells and reticular sub types. These cells were grown in DMEM supplemented with 100  $\mu$ M pyruvate (Sigma), 1.1 mM L-glutamine (Sigma), 10 % FBS and 1 % P/S.

## 2.5 Immunofluorescence assays

### 2.5.1 Cell adhesion

Cell adhesion was either studied through vinculin or integrin immunostaining. After selected culture times (described in the results chapter), cells were washed with phosphate buffered saline (PBS, Invitrogen) and fixed in 4 % formaldehyde at 37 °C for 15 minutes. This fixative was washed 3 times with PBS before incubating the samples with permeabilisation buffer (10.3 g of sucrose, 0.292 g of NaCl, 0.06 g of MgCl<sub>2</sub>, 0.476 g of HEPES buffer in 100 ml of water, pH 7.2 followed by the addition of 0.5 ml Triton X) at 4 °C for 5 minutes. Then, the samples were incubated in 1 % bovine serum albumin (BSA) in PBS at room temperature for 30 minutes to block reactive sites and therefore decrease background fluorescence. For vinculin staining, samples were then treated with a mouse monoclonal anti-vinculin (Sigma, V9131, UK) diluted to 1:400 in 1 % BSA / PBS for 1 hour at room temperature. For integrin staining, samples were treated with monoclonal antibodies against  $\alpha$ 5 (Millipore, AB1928, USA, anti rabbit),  $\beta$ 1 (BD Pharmingen, (EG7, USA, anti rat) and  $\alpha$ V $\beta$ 3 (Millipore, LM609, USA, anti mouse). These were then washed 3 times for 5 minutes (last wash on a shaker) in 0.5 % Tween 20 / PBS. For vinculin detection, a Cy-3-conjugated polyclonal rabbit anti-mouse secondary antibody (Jackson Immunoresearch, UK), diluted 1:200 in 1 % BSA / PBS, with 1:200 BODIPY FL-conjugated phalloidin (Invitrogen, UK) was added and incubated

for 1 hour at room temperature in the absence of light. For the integrins, secondary antibodies against rabbit for  $\alpha 5$  (FITC 1:2000), rat for  $\beta 1$  (RFP 1:2000) and mouse for  $\alpha V\beta 3$  (Cy5 1:2000) (Jackson ImmunoResearch, UK) were used. Samples were again washed 3 times for 5 minutes in 0.5 % Tween 20 / PBS and mounted using Vectashield containing DAPI (Vector Laboratories, UK). Samples were then viewed under a fluorescence microscope (Zeiss AxioObserver- Z1).

### **2.5.2 Osteogenic differentiation**

After 3 weeks, cells were fixed using 4 % formaldehyde in PBS at 37 °C for 15 minutes. Fixative was removed and washed with PBS before the addition of permeabilising buffer (10.3 g of sucrose, 0.292 g of NaCl, 0.06 g of MgCl<sub>2</sub>, 0.476 g of HEPES buffer in 100 ml of water, pH 7.2 followed by the addition of 0.5ml Triton X) for 5 minutes at 4 °C. Permeabilising buffer was removed and PBS/BSA 1 % was added for 5 minutes at 37 °C to block reactive sites. This was followed by the addition of the primary antibody (1:50 in PBS/BSA 1 %) osteocalcin (OCN, mouse monoclonal, sc-365797, UK) and osteopontin (OPN, mouse monoclonal, sc-21742, UK) (Santa Cruz Biotechnology, UK) for 1 and a half hours at 37 °C. 100  $\mu$ L was added to ensure the coverslips were submerged. The samples were next washed with 0.5 % Tween 20 in 100 mL PBS 3 times for 5 minutes. A secondary, biotin-conjugated antibody (1:50 in PBS/BSA, monoclonal horse antimouse (IgG), (Vector Laboratories) was added for 1 hour at 37 °C followed by washing with 0.5 % Tween 20 in 100 mL PBS 3 times for 5 minutes. Simultaneously, rhodamine-conjugated phalloidin was added for the duration of this incubation (1:50 in PBS/BSA 1 %, Life Technologies). A FITC-conjugated streptavidin third layer was added (1:50 in PBS/BSA 1 %, Vector Laboratories) at 4 °C for 30 minutes, and given a final wash with 0.5 % Tween 20 in 100 mL PBS 3 times for 5 minutes. The coverslips were then inverted onto glass slides with DAPI stain (Vector Laboratories, UK). Samples were then viewed under a fluorescence microscope (Zeiss AxioObserver- Z1).

**Table 2.1. Antibodies and suppliers used in this thesis.**

<b>Antibodies</b>	<b>Supplier</b>
<b>Primaries</b>	
Vinculin	Sigma (V9131)
$\alpha_5$	Millipore (AB1928)
$\beta_1$	BD Pharmingen (EG7)
$\alpha_v\beta_3$	Millipore (LM609)
Osteocalcin	Santa Cruz (SC-365797)
Osteopontin	Santa Cruz (SC-21724)
<b>Secondaries</b>	
Cy3	Jackson ImmunoResearch
FITC	Jackson ImmunoResearch
RPF	Jackson ImmunoResearch
Cy5	Jackson ImmunoResearch
Biotin	Vector Laboratories
FITC-conjugated-Steptavidin	Vector Laboratories

## 2.6 von Kossa staining

MSCs were seeded at 5,000 cells/cm<sup>2</sup> and cultured on freshly prepared FN coated glass and *L. lactis*-FN biofilms for 28 days. Cells were fixed with 4 % formaldehyde in ultrapure water for 5 minutes and then a 5 % silver nitrate solution in H<sub>2</sub>O was added to ensure the coverslips were fully submerged and exposed to UV light for 30 minutes. After washing in deionised water, 5 % sodium thiosulphate was added to the samples for 10 minutes and then samples were washed with warm tap water for 10 minutes. After another wash with deionised water, the samples were counterstained with nuclear fast red for 10 minutes and washed again with deionised water. Finally the samples were rinsed with 70 % ethanol and observed in a phase-contrast optical microscope (Zeiss Axio Observer-Z1).

## 2.7 Bacterial viability

To study viability of the bacteria, the BacLight LIVE/DEAD kit (Life Technologies, UK) was used. Biofilms were grown as mentioned previously and transferred to DMEM, DMEM was supplemented with either 1 % penicillin-streptomycin (P/S), DMEM with 10  $\mu$ g/mL tetracycline (TC) or DMEM with 5 and 10  $\mu$ g/mL sulfamethoxazole and viability was tested at 1, 2, 3 and 4 weeks. The biofilm was washed once with sterile NaCl 0.85 % w/v solution

and incubated for 30 minutes using SYTO9 (5  $\mu\text{M}$ ) and propidium iodide (30  $\mu\text{M}$ ) in NaCl 0.85 % w/v. After this, the samples were washed with PBS and mounted using Vectashield without DAPI (Vector Laboratories, UK) and imaged immediately on a Zeiss AxioObserver-Z1. The viability was determined as the ratio between the viable and total number of bacteria. ImageJ was used to analyse the pictures taken.

## **2.8 Image analysis**

Image analysis was completed using the Fiji-ImageJ software (Schindelin, Arganda-Carreras et al. 2012). Images were acquired using a Zeiss AxioObserver Z1 (unless stated otherwise) fitted with an Andor camera. 10, 20, 40 and 63 x objectives were used and images were saved in 8-bit per channel RGB BMP format.

## **2.9 Statistical analysis**

All statistical analysis was performed with GraphPad Prism 6. One way or two way ANOVAs (analysis of variance) were completed depending on the data present (two way ANOVAs were completed when grouped data was tested against two independent variables). A one way ANOVA was used when there were more than two independent groups (not grouped data). A two way ANOVA was used for group data as its purpose is to test if there is an interaction between the two independent variables on the dependent variable. Firstly, data was checked for normality to determine the type of post-hoc test used. If data were normally distributed, a Tukey post-hoc test was used. Conversely, for data that were not normally distributed, a Bonferroni post-hoc test was used. Statistical significance levels are indicated by a number of one to four asterisks that indicate the following levels of significance: \* $p < 0.05$ , \*\* $p < 0.01$ , \*\*\* $P < 0.001$  and \*\*\*\* $p < 0.0001$ .

# 3. Cell-bacteria co-cultures and initial differentiation studies

## Summary

This chapter focusses on the effect of the fibronectin (FN) fragment (FNIII<sub>7-10</sub>) on cell adhesion and the ability of the interface to sustain mesenchymal stem cell (MSC) differentiation in response to externally added bone morphogenetic protein-2 (BMP-2). C2C12 murine myoblasts and MSCs were cultured on FNIII<sub>7-10</sub> and non-FN expressing bacteria (from here on denoted *L. lactis*-FN and *L. lactis*-empty respectively) and their behaviour was assessed. BMP-2 was added to the medium to induce osteogenic differentiation and compared to a control surface of FN coated glass. The results demonstrate that differentiation on the biofilm is approximately equal to that of a FN coated surface.

\*Results in this chapter are partially published in: Hay, J. J., Rodrigo-Navarro, A., Hassi, K., Moulisova, V., Dalby, M. J., & Salmeron-Sanchez, M. (2016). Living biointerfaces based on non-pathogenic bacteria support stem cell differentiation. *Scientific reports*, 6. 10.1038/srep21809

### 3.1 Introduction

The requirement for synthetic materials that mimic the characteristics of the extracellular matrix (ECM) is essential in biomedical engineering to comprehend the complex and dynamic behaviour of cells. Cells interact with different structures of the ECM, namely via physical interactions such as cell geometry and topography at the micro and nanoscale, these micro or nanoenvironments can be used to ultimately control cell behaviour or direct cell fate (Pittenger 2008, Guilak, Cohen et al. 2009). Previously, samples have been coated with a layer of adhesive proteins such as fibronectin (FN), peptides or growth factors as cells are incapable of direct interaction with biomaterials (Grinnell 1986, Dsouza, Ginsberg et al. 1991, Aumailley and Gayraud 1998, Hench and Polak 2002, Shin, Jo et al. 2003). These surfaces are static and provide cells with only one behavioural cue, therefore engineering dynamic surfaces that allow controlled regulation is now at the forefront of biomedical engineering. These surfaces have the potential to provide spatiotemporal triggers that can recapitulate critical characteristics of the ECM and can therefore be used in myriad biomedical fields, ranging from tissue engineering to molecular biology. There have been many recent attempts at synthetic replication of the ECM, a large percentage of which use an extracellular trigger to alter the surrounding environment which can direct cellular behaviour, these include light (Wirkner, Weis et al. 2011, Lee, Garcia et al. 2015), temperature (Ebara, Yamato et al. 2004) and enzymes (Todd, Scurr et al. 2009, Zelzer, Scurr et al. 2012). Significant efforts have been directed toward utilising the adhesive peptide arginine-glycine-aspartic acid (RGD), found in many extracellular matrix proteins such as FN, vitronectin and laminin allowing the user to control cell adhesion (Pierschbacher et al, 1983). We hypothesise that biofilms formed by non-pathogenic bacteria can be utilised to accomplish a successful dynamic surface. They can be genetically modified to express or secrete different proteins which can be used to direct cell behaviour and ultimately control stem cell fate. In that case, bacterial cell to mammalian cell communication can be facilitated on the level of the bacterial biofilm interface due to bacterial capability to colonise many different biomaterials to form a monolayer.

This chapter focuses on highlighting the dynamic interaction between bacterial and mammalian cells by using different microscopic techniques, such as scanning electron microscopy and immunofluorescence, compounded with molecular techniques. This chapter

also shows the ability of the interface to sustain mesenchymal stem cell (MSC) differentiation.

We use the previously characterised *L. lactis* strain that constitutively expresses, via the P1 lactococcal promoter, a fusion protein made of the FNIII<sub>7-10</sub> fragment of the human fibronectin with GFP fused upstream, as a reporter protein (Saadeddin, Rodrigo-Navarro et al. 2013, Rodrigo-Navarro, Rico et al. 2014, Hay, Rodrigo-Navarro et al. 2016). This protein is efficiently located in the bacterial cell wall by using a secretion peptide and an anchoring signal. The expressed FNIII<sub>7-10</sub> fragment contains the RGD adhesion motif on the III<sub>9</sub> repeat and the PHSRN synergy motif on the III<sub>10</sub> repeat. These two motifs interact with the  $\alpha 5\beta 1$  integrin, amongst others (Giancotti and Ruoslahti 1999).

In this chapter, we show C2C12 murine myoblast and MSC behaviour in response to the FNIII<sub>7-10</sub> exposed on the bacterial cell wall shown in Figure 3.1A. In addition to the adhesive cue from the FNIII<sub>7-10</sub> fragment, the osteogenic growth factor, bone morphogenetic protein 2 (BMP-2) (mechanism shown in Figure 3.1B) can induce the differentiation of MSCs towards osteoblasts.

BMP-2 binds to cells via BMPRs (bone morphogenetic protein receptors), of which there are many. BMP-2 signalling is initiated upon BMP-2 binding to BMPRI and the subsequent recruitment of other BMPRs is essential for proper signal propagation. Normally, two of each type of BMPRI and BMPRII are needed to form a ternary homocomplex which leads to the activation of SMADs. SMADs are a group of intracellular proteins that transduce extracellular signals into downstream gene activation. In terms of BMP-2, BMPR activation leads to the recruitment of the pathway restricted SMADs 1, 5 and 8 which recruit the common mediator SMAD 4 (Itoh, Itoh et al. 2000, Moustakas, Souchelnytskyi et al. 2001, Derynck and Zhang 2003). This complex migrates to the nucleus and induces expression of osteogenic genes in the nucleus, represented in Figure 3.1 B (Hay, Rodrigo-Navarro et al. 2016).

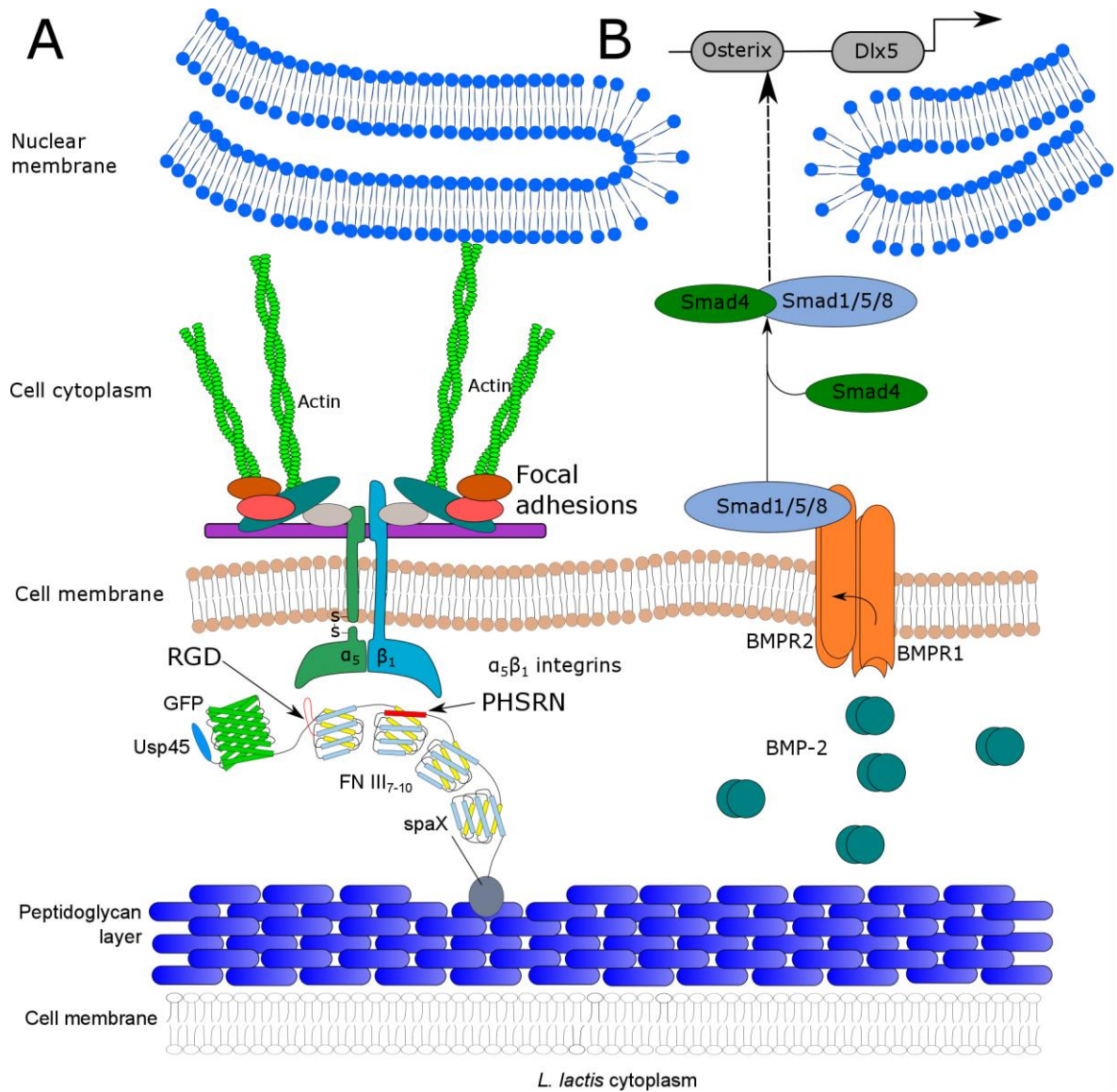


**Figure 3.1. Conceptual overview of the system.** (A) *L. lactis* biofilm expressing the III7–10 fragment of the human fibronectin on its cell wall, fused to green fluorescent protein (GFP) as a reporter, acting as a biointerface for bone marrow-derived human mesenchymal stem cells. (B) Recombinant human BMP-2 (rhBMP-2) was added in the cell culture medium at 100 ng/mL to induce osteogenic differentiation. BMPR1/2 signalling through the Smad pathway leads to activation of the transcription factors Osterix, RunX2 and Dlx5 which induces expression of proteins involved in osteogenic differentiation (Hay, Rodrigo-Navarro et al. 2016).

## 3.2 Materials and methods

### 3.2.1 Scanning electron microscopy (SEM)

MSCs and C2C12s were seeded at 5,000 cells/cm<sup>2</sup> and were fixed in either 2 % glutaraldehyde / 2 % paraformaldehyde / 0.15 M sodium cacodylate buffer / 0.15 % alcian blue for 2 hours at 4 °C or in 1.5% glutaraldehyde/0.1 M sodium cacodylate buffer fix for 1 hour at 4 °C. After fixation, these were then washed with 0.15 M sodium cacodylate buffer 5 times before 1 hour incubation in 1 % osmium tetroxide/0.1 M sodium cacodylate buffer. Samples were then washed 3 times in distilled water and stained with 0.5 % uranyl acetate/distilled water for 1 hour in the dark. Samples were washed again with distilled water before dehydration through an ethanol gradient (30 %, 50 %, 70 % and 90 % for 10 minutes each) with 100 % ethanol used 4 times 5 minutes to fully dry the sample. Samples were then loaded onto a POLARON E3000 Critical Point Dryer (Liquid CO<sub>2</sub>) for 1 hour 20 minutes and then given a gold/palladium coat using a POLARON SC515 SEM COATER and viewed on a JEOL6400 SEM running at 10 kilovolts.

### 3.2.2 Quantitative real-time PCR (qPCR)

qPCR protocol is split into 3 sections:

#### 1. RNA extraction

A cell density of 20,000 cells/cm<sup>2</sup> were used for qPCR experiments. Cells were grown for 14 days in the same conditions as stated previously on fibronectin coated and *L. lactis*-FN coated PEA coverslips. RNA extraction was performed using the Qiagen RNA extraction kit, briefly: cells were lysed with RLT buffer and homogenised prior to the addition of 70 % ethanol. Samples were then transferred to an RNeasy MinElute spin column and centrifuged for 30 seconds at 8000 g and the flow through was discarded. Buffer RW1 was added to the column and centrifuged for 30 seconds at 8000 g and the flow through was discarded. DNase stock solution was added to buffer RDD and mixed. This was then added to the columns and left for 15 minutes at room temperature. Buffer RW1 was added to the columns and centrifuged for 30 seconds at 8000 g and the collection tube was discarded. A new collection tube was added and buffer RPE was added to the column and spun for 30 seconds at 8000 g and flow through was discarded. Next, 80 % ethanol was added and centrifuged for 2 minutes at 8000 g and collection tube discarded. A new collection tube was added and the column was spun at full speed for 5 minutes to dry the membrane and the collection tube was

discarded. A new collection tube was added and RNase free water was added to the column and centrifuged for 1 minute at 16,000 g and the collection tube was kept.

## **2. Reverse transcription**

200 ng of template RNA (when possible) was added to a tube containing reverse transcriptase master mix (Qiagen) and incubated for 15 mins at 42 °C before raising the temperature to 92 °C for 3 minutes.

## **3. Quantification**

qPCR was performed on an ABI7500 thermal cycler using the SYBR Green relative standard method. The SYBR Green master mix was bought from Applied Biosystems, which comprises SYBR Green I dye, AmpliTaq DNA polymerase, dNTPs with dUTP, and a PCR reaction buffer. SYBR Green I dye detects double-stranded DNA, AmpliTaq DNA polymerase synthesises new DNA, and the dUTP reduces carryover contamination. qPCR was started with the cDNAs for each sample and each sample was scaled down to its corresponding RNA concentration of 5 ng/μL. SYBR Green master mix, 2 μL of primer pair (forward and reverse primer) and 1 μL of cDNA sample were mixed up to a final volume of 20 μL for each well (cells isolated from six well plate). Negative controls (samples without reverse transcriptase) and blanks (reactions without cDNA samples) were made to ensure the correct functionality through the monitoring of genomic DNA contamination and substrate fluorescence background respectively. Three technical replicates were run for each experiment. The samples were initially treated with heat activation for 5 minutes at 95 °C, that was followed by a 2 step cycle of 10 seconds at 95 °C and 30 seconds at 60 °C for 40 cycles to allow for elongation. Gene expression was normalised against the house keeping gene, GAPDH (primers shown in Table 3.1).

Primers were synthesised using the Roche universal probe library assay design centre.

**Table 3.2. Primers used in the qPCR gene expression analysis.**

<b>Gene</b>	<b>Pair</b>	<b>Sequence (5' - 3')</b>
Alcam <i>Self Renewal</i>	Forward	ACG ATG AGG CAG AGA TAA CT
	Reverse	CAG CAA GGA GAC CAA C
CD63 <i>Self Renewal</i>	Forward	GCT GTG GGG CTG CTA ACT AC
	Reverse	ATC CCA CAG CCC ACA GTA AC
Osteocalcin <i>Osteogenic</i>	Forward	CAG CGA GGT AGT GAA GAG ACC
	Reverse	TCT GGA GTT TAT TTG GGA GCA G
Osteopontin <i>Osteogenic</i>	Forward	AGC TGG ATG ACC AGA GTG CT
	Reverse	TGA AAT TCA TGG CTG TGG AA
GAPDH <i>Housekeeping</i>	Forward	TCA AGG CTG AGA ACG GGA A
	Reverse	TGG GTG GCA GTG ATG GCA

### 3.3 Results

It is important to note that the strain of bacteria used in this chapter is the previously characterised MG1363. This strain and the FNIII<sub>7-10</sub> have been characterised in previous publications (Saadeddin, Rodrigo-Navarro et al. 2013, Rodrigo-Navarro, Rico et al. 2014, Hay, Rodrigo-Navarro et al. 2016) and a thesis and have been used in this chapter to highlight MSC behavior at longer time points. The future chapters highlight the use of different strains, namely NZ9000 and NZ9020.

#### 3.3.1 Bacterial viability and metabolism

MSCs require four weeks for terminal differentiation to osteoblasts (Stein, Lian et al. 1990, Pittenger, Mackay et al. 1999, Agarwal, Gonzalez-Garcia et al. 2015) and thus it was imperative to deduce bacterial viability up to this time point as the stability of the biofilm modulates cell adhesion. Previous to this work, the biofilms were seeded over glass coverslips as the maximum culture time used was four days (Rodrigo-Navarro, Rico et al. 2014). However, upon culturing the biofilm for longer time points, it became apparent that a new surface was needed as large areas of the biofilm began to detach from the surface after seven days. Glass is a hydrophilic surface, and whilst keeping viability values high (~60 %), the relatively weak adhesion was insufficient to allow long term biofilm formation.

To overcome this obstacle, we used the synthetic polymer poly (ethyl acrylate) (PEA). This has previously been used in mammalian cell culture (Salmeron-Sanchez, Rico et al. 2011) and was found to be particularly well suited for bacterial adhesion (An and Friedman 1998, van Oss, Wu et al. 1998, Van Oss 2002). PEA is a hydrophobic, non-biodegradable polymer and thus, is a good choice for bacterial adhesion. The strain of *L. lactis* used in these experiments was MG1363, a derivative of *L. lactis* subsp. *cremoris* TIL672, which features a hydrophobic surface. The extended Derjaguin-Landau-Verwey-Overbeek model (XDLVO) (Bayouhdh, Othmane et al. 2009) states that hydrophobicity plays an important role in surface interaction. This model explains the interaction in terms of surface free energy of the interacting surfaces, and considers the solid-bacteria, solid-liquid and bacteria-liquid interfaces when calculating the free energy. A practical explanation at the molecular level is that the interaction between two apolar moieties immersed in water is the consequence of hydrogen-bonding energy of cohesion of the water molecules surrounding them, and therefore, a hydrophobic surface is a stronger candidate for bacterial adhesion and biofilm creation, at least with this strain. Nevertheless, *L. lactis* proliferate continuously if nutrients are available and convert any suitable carbon source into lactic acid (De Vuyst and

Vandamme 1992). The build-up of this organic acid unavoidably leads to a decrease in pH of the medium, which is detrimental to mammalian cell viability. It has been previously outlined that tetracycline (TC) used at 10  $\mu\text{g}/\text{mL}$  is sufficient to impede bacterial metabolism without affecting mammalian cells for up to four days (Rodrigo-Navarro, Rico et al. 2014). TC is a bacteriostatic antibiotic that inhibits bacterial protein synthesis by binding to the 30S subunit of bacterial ribosomes, which hinders the attachment of charged aminoacyl tRNA (transfer Ribonucleic acid) to the A site (Geigenmuller and Nierhaus 1986). Due to the differentiation characteristics of MSCs, it was essential to increase this time course up to four weeks. To increase the efficiency of lactic acid retardation, a mixture of penicillin/streptomycin (P/S) at 100 U/mL was also tested. P/S is a bactericidal antibiotic and interferes with the synthesis of the peptidoglycan cell wall, leading to cell lysis (Park and Strominger 1957). These approaches were chosen in an attempt to control the biofilm in a bacteriostatic manner by preventing initial cell death and avoiding acidification of the medium. Figure 3.2 shows *L. lactis*-FN viability at 1, 2, 3 and 4 weeks.

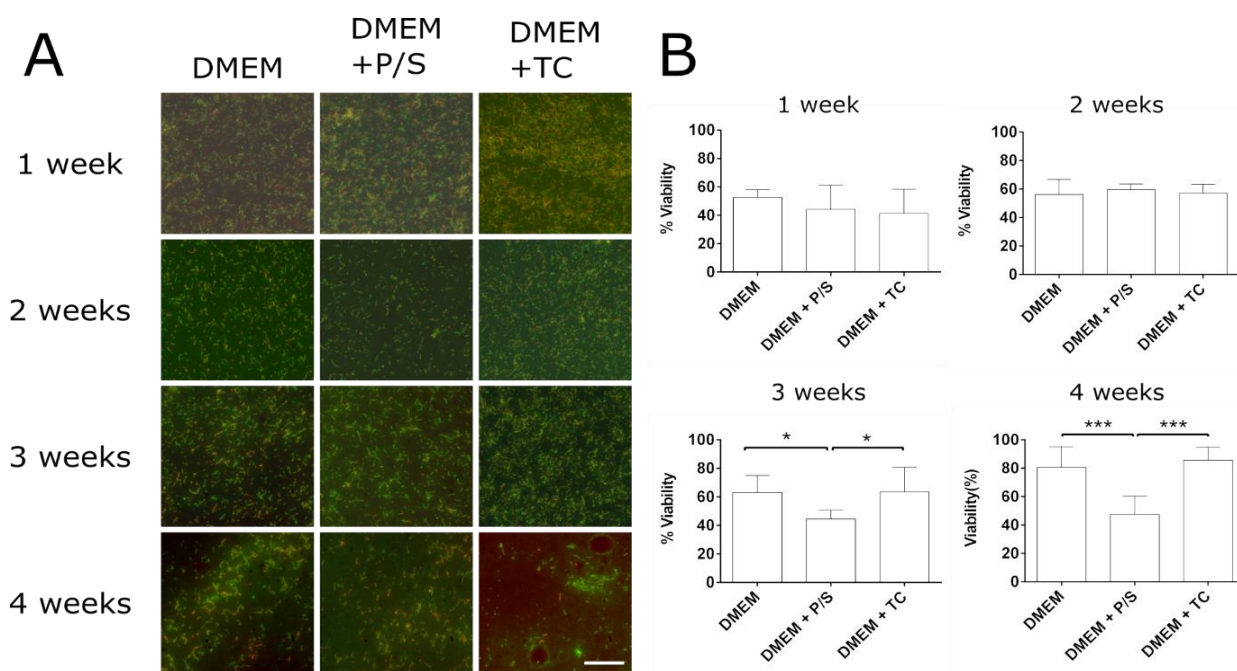


**Figure 3.2. *L. lactis* biofilm viability.** Biofilms of *L. lactis*-FN were produced on a poly (ethyl acrylate) (PEA) surface and cultured for one to four weeks with DMEM, DMEM supplemented with 100 U/mL of penicillin/streptomycin (DMEM+ P/S) and DMEM supplemented with 10  $\mu\text{g}/\text{mL}$  tetracycline (DMEM+ TC). (A) After the selected time points, biofilms were washed and their viability assessed using the commercial BacLight viability kit (Life Technologies). This kit stains viable cells in green and non-viable cells in red. Viability was calculated by analysing the total amount of cells stained in green versus the amount of cells stained in red and green. (B) After three weeks, viability values were found to be higher in biofilms cultured with DMEM or DMEM+ TC than in biofilms cultured with DMEM+ P/S. This result might be attributed to the fact that P/S is bacteriolytic in comparison to TC, which is bacteriostatic. There is an increase in viability values of the four week biofilms that can be attributed to the detachment of non-viable cells. Scale bar size is 50  $\mu\text{m}$ . 10 images were taken per condition from three technical replicates. Data is presented as mean  $\pm$  SD, and was analysed with a one way ANOVA test with a Tukey post-hoc test. Statistical significance levels are \* $p < 0.05$  and \*\*\* $p < 0.001$ .

*L. lactis*-empty was not investigated as this strain has been proven to be unable to bind integrins and thus mammalian cells cannot attach due to the lack of adhesive cues from the FNIII<sub>7-10</sub> fragment (Saadeddin, Rodrigo-Navarro et al. 2013, Rodrigo-Navarro, Rico et al. 2014, Hay, Rodrigo-Navarro et al. 2016). *L. lactis* could be seen to have formed stable biofilms at all-time points on the material surface (Figure 3.2A). Figure 3.2B shows the percentage of living bacteria calculated by analysing the total number of living cells (green) versus the total cell number, stated as living cells (green) plus dead cells (red) from Figure 3.2A. Bacterial viability was constant at approximately 50 % after one week with the highest viability value found in the antibiotic free samples. After two weeks, viability was again seen to be similar between the sample sets, and had increased to approximately 55 %. After three weeks the viability for DMEM + P/S (44 %) was found to be significantly lower than in DMEM (63 %) and DMEM + TC (63 %). This difference was further confirmed by the four week result, again, the viability for bacteria grown in DMEM + P/S (47 %) was significantly lower than both the DMEM (81 %) and DMEM + TC (85 %) conditions. The data shown in Figure 3.2 initially suggests that viability increases as a function of time. It is apparent from Figure 3.3 that as time increases, the surface density of the biofilm decreases. Figure 3.3 shows the surface coverage of the biofilm in colony forming units. These graphs confirm what can be inferred from Figure 3.2A. After two weeks of culture, large portions of the biofilm begin to detach from the surface. Non-viable cells would detach from the surface, and the presence of antibiotic prevents further proliferation of the populations, thus increasing the ratio of viable to non-viable bacteria. However, it can be seen that after four weeks, bacteria are still present on the substrate surface with a similar morphology to those observed at shorter time points.

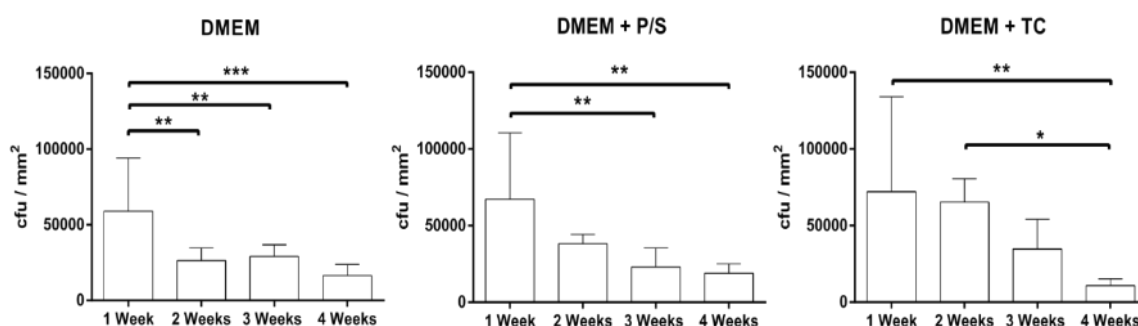


**Figure 3.3. Biofilm coverage after one, two, three and four weeks.** Biofilm coverage was calculated as the percentage of the surface covered by bacteria, expressed as cfu (colony forming units) per square millimeter. We found that a large proportion of the biofilm had detached as the culture time increased, explaining the rise in viability found in Figure 3.2. This results suggests that biofilms produced on PEA, a hydrophobic polymer, can serve as a substrate for long-term stem cell culture. 10 images were quantified per condition from three technical replicates. Data is presented as mean  $\pm$  SD, and was analysed with a one way ANOVA test with a Tukey post-hoc test. Statistical significance levels are \* $p < 0.05$ , \*\* $p < 0.01$  and \*\*\* $p < 0.001$ .

### 3.3.2 Cell adhesion and morphology

Cell adhesion was assessed through scanning electron microscopy (SEM) and vinculin immunostaining. Firstly, C2C12 murine myoblast cells were seeded over *L. lactis*-empty, *L. lactis*-FN and FN coated glass for three hours. These experiments were completed in the absence of FBS (unless stated otherwise), to rule out the presence of any FN deposition from serum influencing the material surface, except for that displayed by *L. lactis*-FN or the FN coat. Figure 3.4 shows SEM images of C2C12s seeded over *L. lactis*-empty biofilms after three hours. It can be seen from this that cells remain in a rounded morphology, and show no protrusions or lamellipodia to attach to the surface.

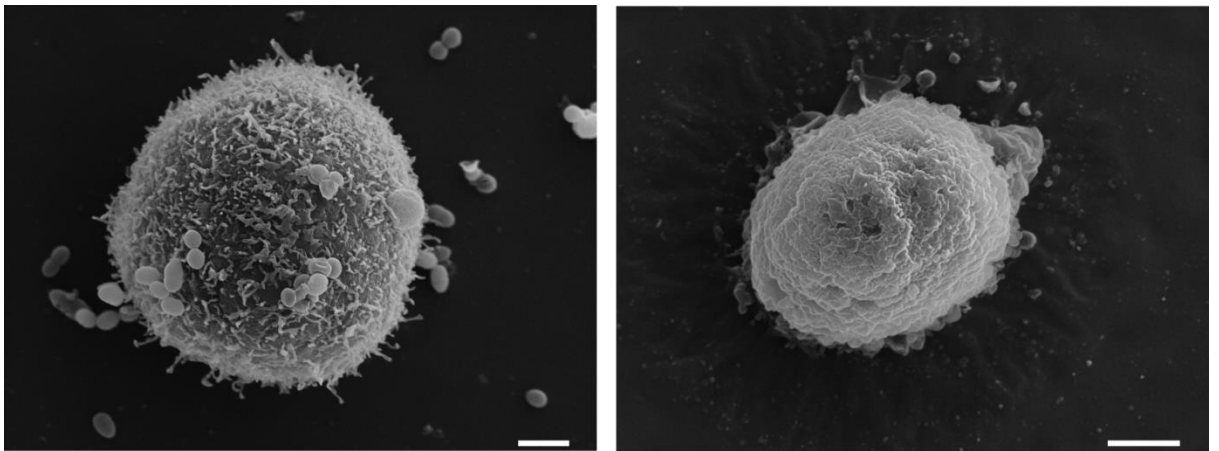


**Figure 3.4. High magnification SEM images of C2C12 murine myoblasts seeded over *L. lactis*-empty after three hours.** The mammalian cells can be seen as the larger spherical shapes, whereas the bacteria can be seen as clusters of smaller spheres. The mammalian cells can be seen as rounded forming no protrusions to the bacteria. Scale bar = 2  $\mu\text{m}$ .

Figure 3.5 shows SEM images of C2C12 cells seeded over *L. lactis*-FN biofilms. It is instantly apparent from Figure 3.5A that cell morphology is drastically affected by the presence of the FNIII<sub>7-10</sub> fragment in the bacterial cell wall. Cells can be seen to spread and form filopodia. Figure 3.5B is a magnified portion of 3.5A shown by the red square and shows a cellular protrusion over four bacteria. Figure 3.5C and 3.5D clearly show a filopodia like projection from the cell straight to the cell wall of a bacteria. This evidence suggests that the FNIII<sub>7-10</sub> fragment available in the bacterial cell wall is able to induce cell adhesion.

Figure 3.6 shows SEM images of C2C12 cells seeded over a FN coated glass coverslip after three hours. Again, the difference in morphology between these cells and the cells on the *L. lactis*-empty is clear (Figure 3.4). Cell morphology is similar between the FN coat and *L. lactis*-FN. These results support the work completed previously (Saadeddin, Rodrigo-Navarro et al. 2013, Rodrigo-Navarro, Rico et al. 2014). On the *L. lactis*-empty, no adhesion

can occur as there are no proteins present that allow integrin interaction and thus the cells remain in a rounded morphology. On both the *L. lactis*-FN and FN coated surface, mammalian cell integrins can associate with the RGD domains of FN and spread.

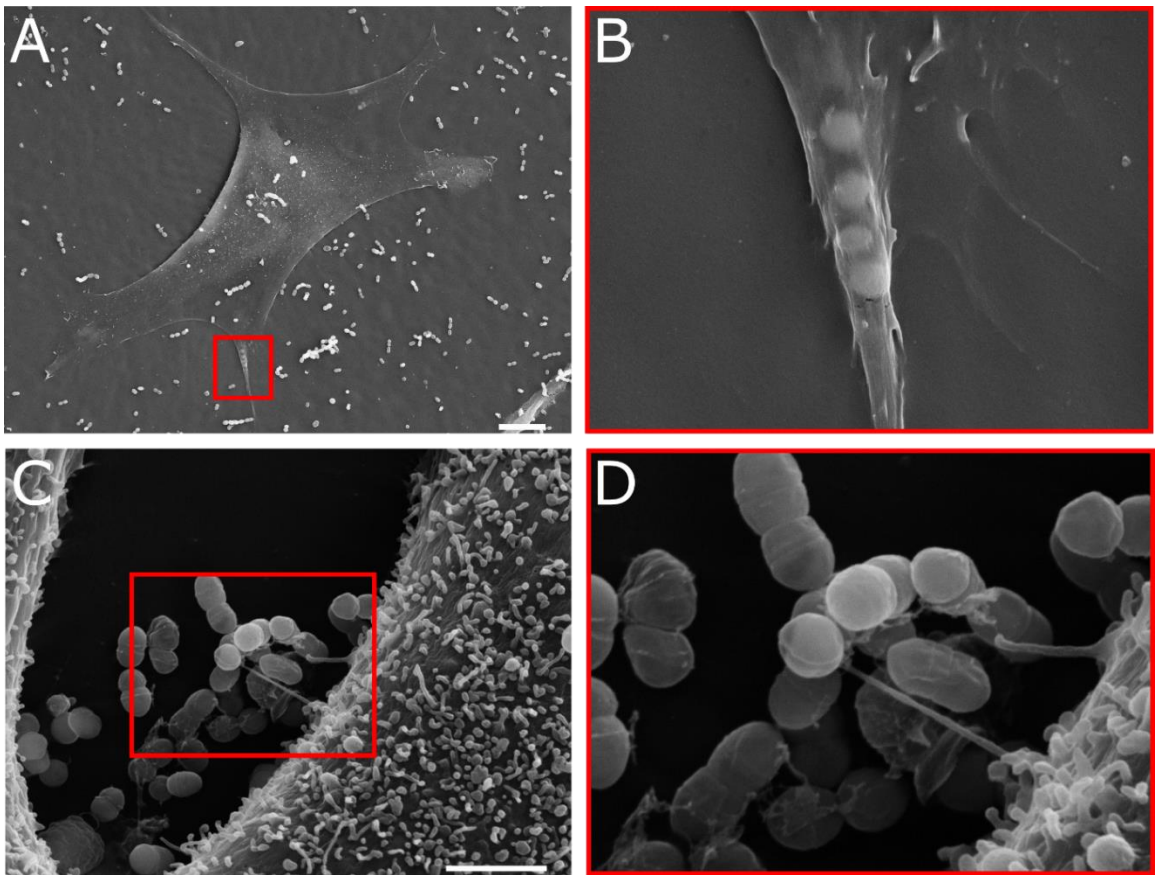


**Figure 3.5. Low (A and C) and high magnification (B and D) SEM images of C2C12 murine myoblasts interacting with *L. lactis*-FN after three hours. (A).** C2C12 cells are spread with a magnified region (red square) shown in **B**. This magnified image shows an extension of the cell on top of four bacteria. **(C).** A region of a C2C12 cell with a filopodia like projection contacting the cell wall of a bacterial cell with a magnified region shown in **D** (red square). These images confirm the presence of FNIII<sub>7-10</sub> in the cell wall of the bacteria induce mammalian cell spreading and adhesion. Scale bar = 10 and 2  $\mu$ m for A and C respectively.

These images shown (Figures 3.4, 3.5 and 3.6) were taken after fixing the cells with 1.5 % glutaraldehyde/0.1 M sodium cacodylate buffer mix. It was noted that there was a major difference between these images and when the sample was viewed under the microscope before the fixation process, an extremely large proportion of bacteria had dissociated from the sample. The experiment was repeated and the fixation process was altered with the addition of 0.15 % alcian blue, a cationic fixative that allows for a higher degree of bacterial fixation (Erlandsen, Kristich et al. 2004). This allows us to have a more accurate representation of what was occurring on the coverslip. Figure 3.7 shows SEM images of C2C12 cells seeded over *L. lactis*-empty (A and B) and *L. lactis*-FN (C and D) after three hours. Figure 3.7A and 3.7C show low magnification images of the cellular interaction with

*L. lactis*-empty and *L. lactis*-FN respectively. Many more bacteria can be seen utilising this fixation method when compared with the previous method, even with the same seeding density. Figure 3.7B and 3.7D (larger image seen in Annex Figure 8.1) show high resolution images of the cellular interaction with *L. lactis*-empty and *L. lactis*-FN respectively. Figure 3.7B shows four rounded C2C12 cells surrounded by bacteria, which is in stark contrast to the images shown in Figure 3.4. Figure 3.7D shows two spread C2C12 cells, again, surrounded by bacteria. The C2C12s fixed with this method can be seen to interact (highlighted with the red arrows, larger image found in Annex Fig 8.1) with many more bacteria than seen in Figure 3.5. Fixation with this method allows for a more representative image of what is occurring on the coverslip.

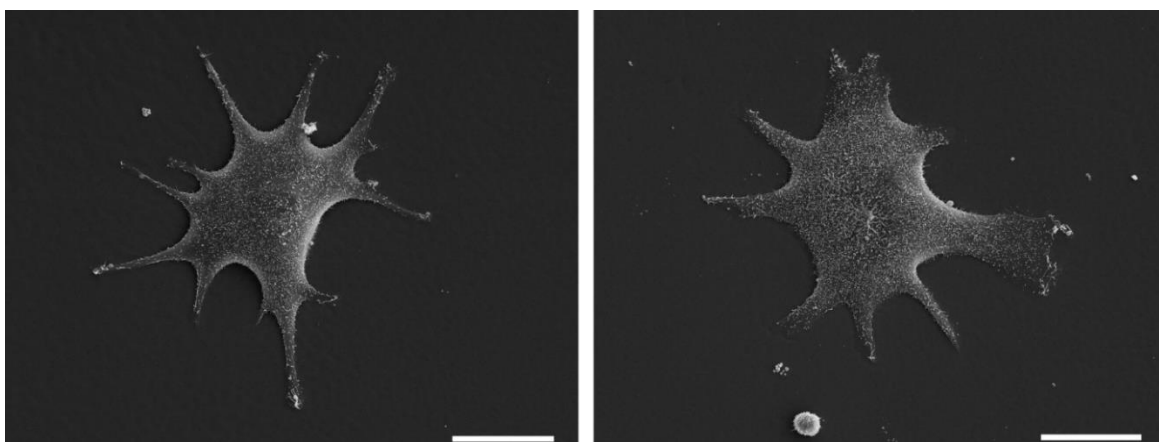


**Figure 3.6. Low magnification SEM images of C2C12 murine myoblasts seeded over FN coated glass after 3 hours.** The cells can be seen to form a spread morphology, adhered to the surface. These cells strongly resemble the shape of the mammalian cells on the *L. lactis*-FN sample. Scale bar = 20  $\mu$ m.

MSCs ability to interact with *L. lactis*-FN compared to FN coated surface and *L. lactis*-empty were next assessed. MSC spreading after three hours was found to be directly related to the availability of FN to the MSCs. Figure 3.8 shows SEM images after three hours (without FBS) and 1 week (with FBS) of MSC culture. From these images, it became apparent that the FNIII<sub>7-10</sub> fragment in the bacterial cell wall is essential to develop adhesion structures after three hours, since MSCs cultured on top of *L. lactis*-empty biofilms kept a rounded shape, with no sign of adhesion. The morphology of the MSCs on the FN coated surface and *L. lactis*-FN appear similar. It is clear that the initial cell interaction determines cell morphology and it is distinctly affected by the availability of the FNIII<sub>7-10</sub> fragment on the bacterial cell wall. After one week, cell morphology on all surfaces becomes more similar. This is likely due to the addition of 1 % foetal bovine serum (FBS) to the culture media, which is necessary to ensure the viability of the MSCs in the long-term.

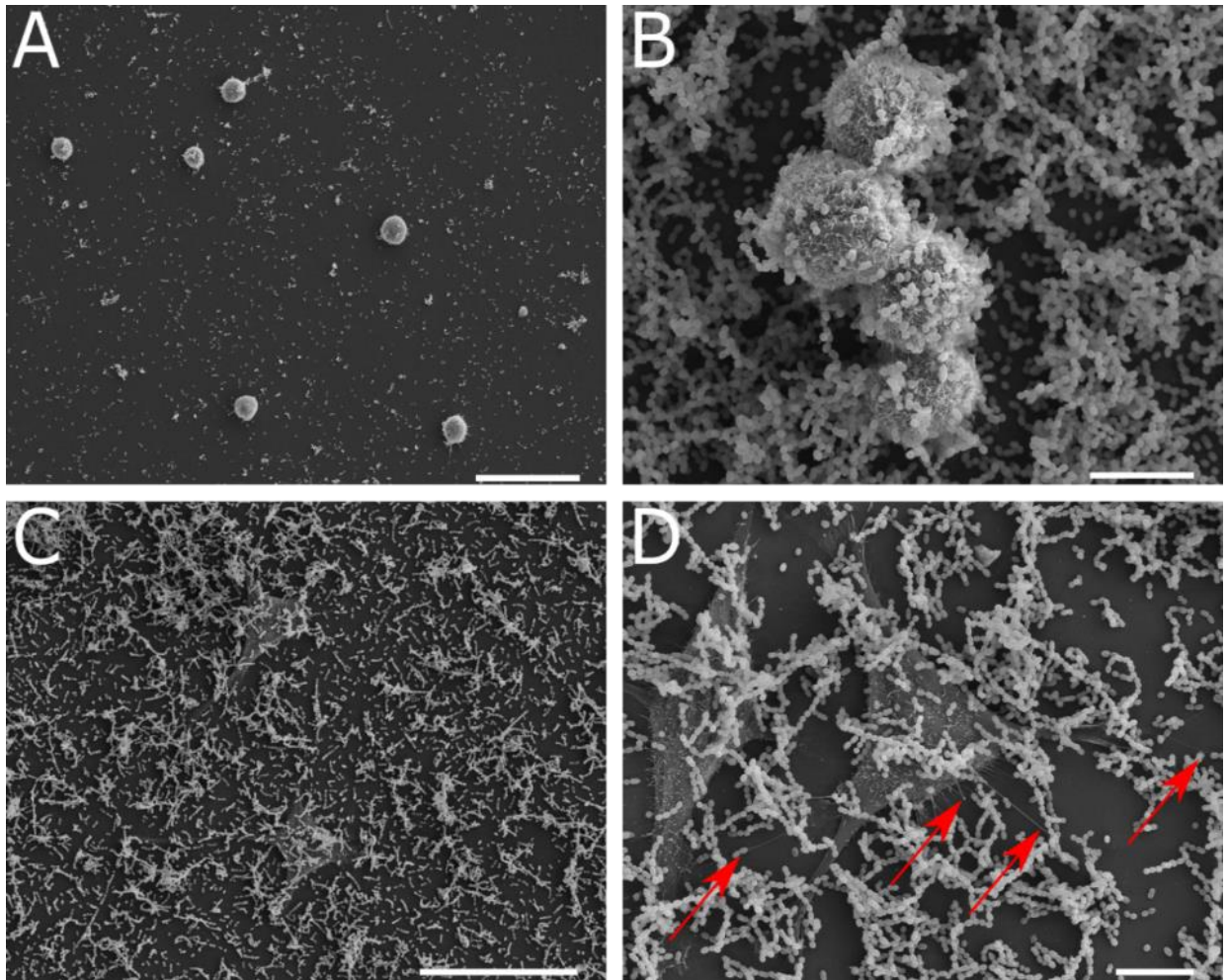


**Figure 3.7. Low and high magnification SEM images of C2C12 murine myoblasts under alcian blue fixative after 3 hours.** Many more bacteria can be seen utilising this fixative when compared with the previous method giving a much more accurate representation of what is occurring on the coverslip. **A** and **B** represent cells on the *L. lactis*-empty (low and high magnification respectively) samples. **C** and **D** represent cells on the *L. lactis*-FN (low and high magnification respectively) samples. A larger picture of **D** can be seen in the Annex Figure 8.1. It can be seen in **D** that the cells have many more protrusion structures to bacteria (highlighted by the red arrows). Scale bar = 50  $\mu\text{m}$  for **A** and **C** and 10  $\mu\text{m}$  for **B** and **D**.

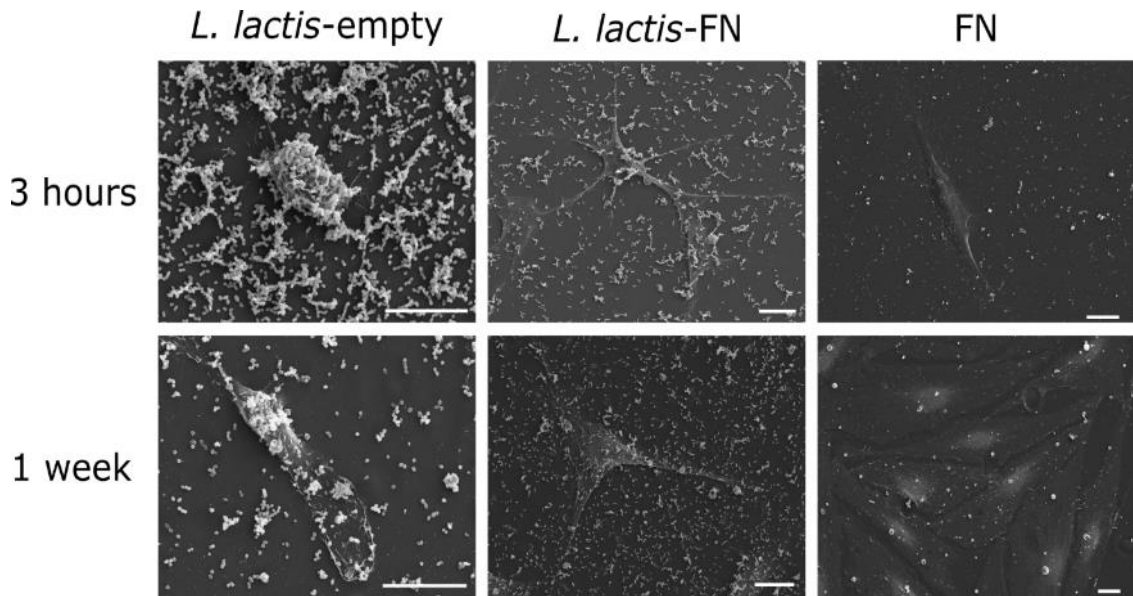


**Figure 3.8. Morphological study of the hMSCs by SEM.** MSC behaviour on the *L. lactis*-FN and *L. lactis*-empty biofilms, and FN-coated surface was assessed by scanning electron microscopy. Cells were cultured for three hours in absence of FBS and for one week with 1 % FBS, in this case to ensure cell viability. MSCs cultured for three hours on the *L. lactis*-empty biofilm kept a round shape, while in the *L. lactis*-FN and in the FN-coated surface showed adherence and spreading. On the other hand, in the one week cultures, due to the need to use FBS to ensure viability, cells showed an elongated shape with evidences of adhesion behaviour. Nevertheless, MSCs showed different features in the *L. lactis*-FN compared to the *L. lactis*-empty biofilm, this behaviour can be attributed to the presence of the III<sub>7-10</sub> fragment exposed on the *L. lactis* cell wall. Cells cultured on the FN-coated surface displayed higher proliferation ratios. Scale bar = 20  $\mu$ m.

After initial SEM studies, MSC adhesion was explored through vinculin immunostaining, a protein present in focal adhesion complexes (Humphries, Wang et al. 2007, del Rio, Perez-Jimenez et al. 2009, Kanchanawong, Shtengel et al. 2010, Case, Baird et al. 2015). This experiment was completed to ascertain if there were any changes in focal adhesion complexes across the surfaces. Figure 3.9 shows vinculin staining on the surfaces after three hours and one day. After three hours, MSCs cultured on *L. lactis*-empty display a rounded morphology with no signs of adhesion, a result similar to SEM. Whereas MSCs cultured on the FN coated surface and *L. lactis*-FN display evidence of spreading and adhesion; the nascent focal adhesions could be seen at the edges of the cell lamellae (see arrows Figure 3.9). After one day, cells on all surfaces have spread and adhered to the surfaces. The presence of vinculin on the *L. lactis*-empty is likely due to the addition of FBS to the media. FBS contains many proteins and molecules essential for long term cell culture such as, albumin, antichymotrypsin, apolipoproteins, biotin, and growth supporting factors, however, it also comprises many cell adhesive glycoproteins which become adsorbed to the sample surface (Hayman and Ruoslahti 1979, Zheng, Baker et al. 2006). Nevertheless, and more

critically, MSCs cultured on the FN coat and *L. lactis*-FN displayed many more and more developed focal adhesions, which is highlighted by the larger dash morphology when compared against *L. lactis*-empty, where the adhesions are strictly punctate, dot shaped focal complexes.

Focal adhesions were again explored after three and seven days (Figure 3.10A). All cells display adhesion complexes and a spread morphology, regardless of the sample surface. This may again be due to the presence of FN, amongst other adhesive proteins in the FBS (Taub 1990). After cells become attached to a surface, they begin to secrete their own matrix, allowing other cells to migrate and grow. After three days, it can be inferred from the graphs (Figure 3.10B) that the FBS, combined with the matrix secreted by the cells has allowed cell adhesion to become uniform across all sample sets.

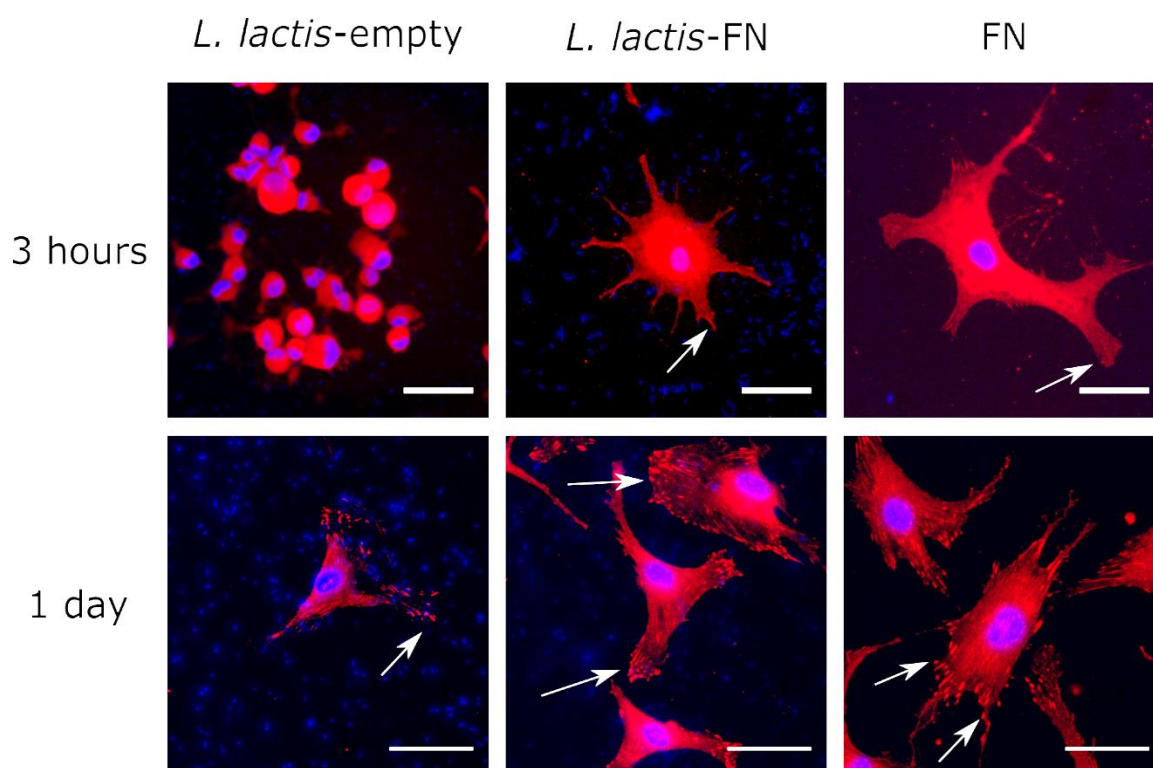


**Figure 3.9. Adhesion assessment of hMSCs cultured on *L. lactis*-empty, *L. lactis*-FN and FN-coated surface.** Cells were cultured for three hours in absence of FBS and one day with 1 % FBS with an initial density of 5,000 cells/ cm<sup>2</sup>. After selected times, cells were fixed and immunostained against vinculin (red) and DAPI (blue). MSCs cultured for three hours in the *L. lactis*-empty biofilm showed no sign of adhesion, keeping a round shape, while in the *L. lactis*-FN and FN surfaces there is evidence of spreading and adhesion, although focal adhesion complexes are not fully developed. After one day, there are focal adhesion (FA) complexes in the three different conditions; the presence of FA in cells cultured on *L. lactis*-empty biofilm is most probably due to the presence of FBS in the medium. Cells cultured on the *L. lactis*-FN biofilm and FN-coated surface displayed more developed FA complexes compared to *L. lactis*-empty biofilm, suggesting that the already present fibronectin in the surface (either on the *L. lactis* cell wall or grafted on the surface) enhances the development of this FA complexes. Scale bar = 50  $\mu$ m.

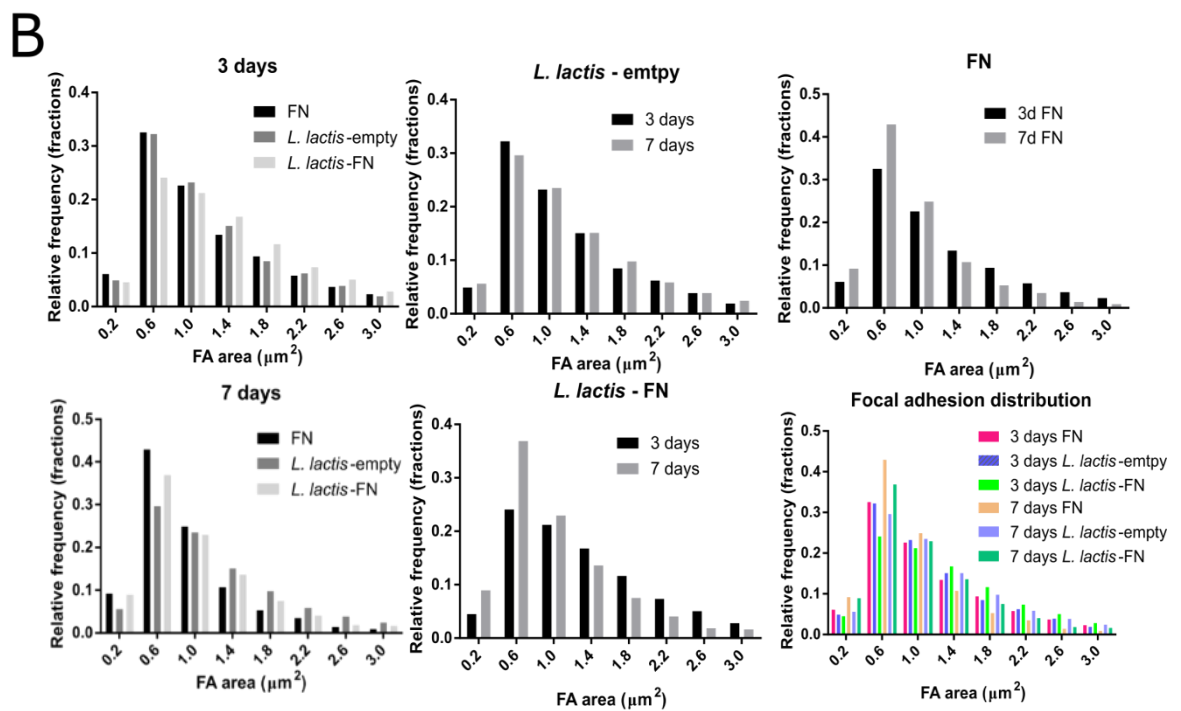
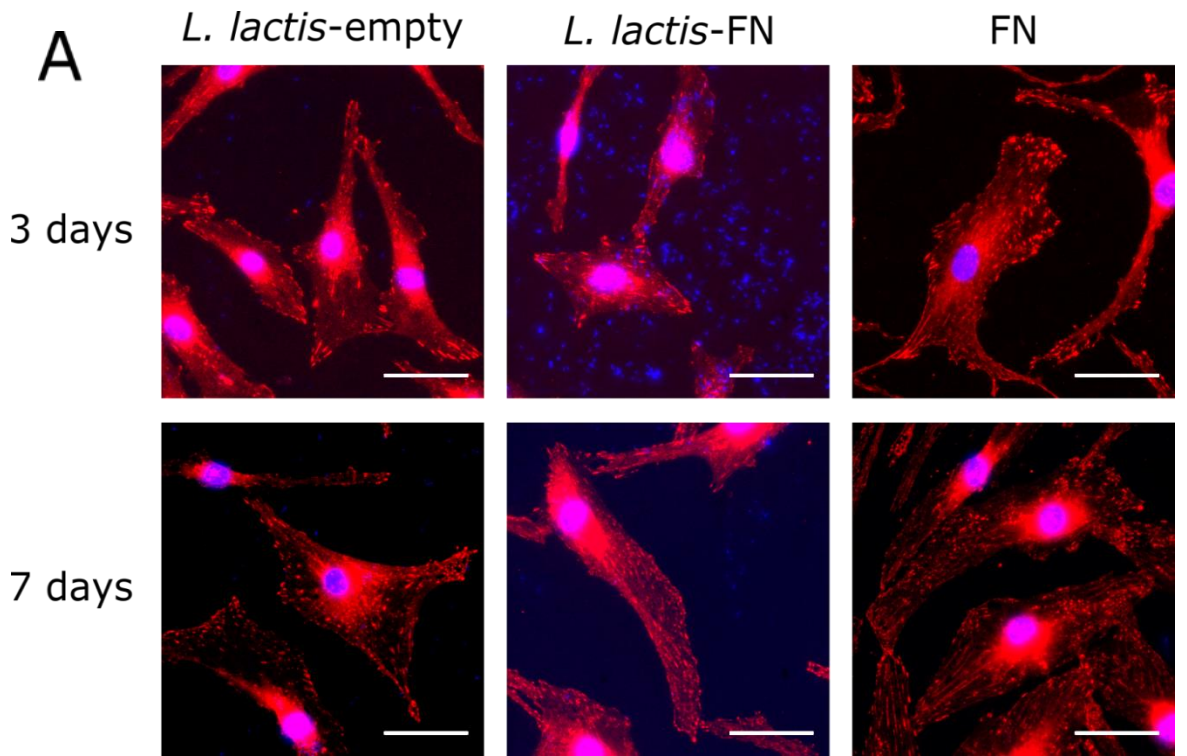


**Figure 3.10. Long term focal adhesion analysis.** Image **A** shows focal adhesion analysis performed on MSCs after three and seven days of culture on *L. lactis*-empty, *L. lactis*-FN and FN coated glass. MSCs were cultured in DMEM supplemented with 10  $\mu\text{g}/\text{mL}$  tetracycline and 1 % FBS and after the selected time points, fixed and immunostained for vinculin (red), while nuclei were stained with DAPI (blue). A minimum of 12 individual, isolated cells per condition were analysed to check area and number of focal adhesion complexes. The graphs in **B** show that there is no difference between focal adhesion distribution between time, nor surfaces, probably due to the fact that the FBS added to the cell culture medium is helping in the initial adhesion steps, via fibronectin, vitronectin and collagen present in the serum. After this initial adhesion, MSCs start to secrete their own ECM proteins, leading to a very similar behavioural profile across the sample sets. A minimum of 24 cells were used per condition from three technical replicates. Data was analysed with a one way ANOVA test with a Tukey post-hoc test. No statistical differences were seen. Scale bar = 50  $\mu\text{m}$ .

After vinculin staining, a more specific staining for integrins was completed. Figure 3.11 shows integrin ( $\alpha 5$ ,  $\beta 1$  and  $\alpha \nu \beta 3$ ) staining of MSCs on differently functionalised glass coverslips after 75 minutes. 75 minutes was chosen as a time point as after this time, the cells begin to secrete their own matrix and integrin binding begins to become more uniform (Sternlicht and Werb 2001). This experiment was set up to highlight if the FNIII<sub>7-10</sub> expressing strain engages  $\alpha 5 \beta 1$  compared to  $\alpha \nu \beta 3$ . This is due to the fact that our FNIII<sub>7-10</sub> fragment houses PHSRN and RGD, which is thought to be essential for  $\alpha 5 \beta 1$  binding (Ebara, Yamato et al. 2008).

As can be seen from Figure 3.11 the samples that display no FN (no FN coat and *L. lactis*-empty) show rounded cells, indicative of no adhesion. Cells seeded upon coverslips functionalised with either a FN coat or FNIII<sub>7-10</sub> expressing *L. lactis* are spread, with good integrin staining in all channels. It is apparent that  $\alpha \nu \beta 3$  staining is higher on the FN coat than in *L. lactis*-FN as can be seen in the graphs in Figure 3.12. The  $\alpha 5$  and  $\beta 1$  channels on the *L. lactis*-FN confirm good co-localisation of these integrin subunits, which can be seen in the composite images. Focal adhesion structure can be seen to be distinctly different in the FN positive and negative samples. In the FN positive samples, integrin structures are seen to be much larger and more numerous as can be seen by the dashed morphology. Conversely, the samples without FN display structures that are dot shaped and more punctate. These results are highly similar to the three hour vinculin staining shown previously (Figures 3.9 and 3.10).

The number of unique focal adhesions, integrin area per cell and average integrin cluster size in MSCs was calculated from the images analysing 16 cells per condition. The samples on surfaces with no FN are not shown for average integrin cluster size as upon quantifying the samples, it became apparent that the low number of focal adhesions relative to integrin area per cell resulted in an extremely high average integrin size per cell. As can be seen from Figure 3.12A, the number of unique focal adhesions per cell is greatly increased on the FN coated surfaces when compared against surfaces without FN. In the *L. lactis*-FN sample,  $\alpha 5$  shows the highest number of unique adhesion structures, whereas on the FN coat,  $\alpha \nu \beta 3$  shows the highest number of adhesions. Figure 3.12B displays the average integrin area per cell and shows that cells on surfaces without FN have a much lower total integrin area than FN functionalised surfaces with  $\alpha 5$  having the highest area per cell in *L. lactis*-FN. Conversely, integrin area is almost uniform across  $\alpha 5$ ,  $\beta 1$  and  $\alpha \nu \beta 3$  on the FN coat. Most interestingly, *L. lactis*-FN displays a similar integrin area per cell for  $\alpha \nu \beta 3$  to the non-FN expressing cells. Figure 3.12C displays the average integrin size. It can be noted that average

integrin cluster size was highest on the FN coat. Integrin cluster size on the FN coat is fairly uniform with  $\alpha5$ ,  $\beta1$  and  $\alpha v\beta3$  all displaying similar areas with no statistically significantly different focal adhesion sizes. Contrariwise, on the *L. lactis*-FN samples,  $\alpha v\beta3$  shows the smallest integrin size with  $\alpha5$  and  $\beta1$  being roughly equivalent.

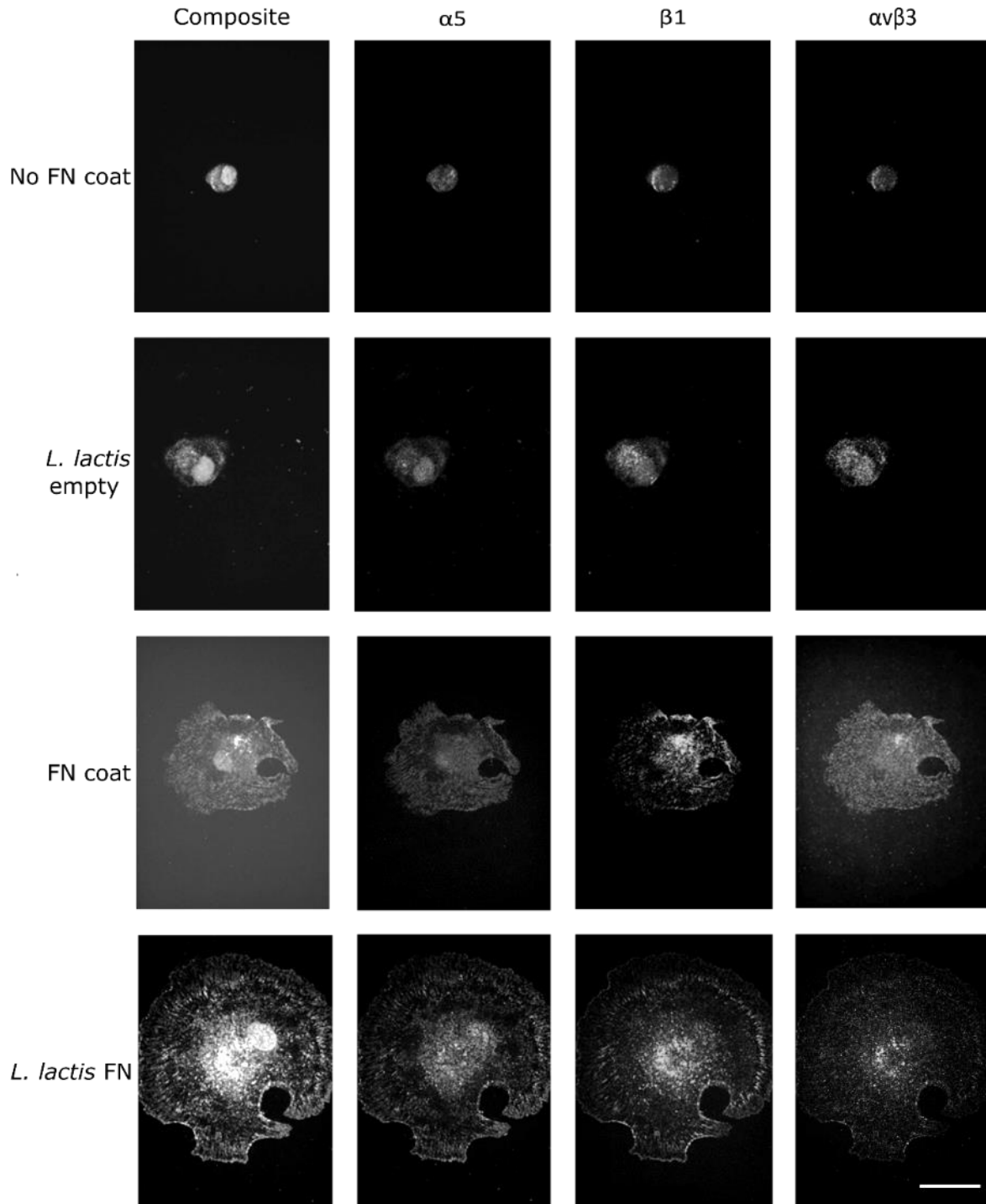


**Figure 3.11. Immunofluorescent images of MSCs stained for integrin  $\alpha5$ ,  $\beta1$  and  $\alpha v\beta3$ .** Cells were fixed 75 minutes after seeding. Images were taken at 63x, from top to bottom, no FN coat, *L. lactis* empty, FN coat and *L. lactis*-FN and from left to right, composite image,  $\alpha5$ ,  $\beta1$  and  $\alpha v\beta3$ . Cell spreading was seen in all FN samples. Scale bar = 50  $\mu$ m.

The differences in integrin binding between the FN coat and *L. lactis*-FN may be explained by the structure of FN and how integrins interact with FN. *L. lactis*-FN only displays FNIII<sub>7-10</sub> which houses the RGD and PHSRN motifs whereas the FN coat displays the whole molecule. On the FN coat, average focal adhesion area is seen to be higher for all integrins than for *L. lactis*-FN showing that the natural protein is able to induce a better cell response. There is a statistically significant difference between  $\alpha\beta3$  and  $\alpha5$  on the *L. lactis*-FN whereas there is no difference on the FN coat. This difference in integrin binding on *L. lactis*-FN could be due to the binding of  $\alpha5\beta1$  to RGD in the presence of PHSRN when there is an absence of the whole FN protein. This data describes a preferential binding of  $\alpha5\beta1$  over  $\alpha\beta3$  for MSCs seeded over *L. lactis*-FN.

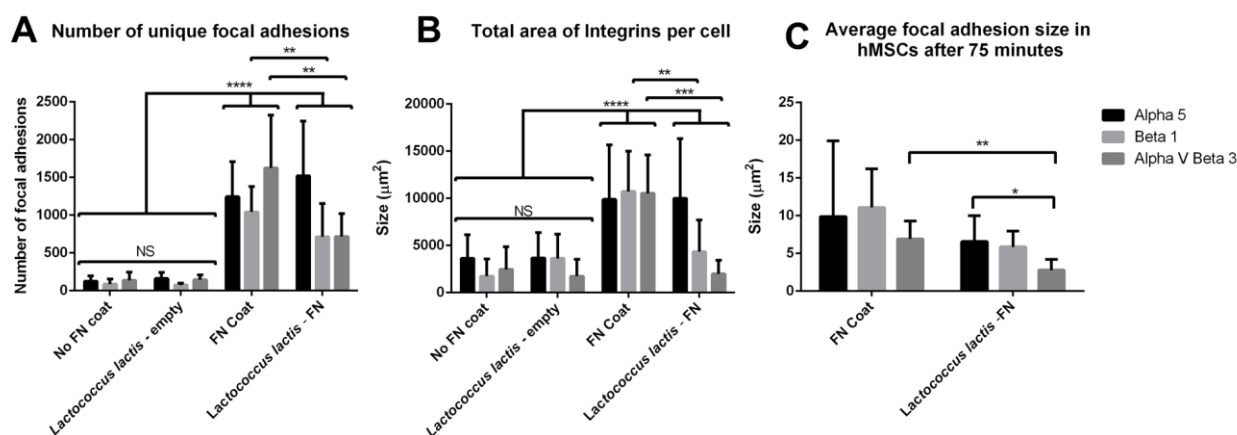


**Figure 3.12. Graphs detailing integrin adhesion after 75 minutes.** Graphs were constructed from 16 pictures per sample. **A** = Number of unique focal adhesions, **B** = integrin area per cell and **C** = Average integrin size. Cells seeded over non-FN samples show low adhesion number and integrin area, conversely, cells on FN samples show more and larger adhesion structures. Cells on *L. lactis* samples do not use  $\alpha\beta3$  as regularly as on a FN coated surface. A minimum of 16 cells were analysed per condition from three technical replicates. Data is presented as mean  $\pm$  SD, and was analysed with a one way ANOVA test with a Tukey post-hoc test. \*  $p < 0.05$ , \*\*  $p < 0.01$  and \*\*\*\*  $p < 0.0001$ .

### 3.3.3 Mesenchymal stem cell differentiation

#### Immunohistochemistry

BMP-2 was used to determine the ability of the biofilm to sustain MSC differentiation towards an osteoblastic phenotype. The bone specific proteins osteocalcin (OCN), osteopontin (OPN) as well as phosphate deposition (von Kossa) as part of matrix mineralisation were used to determine the reaction of MSCs to the addition of 100 ng/mL BMP-2. Figure 3.13 shows OCN staining after 21 days. Cells were cultured on FN coated glass as a control, and *L. lactis*-FN. Samples treated with 100 ng/mL BMP-2 show statistically significantly more OCN than non-treated samples by factors of 7.6 and 3 on the

FN coated surface and the *L. lactis*-FN surfaces respectively as can be seen in Figure 3.13A. Moreover, both samples with added BMP-2 were found to be statistically similar ( $p < 0.05$ ). Both samples with added BMP-2 showed high variance in the data as seen by the large error bars. Upon viewing the cells under fluorescence microscopy, it became apparent that some cells showed high amounts of OCN whereas some cells showed very little or no stain whatsoever (as shown in Figure 3.13A), this is the cause of the high standard deviation shown in Figure 3.13B. This could also be caused by undesired differentiation of the MSCs as well as 'stemness' retention as these cells would not produce any OCN. Standard deviation was low across the samples with no BMP-2 addition showing similar results were found in all replicates. These results demonstrate that the biofilm can sustain MSC differentiation. Figure 3.13C shows the number of cells per coverslip. Samples without added BMP-2 showed higher cell numbers in both sample sets. The cell count on the biofilm was found to be higher than on the FN in both the BMP-2 positive (statistically significant  $p < 0.05$ ) and negative media ( $p < 0.001$ ). This is likely caused by cell cycle inhibition. In terminal somatic cell culture models, inhibition of the cell cycle is usually a requisite for differentiation, and vice versa (Lathrop, Thomas et al. 1985, Budirahardja and Gonczy 2009, Hindley and Philpott 2012). By adding a growth factor to the medium, we can pull the cells from the cell cycle and hence proliferation, and force them to enter terminal differentiation. Figure 3.14 shows OPN staining after 21 days. Cells were cultured on FN coated glass and *L. lactis*-FN, both with and without 100 ng/mL BMP-2. More OPN was found in the BMP-2 positive samples on both substrates, by a factor of 1.6 (statistically significant  $p < 0.01$ ) and 1.1 (not statistically significant) for the FN coated glass and *L. lactis*-FN respectively as can be seen in Figure 3.14B. The differences in expression of OPN compared to OCN are not as striking, but do give a positive result. The fact that all cells are seen to express OPN (green area surrounding the nucleus) shows that all cells have begun differentiation towards an osteoblastic phenotype, this may be a phenomenon of the surface characteristics, and stiffer surfaces favour osteoblastic differentiation (Engler, Sen et al. 2006). The fact that BMP-2 addition only increases differentiation levels leads us to the conclusion that the growth factor is indeed responsible for the additional differentiation.

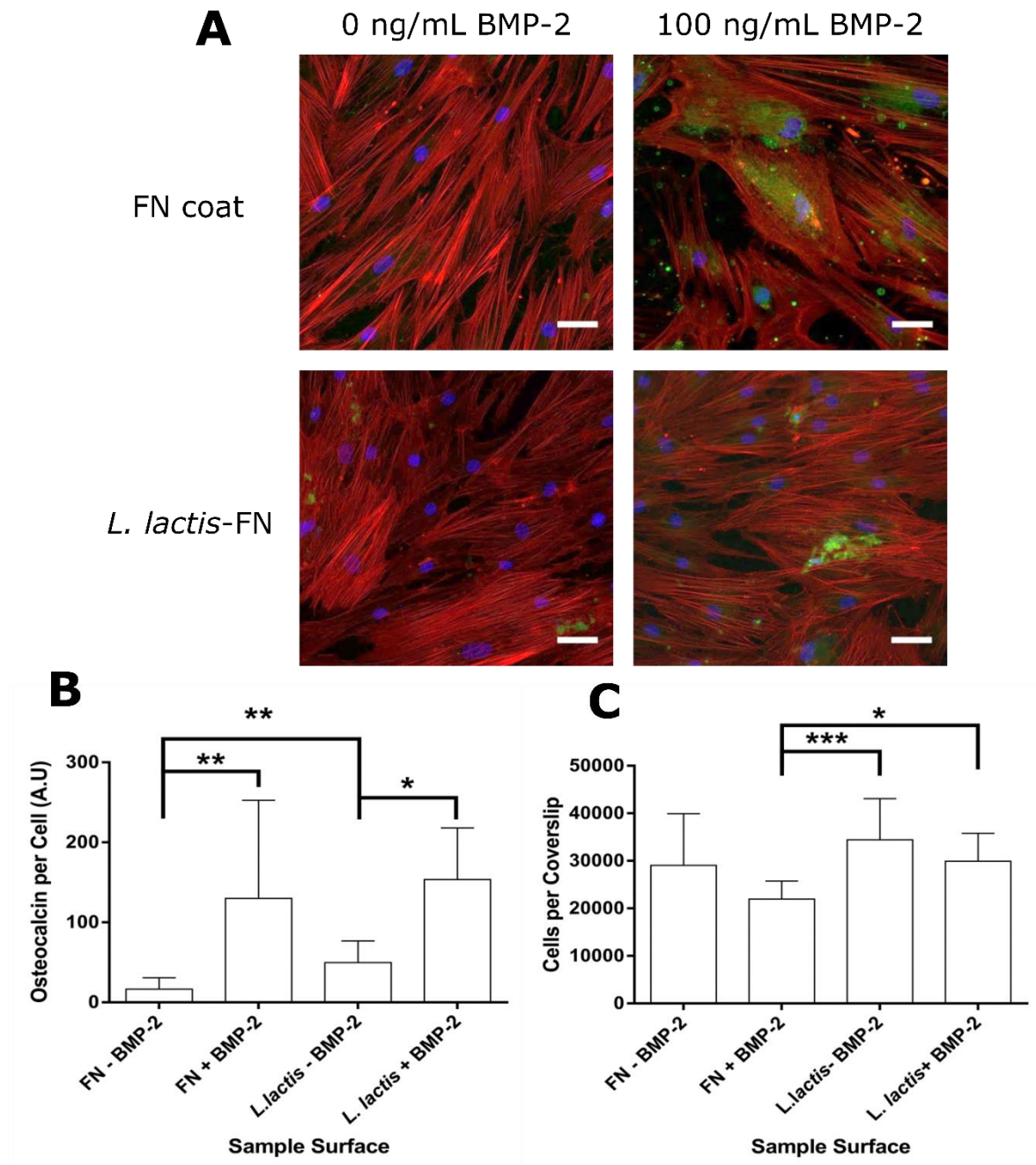


**Figure 3.13. Osteocalcin and cell count after three weeks of culture.** **A.** Cells stained for osteocalcin (green), actin (red) and DNA (blue) from left to right: FN 0 ng/mL BMP-2, FN 100ng/mL BMP-2, *L. lactis*-FN 0 ng/mL BMP-2 and *L. lactis*-FN 100 ng/mL BMP-2. **B.** Graph shows OCN area per cell  $\pm$  standard deviation of the sample sets (460, 269, 452 and 386 cells respectively). Total integrated density corresponding to the green channel (osteocalcin) was quantified using ImageJ. **C.** Graph shows MSCs per coverslip  $\pm$  standard deviation of the sample sets (2226, 1684, 2639 and 2295 cells respectively) from three technical replicates. OCN expression was much higher on the samples with added BMP-2. Data is presented as mean  $\pm$  SD and analysed with a one way ANOVA with a Tukey post-hoc test, \*  $p < 0.05$ , \*\*  $p < 0.01$  and \*\*\*  $p < 0.001$ . Scale bar = 50  $\mu$ m.

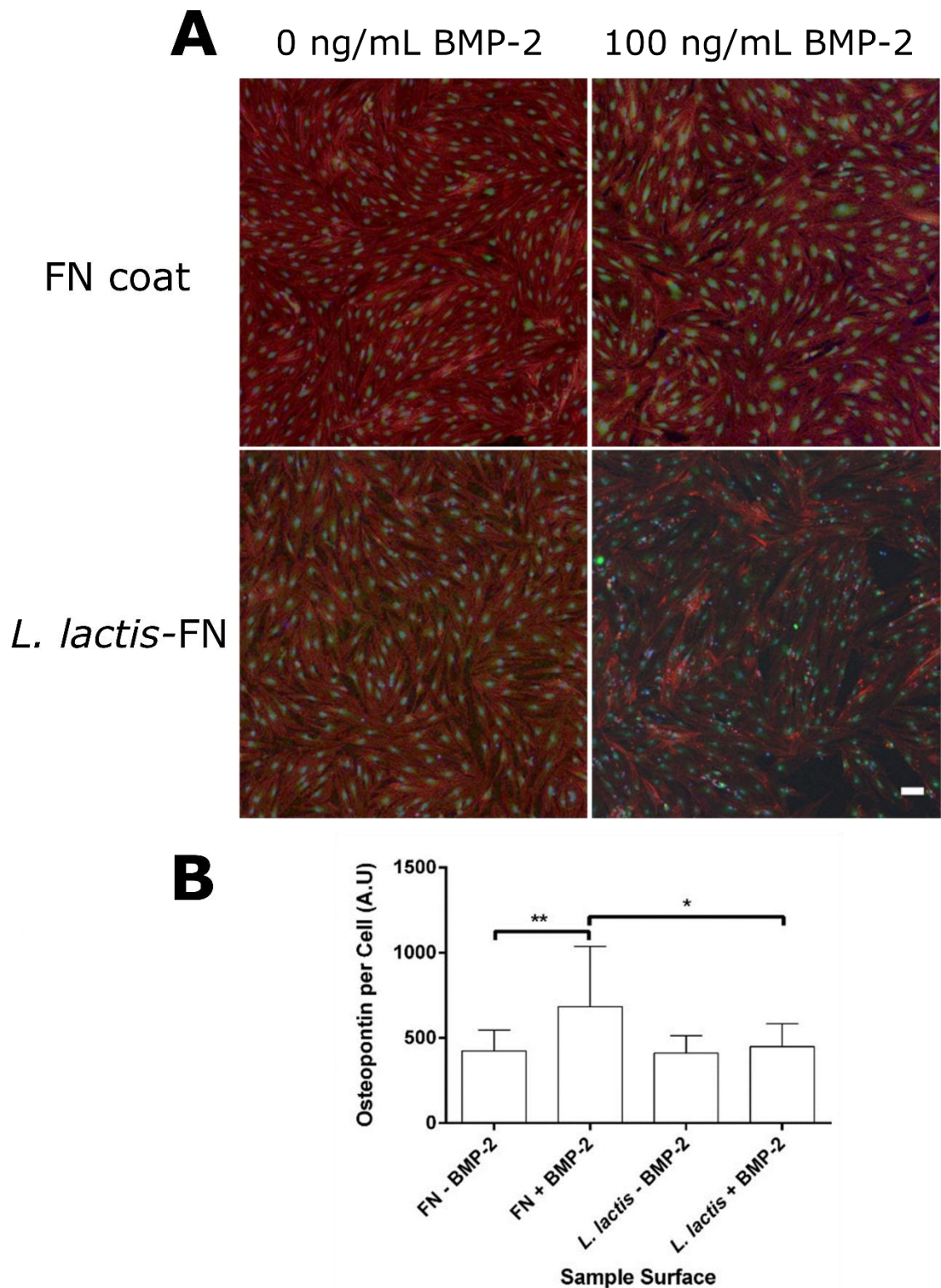


**Figure 3.14. Osteopontin production by cells.** **A.** Cells were grown for three weeks and stained for OPN (green), actin (red) and the nucleus (blue), the top row shows MSCs grown on FN coated PEA glass coverslips, the bottom row shows MSCs grown on *L. lactis*-FN PEA glass coverslips. The first column denotes 0 ng/mL BMP-2 and the second with 100 ng/mL BMP-2. **B.** Graph shows OPN area per cell  $\pm$  standard deviation of the sample sets (572, 347, 562 and 402 cells respectively) from three technical replicates. OPN expression was roughly equivalent across sample sets, with the exception of FN + 100 ng/mL BMP-2 where more OPN was observed. Data is presented as mean  $\pm$  SD and was analysed with a one way ANOVA test with a Tukey post-hoc test. Statistical significance levels are \* $p < 0.05$ , \*\* $p < 0.01$ . Scale bar = 100  $\mu$ m.

In addition to differentiation, it was important to check whether the bacteria were still present after three weeks of co-culture. Figure 3.15 shows that the biofilm is still visible and marked as purple dots, with the MSC nuclei in blue. It is abundantly clear that the bacterial density is lower than at the beginning, where the coverage can be as high as 27%, but in this case in particular, where *L. lactis* is providing only the adhesion cue, the importance of the biofilm is less essential than the differentiation cues provided by the BMP-2 supplemented in the medium. Further to this, the sample preparation involved in immunohistochemistry staining washes out a large proportion of the bacteria.

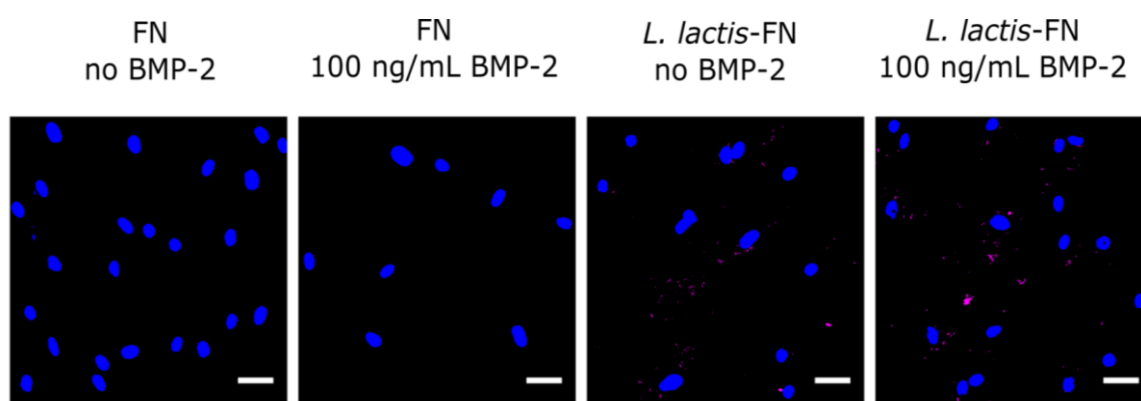


**Figure 3.15. Cell and bacterial coverage after 3 weeks.** Reconstructed DAPI images from left to right, cells were cultured on a FN-coated surface with and without BMP-2 at 100 ng/mL and on *L. lactis*-FN biofilm, again with and without BMP-2 at 100 ng/mL. Mammalian cell nuclei are seen in blue and bacterial DNA are seen in purple. Mammalian cells can still be seen after 3 weeks in co-culture with bacterial cells. Scale bar = 50  $\mu$ m.

### Matrix mineralisation

A third population of MSCs were grown for 28 days before analysing phosphate deposition shown in Figure 3.16. Matrix mineralisation was assessed via a von Kossa stain. Active osteoblasts deposit phosphate as a primary step of bone development and is therefore suggestive of terminal osteogenic differentiation. As can be seen from Figure 3.16, little phosphate deposition has been observed in the BMP-2 negative samples. In comparison, distinctly more phosphate (black deposits highlighted by red arrows) could be found in the BMP-2 positive samples thus showing that mineralisation of the ECM has occurred, a prerequisite for successful bone formation.

Together, the results confirm the ability of the living interface to support long-term MSC viability and trigger functionality, including mature differentiation with deposition of mineralised matrix.

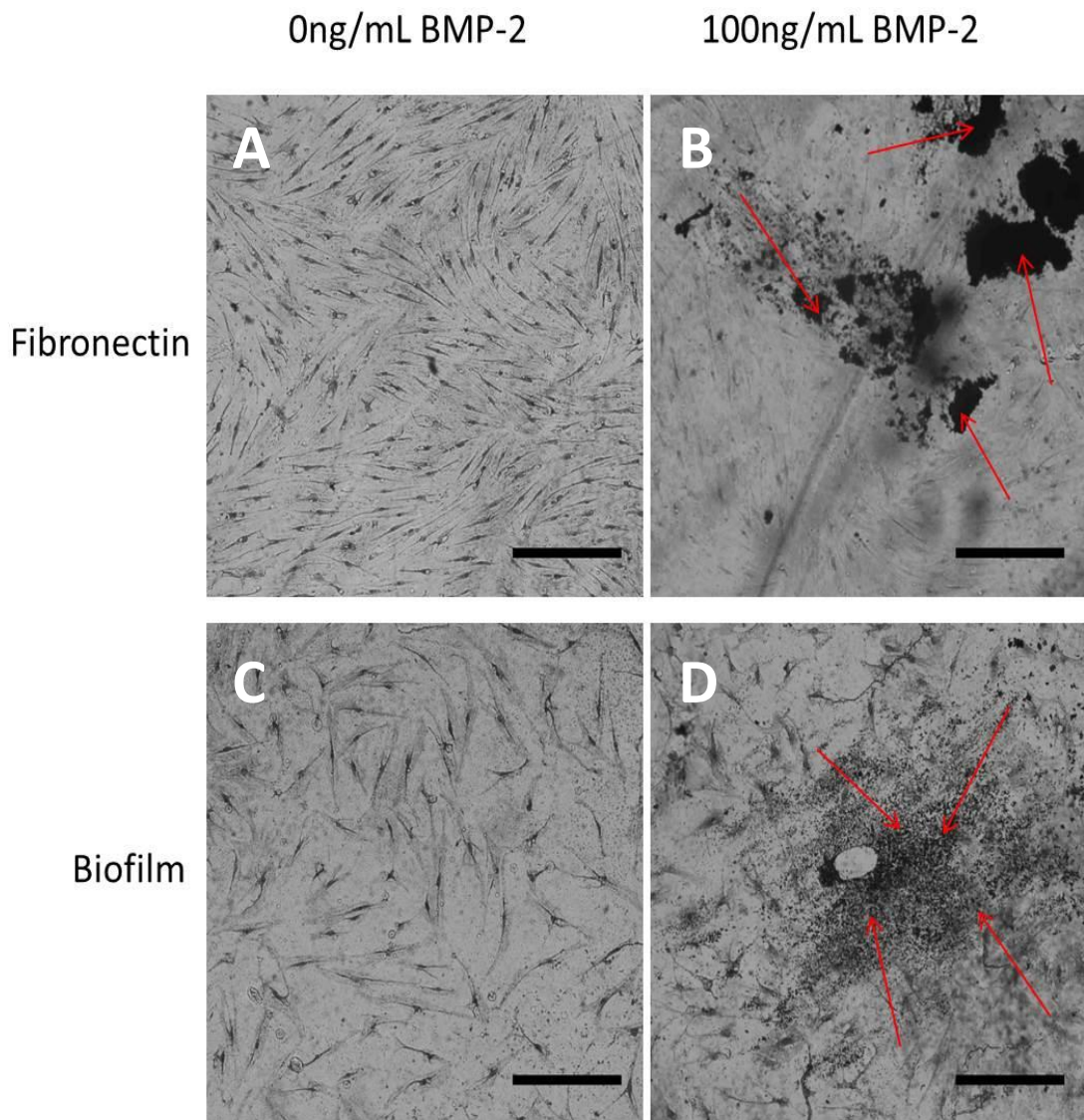


**Figure 3.16. Extracellular matrix mineralisation.** Mineralisation (phosphate deposition) was assessed with a von Kossa stain. MSCs were cultured for 28 days on a surface coated with FN (top row) and on *L. lactis*-FN biofilms (bottom row). After staining, cells were imaged in a Zeiss AxioObserver Z1 microscope using phase contrast. Cultures treated with BMP-2 showed black areas corresponding to phosphate deposits produced by the MSCs, while in the untreated cultures there is no evidence of mineralization. Scale bar size is 300  $\mu$ m.

### Gene expression analysis

A fourth population of MSCs were grown at 20,000 cells per  $\text{cm}^2$  for 14 days on FN and *L. lactis*-FN with and without 100 ng/mL BMP-2. Cells were grown in the same medium as previous experiments; however, the number of cells was increased to aid in the harvesting of enough RNA for qPCR analysis. The gene expression profiles of MSCs after two weeks of culture are shown in Figure 3.17 (normalised to glyceraldehyde 3-phosphate dehydrogenase (GAPDH)). The most notable difference can be seen between the BMP-2

positive and BMP-2 negative samples in which the expression of the ‘stemness’ markers ALCAM and CD63 are down-regulated in comparison with the BMP-2 negative samples. This illustrates the reduction in the expression of ‘stemness’ related mRNA and thus a decrease in protein expression therefore altering the cells behaviour and consequently, phenotype.

However, the expression of the osteogenic markers OPN and OCN display a similar expression level. After two weeks of culture, these markers are expected to be upregulated in an osteogenic culture (Yang, McNamara et al. 2014). Lian and Stein *et al.* described different markers of osteogenesis at differing time points, and OCN and OPN are shown as later markers (three or four weeks as opposed to two used in the experiment) (Stein, Lian et al. 1990). However, compounded with the previous histological and matrix mineralisation results, showing a large increase in OCN levels after three weeks and phosphate deposition after four weeks under the same conditions, it seems sensible to assume osteogenic differentiation has occurred.

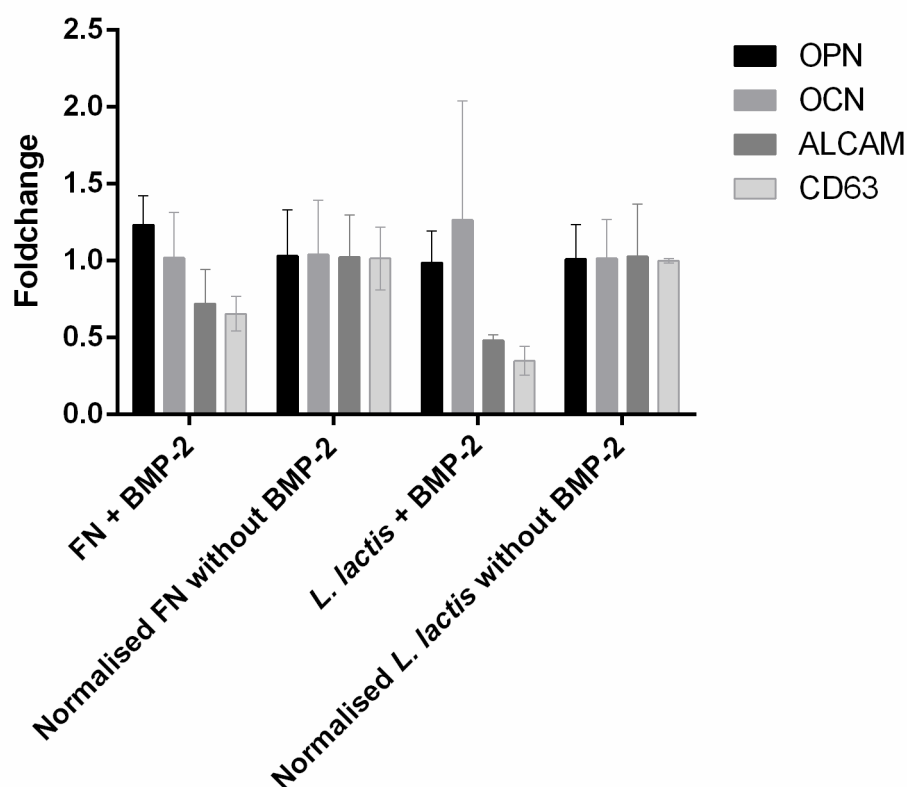


**Figure 3.17. Gene expression analysis of MSCs after 14 days.** From left to right, cells were cultured on a FN-coated surface with and without BMP-2 at 100 ng/mL and on *L. lactis*-FN biofilm, again with and without BMP-2 at 100 ng/mL. The gene expression has been normalised to glyceraldehyde 3-phosphate dehydrogenase (GAPDH). The most notable difference can be seen in the self-renewal genes, ALCAM and CD63 where their expression is downregulated in the BMP-2 positive samples. Three technical replicates were used per condition. Data is presented as mean  $\pm$  SD and was analysed with a two way ANOVA with a Tukey post-hoc test. No statistical differences were found.

### 3.4 Discussion

*In vivo*, adult stem cells survive within a specialised environment known as the niche (Yin and Li 2006, Li and Clevers 2010). The niche is made up of both cellular and non-cellular components, including resident stem cells, support cells, and the ECM that, together, regulate stem cell self-renewal (Engelhardt 2001, Yin and Li 2006, Xie 2008, Li and Clevers 2010, Mendez-Ferrer, Michurina et al. 2010). Once these cells are removed from their natural environment and placed on tissue culture plastics, which are distinctly different from the *in vivo* niche, MSCs begin to spontaneously differentiate into a heterogeneous population of mainly fibroblasts (Papadimitropoulos, Piccinini et al. 2014). This is undesirable for tissue engineering and provides a large obstacle in regenerative medicine.

Previous attempts at synthesising a dynamic niche for MSC proliferation and differentiation include the functionalisation of material surfaces with cell adhesive motifs, or incorporating protease degradable fragments in polymer hydrogels that allow changes in the material structure as cells secrete proteases to remodel the ECM (Garcia, Vega et al. 1999, Todd, Scurr et al. 2009, Khetan, Guvendiren et al. 2013). Dynamic surfaces have also been engineered to present cell adhesive RGD domains on demand (Todd, Scurr et al. 2009, Zelzer, Scurr et al. 2012, Weis, Lee et al. 2013, Roberts, Sahoo et al. 2016). In addition to adhesion, the dynamic release of growth factors in a controlled way to support cell differentiation have been tested (Lutolf and Hubbell 2005, Ma 2008, Makarenkova, Hoffman et al. 2009, Moon, Hahn et al. 2009, Silva, Richard et al. 2009, Phelps, Landazuri et al. 2010).

As seen in previous publications (Rodrigo-Navarro, Rico et al. 2014, Hay, Rodrigo-Navarro et al. 2016), a system has been proposed where mammalian cells can survive and differentiate on engineered non-pathogenic bacteria. This genetically engineered strain of *L. lactis*, a food grade, gram-positive bacterium with very low production of lipopolysaccharide (LPS) has been modified to present a fibronectin fragment (III<sub>7-10</sub>) tethered to its peptidoglycan layer by the *Staphylococcus aureus* protein A, making it available for mammalian cell integrins. This fragment houses the RGD and PHSRN synergy sequences which promotes cell adhesion and differentiation (Aumailley, Gurrath et al. 1991, Dsouza, Ginsberg et al. 1991, Salmeron-Sanchez and Dalby 2016). We have shown that this FNIII<sub>7-10</sub> fragment can induce adhesion in a variety of cell lines including NIH3T3, C2C12 and MSCs, and that the intracellular cascades activated are the same as when the cells are seeded

over FN coated glass (Saadeddin, Rodrigo-Navarro et al. 2013, Rodrigo-Navarro, Rico et al. 2014).

The FNIII<sub>7-10</sub> fragment contains the RGD adhesion and the PHSRN synergy motifs. RGD interacts with a wide variety of integrins, however, when combined with the synergy motif, a specific interaction with integrin  $\alpha 5\beta 1$  is able to occur. Signalling initiated with this specific integrin has been linked to enhanced osteogenic differentiation in MSCs (Agarwal, Gonzalez-Garcia et al. 2015). In addition to FNIII<sub>7-10</sub>, the known osteoinducer BMP-2 has also been used. The combination of FNIII<sub>7-10</sub> expressed in the bacterial cell wall and BMP-2 added to the culture media has proven an effective means of inducing osteoblastic differentiation in MSCs.

This bacterial strain produces stable biofilms that allow us to co-culture mammalian cells. The formation of the biofilm begins when individual bacteria begin to adhere to the surface. This process is governed by weak non-specific forces such as Van der Waals and polar Lewis acid-base interactions (Nishiyama, Sugiyama et al. 2016). This is an initial adherence, and can easily be reversed. Bacterial cells can increase their adherence through the use of cell-wall anchored proteins (CWAPs), these are also known as adhesins. *L. lactis* has several prominent anchor proteins, the most notable being CluA (Godon, Jury et al. 1994, Stentz, Jury et al. 2004) sex factor and the PrtP and NisP proteinases (Godon, Jury et al. 1994, Habimana, Le Goff et al. 2007, Giaouris, Chapot-Chartier et al. 2009). The required force to detach the bacteria from the surface is increased and allows for more bacteria to co-aggregate to the existing ones. The adhesins act by actively remodelling the bacterial surface and lead to the irreversible attachment to the surface. A bacterial community is now established and the bacteria can proliferate and develop the biofilm. *L. lactis* is a bacterial species that produces a low amount of exopolysaccharide and therefore their biofilms usually show a monolayered morphology, lacking the stratified structure found in many other species (Gulot, Georges et al. 2002, Habimana, Meyrand et al. 2009, Saadeddin, Rodrigo-Navarro et al. 2013).

Previously, *L. lactis* biofilms were developed on glass, a hydrophilic surface, and were found to be stable for at least four days in co-culture with mammalian cells (Pittenger 2008). As our experiments were running for four weeks (28 days), it was essential to select an appropriate surface to allow stable bacterial attachment for the time course. A stronger interaction was needed between the biofilm and the underlying surface. To allow for this, a change in material was needed. Surface hydrophobicity plays a role, as is explained by the XDLVO theory (Bayouhdh, Othmane et al. 2009) and therefore a switch to a more

hydrophobic surface was chosen, more specifically, poly (ethyl acrylate) (PEA), spin coated onto glass coverslips to form a thin layer. PEA is a hydrophobic, non-biodegradable synthetic polymer that showed excellent adhesive properties for *L. lactis*. Glass covered with this polymer were found to support good bacterial viability, similar to those found on glass at shorter time points. Moreover, these biofilms were found to be stable for at least 28 days, even in the presence of the bacteriostatic antibiotic TC. TC was used to impede bacterial metabolism and prevent acidification of the medium, enabling survival of the mammalian cells. The basis of using PEA as an alternative to glass is due to the interaction between the bacterial cell wall and the surface. Our *L. lactis* strain MG1363 and NZ9000 are derivatives of the subspecies *cremoris* TIL672 which feature hydrophobic surfaces (Giaouris, Chapot-Chartier et al. 2009). Observations had been made on many occasions, that when this strain is grown in M17 media, they tend to aggregate together to form chains, indicative of its hydrophobicity. The XDLVO theory describes the interaction in terms of free energy of the interacting surfaces (Bayouhd, Othmane et al. 2009). The interaction is not distant dependent and hydrophobic surfaces interact better together than hydrophobic-hydrophilic. A practical explanation at the molecular level is that the interaction between two apolar moieties immersed in water is the consequence of the hydrogen bonding energy of cohesion of the water molecules surrounding them. Therefore, the use of a hydrophobic surface is better suited to support biofilm development, at least with this strain. For other strains, an evaluation of their hydrophobicity should be completed to optimise and improve biofilm development.

The combination of these factors, that is, improved biofilm stability, the bacterially expressed FNIII<sub>7-10</sub> compounded by its integrin related signalling and BMP-2 induced phenotypical change lead to improved osteogenic differentiation in MSCs when compared to FNIII<sub>7-10</sub> signalling alone.

### **3.5 Conclusion**

This chapter has shown that engineered bacteria can be used as an interface between a synthetic surface and mammalian cells to control adhesion and sustain differentiation. Firstly, conditions were optimised to maintain stable biofilms for up to four weeks to allow terminal MSC differentiation. More specifically, there is very little difference between a fibronectin coated surface and our modified bacteria in terms of adhesion and differentiation and that the bacteria holds an advantage over a simple fibronectin coat, in that it can be further modified to produce a superfluity of proteins or growth factors that can be used to alter and direct cell fate. This is advantageous over current systems in that the bacteria can be controlled to express proteins in a spatiotemporal manner; something that is currently unavailable in the literature. We aim to control the interface to allow MSC self-renewal and differentiation, which can then be applied to aid in many strategies to promote tissue repair and regeneration.

# 4. *Lactococcus lactis* cloning and characterisation

## Summary

This chapter focusses on the cloning of bone morphogenetic protein 2 (BMP-2) into the relevant plasmids and their transformation into *Lactococcus lactis*. Both constitutive and inducible expression of BMP-2 was completed and characterised by fusing the biologically active protein to GFP or a hexahistidine tag. The well characterised nisin controlled gene expression system was used to control temporal induction of BMP-2 and FNIII<sub>7-10</sub> fragments. The results demonstrate that the new *L. lactis* is viable and can display BMP-2 and FNIII<sub>7-10</sub> in an inducible fashion.

## 4.1 Introduction

Microbes are ever present in the surrounding environment and are postulated to have been present on earth for 2 billion years before any other living organism (Corliss 1975). They are as such, ubiquitous and have colonised a vast array of environments including the living bodies of most, if not all living organisms (Sagan 1967), have formed colonies on land and in the deepest oceans, can be found in arctic ice and hot springs, and even in the stratosphere (Ferris, Muyzer et al. 1996, Huston, Krieger-Brockett et al. 2000, Wainwright, Wickramasinghe et al. 2004, Hazen, Dubinsky et al. 2010). Bacteria were first witnessed by Anton van Leeuwenhoek in the mid-17<sup>th</sup> century and since, have become extensively studied (Lane 2015).

Since their discovery, it has been proven that microbes play a significant role in the lifestyle and industry of humans. Some cause disease in humans and animals, initiating an economic burden as well as affecting health. On the contrary, some bacteria have proved very useful in industry, particularly in the petroleum, agriculture and food industries. These ‘useful’ bacteria, that is, the ones that are not pathogenic, can be exploited to provide beneficial outcomes, both in health and in industry. This idea of exploitation is not new, some of the earliest biotechnology used prokaryotes in the production of cheese, bread and yoghurt. Cheese production is thought to have originated sometime between 4000-7000 years ago, and thus biotechnology was being used long before the term was coined (Campbellplatt 1994).

The arrival of molecular and synthetic biology has rapidly revolutionised microbiology, through the use of recombinant strains and has opened new possibilities for industry and medicine. The first documented experiments using foreign DNA was in 1944, where DNA from the bacterium *Streptococcus pneumonia* was found to transfer to a genetically different bacterium and its subsequent recombination into the host-cell genome (Avery, Macleod et al. 1944). Ensuing studies substantiated that genetic alteration of a recipient cell can be due to the uptake of exogenous extrachromosomal DNA such as plasmids.

Plasmids are defined as extrachromosomal genetic elements capable of stable autonomous replication in a cell and were first introduced by the molecular biologist Joshua Lederberg in 1952 (Lederberg and Lederberg 1952). Usually, bacterial plasmids are initially recognised by the phenotypic properties they confer on a cell, for example, the ability to promote genetic transfer by conjugation, resistance to drugs and some metal ions, and production of antibiotic proteins and toxins. They are typically smaller in size compared to the genome, but a

bacterium can contain hundreds or thousands of copies of the plasmid (copy number). Many beneficial characteristics have been engineered into plasmids, which allow the user to convey wanted phenotypes to the cell (Debruijn and Lupski 1984). Microbiologists can insert genes, operons or cassettes that give a selective advantage to the host bacterium, often an antibiotic resistance, which allows the selection of the bacterium harbouring the favourable plasmid against the wild type species (Laddy and Weiner 2006). Many positive uses of bacteria have originated through plasmid engineering, such as lactose fermentation (Efstathiou and McKay 1977), proteinase activity (Efstathiou and Mckay 1976) and bacteriophage resistance (Labrie, Samson et al. 2010), amongst many others. Conversely, numerous pathogenic and toxin producing strains harbour their virulence factors on plasmids (Evans, Silver et al. 1975). Scientists can exploit the genetic machinery of bacteria as plasmid vectors allow the delivery of foreign DNA into a cell, to be replicated and maintained in the new host. As such, recombinant DNA technology relies on the alteration of plasmids. We can design plasmids that produce therapeutically advantageous or industrially relevant proteins to combat their associated problems.

More specifically, lactic acid bacteria (LAB), such as *Lactococcus lactis* have a long history of benevolent use by humans. They have been used in food production and as probiotics agents to promote human wellbeing (Cano-Garrido, Seras-Franzoso et al. 2015). Some species of LAB, including *L. lactis* are generally regarded as safe (GRAS) by the US Food and Drug Administration (FDA) and fulfil criteria of the qualified presumption of safety (QPS) according to the European Food Safety Authority (EFSA). Besides their characteristic safety, a great effort has been put toward developing effective molecular tools to use LAB as cell factories for the production of proteins of interest. The lack of effective approaches for regenerative medicine has driven the way for LAB to become an appealing option for biologists to deliver therapeutic molecules to sites of interest. These bacteria have already been used as vectors for delivering functionally active proteins to mucosal tissues for the treatment of gastrointestinal diseases, diabetes, cancer and viral infections (Steidler, Wells et al. 1995, Steidler, Viaene et al. 1998, Schotte, Steidler et al. 2000). A distinctive advantage of LAB over current technologies is the significant decrease in the cost of treatment. These are living organisms and as such would be able to autonomously replicate and synthesise the proteins of interest at the site of delivery.

A novel system has been created where mammalian cells directly interact with *L. lactis* through a fragment of fibronectin (FNIII<sub>7-10</sub>) (Saadeddin, Rodrigo-Navarro et al. 2013, Rodrigo-Navarro, Rico et al. 2014, Hay, Rodrigo-Navarro et al. 2016). Further to this, these

bacteria can be further modified to allow the production of a potent osteogenic growth factor, bone morphogenetic protein 2 (BMP-2) in a variety of forms. The direct contact of mesenchymal stem cells (MSCs) with *L. lactis* through the FNIII<sub>7-10</sub> fragment will allow the precise delivery of BMP-2 directly to the cells. This combination of cell adhesion and growth factor delivery is hypothesised to allow a currently unmet differentiation platform for MSCs. This, compounded by the presence of inducible plasmids allows the user to control the exact amount of growth factor delivery and adhesion to tailor exact MSC differentiation.

## 4.2 Materials and Methods

### 4.2.1 Cloning

A summary of the cloning procedure is as follows:

The plasmid pGEM-T-BMP2, shown in Figure 4.1 was purchased from Sino Biological and transformed into *E. coli*. The biologically active part of the BMP-2 preprotein was isolated and amplified by PCR from the plasmid after miniprep and cloned into pT1NX, between the *usp45* secretion peptide and *spaX* anchor protein. Depending on whether we wanted cell wall bound or secreted expression, the *spaX* was either made part of the open reading frame or a stop codon was placed before the *spaX* gene. The plasmids were created using Gibson Assembly and were transformed into electrocompetent *L. lactis* with exact methods described below.

The primers used to isolate the biologically active form of BMP-2 from pGEM-T-BMP2 (Figure 4.1) are shown below:

**Table 4.1. Isolation of BMP-2 from pGEM-T-BMP2.**

<b>Primer</b>	<b>Sequence 5'-3'</b>	<b>3' Annealing Temperature</b>
BMP-2 Forward	'GTCAGGTGTTTACGCCCAAGCCAAACACAAA CAGC'	62.4 °C
BMP-2 Reverse	'TCTTCCTCTTTTGGATCCTAGCGACACCCACA ACC'	62.4 °C

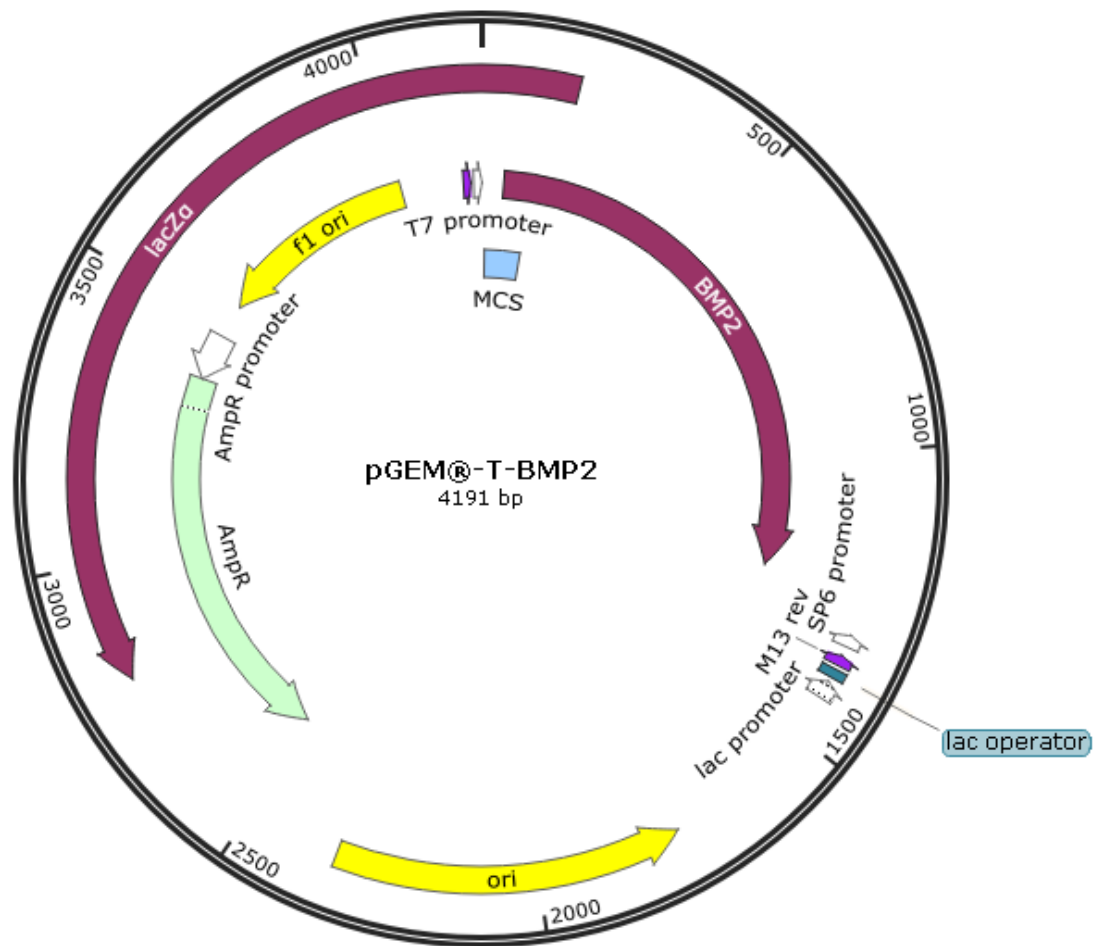


Figure 4.1. Schematic representation of the commercially available pGEM-T-BMP-2 used in this thesis.

#### 4.2.2 Transformation of chemically competent *Escherichia coli* (*E.coli*)

Firstly, agar plates and media were prepared for *E.coli* from Luria-Bertani (LB) media which contains: 10 g/L tryptone, 10 g/L NaCl and 5 g/L yeast extract, for plates, 1.5 % agar was added (Sambrook 2001). After sterilisation by autoclaving, 100 µg/mL ampicillin for pGEM-T (Sino Biological) was added. 100 ng of the plasmid pGEM-T-BMP2 was transferred into NEB 5-alpha competent *E. coli* (high efficiency) cells and incubated on ice for 30 minutes. These were then heat shocked at 42 °C for 30 seconds then placed on ice for 5 minutes. 950 µL of Super Optimal broth with Catabolite repression (SOC) was added and the cells were incubated at 37 °C for 1 hour at 250 rpm before being spread on agar plates and incubated overnight at 37 °C. These transformed cells were then inoculated in LB media and left to grow overnight at 37 °C. A glycerinate was prepared by adding 15% v/v of sterile glycerol to the bacterial culture and then stored at -80 °C for further work.

### **4.2.3 *E. coli* culture**

*Escherichia coli* is a gram-negative aerobic strain which grows in Luria Broth, composed of 10 g/L tryptone, 5 g/L NaCl and 10 g/L yeast extract. This media is then sterilised at 126 °C for 30 minutes. *E. coli* has an optimal growth temperature of 37 °C with shaking, in aerobic conditions (open container). The agar plates were prepared by adding 1 % w/v of agar, sterilising at 126 °C for 20 minutes and pouring into Petri dishes supplemented with the appropriate amounts of antibiotic when needed. Freshly prepared LB agar plates can be stored at 4 °C for several weeks in closed containers.

### **4.2.4 Plasmid isolation from *E.coli***

Bacteria were lysed using the manufacturer's guidelines (GenElute HP Five-Minute Plasmid Miniprep Kit, Sigma Aldrich). Briefly, 40 µL lysis reagent was added to 400 µL of overnight culture in a collection tube and mixed thoroughly before a 2 minute incubation at room temperature. 500 µL of column preparation solution were centrifuged at maximum speed for 15 seconds to prepare the columns, discarding the flow-through. 400 µL of binding solution was added to the lysate and mixed by inverting at least 15 times. This mixture was then transferred to a prewashed binding column and centrifuged for 20 seconds, the flow through was discarded. The column was twice washed using 700 and 200 µL of washing buffer and centrifuged for 20 and 30 seconds respectively, also discarding the flow-through. Finally, 40 µL of water was used to recover the plasmid DNA, by centrifugation at maximum speed for 30 seconds and the plasmid was stored at -20 °C. All centrifugation steps were completed at maximum speed, usually 20,000 g.

### **4.2.5 Plasmid purification**

Post miniprep and PCR, plasmid purification is necessary to remove salts and left over nucleotides and leave pure plasmid for downstream experiments. The PureLink Quick Gel Extraction and PCR Purification Combo Kit from ThermoFisher was used following the manufacturer's guidelines. Briefly, columns were prepared by incubating 500 µL 10 % HCl for 5 minutes before 3 washes with 650 µL of nuclease-free water being centrifuged through the column at 16,000 g for 30 seconds. Four volumes of binding buffer was added to the PCR mix and loaded into the spin columns and centrifuged for 1 minute at 10,000 g. The flow through was discarded and 650 µL of wash buffer was added to the column before spinning for 1 minute at 10,000 g. The flow through was discarded and the column was then

centrifuged at maximum speed for 3 minutes. The column was then placed in a new collection tube and 40  $\mu$ L of nuclease-free water was added to the column and left to incubate for 2 minutes. This was then centrifuged at maximum speed for 1 minute and the DNA product collected and stored at -20 °C until use.

#### **4.2.6 Preparation of *L. lactis* electrocompetent cells**

2 mL culture of *L. lactis* was grown overnight in M17 medium supplemented with 1 % glycine and inoculated into 200 mL of fresh M17 with 1 % glycine and grown at 30 °C. Once the culture had reached an optical density (OD) of 0.6-0.8 at 660 nm the cells were harvested by centrifugation at 3000 g for 10 minutes at 4 °C. This pellet was then washed 3 times in a sterile ice-cold solution of 10 % v/v glycerol and 0.5 M sucrose in ultrapure water. The cells were then resuspended in 1 % of the same wash solution and aliquoted at volumes of 50  $\mu$ L, flash-frozen in liquid nitrogen and stored at -80 °C. Cells stored at this temperature are able to keep their electrocompetency for approximately 6 months.

#### **4.2.7 Polymerase chain reaction (PCR)**

PCR reactions were carried out on a ThermoFisher ProFlex PCR System (ThermoFisher) using Q5 High-Fidelity DNA Polymerase (New England Biolabs).

PCR programs were set up as shown:

1. 1<sup>st</sup> denaturation step: 2 minutes at 95 °C
2. 35 amplification steps:
  - Denaturation, 30 seconds at 95 °C
  - Annealing, 30 seconds at the annealing temperature of each pair of primers
  - Extension, 30 seconds per kilobase of DNA at 72 °C
3. Final extension step: 72 °C for 2 minutes

Specific primers annealing temperatures are shown below:

Primers were designed using New England Biolab's NEBuilder assembly tool and purchased from ThermoFisher.

**Table 4.2. Primers for constitutively secreted biologically active BMP-2 (Usp45-BMP-2).**

<b>Primer</b>	<b>Sequence 5'-3'</b>	<b>3' Annealing Temperature</b>
Forward BMP-2	'GTCAGGTGTTTACGCCCAAGCCAAACACAAA CAGCG'	66.4 °C
Reverse BMP-2	'TCTTCCTCTTTTGGATCTTAGCGACACCCACA ACCCTC'	66.4 °C
pT1NX Forward	'TAAGATCCAAAAGAGGAAGACAAC'	61.6 °C
pT1NX Reverse	'TGATCCACCTCCACCTGATCCTCCACCACCGG CGTAAACACCTGACAAC'	61.6 °C

**Table 4.3. Primers for constitutively secreted BMP-2-GFP (Usp45-BMP-2-GFP).**

<b>Primer</b>	<b>Sequence 5'-3'</b>	<b>3' Annealing Temperature</b>
Forward GFP	'CGTTGTCAGGTGTTTACGCCATGGGTAAAGG AGAAGAAC'	59 °C
Reverse GFP	'CTCCACCACCGTATAGTTCATCCATGCCATG'	59 °C
pT1NX Forward	'CTAGTAGATCCGGCTGCTAAC'	64.7 °C
pT1NX Reverse	'GGCGTAAACACCTGACAAC'	64.7 °C
Linker-BMP-2 Forward	'TGAACTATACGGTGGTGGAGGATCAGGT'	65.8 °C
Linker-BMP-2 Reverse	'TTAGCAGCCGGATCTACTAGTTAGCGACACC CACAACC'	65.8 °C

**Table 4.4. Primers for constitutively cell wall bound BMP-2 (Usp45-BMP-2-spaX).**

<b>Primer</b>	<b>Sequence 5'-3'</b>	<b>3' Annealing Temperature</b>
Forward BMP-2	'GTCAGGTGTTTACGCCCAAGCCAAACACAAA CAGCG'	66.4 °C
Reverse BMP-2	'TCTTCCTCTTTTGGATCGCGACACCCACAACC CTC'	66.4 °C
pT1NX Forward	'GATCCAAAAGAGGAAGACAATAAC'	62.1 °C
pT1NX Reverse	'GGCGTAAACACCTGACAAC'	62.1 °C

**Table 4.5. Primers for constitutively cell wall bound BMP-2-GFP (Usp45-GFP-BMP-2-spaX).**

<b>Primer</b>	<b>Sequence 5'-3'</b>	<b>3' Annealing Temperature</b>
Forward GFP	'CGTTGTCAGGTGTTTACGCCATGGGTAAAGG AGAAGAAC'	59 °C
Reverse GFP	'CGCTGTTTGTGTTTGGCTTGGTATAGTTCATC CATGCCATG'	59 °C
pT1NX -BMP- 2-spaX Forward	'CAAGCCAAACACAAACAG'	64.7 °C
pT1NX-BMP-2- spaX Reverse	'GGCGTAAACACCTGACAAC'	64.7 °C

**Table 4.6. Primers for inducible secreted bound BMP-2-6xHis (Usp45-6xHis-BMP-2).**

<b>Primer</b>	<b>Sequence 5'-3'</b>	<b>3' Annealing Temperature</b>
Forward BMP-2	'CGTTGTCAGGTGTTTACGCCCATCACCATCA CCACCATCAAGCCAAACACAAACAGCG'	66 °C
Reverse BMP-2	'GCAGTACCCATGGCCGTGCCTTAGCGACACC CACAACCCTC'	66 °C
pNZ8123-BMP- 2- Forward	'TAAGGCACGGCCATGGGTACT'	70 °C
pNZ8123-BMP- 2- Reverse	'ATGGTGGTGATGGTGATGGGCGTAAACACC TGACAAC'	70 °C

**Table 4.7. Primers for inducible cell wall bound BMP-2-6xHis (Usp45-6xHis-BMP-2-spaX).**

<b>Primer</b>	<b>Sequence 5'-3'</b>	<b>3' Annealing Temperature</b>
Forward BMP-2	'CGTTGTCAGGTGTTTACGCCCATCACCATCA CCACCATCAAGCCAAACACAAACAG'	60 °C
Reverse BMP-2	'GCAGTACCCATGGCCGTGCCTTATAGTTCGC GACGACG'	60 °C
pNZ8123 - BMP-2-spaX Forward	'GGCACGGCCATGGGTACT'	65 °C
pNz8123-BMP- 2-spaX Reverse	'ATGGTGGTGATGGTGATGGGCGTAAACACC TGACAAC'	65 °C

**Table 4.8. Primers for inducible cell wall FNIII<sub>7-10</sub>-GFP (Usp45-GFP-FNIII<sub>7-10</sub>-spaX).**

<b>Primer</b>	<b>Sequence 5'-3'</b>	<b>3' Annealing Temperature</b>
Forward GFP	'CGTTGTCAGGTGTTTACGCCATGGGTAAAGG AGAAGAACTTTT'	62 °C
Reverse GFP	'GCAGTACCCATGGCCGTGCCTTATAGTTCGC GACGACG'	62 °C
pNZ8123 -FN- spaX Forward	'GGCACGGCCATGGGTACT'	70 °C
pNZ8123-FN- spaX Reverse	'GGCGTAAACACCTGACAACGG'	70 °C

**Table 4.9. Primers for inserting chloramphenicol into pT1NX for the creation of pT2NX.**

<b>Primer</b>	<b>Sequence 5'-3'</b>	<b>3' Annealing Temperature</b>
Forward chloramphenicol	'TTCTATGAGTCGCTTTTG'	56.9 °C
Reverse chloramphenicol	'GTAATCACTCCTTCTTAATTACAAATTTTGA G'	56.9 °C
pT1NX Forward	'AATTAAGAAGGAGTGATTACATGAACTTTA ATAAAATTGATTTAGACAATTG'	57.3 °C
pT1NX Reverse	'TACAAAAGCGACTCATAGAATTATAAAAGC CAGTCATTAGG'	57.3 °C

#### 4.2.8 Gibson Assembly

To join PCR products together to form new plasmids, the Gibson Assembly Master Mix (New England Biolabs) was used. The workflow for a reaction is as follows:

The fragment and vector were mixed in a 2:1 ratio (between 0.03 – 0.2 pmol) in a 0.2 mL microtube before adding the equivalent volume of Gibson Master Mix. This was then incubated for 15 minutes at 50 °C before diluting the volume four times with water. The assembled construct was then transformed into electrocompetent *L. lactis*.

#### **4.2.9 Electroporation of *L. lactis***

50 µL of frozen competent *L. lactis* and sterile electroporation cuvettes (VWR) were chilled on ice for 10 minutes. Then, 1 µL (100-500 ng) of the Gibson reaction product was added to the competent cells. This solution was added to pre-chilled electroporation cuvettes and electroporated at 2000 V (Eppendorf Eporator). The cells were then immediately transferred to a recovery medium of 5 mL M17 + 0.5 % glucose + 20 mM MgCl<sub>2</sub> + 2 mM CaCl<sub>2</sub> and incubated at 30 °C for 2 hours. The cells were then harvested at 3000 g for 10 minutes and resuspended in 50 µL of the same medium and streaked on M17 agar plates supplemented with 0.5 % w/v glucose and erythromycin at 10 µg/mL and left to grow at 30 °C overnight.

#### **4.2.10 Plasmid isolation from *L. lactis***

Plasmid isolation was carried out using a combination of an alkaline lysis protocol (O'Sullivan D and Klaenhammer 1993) and the GenElute five minute plasmid miniprep kit (Sigma). To lyse the bacteria, they were grown until the stationary phase in M17 media supplemented with 0.5 % v/v glucose and appropriate antibiotic and harvested by centrifugation at 3000 g for 10 minutes. The pellet was then resuspended in 200 µL 25 % sucrose containing 1 mg/mL RNase and 30 mg/mL lysozyme and incubated at 37 °C for 15 minutes. Then 400 µL of 0.2 N NaOH and 3 % sodium dodecyl sulphate (SDS) solution was added followed by immediate mixing by inversion and left for 7 minutes. Then, 300 µL of ice cold 3 M sodium acetate (pH 4.8) was added and the solution was vortexed. This solution was then centrifuged at 18,000 g for 15 minutes at 4 °C. The supernatant was recovered and the plasmid was isolated using the GenElute miniprep kit detailed above.

#### **4.2.11 Sequencing**

Samples were sent to Source Bioscience using the SpeedREAD™ service. 100 ng/µL of plasmid DNA and 3.2 pmol/µL of primers were sent to the service and these were sequenced using standard Sanger sequencing. The chromatograms were analysed using the SnapGene software.

The primers used for sequencing are shown below:

**Table 4.10. Primers for sequencing.**

<b>Primer</b>	<b>Sequence 5'-3'</b>
pT1NX	'AGTTCTTGTGGTTACGTGGT'
BMP-2	'CGGAAACGCCTTAAGTCCA'
GFP	'ACGTGCTGAAGTCAAGTTTGA'
pNZ8123 Forward	'CGAGCATAATAAACGGCTCTG'
pNZ8123 Reverse	'CTATCAATCAAACGAACACGTGC'

#### **4.2.12 Agarose gel preparation**

0.8 % agarose gels were used to visualise plasmids. Briefly 1 µg of plasmid was added to the agarose gel stained with SYBR safe. 2-Log DNA Ladder (0.1-10 KB) (New England Biolabs) was added as a marker and gels were run until the bands of the ladder could be seen separately. Prior to running the gel, plasmids were linearised using either EcoRI or NgoMIV.

#### **4.2.13 Preparation of the nisin stock**

Nisin was purchased from Sigma (N5764) and a stock of 1 mg/mL in 0.05 % acetic acid was prepared. The nisin was left to dissolve for 10 minutes at room temperature before centrifugation at 20,000 RPM for 1 minute to pellet the insoluble material. The supernatant was removed and stored at -20 °C. This stock was diluted to the desired concentration in water prior to use as less concentrated solutions of nisin are unstable (Mierau and Kleerebezem 2005).

#### **4.2.14 GFP Assay**

Bacteria were grown in GM17 with appropriate antibiotic in standing cultures for 24 hours before harvesting at 7000 g for 5 minutes and washing with M9 before resuspension in GM9 for 24 hours. The cells were then harvested at 7000 g for 5 minutes before the supernatant was neutralised with NaOH and left for 1 hour. The supernatant was then transferred to a black 96 well plate for fluorescence reading. The excitation wavelength was set to 395 nm and emission was set to 508 nm using an Infinite 200 PRO NanoQuant Plate Reader from Tecan.

#### **4.2.15 Western blot**

##### **Constitutive cell wall expression**

1 mL of standing culture was taken and lysed with the addition of 200  $\mu$ L of 25% sucrose and 30 mg/mL lysozyme for 30 minutes at 37 °C. Then, 400  $\mu$ L of 3 % SDS was added and incubated for 7 minutes at room temperature and then immediately placed on ice. 60  $\mu$ L of the lysate was mixed with 20  $\mu$ L of 4x Laemmli buffer and boiled at 95 °C for 5 minutes and then 30  $\mu$ L was loaded into a 4-20 % gel (New England Biolabs).

The gels were then run at 50 V for 2 hours. The proteins were then transferred to a 0.45  $\mu$ m pore size polyvinylidene fluoride (PVDF) membrane at 25 V for 45 minutes. The membrane was then blocked with 5 % milk in PBS for 1 hour on a shaker. The primary antibody (anti GFP (Clonotech) 1:7500 in 5 % milk-TBS-0.1 % Tween-20) was then added and left overnight at 4 °C. The sample was then washed 4 times for 5 minutes each in PBS-0.5 % Tween. The secondary antibody (Rabbit antimouse 1:20,000 with HRP in 2 % milk with PBS-0.5 % Tween, General Electric Healthcare) was then added for 1 hour on a shaker. The sample was then washed 6 times for 5 minutes with TBS-0.1 % Tween. The substrate ECL Prime WB Detection Agent (GE Healthcare) was then added and incubated for 5 minutes. Chemiluminescence was then imaged using the Syngene PXi 5 gel documentation system.

##### **Inducible cell wall expression.**

Cultures were grown in GM17 overnight before a 1 % inoculation into fresh GM17. After 1 hour, nisin was added at desired concentrations (see results section) and left for 5 hours before lysis and western blotting using the method described above. The primary antibodies (anti 6x HisTag (His.H8, ThermoFisher, UK) 1:2500 in 5 % milk-TBS-0.1 % Tween-20 for BMP-2W and HFN7.1 (Developmental Studies Hybridoma Bank, University of Iowa, USA) 1:1000 in 5 % milk-TBS-0.1 % Tween-20).

#### **4.2.16 Enzyme Linked Immunosorbent Assay (ELISA)**

Bacteria were grown overnight before fresh GM17 was inoculated with 1 % bacterial culture. After 1 hour, nisin was added at desired concentrations (0, 0.1, 0.5, 1 and 10 ng/mL) and left for 5 hours. A competitive ELISA (His-Tag Protein ELISA Kit, Cell Biolabs Inc, UK) was completed. Briefly, the plate was coated with polyhistidine and left overnight and samples and standards were added for 10 minutes on an orbital shaker. Standards were obtained from the kit. Anti-6xHis antibody was added to the wells for 2 hours before washing with wash buffer 5 times. Secondary antibody was added for 1 hour on an orbital shaker before washing

5 times. Then, substrate solution was added for 8 minutes before stopping and absorbance was read on an Infinite 200 PRO NanoQuant Plate Reader from Tecan at 450 nm.

## 4.3 Results

In order to utilise the power of *L. lactis* inducible systems, we had to change strain from MG1363 (used in the previous chapter) to NZ9000 and its derivatives. This is due to the fact that MG1363 does not harbour the nisin receptor needed for intracellular signalling and promoter activation. This chapter will focus on the cloning procedures and basic mammalian cellular response to these new clones.

### 4.3.1 NZ9000 FNIII<sub>7-10</sub>-GFP and BMP-2 strains

As there are no commercially available kits for the detection and quantification of bacterially expressed BMP-2, the synthesised proteins were tagged with either GFP or a 6x HisTag. The epitope of antibodies against BMP-2 bind to the glycosylated region of BMP-2 (information obtained from PeproTech). Bacteria do not possess the machinery to complete the same post-translational modifications as mammalian cells (Caina, Solis et al. 2014) and therefore a tag was needed.

For the constitutive clones, GFP was cloned into both cell wall and secreted clones for detection. This allowed the direct measurement of GFP by both western blot and fluorescence to detect the protein. Four clones were completed, cell wall expressing BMP-2 with and without GFP and secreted BMP-2 with and without GFP.

For the inducible clones, FNIII<sub>7-10</sub>-GFP and BMP-2 with a 6x HisTag were used. This allowed the direct measurement by western blot and ELISA. Two clones were completed, cell wall bound BMP-2 and secreted BMP-2.

To quantify FNIII<sub>7-10</sub> production, either antiGFP (constitutive) or antiFN (inducible) antibodies were used.

#### Constitutive expression

##### Cell wall expressing BMP-2 in NZ9000

Expression and localisation of cell wall bound BMP-2 was confirmed utilising a variety of methods. Firstly, sequencing an isolated plasmid from the clones highlighted an in-frame insertion of a 1.7 kb fragment, corresponding to GFP-BMP-2 and an insertion of 1 kb for BMP-2 without GFP.

Further confirmation was ascertained by western blot as shown in Figure 4.2. As described in the Materials and Methods section, *L. lactis* was lysed and the lysate was run on a gel and transferred for western blotting. The blot displayed bands at 60 kDa which is equivalent to that of GFP-BMP-2-SpA whereas control GFP which has a molecular weight of 26.9 kDa was found at 27 kDa. The bacterially expressed GFP band was found to be at a higher molecular weight as it is also fused to spaX and BMP-2. GFP was also used to make a standard curve to determine the concentration of BMP-2 per bacteria. Band densitometry analysis was used, finding a linear relationship between band density and protein amount. Based on this, it was determined that 37.5 and 18.7  $\mu$ L of standing culture contains approximately  $1.2 \pm 0.2$  and  $0.44 \pm 0.04$   $\mu$ g of GFP-BMP-2 respectively. Using these estimations, the approximate density of BMP-2 molecules that a mammalian cell can interact with is roughly 55,000 per bacterial cell, assuming a molecular weight of 60 kDa and fully saturated media containing  $2.2 \times 10^9$  bacteria per mL. This is equal to  $6.65 \text{ ng/cm}^2$  of cell wall bound BMP-2.

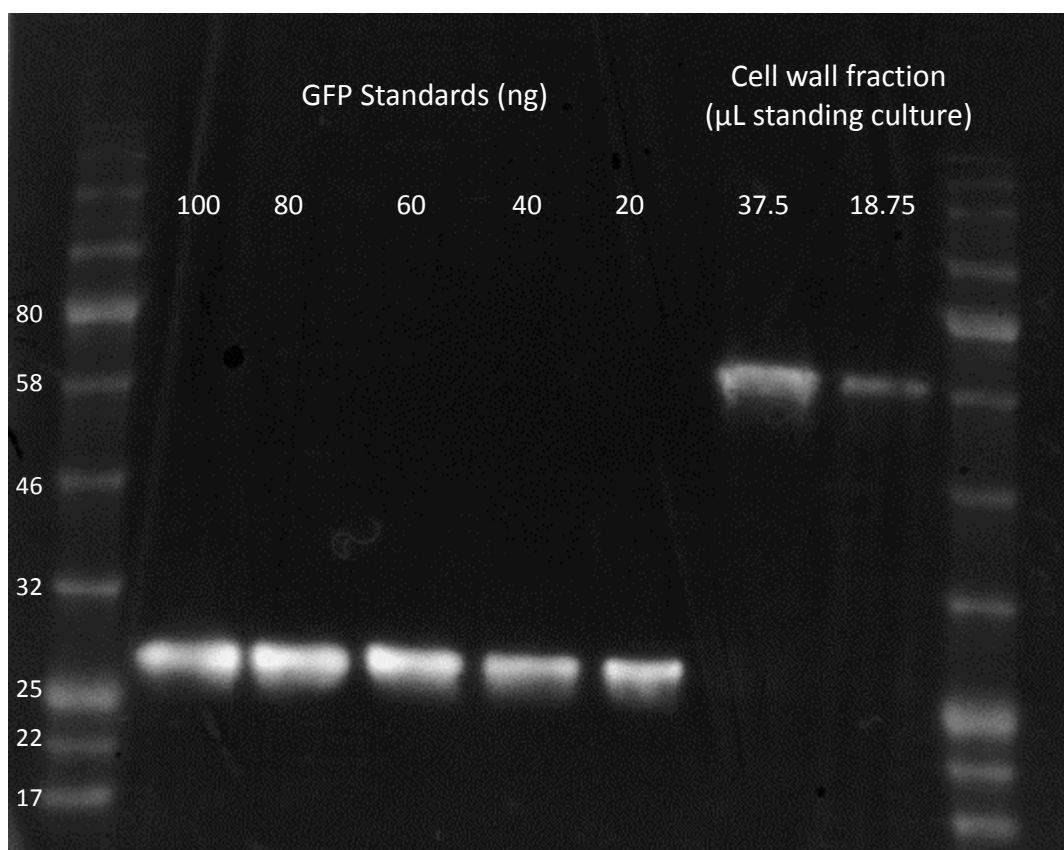


**Figure 4.2 Western blot against constitutive NZ9000 cell wall bound GFP-BMP-2.** From left to right colour prestained protein ladder (NEB), GFP standards at 100, 80, 60, 40 and 20 ng and 37.5 and 18.75  $\mu$ L cell wall fractions of standing culture and colour prestained protein ladder (NEB). GFP has a molecular weight of 26.9 kDa and can be seen at approximately 28 kDa and GFP-BMP-2-spaX has a molecular weight of 60 kDa and can be seen at 60 kDa. Three western blots were completed to allow quantification.

These results suggest that the anchoring of the protein by *spaX* and the fusion of BMP-2 and GFP can be easily expressed and are not detrimental to bacterial viability. *L. lactis*-BMP-2 cell wall and *L. lactis*-BMP-2 fused to GFP cell wall will now be known as *L. lactis*-BMP-2W and *L. lactis*-BMP-2WGFP respectively.

### **Expression of secreted BMP-2 in NZ9000**

Expression of secreted BMP-2 was confirmed in a different manner to cell wall expression. Again, sequencing the isolated plasmid from bacterial cells revealed the inclusion of an in-frame 1.7 kb fragment comprising GFP and BMP-2 with a stop codon between BMP-2 and *spaX*, preventing the synthesis of the *spaX* anchor, allowing protein secretion and another 1 kb insertion for BMP-2 without GFP.

A fluorescence assay was used to verify the presence of GFP from the clones. GFP shows fluorescence when it is excited with light at 395 nm and emits at 508 nm. Bacterial supernatant was loaded into 96 well plates and the fluorescence was measured. Figure 4.3A shows the GFP fluorescence of the bacterial supernatant under differing conditions. It has been proven that increasing the pH of the solution over 10 further increases the fluorescence which would further support the presence of GFP. In addition to pH, the presence of oxygen is essential for the maturation of the chromophore, and therefore, the bacteria had to be grown aerobically (Landete, Langa et al. 2015). As can be seen from Figure 4.3A, GFP fluorescence is statistically significantly higher in the aerobically grown samples, and the highest in the pH 12 samples. A standard curve was created using GFP at known concentrations allowing us to ascertain the amount of GFP in the *L. lactis* samples shown in Figure 4.3B. As GFP and BMP-2 are at a 1:1 ratio the total amount of GFP will be the same as BMP-2. Using the standard curve, it was found that we had 970 ng/mL of BMP-2 monomers, to be biologically active, BMP-2 needs to dimerise, and therefore we theoretically have 485 ng/mL of BMP-2 in a fully saturated culture of *L. lactis* after 1 day. *L. lactis*-BMP-2 secreted and *L. lactis*-BMP-2 fused to GFP secreted will now be known as *L. lactis*-BMP-2S and *L. lactis*-BMP-2SGFP respectively.

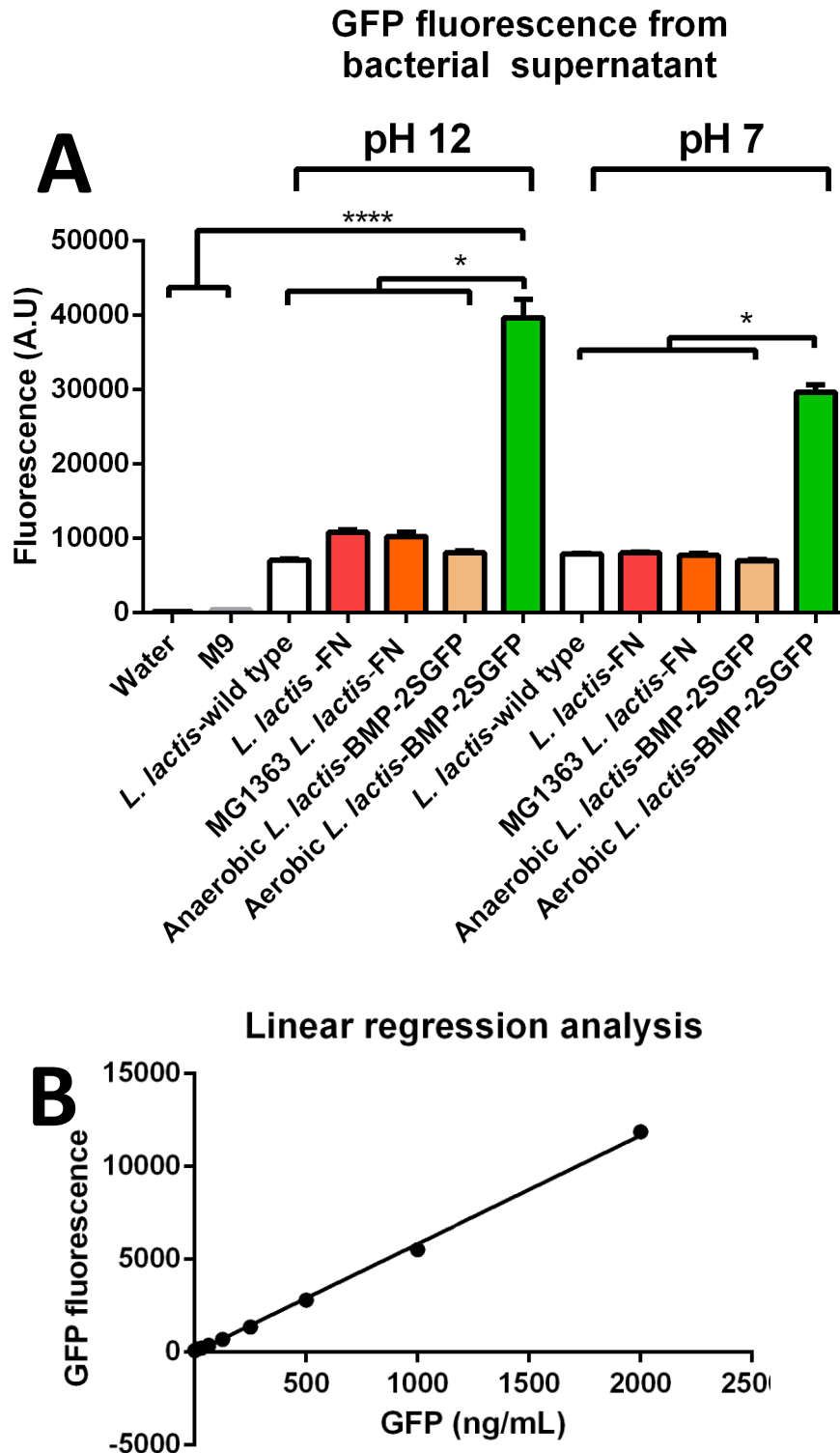


**Figure 4.3. GFP fluorescence assay to confirm the presence of constitutive BMP-2-GFP from NZ9000.** (A) GFP fluorescence is higher at higher pH so fluorescence at pH 7 and 12 were tested. (B) GFP at known concentrations was used for linear regression analysis in the quantification of *L. lactis*-BMP-2-GFP. Significance levels are \* $p < 0.05$  and \*\*\*\* $p < 0.0001$ . Three technical replicates were completed to allow quantification. Data is presented as the mean  $\pm$  SD and analysed with a one way ANOVA with a Tukey post-hoc test.

## FNIII<sub>7-10</sub> fragment expression in NZ9000

The FNIII<sub>7-10</sub> expressing plasmid from MG1363 was purified and transformed into electrocompetent NZ9000 using methods described previously. This was again isolated and sent for sequencing. The sequencing data showed an insert corresponding to FNIII<sub>7-10</sub>-GFP of 2.3 kb. Further to sequencing, a western blot shown in Figure 4.4 was completed showing the presence of GFP at approximately 85 kDa. GFP-FNIII<sub>7-10</sub>-SpA has a molecular weight of 87.4 kDa and therefore the weight is slightly off. However, the sequence data shows the correct insertion and the presence of GFP is confirmed. GFP was used as a standard to create a standard curve for the accurate quantification of GFP in the bacterial cell wall fragments and it was found that there were approximately 6.36 ng/cm<sup>2</sup> of FNIII<sub>7-10</sub> for mammalian cells to interact with.

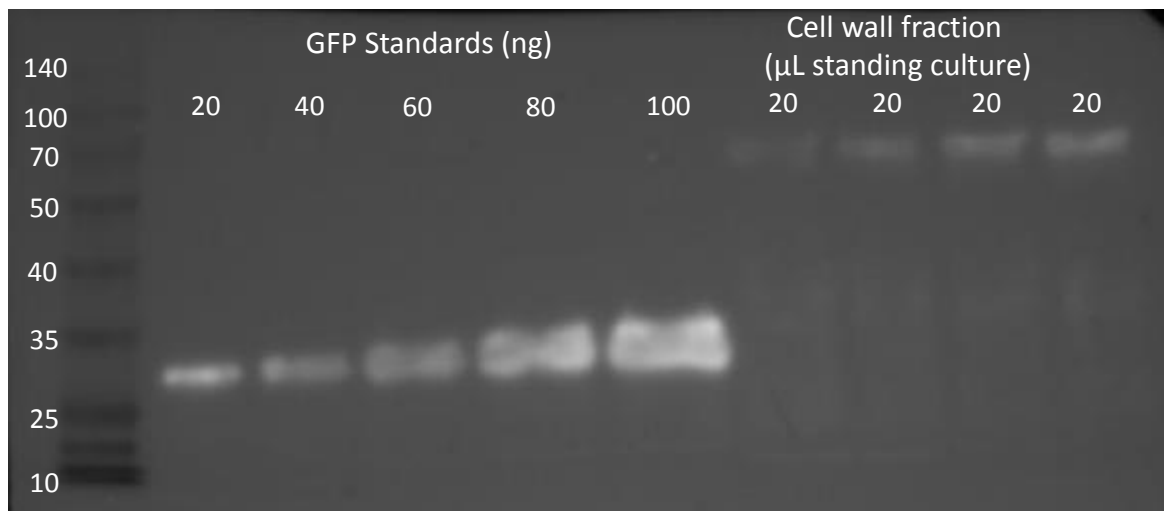


**Figure 4.4. Western Blot against constitutive NZ9000 cell wall bound FNIII<sub>7-10</sub>-GFP.** From left to right colour prestained protein ladder (NEB), GFP standards at 20, 40, 60, 80 and 100 ng and 20 μL cell wall fractions of standing culture. GFP has a molecular weight of 26.9 kDa and can be seen at approximately 28 kDa and GFP-FNIII<sub>7-10</sub>-spaX has a molecular weight of 87 kDa and can be seen at 80 kDa. Three western blots were completed to allow quantification.

## Inducible expression

### Cell wall expressing BMP-2 in NZ9000

Plasmids were isolated and sent for sequencing. An insertion of 999 bp was found corresponding to Usp45, 6x HisTag, BMP-2 and spaX. Further to sequencing, a western blot against the HisTag was completed. Nisin was added at differing concentrations (0, 0.5, 1, 5 and 10 ng/mL) one hour after fresh M17 was inoculated with 1 % of saturated bacterial culture and left to grow for five hours before a western blot was completed against the 6x Histag sequence. FNIII<sub>7-10</sub>-Histag was used to make a standard curve and band densitometry analysis was used to calculate protein expression. Figure 4.5A shows that upon increasing

amounts of nisin, more BMP-2W was found in the blot. Figure 4.5B highlights that production of protein increases as a function of nisin addition. At 10 ng/mL of nisin, BMP-2W was found at 8.79ng/cm<sup>2</sup>. The dotted line on the graph represents the amount of BMP-2W-GFP present in the constitutive clone (6.65 ng/cm<sup>2</sup>). The blot also shows that the nisA promoter is not leaky as there is no protein found in the 0 ng/mL channel. Protein expression was seen to be highest in the 10 ng/mL sample, being marginally higher than protein expression in the constitutive samples.

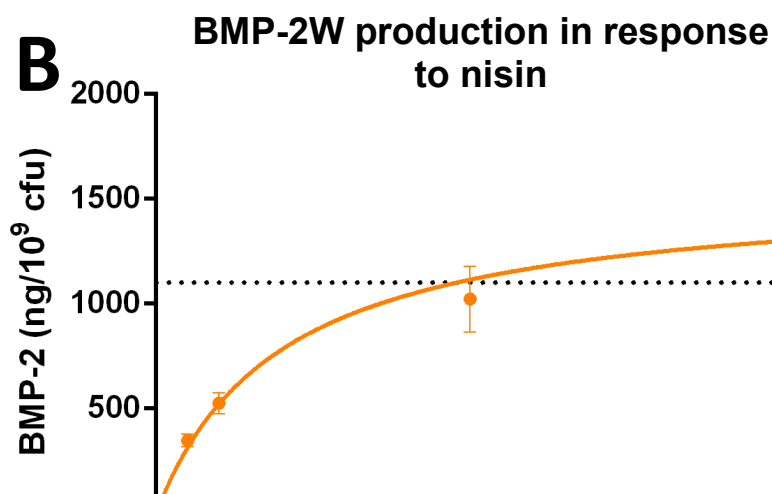
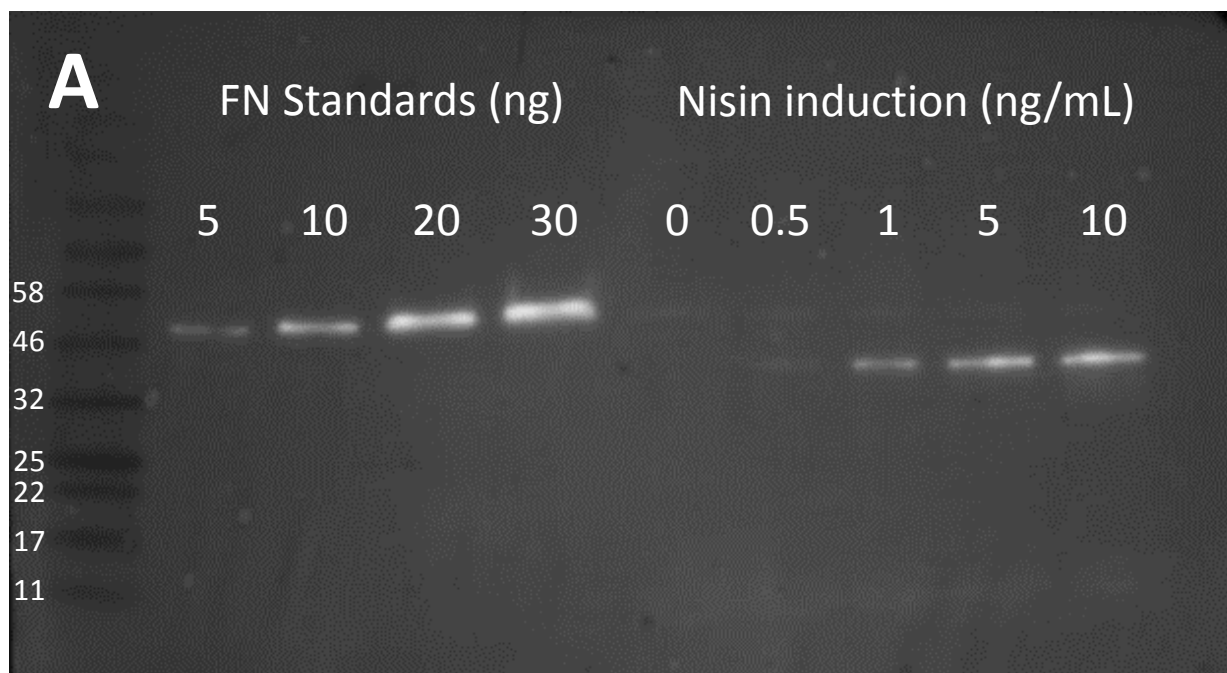


**Figure 4.5. Western blot against inducible NZ9000 cell wall bound BMP-2.** (A) From left to right colour prestained protein ladder (NEB), FN standards at 5, 10, 20 and 30 ng and 20  $\mu$ L cell wall fractions of standing culture under different nisin induction profiles. FN standard has a molecular weight of 44 kDa and can be seen at approximately 46 kDa and BMP-2W-spaX has a molecular weight of 32 kDa and but can be seen above 32 kDa. (B) A plot of BMP-2W concentration at different levels of inducer shows protein expression at 10 ng/mL is slightly higher than in the constitutive clone. The plotted line follows the equation  $Y = B_{max} * X / (K_d + X)$ ,  $R^2 = 0.9765$ . The dotted line represents protein expression in the constitutive clone. Three western blots were completed to allow quantification.

### Secreted expression of BMP-2 in NZ9000

Plasmids were isolated and sequenced in the same manner as described previously. An inframe insertion of 442 bp corresponding to Usp45, 6x HisTag, BMP-2 followed by a stop codon was found. Further to sequencing, an ELISA for the 6x HisTag was completed (Figure 4.6). Nisin was added at differing concentrations (0, 0.1, 0.5, 1 and 10 ng/mL) one hour after fresh M17 was inoculated with 1 % of saturated bacterial culture and left to grow for five hours before completing a competitive ELISA. It was found that at 10 ng/mL (plateau reached at approximately 2 ng/mL of nisin) BMP-2 was secreted at 18.6  $\mu$ g/mL, a value 46 times greater than that from the constitutive clone.

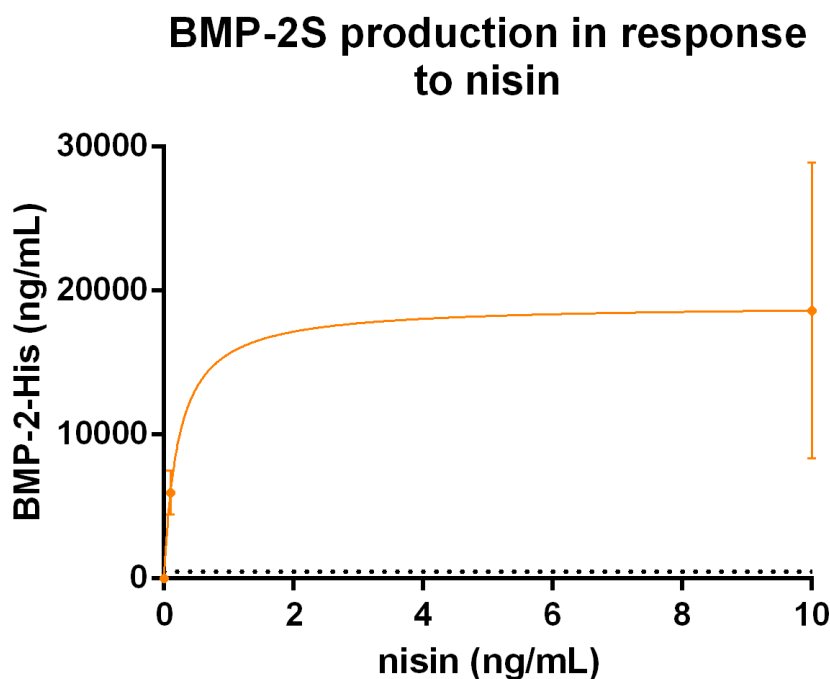


**Figure 4.6. ELISA data for inducible NZ9000 secreted BMP-2.** Protein production was seen to increase upon additive amounts of nisin up to 2 ng/mL where a plateau in protein production was seen. Maximal expression was found to be 18.6  $\mu$ g/mL. The plotted line follows the equation  $Y = B_{max} * X / (K_d + X)$ ,  $R^2 = 0.8389$ . Three technical replicates were completed to allow quantification.

### FNIII<sub>7-10</sub> fragment expression in NZ9000

Sequencing the isolated plasmid revealed an insert corresponding to FNIII<sub>7-10</sub>-GFP of 2.3 kb. A western blot against FNIII<sub>7-10</sub> was completed to further ascertain protein expression. Nisin was added at differing concentrations (0, 0.1, 0.5, 1 and 10 ng/mL) one hour after fresh M17 was inoculated with 1 % of saturated bacterial culture and left to grow for five hours.

Figure 4.7A shows a western blot against FNIII<sub>7-10</sub> and the corresponding amounts of FNIII<sub>7-10</sub>-GFP produced. Figure 4.7B illustrates a plateau of FNIII<sub>7-10</sub>-GFP production at approximately 2 ng/mL of nisin in the media. The dotted line on the graph represents the amount of FNIII<sub>7-10</sub> present in the constitutive clone. This shows that when the nisA promoter of pNZ8123 is activated, it is roughly 120 (853 ng/cm<sup>2</sup> vs 6.36ng/cm<sup>2</sup>) times stronger than the P1 promoter found in pT1NX, at least for FNIII<sub>7-10</sub> production. The blot also shows no induction in the 0 ng/mL channel showing that the promoter is not leaky.

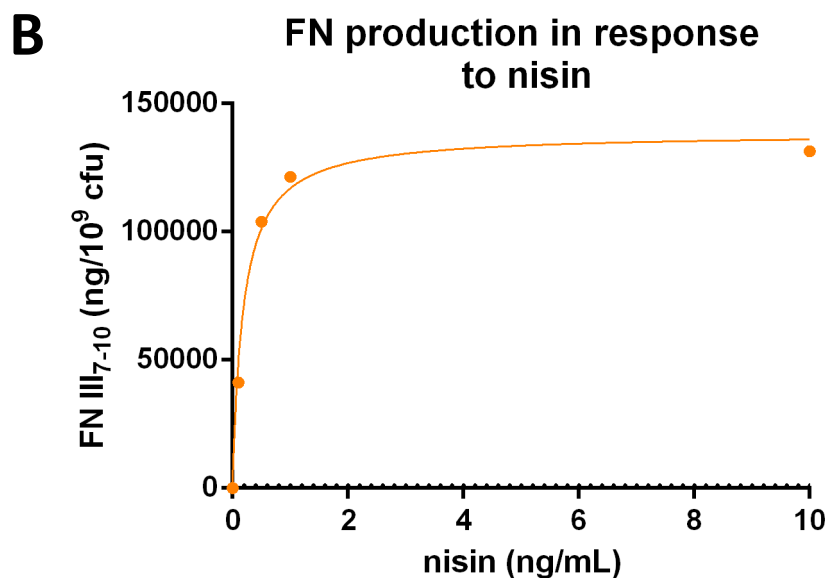
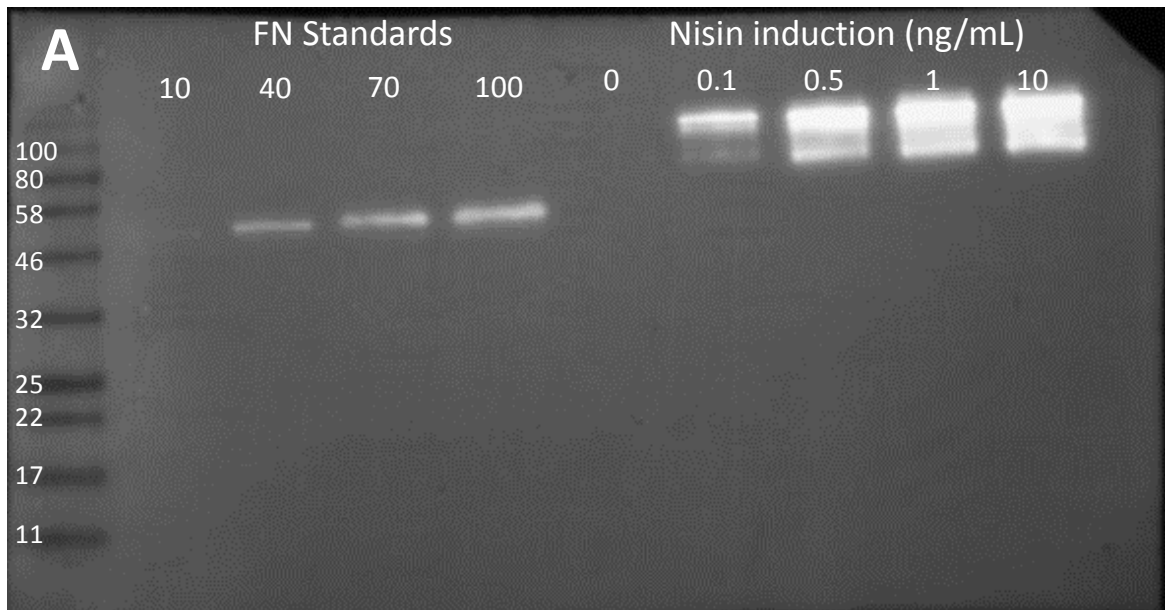


**Figure 4.7. Western blot against inducible NZ9000 cell wall bound FNIII<sub>7-10</sub>-GFP under different concentrations of nisin.** (A) From left to right colour prestained protein ladder (NEB), FN standards at 10, 40, 70 and 100 ng, FNIII<sub>7-10</sub>-GFP at 0, 0.1, 0.5, 1 and 10 ng/mL nisin. FNIII<sub>7-10</sub>-HisTag standard has a molecular weight of 44 kDa and can be seen at approximately 46 kDa and GFP-FN-spaX has a molecular weight of 87 kDa and can be seen at a this approximate molecular weight. (B) Below, a plot of FNIII<sub>7-10</sub> concentration at different levels of inducer shows a plateau of production at approximately 2 ng/mL. The plotted line follows the equation  $Y = B_{max} * X / (K_d + X)$ ,  $R^2 = 0.9998$ . The dotted line represents protein expression in the constitutive clone. One replicate was used to quantify protein expression.

### 4.3.2 Bacterial viability

As discussed in the previous chapter, MSCs must be cultured for 3-4 weeks before late markers of osteogenesis are expressed. Therefore, bacterial viability up to this time point must also be studied to allow for continuous ligand (FNIII<sub>7-10</sub>) and growth factor delivery (BMP-2). The use of antibiotic is also essential to prevent overgrowth of bacteria. Previously, the use of tetracycline (TC) was used as it is bacteriostatic in its nature and retards the metabolism of the biofilm. We found that adding TC at 10 µg/mL was sufficient to prevent bacterial cell growth but not potent enough to kill the bacteria (Saadeddin, Rodrigo-Navarro et al. 2013, Rodrigo-Navarro, Rico et al. 2014, Hay, Rodrigo-Navarro et al. 2016). However, as TC acts by blocking protein synthesis (Geigenmuller and Nierhaus 1986), a new antibiotic needed to be chosen. The use of TC would block the synthesis of BMP-2 and thus prevent osteogenesis of MSCs. Sulfamethoxazole (SMX) acts as an analogue to a prime precursor in the folate synthesis pathway in both gram positive and negative bacteria. Folate is an essential metabolite for bacterial growth and replication as it is used for both DNA synthesis of thymidylate and purine bases and amino acid synthesis. Therefore, blocking folate production leads to the obstruction of bacterial cell growth and therefore SMX is considered a bacteriostatic antibiotic (Burchall 1973, Hitchings 1973). SMX's capability to impede bacterial cell growth was tested at different concentrations and can be seen in Figure 4.8A. It can be seen that bacterial viability in DMEM without antibiotic is good, as was shown in the previous chapter. Two different concentrations of SMX were studied, 5 and 10 µg/mL. Bacteria in the 10 µg/mL samples were seen to be less viable than in the 5 µg/mL samples. Moreover, the 5 µg/mL samples also managed to impede bacterial cell growth. This can also be seen in the graphs seen in Figure 4.8B. For future experiments, the use of 5 µg/mL SMX was chosen as it is concentrated enough to prevent bacterial growth whilst also keeping the biofilm healthy. This is essential as the preservation of the biofilm is of utmost importance for the continuous signalling of the FNIII<sub>7-10</sub> fragment and BMP-2.

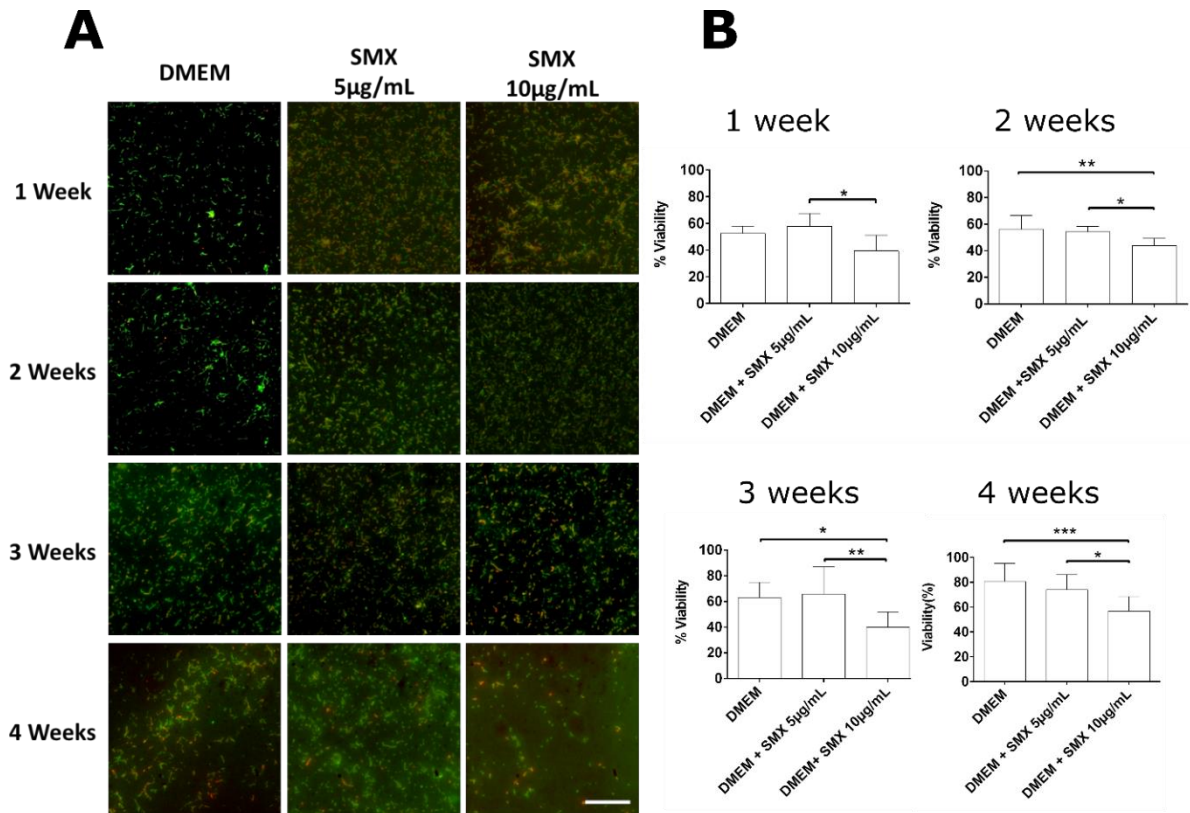


**Figure 4.8. Bacterial viability.** (A) Biofilms of *L. lactis*-FN were produced on a poly (ethyl acrylate) (PEA) surface and cultured for 1 to 4 weeks with DMEM, DMEM supplemented with 5 µg/mL sulfamethoxazole (DMEM + SMX 5). After selected time points, biofilms were washed and their viability assessed using the commercial BacLight viability kit (Life Technologies). This kit stains viable cells in green and non-viable cells in red. Viability was calculated by analysing the total amount of cells stained in green versus the amount of cells stained in red and green. Scale bar is 100 µm. (B) Bacteria were seen to be less viable on DMEM SMX 10 µg/mL at all time points. Viability results were similar between DMEM and DMEM SMX 5 µg/mL. 10 images were taken from three technical replicates. Data is presented as mean ± SD and was analysed by a one way ANOVA test with a Tukey post-hoc test. Significance levels are \*p < 0.05, \*\*p < 0.01 and \*\*\*p < 0.001.

### 4.3.3 Mammalian cell viability on NZ9000

Cell viability was explored using the constitutive expression clones only. MSCs were seeded over different BMP-2 clones with *L. lactis*-FN, *L. lactis*-empty and FN-coated samples as controls for 4 weeks as this is the time required for terminal MSC differentiation.

As can be seen in Figure 4.9, MSC viability on all bacterial samples is seen to decrease over four weeks. MSCs seeded onto the FN coat show approximately 100 % viability at all time points. After one day, MSCs on all surfaces, have 100 % viability, but after this time point, cell viability begins to decrease. MSCs on the *L. lactis*-BMP-2S bacteria began to die after one day as is seen by the steep decrease on the chart after one day. There were no cells left on the samples after four days. Conversely, MSCs on all other bacterial types showed good viability up to day 14, but were severely diminished by day 21.

This decrease in cell viability may be due to the acidification of the medium, even in the presence of tetracycline, as the DMEM was seen to become yellow in colour. NZ9000 is a much more metabolically active strain than MG1363 (used in the previous chapter) and thus produces lactic acid at much higher rates. Loss of viability may also be compounded by the fact that the media had to be changed at least once a day due to the acidification of the media, and therefore, any growth factors secreted by the cells would be removed, thus altering their behaviour further. The most striking result from this experiment is the complete death of cells after one day on the *L. lactis*-BMP-2S clones. The *L. lactis*-BMP-2S-GFP did not display this result. MSC death may be due to a toxic concentration of BMP-2 in the media. However, upon searching the literature, there were no reports of BMP-2 toxicity to MSCs at this concentration.

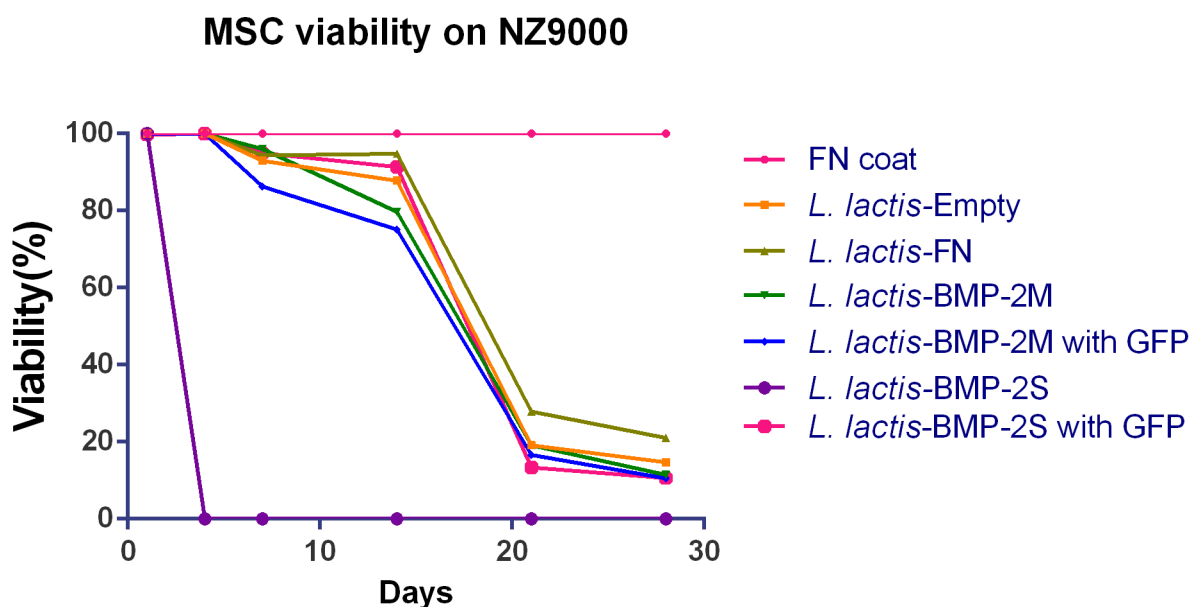


**Figure 4.9. Mesenchymal stem cell viability on NZ9000 *L. lactis* clones.** MSC viability was seen to decrease over 4 weeks on all NZ9000 *L. lactis* clones whilst viability on the FN coat was seen to stay high. 10 images were taken per condition from three technical replicates.

To deduce *L. lactis* derived BMP-2 toxicity to the cells, co-cultures of *L. lactis*-FN and *L. lactis*-BMP-2S clones were made, therefore, theoretically halving the amount of BMP-2 that the cells can interact with. Figure 4.10 shows MSC and C2C12 viability after five days on *L. lactis*-FN, *L. lactis*-BMP-2S and 50:50 co-cultures of *L. lactis*-FN and *L. lactis*-BMP-2S. As is seen in Figure 4.10, cell viability is drastically decreased in the *L. lactis*-BMP-2S samples, albeit, not complete cell death after four days as was shown in Figure 4.9. Interestingly, cell death is seen to be statistically significantly higher in MSCs when compared against C2C12s on *L. lactis*-BMP-2S. Cell viability in both MSCs and C2C12s on

*L. lactis*-FN was seen to be close to 100 % whilst the co-cultures of *L. lactis*-FN and *L. lactis*-BMP-2S display an intermediate cell viability, approximately 77 % for both MSCs and C2C12s. This result demonstrates that either the presence of the FNIII<sub>7-10</sub> fragment in the *L. lactis* cell wall or the decreased amount of BMP-2 produced by decreasing the amount of *L. lactis*-BMP-2S bacteria positively affects cell viability.

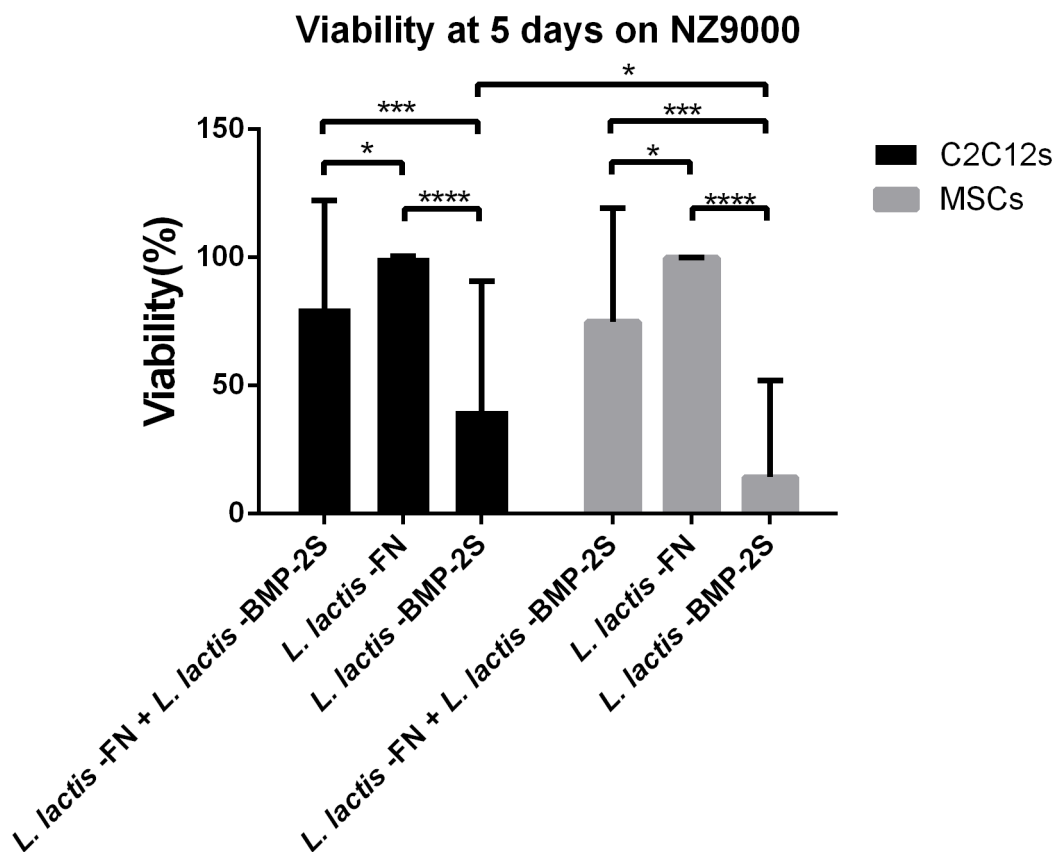


**Figure 4.10. MSC and C2C12 viability on *L. lactis*.** Viability values of co-cultures are seen to be higher than *L. lactis*-BMP-2S in both MSCs and C2C12s after 5 days. 10 images were taken per condition from three technical replicates. Data is presented as mean  $\pm$  SD and analysed with a two way ANOVA test with a Tukey post-hoc test. Significance levels are \* $p < 0.05$ , \*\*\* $p < 0.001$  and \*\*\*\* $p < 0.0001$ .

It was thus decided to use a metabolically different strain of NZ9000, NZ9020. In NZ9020, both known lactate dehydrogenase genes are knocked out and it is therefore unable to produce as much lactate as a fermentation end product, therefore decreasing the acidity of the media, keeping the pH neutral (Bongers, Hoefnagel et al. 2003). The lactate dehydrogenase genes were replaced with an erythromycin and tetracycline resistance and therefore the clones could be screened for. If NZ9020 is grown under aerobic conditions, it displays an almost complete loss of lactate production, and acetoin is found to be the main end product of fermentation, complete data can be found in Table 4.11. The presence of O<sub>2</sub> allows the cells to maintain their redox balance through the activity of endogenous NADH

oxidase. This sustains sugar fermentation without the production of lactic acid. However, under aerobic conditions, the rate of sugar fermentation is decreased, and the metabolic end products are also shifted to ethanol. This suggests that these pathways are using ethanol as an alternative electron sink, since the enzymatic conversions involved include reducing steps that use NADH as a cofactor. To combat the use of ethanol as an electron sink, many authors have described the use of heme in *L. lactis* aerobic respiration (Sijpesteijn 1970, Ritchey and Seely 1976, Arioli, Zambelli et al. 2013). By inhibiting fermentative metabolism (anaerobic respiration) under respiration permissive conditions (heme plus oxygen), oxidation of NADH is shifted toward the electron transport chain via cytochrome bd oxidase. This would enable the successful culture of *L. lactis* without the inevitable decrease in pH that is so detrimental to mammalian cell culture. Figure 4.11 highlights the use of hemin in aerobic respiration in *L. lactis*.

Figure 4.12 shows the final pH of bacterial cell supernatant using different strains. As can be seen, the pH in NZ9020 cell supernatant is higher than NZ9000 due to the lack of lactic acid being produced. The use of hemin further increases the pH. These results suggest that using NZ9020 aerobically with hemin at 5 µg/mL will be best for mammalian cell culture. All long term mammalian cell co-culture with NZ9020 used hemin from hereon.

**Table 4.11. *L. lactis* metabolism under different conditions (Bongers, Hoefnagel et al. 2003).**

Strain	Aerobe	Final OD	Final pH	Concentration (mmol/L) of product formed						
				Lactate	Formate	Acetate	Acetoin	Butanediol	Ethanol	Pyruvate
NZ9000	+	2.9	5.13	42.7	ND	8.7	ND	0.1	ND	ND
	-	2.53	4.87	52	ND	1.2	ND	ND	ND	ND
NZ9020	+	2.68	6.27	0.6	ND	12	17.9	0.1	1.4	2.6
	-	2.89	5.54	1.5	ND	10	5.6	ND	25.2	0.5

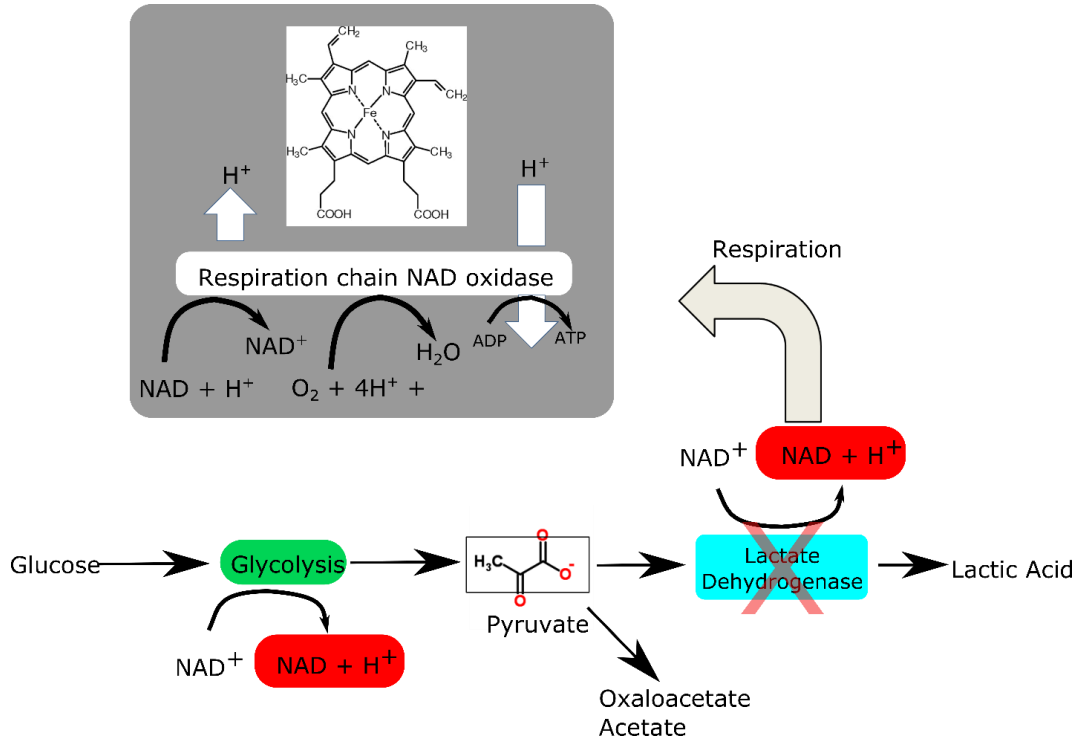


Figure 4.11. Simplified representation of glycolysis, homolactic, and mixed-acid fermentations and heme-dependent respiration in *L. lactis*.

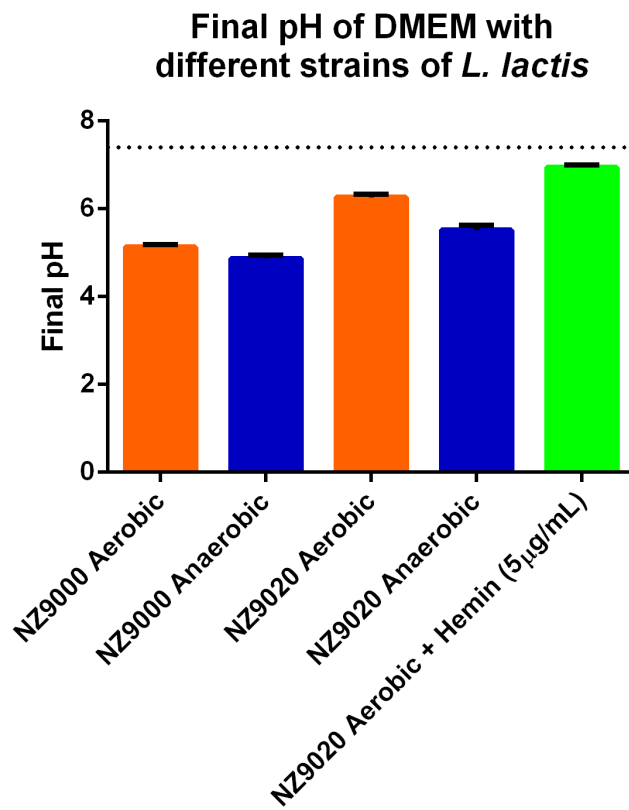


Figure 4.12. pH of M17 after 1 day of *L. lactis* growth. The pH of cultures after 1 day of growth were measured in both NZ9000 and NZ9020 when grown aerobically and anaerobically. In addition, NZ9020 grown aerobically with 5 µg/mL hemin was also tested. The dotted line represents pH 7.4, the closest growth conditions to that preferred by mammalian cells. The closest *L. lactis* to this was reached by aerobic NZ9020 with the use of hemin at 5 µg/mL. Three technical replicates were completed per sample and data is presented as mean ± SD.

#### **4.3.4 NZ9020 FNIII<sub>7-10</sub> fragment and BMP-2 expressing bacteria**

As discussed, NZ9020 is a less metabolically active strain of NZ9000 designed by Bongers *et al.* (Bongers, Hoefnagel *et al.* 2003) at Nizo Food Research in the Netherlands. It has had both its known lactate dehydrogenase enzymes removed and therefore its metabolism has been disrupted. This leads to a general decrease in growth and protein expression when compared with NZ9000. Further to this, in order to be able to screen for successful lactate dehydrogenase knockouts, the genes were replaced with tetracycline and erythromycin resistances. This posed problems for the constitutive clones as pT1NX has an erythromycin resistance gene. Therefore screening successful clones with erythromycin would be impossible, so pT1NX had to be altered. The chloramphenicol resistance gene from pNZ8123 was isolated and used to replace the erythromycin resistance gene in pT1NX, effectively creating a new plasmid that could be screened for. This new plasmid has been denoted pT2NX, and it has been used for all the constitutive protein production in NZ9020. This section shows the characterisation of constitutive and inducible expression of cell wall anchored FNIII<sub>7-10</sub> and both cell wall bound and secreted versions of BMP-2.

##### **Constitutive expression**

##### **Cell wall expressing BMP-2 in NZ9020**

Again, sequencing an isolated plasmid from the transformed bacteria highlighted an inframe insertion of a 1.7 kb fragment, corresponding to GFP-BMP-2 and an insertion of 1 kb for BMP-2 without GFP.

Further confirmation was ascertained by western blot as shown in Figure 4.13. Cell wall fragments were isolated as before and were run on a gel and transferred for western blotting. The blot displayed bands in the cell wall fraction at 60 kDa which is equal to that of GFP-BMP-2-SpaX. GFP was again added as a control and standard and was found at 27 kDa; GFP has a molecular weight of 26.9 kDa. The GFP standard curve was used to determine the concentration of BMP-2 per bacteria. Band densitometry analysis found a linear relationship between band density and protein amount. Based on this, it was determined that 20  $\mu$ L of standing culture contains approximately  $0.8 \pm 0.14$   $\mu$ g of GFP-BMP-2. Using these estimations, the approximate density of BMP-2 molecules that a mammalian cell can interact with is approximately 40,000 per bacterial cell, assuming a molecular weight of 60 kDa and fully saturated media containing  $2.2 \times 10^9$  bacteria per mL. This is equivalent to 4.84 ng/cm<sup>2</sup> of cell wall bound BMP-2. This is a lower amount of BMP-2W than was found for NZ9000 but this is expected due to the lower metabolic activity of NZ9020.

These results also suggest that the presence of BMP-2W and BMP-2W-GFP are not detrimental for bacterial viability of the NZ9020 strain.

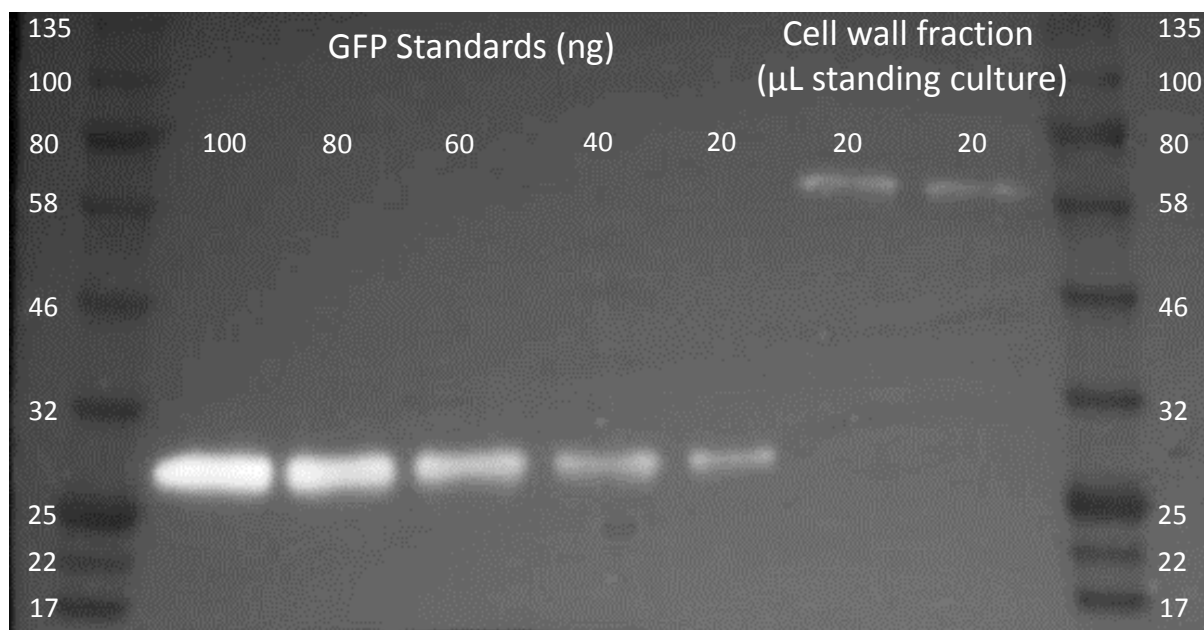
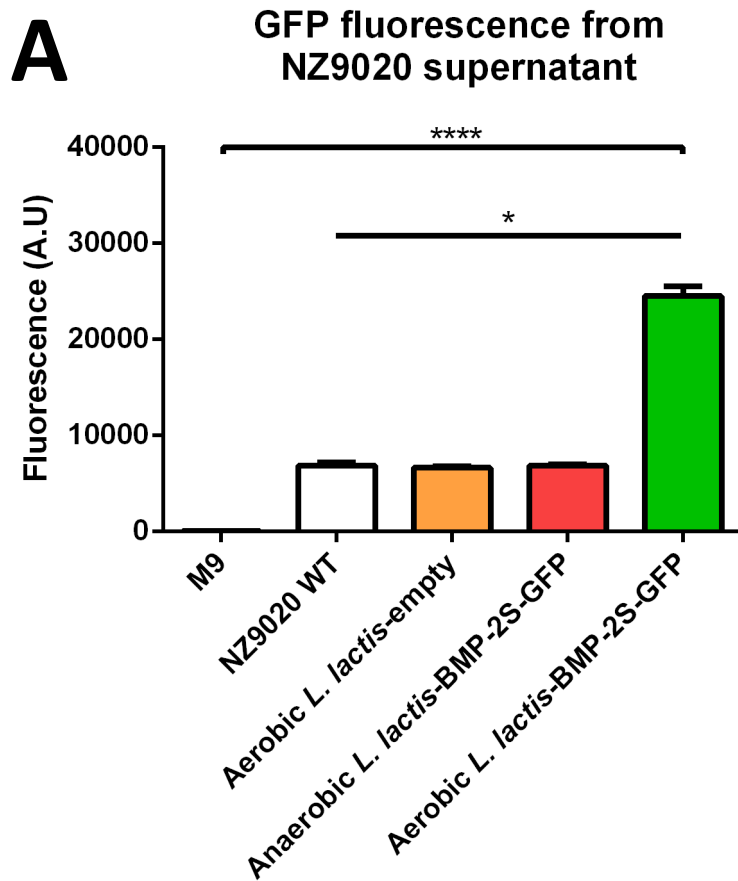


**Figure 4.13. Western blot against constitutive NZ9020 cell wall bound GFP-BMP-2.** From left to right colour prestained protein ladder (NEB), GFP standards at 100, 80, 60, 40 and 20 ng and 20 µL cell wall fractions of standing culture and colour prestained protein ladder (NEB). GFP has a molecular weight of 26.9 kDa and can be seen at approximately 28 kDa and GFP-BMP-2-spaX has a molecular weight of 60 kDa and can be seen at 60 kDa. Three western blots were completed to allow quantification.

### Secreted expression of BMP-2 in NZ9020

Expression of constitutive secreted BMP-2 in NZ9020 was completed in the same manner as for NZ9000. Plasmids were isolated and sequenced, the plasmid revealed the inclusion of an inframe 1.7 kb fragment comprising GFP and BMP-2 with a stop codon between BMP-2 and *spaX* allowing protein secretion. A fluorescence assay was again completed showing the presence of GFP in the bacterial supernatant shown in Figure 4.14A. As was seen with NZ9000, GFP fluorescence was seen to be highest in the aerobically grown *L. lactis* BMP-2S-GFP samples. A standard curve shown in Figure 4.14B was made and highlighted that NZ9020 secretes 598 ng/mL of BMP-2S-GFP, which due to the need for dimerisation translates to a working concentration of 299 ng/mL of biologically active BMP-2. This is again, lower than the amount found from NZ9000.



**B** Linear regression analysis

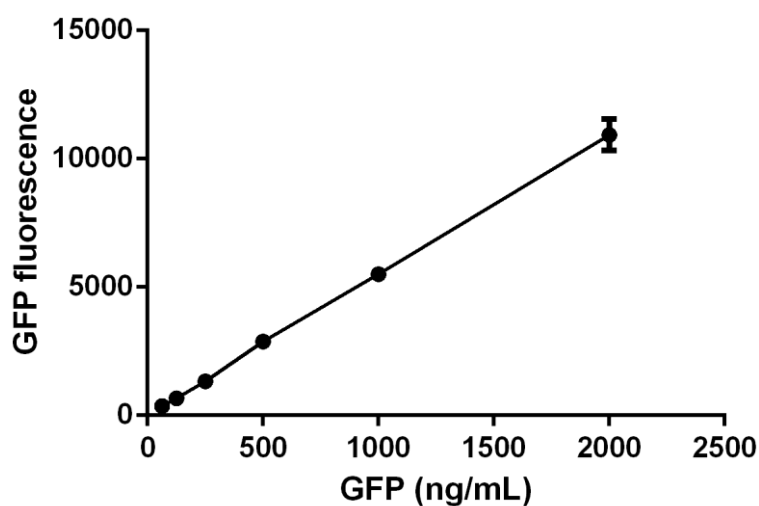


**Figure 4.14. GFP fluorescence assay to confirm the presence of constitutive NZ9020 BMP-2-GFP.** (A) GFP at known concentrations was used for linear regression analysis (B) in the quantification of *L. lactis*-BMP-2-GFP. Data is presented as mean  $\pm$  SD and was analysed by a one way ANOVA test with a Tukey post-hoc test. Significance levels are \* $p < 0.05$  and \*\*\*\* $p < 0.0001$ . Three technical replicates were used for quantification.

## FNIII<sub>7-10</sub> fragment expression in NZ9020

Insertion of the gene was again seen via sequencing data showing an insert of 2.3 kb, corresponding to Usp45, GFP, FNIII<sub>7-10</sub> and the spaX anchor. Figure 4.15 shows a western blot against GFP for quantitation of FNIII<sub>7-10</sub>. GFP was once again used to make a standard curve to ascertain the concentration of FNIII<sub>7-10</sub> per bacteria. Band densitometry analysis was used, finding a linear relationship between band density and protein amount. Based on this, the approximate density of FNIII<sub>7-10</sub> in 1 mL of saturated culture contained 5.84 ng/cm<sup>2</sup> of protein, a similar result to that found for FNIII<sub>7-10</sub> when synthesised in MG1363 and NZ9000 (6.36 ng) (Saadeddin, Rodrigo-Navarro et al. 2013).

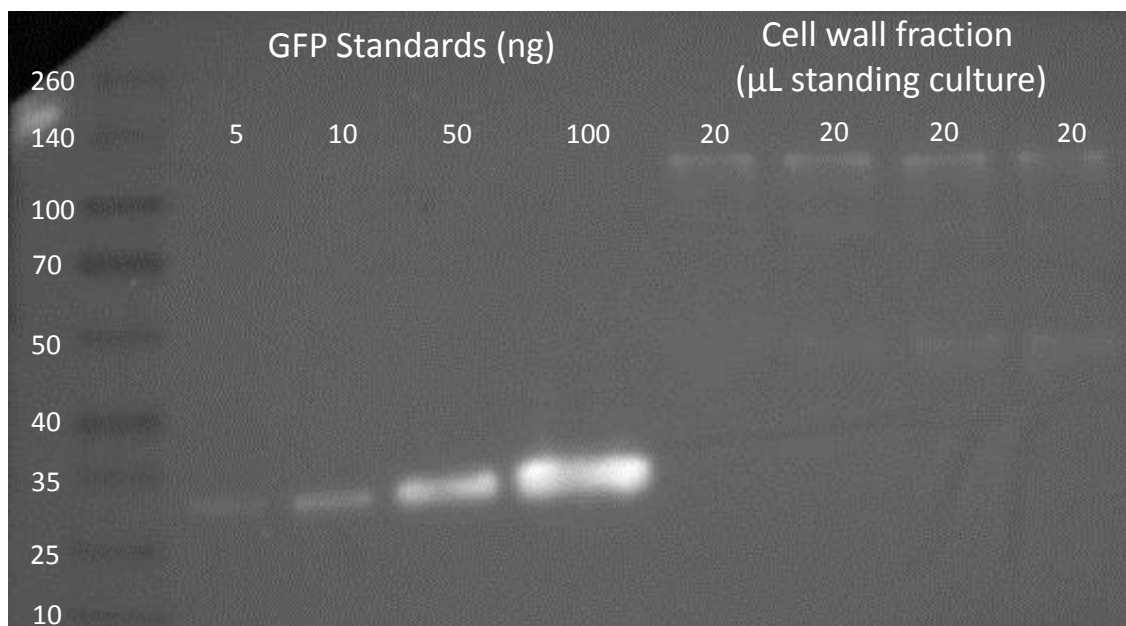


**Figure 4.15. Western blot against constitutive NZ9020 cell wall bound FNIII<sub>7-10</sub>-GFP.** From left to right colour prestained protein ladder (NEB), GFP standards at 5, 10, 50 and 100 ng and 20 μL cell wall fractions of standing culture. GFP has a molecular weight of 26.9 kDa and can be seen at approximately 28 kDa and GFP-FNIII<sub>7-10</sub>-spaX has a molecular weight of 87 kDa and but can be seen above 100 kDa. Three western blots were completed to allow quantification.

## Inducible expression

### Cell wall expressing BMP-2 in NZ9020

Plasmids were isolated and sent for sequencing. An insertion of 999 bp was found corresponding to Usp45, 6x HisTag, BMP-2 and spaX. Further to sequencing, a western blot against the HisTag was completed. Nisin was added at differing concentrations (0, 0.5, 1, 5 and 10 ng/mL) one hour after fresh M17 was inoculated with 1 % of saturated bacterial culture and left to grow for five hours before a western blot (Figure 4.16A) was completed against the 6x Histag sequence. FNIII<sub>7-10</sub>-Histag was used to make a standard curve and band

densitometry analysis was used to calculate protein expression. It is apparent from Figure 4.16A that nisin induction at different concentrations induces different protein expression, which has been quantified in Figure 4.16B. Interestingly, protein expression is seen to be higher in NZ9020 than in NZ9000 (Figure 4.5), however, this is only at the 10 ng/mL sample. NZ9000 protein expression was seen to be higher at the other nisin induction concentrations. The dotted line represents the amount of BMP-2W-GFP synthesised in the constitutive samples. Protein expression under the *nisA* promoter (pNZ8123) is seen to be much higher than under the P1 promoter (pT1/2NX). No protein expression was found in the 0 ng/mL nisin sample showing that the promoter is not leaky.

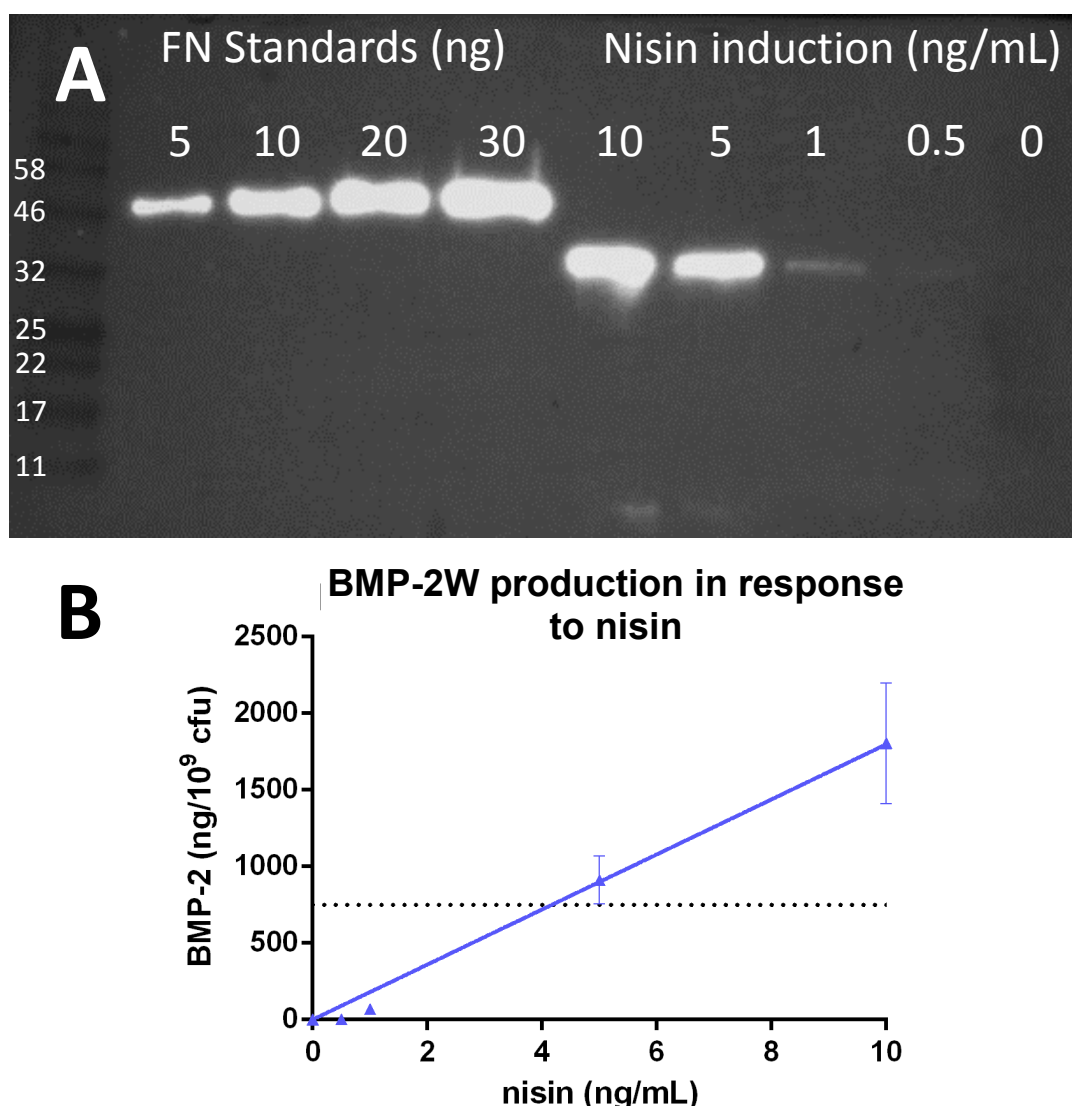


**Figure 4.16. Western blot against inducible NZ9020 cell wall bound BMP-2.** (A) From left to right colour prestained protein ladder (NEB), FN standards at 5, 10, 20 and 30 ng and 20  $\mu$ L cell wall fractions of standing culture under different nisin induction profiles. FN standard has a molecular weight of 44 kDa and can be seen at approximately 46 kDa and BMP-2W-*spaX* has a molecular weight of 32 kDa and but can be seen above 32 kDa. (B) A plot of BMP-2W concentration at different levels of inducer shows protein expression at 10 ng/mL is approximately double to that found in the constitutive clone. The dotted line represents protein expression in the constitutive clone. The plotted line follows the equation  $Y = B_{max} * X / (K_d + X)$ ,  $R^2 = 0.9475$ . Three western blots were completed to allow quantification.

### Secreted expression of BMP-2 in NZ9020

Plasmids were isolated and sequenced. An inframe addition 442 bp corresponding to Usp45, 6x HisTag, BMP-2 followed by a stop codon was found. An ELISA for 6x HisTag was also completed (Figure 4.17) to deduce BMP-2 concentration. Nisin was added at differing concentrations (0, 0.1, 0.5, 1 and 10 ng/mL) one hour after fresh M17 was inoculated with 1 % of saturated bacterial culture and left to grow for five hours before completing a competitive ELISA. It was found that protein expression was highest at 10 ng/mL of nisin (plateau was reached at approximately 2 ng/mL nisin) at 183 ng/mL, a value that is less than that observed in the constitutive clone (299 ng/mL).

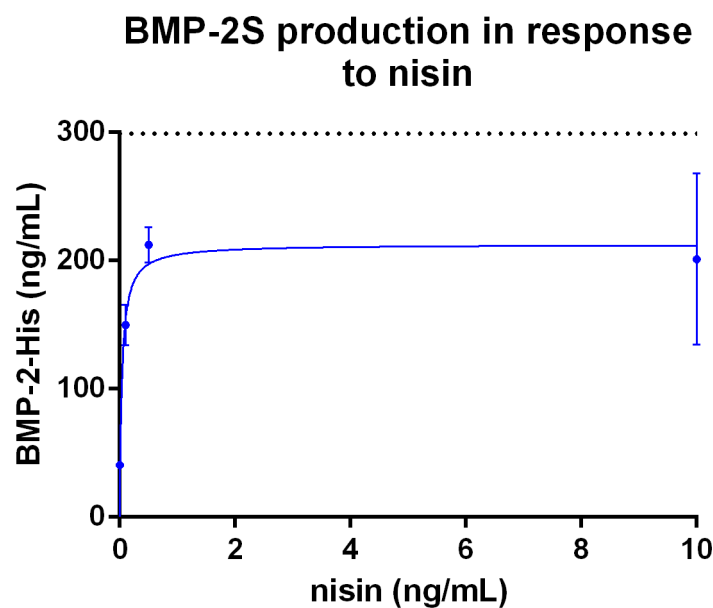


**Figure 4.17. ELISA data for inducible NZ9020 secreted BMP-2.** Protein production was seen to increase upon additive amounts of nisin up to 2 ng/mL where a plateau in protein production was seen. Maximal expression was found to be 183 ng/mL. The plotted line follows the equation  $Y = B_{max} * X / (K_d + X)$ ,  $R^2 = -3.958$ . Three technical replicates were used to quantify BMP-2 secretion.

### FNIII<sub>7-10</sub> fragment expression in NZ9020

Sequencing isolated plasmid revealed an insert corresponding to FNIII<sub>7-10</sub>-GFP of 2.3 kb. A western blot against FNIII<sub>7-10</sub> was also completed to ascertain protein expression. Nisin was added at differing concentrations (0.1, 1, 5 and 10 ng/mL) one hour after fresh M17 was inoculated with 1 % of saturated bacterial culture and left to grow for five hours. Figure 4.18A shows a western blot against GFP and the corresponding amounts of FNIII<sub>7-10</sub> produced. Figure 4.18B shows a graphical representation of FNIII<sub>7-10</sub> production under nisin and shows a different result to that of NZ9000, there is less protein expression in NZ9020

(359 ng/cm<sup>2</sup> against 853 ng/cm<sup>2</sup>). The dotted line represents the amount of FNIII<sub>7-10</sub> found in the NZ9020 constitutive plasmid, protein expression under the nisin promoter is 62 times higher than under P1.

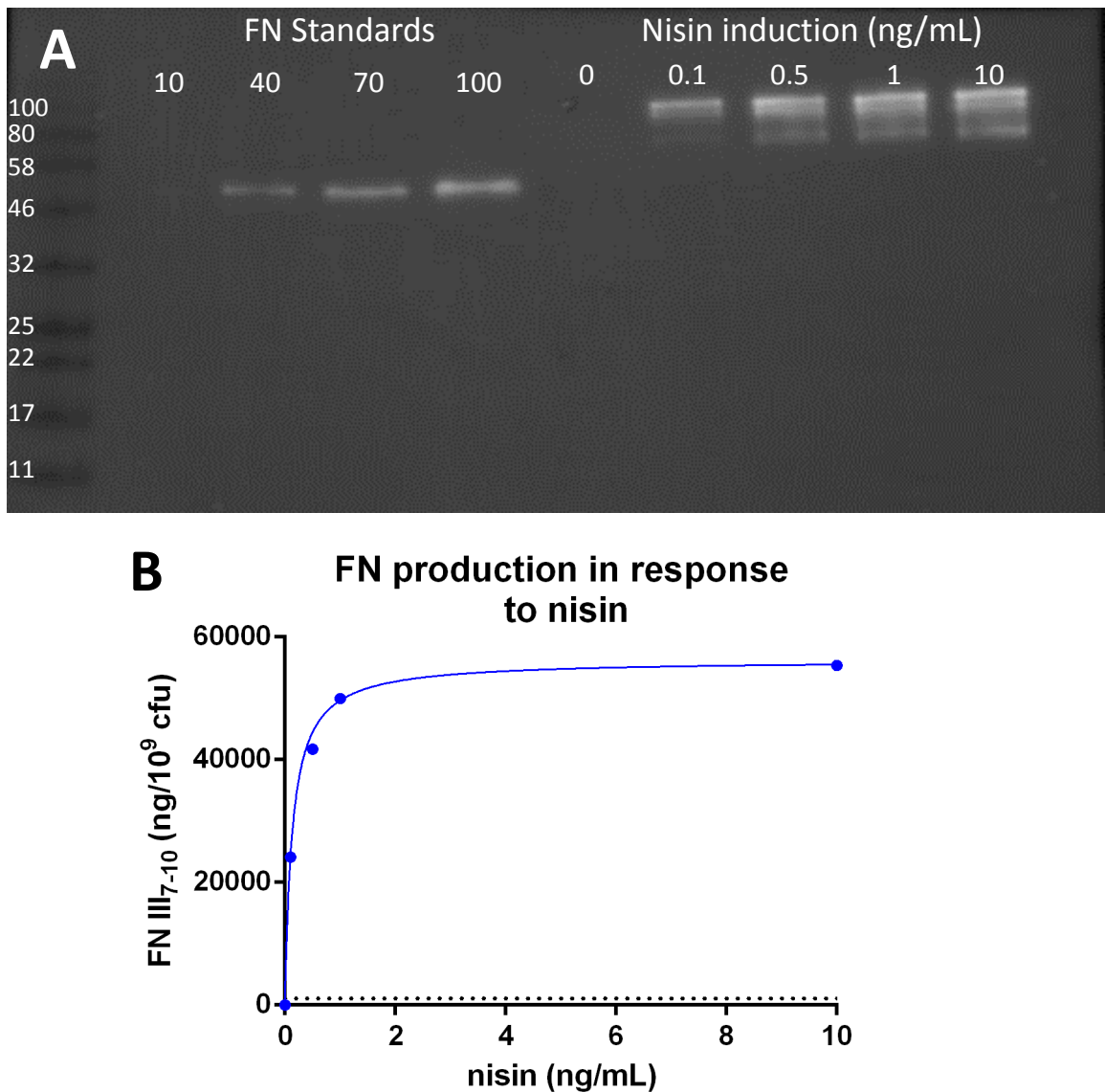


**Figure 4.18. Western blot against inducible NZ9020 cell wall bound FNIII<sub>7-10</sub>-GFP under different concentrations of inducer. (A)** From left to right colour prestained protein ladder (NEB), FN standards at 10, 40, 70 and 100 ng, FNIII<sub>7-10</sub>-GFP at 0, 0.1, 0.6, 1 and 10 ng/mL nisin. FN standard has a molecular weight of 44 kDa and can be seen at approximately 46 kDa and GFP-FNIII<sub>7-10</sub>-spaX has a molecular weight of 87 kDa and can be seen at this approximate weight. **(B)** A plot of FNIII<sub>7-10</sub> concentration at different levels of inducer shows a plateau of production, at approximately 2 ng/mL. The dotted line represents protein expression in the constitutive clone. The plotted line follows the equation  $Y = B_{max} * X / (K_d + X)$ ,  $R^2 = 0.9942$ . One replicate was used to quantify protein expression.

### 4.3.5 Mammalian cell viability on NZ9020

As can be seen from Figure 4.19, mammalian cell viability on NZ9020 grown with hemin is drastically different compared to NZ9000 (Figure 4.9). MSCs are seen to be at 99 % viability up until 21 days on all sample substrates. Unlike NZ9000, there is no rapid viability decrease on *L. lactis*-BMP-2S after one day, and there is also no slight viability decrease on the other *L. lactis* samples after 14 days. This is due to the lack of lactic acid production in NZ9020 when compared with NZ9000. Also, the presence of hemin allows this bacterium to utilise aerobic respiration more effectively. Viability on the FN coat is seen to be 99 % for the whole four weeks with no statistical differences at any time point, whereas, viability drops to approximately 95 % after 21 days on all bacterial substrates. The exact reason for this is not known, but the small increase in acetoin in the medium may cause the small increase in cell death. Overall, mammalian cells cultured over NZ9020 show a much higher cell viability than on NZ9000 (Figure 4.9).

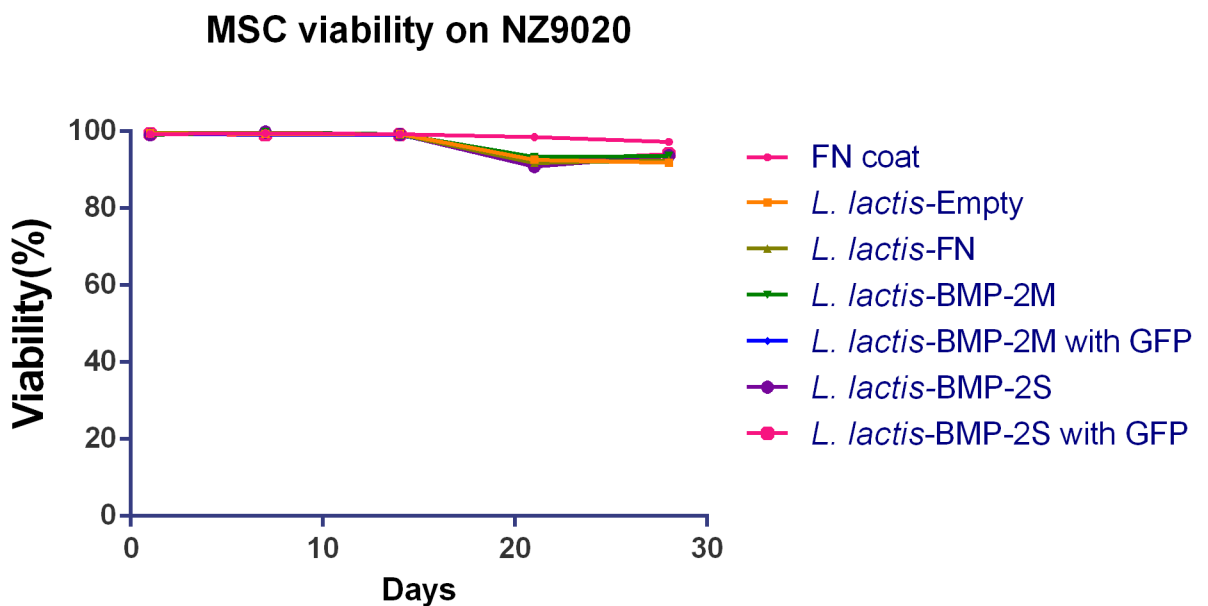


**Figure 4.19. Mesenchymal stem cell viability on NZ9020 *L. lactis* clones.** MSC viability was seen to be more stable on all NZ9020 *L. lactis* clones. Viability on the FN coat was also seen to stay high. 10 images were taken per condition from three technical replicates.

## 4.4 Discussion

*L. lactis* is a gram positive lactic acid bacterium that has been used for centuries in food fermentation. However, within the last 35 years, great progress has been made in using this organism in genetic engineering for the therapeutic delivery of proteins. More specifically, the HPV-16 E7 antigen was cloned and synthesised in a secreted form to aid in the fight against cancer (Benbouziane, Ribelles et al. 2013). Interleukin 27 has also been engineered to be secreted using the same plasmid used in this thesis (pT1NX) to alleviate the symptoms of colitis in mice (Hanson, Hixon et al. 2014). This organism can be used to produce proteins in a constitutive and inducible fashion which has been described in this chapter. The use of gram positive bacteria for heterologous protein production proves to be a useful choice due to easy protein secretion.

Furthermore, the gold standard for bacterially produced recombinant proteins has been *E. coli*. However, the most commonly used production strategies for *E. coli* utilise intracellular or periplasmic expression and involve expensive and potentially problematic downstream purification processes. Moreover, LPS should be removed from proteins needed to be administered to humans. The presence of LPS makes protein use in humans impossible. Moreover, expressed proteins are likely to be hidden in a mesh of bacterial ECM (Froon, Dentener et al. 1995, Maestroni 2001).

In addition to previous publications where FNIII<sub>7-10</sub> was produced in *L. lactis* MG1363 (Saadeddin, Rodrigo-Navarro et al. 2013, Rodrigo-Navarro, Rico et al. 2014, Hay, Rodrigo-Navarro et al. 2016), we have demonstrated the completion of BMP-2 expressing *L. lactis* NZ9000 and NZ9020. This known osteoinducer has the capability to induce the differentiation of MSCs to osteoblasts as was shown in the previous chapter.

The genetic modification of this strain has been completed using the versatile Gibson assembly technique (Gibson, Young et al. 2009) whereby primer overlaps are designed to allow the quick and efficient annealing of multiple fragments. With the correct primer design, facilitated by easy design software and commercial availability, Gibson assembly has fast become an extremely powerful and highly used technique. Overlaps can be designed in a single primer and PCR allows the elongation of large plasmid backbones which can be modified with the addition of other DNA sequences by the overhanging primers.

The data has demonstrated that FNIII<sub>7-10</sub> can be produced in both NZ9000 and NZ9020 with both pT1NX for constitutive expression and pNZ8123 for inducible expression and that

protein production under the nisin promoter is directly controlled by nisin concentration in the media.

Furthermore, it can be concluded from the results that BMP-2 has been synthesised in both cell wall bound and secreted forms by the inducible and secreted plasmids. This was confirmed by the addition of a fusion GFP or His-tag reporter protein. GFP is a widely used expression reporter originally cloned from the jellyfish *Aequorea Victoria* and displays a bright green fluorescence when illuminated under ultraviolet light (Tsien 1998).

Another widely used reporter protein is the polyhistidine tag (Hochuli, Bannwarth et al. 1988). Histidine clusters of a minimum of four repeats interact with divalent cations that, when immobilised with metal ion matrices, electron donor groups on the histidine imidazole ring readily form coordination bonds with the immobilised transition metal (Block, Maertens et al. 2009). Peptides containing sequences of consecutive histidine residues are efficiently retained on immobilised metal-affinity chromatography (IMAC) columns. Following washing of the matrix material, peptides containing polyhistidine sequences can be easily eluted by either adjusting the pH of the column buffer or by adding free imidazole (Terpe 2003, Block, Maertens et al. 2009). The proteins were expressed with the Usp45 secretion peptide and SpaX anchoring protein allowing either cell wall bound or secreted expression. Western blots, ELISAs and fluorescence assays were used to ascertain protein production levels in NZ9000 and NZ9020.

Interestingly, it was mostly found that protein production was slightly higher in NZ9000 than NZ9020 due to the discrepancies in the metabolic activity of the strains. For all proteins except BMP-2W, NZ9000 was found to synthesise more protein than NZ9020.

A large disparity in protein concentration under the nisin promoter was found between FNIII<sub>7-10</sub> and BMP-2W. Under the P1 promoter, protein expression was seen to be highly similar for BMP-2W and FNIII<sub>7-10</sub> in both NZ9000 and NZ9020. However, under nisin expression, FNIII<sub>7-10</sub> was seen to be expressed at much higher amounts. Reasons for this could vary from simple steric hindrance (FNIII<sub>7-10</sub> fragment is much further from the bacterial cell wall and can therefore be more easily accessed) to codon optimisation (Gold 1988, deRuyter, Kuipers et al. 1996). Further to this, the size and conformation of the protein can often have an effect on the efficiency of synthesis (Francis and Page 2010, Sabate, de Groot et al. 2010, Bonde, Pedersen et al. 2016). BMP-2S under the nisin promoter was also seen to have a large protein expression increase compared to P1 in NZ9000. However, BMP-2S under the nisin promoter in NZ9020 was seen to decrease in protein expression compared to P1. The increase in

NZ9000 BMP-2S under the nisin promoter compared to P1 and decrease in BMP-2S expression in NZ9020 under the same conditions is difficult to explain. It is well known that the nisin promoter is stronger than P1 (deRuyter, Kuipers et al. 1996) and this explains why expression is higher in the inducible plasmid for most cases. It is important to note that the constitutive bacteria for BMP-2S were grown in M9 media, not M17 and this could have an effect on protein expression. We do not have a satisfactory explanation, and this would have to be tested further to ascertain a firmer conclusion. It is apparent from the results that the protein is present, and at high enough levels (>100 ng/mL) to induce the differentiation of MSCs. Table 4.12 shows the amount of protein expression for all *L. lactis* clones.

**Table 4.12. Quantitation of *L. lactis* protein expression**

	<b>NZ9000</b>	<b>NZ9020</b>
<b>Constitutive FNIII<sub>7-10</sub></b>	6.36 ng/cm <sup>2</sup>	5.84 ng/cm <sup>2</sup>
<b>Inducible FNIII<sub>7-10</sub></b>	853 ng/cm <sup>2</sup>	359 ng/cm <sup>2</sup>
<b>Constitutive BMP-2W</b>	6.65 ng/cm <sup>2</sup>	4.84 ng/cm <sup>2</sup>
<b>Inducible BMP-2W</b>	8.79 ng/cm <sup>2</sup>	11.16 ng/cm <sup>2</sup>
<b>Constitutive BMP-2S</b>	485 ng/mL	299 ng/mL
<b>Inducible BMP-2S</b>	18.6 µg/mL	183 ng/mL

The use of the NZ9020 strain was due to the high metabolic activity of NZ9000 as it was found that the high production of lactic acid resulted in the death of MSCs in the co-culture. To overcome this, the double lactate dehydrogenase knockout NZ9020 was genetically engineered and MSCs were seeded onto these bacteria instead. It was found that MSC viability was found to stay high, similar to that of a FN coated glass coverslip.

The creation of genetically engineered *L. lactis* NZ9020 expressing BMP-2 and FNIII<sub>7-10</sub> fragments has been shown to keep MSCs viable and that these proteins are expressed at high levels in both constitutive and inducible fashions.

## 4.5 Conclusion

This chapter has shown that *L. lactis* NZ9000 and NZ9020 can be engineered to display and express FNIII<sub>7-10</sub> and BMP-2. Furthermore, the use of SMX at 5 µg/mL has a similar effect to that of TC at 10µg/mL in terms of bacterial viability. SMX however, does not prevent bacterial protein expression like TC and can therefore be used in conjunction with BMP-2 expressing clones.

Regrettably, the use of NZ9000 was deemed detrimental to mammalian cell viability and a lactate dehydrogenase knockout was used to combat this problem. This NZ9020 has had both its known lactate dehydrogenase genes knocked out and has therefore had its metabolism sufficiently altered to produce less lactic acid and allow for longer term cell culture. However, the use of this bacteria leads to a general decrease in protein expression when compared with NZ9000.

Most interestingly, the system was transformed to allow for the inducible expression of proteins through the well characterised NICE system (Kuipers, de Ruyter et al. 1998, Mierau and Kleerebezem 2005, Mierau, Olieman et al. 2005). It was found that protein production was reliant on nisin addition to the media and that the amount of protein production was concentration dependent. Furthermore, the promoter is not leaky, which is demonstrated by the absence of protein in cultures where no nisin was added.

We aim to establish a surface whereby MSCs are adhered to the surface by the FNIII<sub>7-10</sub> fragment and the expression of BMP-2, either cell wall bound or secreted can induce the differentiation of these cells into osteoblasts.

# 5. Cell-bacteria interaction dynamics

## Summary

This chapter focusses on how *L. lactis* and mammalian cells interact with one another and how this co-culture can affect bacterial and mammalian cell behaviour. Basic cell attachment to constitutive and inducible *L. lactis* was investigated for the FNIII<sub>7-10</sub> expressing bacteria. Proliferation of MSCs on FNIII<sub>7-10</sub> and BMP-2 expressing clones was also investigated to ascertain the health and differentiation capabilities of the bacterial strains in the short term. Lastly, bacterial internalisation by mammalian cells was explored as previous studies showed potential for the mammalian cells to engulf the bacteria. The results in this chapter demonstrate that *L. lactis* NZ9000 and NZ9020 can sustain cell adhesion on both the constitutive and inducible clones and that cell size is proportional to the amount of inducer. Also, mammalian cells are able to proliferate on all clones of *L. lactis* and proliferation is lowest on the BMP-2 secreting clones. Murine C2C12 cells as well as murine RAW macrophages are also able to engulf all strains of *L. lactis* but rate of uptake is limited by the presence of a protein in the bacterial cell wall.

## 5.1 Introduction

It is thought that mitochondria are the progeny of bacteria, initially kept by higher cells in symbiosis due to their capacity to consume atmospheric oxygen and produce energy (Sagan 1967, Margulis and Bermudes 1985). If this is true, this shows a long standing interaction between bacteria and eukaryotic cells. However, not all prokaryotic-eukaryotic interactions end so well. Some bacteria are pathogenic and can cause a disease state in their host. Similarly, some eukaryotic cells prey on prokaryotic cells. Microbial phagocytic defence may have evolved in response to these pathogenic bacteria. However, the usual outcome between a microbe and its host does not lead to a disease state. To test bacterial-mammalian cell dynamics, an internalisation assay was developed to establish whether C2C12 cells were able to engulf bacteria. RAW macrophage-like cells were also included to test whether the internalisation of bacteria was unique to immune cells only.

We can exploit these non-pathogenic bacteria to become cell factories for the production of probiotics, through cell adhesion and differentiation.

Cell adhesion is crucial for the survival, proliferation and differentiation of cells to form higher structures such as tissues and organs. The architecture of organs is therefore modulated by cell adhesion and adhesion systems should be regarded as mechanisms that translate basic genetic information into complex phenotypes. Upon attachment to a functionalised surface, cells begin to proliferate. There is evidence that signals arising from focal adhesions directly communicate with pathways that regulate proliferation (Giancotti and Ruoslahti 1999).

However, proliferation and differentiation are closely coupled, and are intricately linked. Self-renewal and differentiation are associated with the cell-cycle and this enables tissue specification, organ homeostasis and potentially tumourigenesis. Tissue differentiation and maintenance is guided by the coordination between differentiation and proliferation of specific progenitor cells. The importance of these mechanisms has been displayed by many authors for many different organs such as the brain, gut and skin (Fuchs 2009, Lange and Calegari 2010, Li and Clevers 2010).

In the established model of mammalian cell cycle control, the retinoblastoma protein functions to direct cell fate. The retinoblastoma protein functions to restrict cells from entering S phase by binding and sequestering the E2f activators E2f1, E2f2 and E2f3. These are largely regarded as the ultimate effectors that commit cells to enter and progress through

S phase towards self-renewal. In differentiating cells, such as MSCs, E2f1-3 function as a complex with retinoblastoma proteins allowing the silencing of E2f targets and assist in the exit from the cell cycle (Chong, Wenzel et al. 2009). The E2f1 transcription factor acts a molecular switch between proliferation and differentiation and can bind to phosphorylated retinoblastoma protein. Unbound, E2f1 promotes G1 to S phase transition. However, upon complex formation between retinoblastoma protein and E2f1, G1 to S phase is inhibited (Johnson, Schwarz et al. 1993). Accumulation of phosphorylated retinoblastoma protein allows the switch from proliferation to differentiation as it has been reported to interact with transcription factors that are specific to osteogenesis and adipogenesis (RUNX2 and PPAR $\gamma$ ) (Docheva, Padula et al. 2008). Figure 5.1 shows a schematic detailing the stages of MSC differentiation and proliferation.

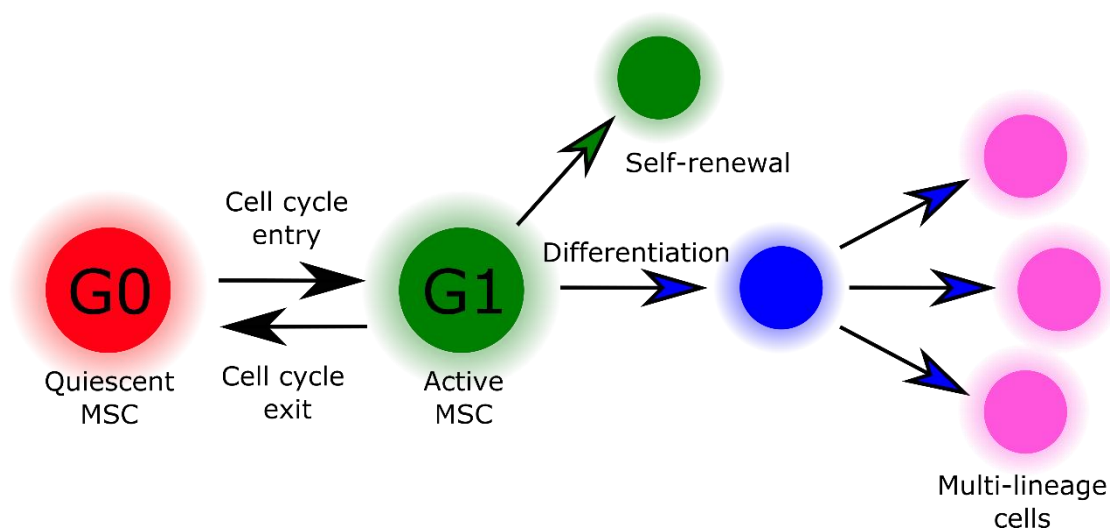


**Figure 5.1. MSC cell cycle schematic.** Quiescent MSCs in G0 phase can either self-renew or differentiate.

## **5.2 Materials and methods**

### **5.2.1 Nisin induction for cell adhesion**

Biofilm production and cell seeding was the same as detailed for previous cell adhesion experiments. However, nisin was added to the cultures at the same time as the mammalian cells at 0, 0.5, 5 and 10 ng/mL. Cells were left to attach for five hours and stained for actin, vinculin and nuclei using antibodies and methods detailed previously.

### **5.2.2 Cell proliferation**

MSCs were seeded over *L. lactis* clones at 5,000 cells/cm<sup>2</sup> for one and three days to measure cell proliferation at these time points. 6 hours prior to fixation, 1 mM BrdU (5-bromo-2-deoxyuridine) was added to each well in DMEM. Cells were fixed and permeabilised using standard methods described previously. These were then blocked with 1 % BSA in PBS at 37 °C for 10 minutes. The GE Healthcare Cell Proliferation Kit was used from this point to stain the cells. The mouse monoclonal anti BrdU was added with DNase to ensure the primary antibody was able to reach the DNA and incubated at 37 °C for 2 hours. Samples were washed using the standard protocol and the addition of phalloidin (Life Technologies, UK) and a Cy3 conjugated anti mouse secondary antibody (Jackson Immunoresearch, UK) was added for 1 hour at 37 °C. Cells were washed and mounted using Vectashield with Dapi (Vector Laboratories, UK) and viewed under a Zeiss AxioObserver.Z1 fluorescence microscope.

### **5.2.3 Bacterial internalisation**

Biofilms were established using the methods as described previously. Both C2C12 and RAW macrophages were seeded over the biofilms at 5,000 cells/cm<sup>2</sup> and left to grow for 16 hours. The cells were trypsinised for five minutes at 37 °C before centrifugation at 1300 RPM for five minutes. This addition of trypsinisation for five minutes was found to remove most mammalian cells but left a majority of bacterial cells attached to the coverslip. To further separate the cell types, the centrifugation step allowed the pellet of the mammalian cells whilst leaving the bacteria in the supernatant to be discarded. This cell pellet was

resuspended and seeded over FN coated coverslips (using the same methods as described previously) for five hours to allow cell attachment. Any bacteria present should either be inside or stuck to the outside of the bacteria. A Nikon Eclipse Ti Confocal microscope fitted with a Scmos camera using the Volocity software (Piltti, Haus et al. 2011) was used to visualise the samples. To establish the localisation of the bacteria, the co-localisation plugin was used whereby the software can evaluate the overlap of two dyes and thus be highly specific to bacteria that are inside the mammalian cells.

## 5.3 Results

### 5.3.1 Cell adhesion

Cell adhesion to constitutive and inducible FNIII<sub>7-10</sub> in NZ9000 and NZ9020 was tested using different amounts of nisin, ranging through 0, 0.5, 5 and 10 ng/mL which can be seen in Figure 5.2. NZ9000 was used as well as NZ9020 as the short time point used is not detrimental to cell viability and gives us insight into how protein expression differs between the strains. It can be seen in the constitutive samples that the presence of the FNIII<sub>7-10</sub> fragment in both NZ9000 and NZ9020 *L. lactis* induces cell spreading, similar to the FN coated sample with very comparable values; NZ9000 and NZ9020 both show cell areas of 2527 and 2672  $\mu\text{m}^2$  respectively. The cells on the FN coat show cell areas of 3125  $\mu\text{m}^2$  which is higher than either NZ9000 or NZ9020 under the constitutive promoter. These results have been demonstrated before using a different strain of *L. lactis* known as MG1363 (see Chapter 3).

Most interestingly, the nisin controlled FNIII<sub>7-10</sub> protein expression samples show striking results. Upon additive amounts of nisin, cell spreading increases. These results have been quantified and can be seen in Figure 5.3

The empty samples, that is, the ones displaying no FN, show the smallest cell area being comparable between sample sets, all the cells found on these surfaces show similar cell areas. Cells seeded onto the constitutive FNIII<sub>7-10</sub> samples show similar results to that of a FN coat and are higher than their respective empty samples. Interestingly, cell area is seen to increase in both the NZ9000 and NZ9020 samples upon higher amounts of nisin added to the system. This also agrees with the results from the western blot, as more nisin is added, more GFP-FNIII<sub>7-10</sub> is found (see Chapter 4, Figures 4.7 and 4.17). This increased amount of FNIII<sub>7-10</sub> presented to the mammalian cells would allow for more cell spreading. Further to this, cell spreading on NZ9020 is seen to be lower than in NZ9000. This is likely due to the fact that this strain is much more metabolically slower than NZ9000 and therefore the five hours may not be enough time for the bacteria to synthesise enough FNIII<sub>7-10</sub> to give a similar response to that seen in NZ9000. It can be seen that cell spreading on NZ9000 FNIII<sub>7-10</sub> expressing clones when stimulated with 10 ng/mL of nisin is the highest, albeit, only slightly higher than the FN coated surface. It is most likely higher than the constitutive expression as the *nisA* promoter is stronger than P1; and therefore, more FNIII<sub>7-10</sub> can be produced.

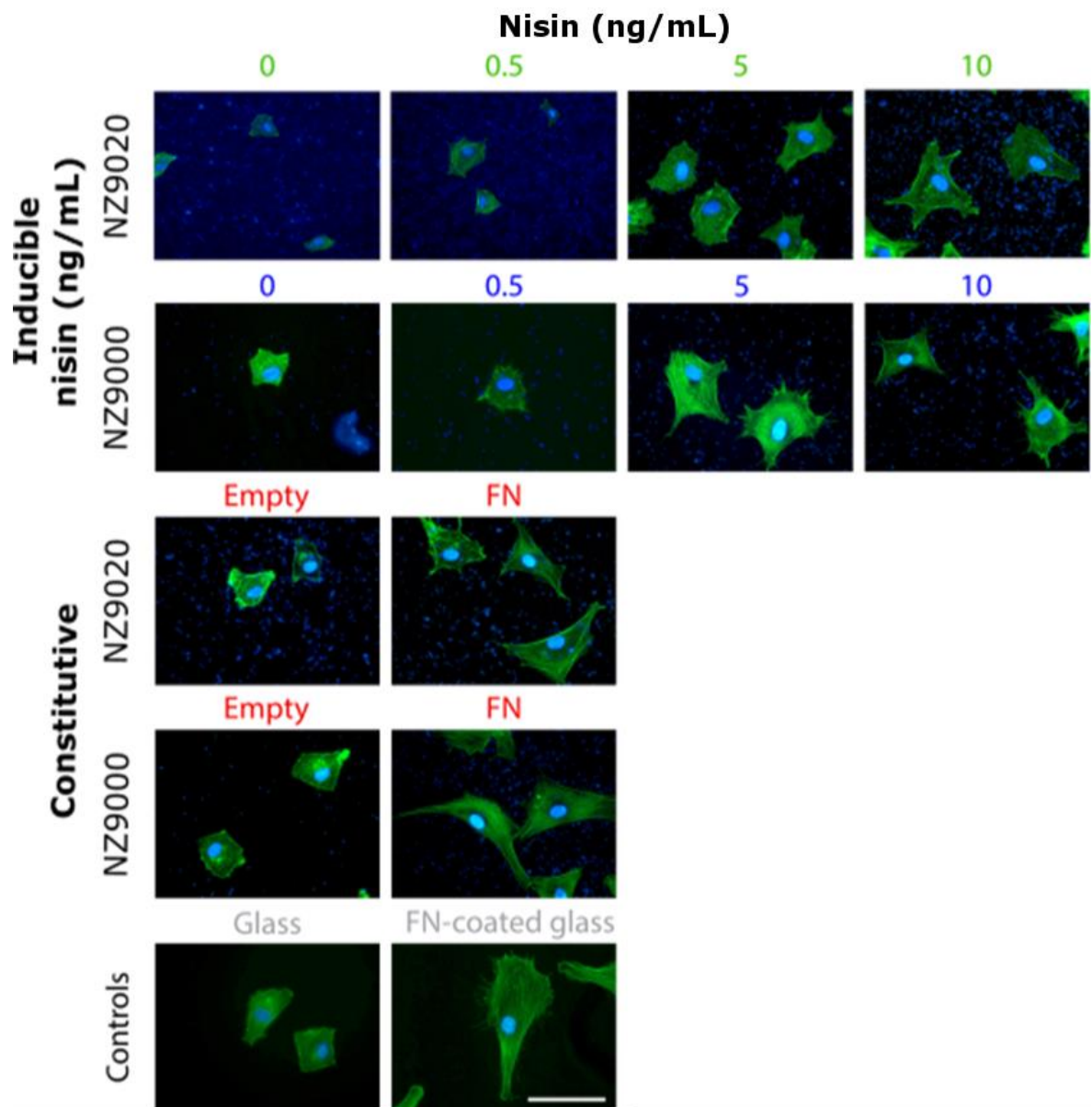


**Figure 5.2. MSC adhesion to inducibly expressed FNIII<sub>7-10</sub> from *L. lactis*.** Top images show cell adhesion in response to FNIII<sub>7-10</sub> production under nisin induction in inducible *L. lactis*-FN clones for both NZ9000 (top) and NZ9020 (bottom). Middle images show cell adhesion to *L. lactis*-FN constitutive clones for both NZ9000 (top) and NZ9020 (bottom). Bottom images show cell adhesion to FN coated and non-FN coated glass. All images taken after five hours. Upon increasing nisin addition, cell area is seen to increase. This is due to more FNIII<sub>7-10</sub> being available in the bacterial cell wall. Green is actin, blue is DNA. Scale bar = 100  $\mu$ m.

### Cell area of hMSCs after 5 hours on FN expressing L. lactis

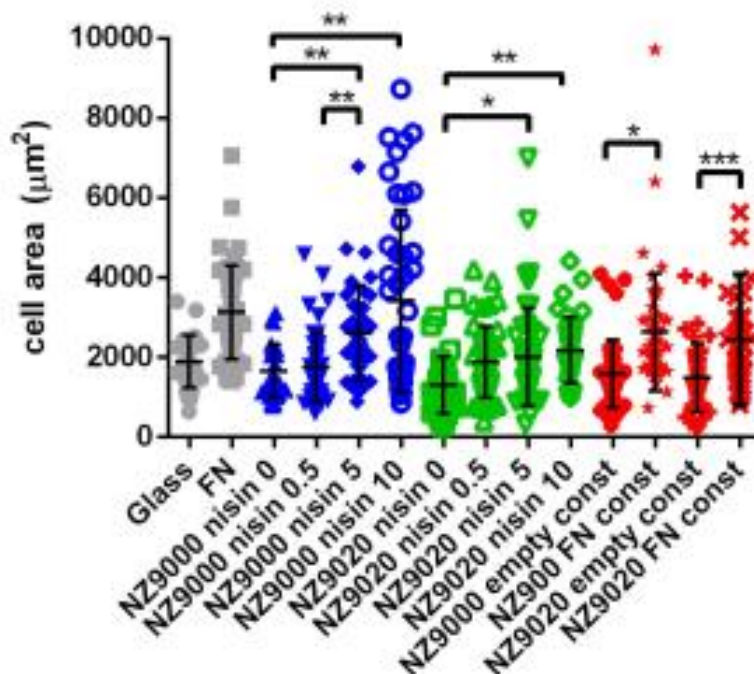


**Figure 5.3. Graphical representation of cell area after nisin induction.** Increasing amounts of nisin are seen to lead to an increase in cell area in both NZ9000 and NZ9020 (statistically significant). Cell area in NZ9000 with 5 and 10 ng of nisin shows higher cell area than on constitutive clones. Conversely, cell area on NZ9020 is lower than the constitutive clones, likely due to the slower metabolism rates. A minimum of 27 cells were used. Data is displayed as mean  $\pm$  SD and was analysed with a one way ANOVA test with a Tukey post-hoc test. Statistical significance levels are \* $p < 0.05$ , \*\* $p < 0.01$  and \*\*\* $p < 0.001$ .

### 5.3.2 Cell proliferation

Cell proliferation was studied on NZ9020 only as the long-term cultures will only be completed on this strain due to detrimental effect NZ9000 has on the long-term cell viability of MSCs. Figure 5.4 shows the percentage of new cells formed within six hours after the addition of 5-bromo-2'-deoxyuridine (BrdU) after one day (orange) and three days (blue) on constitutively expressed protein. BrdU is a brominated analogue of thymidine and is incorporated into cell DNA at the S phase of the cell cycle. Upon addition to the media, BrdU can replace thymidine in the cell's DNA and be stained for with an anti-BrdU antibody

(Zhang, Zhi et al. 2010). MSCs were seeded over different *L. lactis* strains and the percentage of BrdU positive cells was calculated. At day one, cell proliferation on glass, FN coat, *L. lactis*-BMP-2W, *L. lactis*-BMP-2WGFP and *L. lactis*-BMP-2SGFP are all roughly equivalent. Proliferation on *L. lactis*-empty and *L. lactis*-FN are much higher with 20 % of the total cell count being BrdU positive. Conversely, cell proliferation was seen to be lowest on the FN coat with 100 ng/mL of BMP-2 added and *L. lactis*-BMP-2S with less than 5 % of cells being BrdU positive. A similar trend was seen for the three day experiment. Again, the lowest cell proliferation was seen on the FN coat with 100 ng/mL of BMP-2 added and *L. lactis*-BMP-2S at about 3 % of total cells being BrdU positive. All other samples show similar values with approximately 10 % of cells being BrdU positive. At three days *L. lactis*-empty and *L. lactis*-FN show similar results to the other samples as opposed to being higher at one day.

### Percentage of new cells 6 hours after addition of BrdU

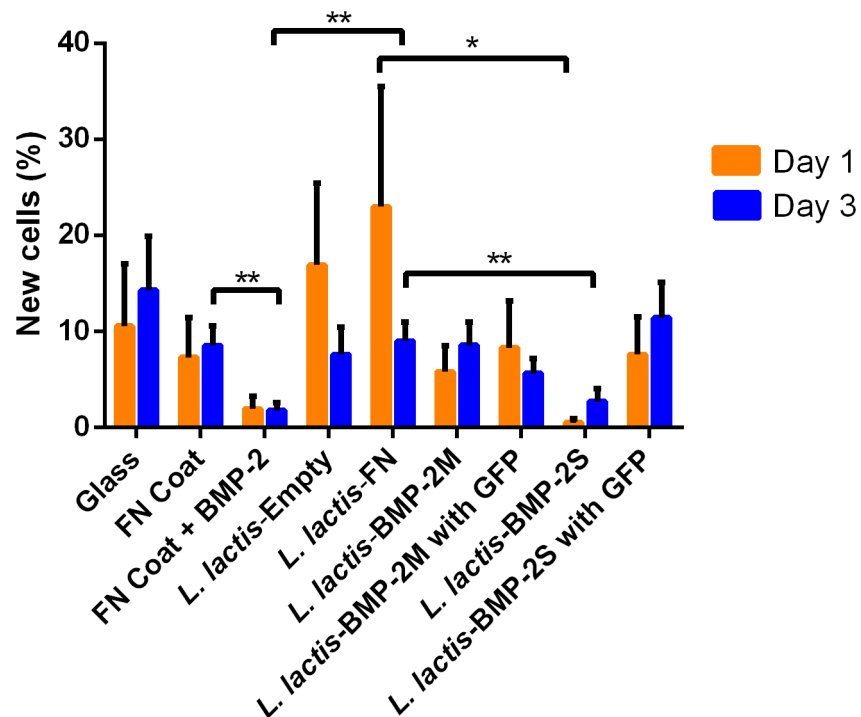


**Figure 5.4. Cell proliferation on differing constitutive *L. lactis* clones.** The cells were cultured for one and three days and quantified according to BrdU incorporation into the nucleus. Cell proliferation on most samples is approximately 10 % new cells over a six hour period where as cells cultured in the BMP-2 positive control and *L. lactis*-BMP-2S show much lower proliferation rates. A minimum of five images were analysed from three technical replicates. Data are reported as the mean  $\pm$  SD and was analysed by a two way ANOVA with a Bonferroni post-hoc test (data not normally distributed). Statistical significance levels are \* $p < 0.05$ , \*\* $p < 0.01$ .

Figure 5.5 shows cell proliferation in response to the inducible clones. In this experiment, only *L. lactis*-BMP-2S and *L. lactis*-FN were used as the *L. lactis*-BMP-2W and both BMP-2-GFP expressing clones showed no change in cell proliferation compared to on the FN coat. Further to this, a co-culture of *L. lactis*-FN and *L. lactis*-BMP-2S was also tested. Nisin was added at 10 ng/mL to allow maximal protein synthesis. A similar trend to that observed on the constitutive clones can be seen where the lowest cell proliferation was found on the FN coat with 100 ng/mL BMP-2 and the *L. lactis*-BMP-2S at both day one and day three. Cell proliferation on the FN coat, *L. lactis*-empty and *L. lactis*-FN are also very similar to those seen on the constitutive clones at around 10 % on day one with lower proliferation rates by day three. The co-culture of *L. lactis*-FN and *L. lactis*-BMP-2S shows an intermediate proliferation rate, between that of single *L. lactis*-FN and *L. lactis*-BMP-2S. This result, although not statistically significantly different from either single clone culture could be due to the lower levels of BMP-2 secreted; due to there being half the amount of *L. lactis*-BMP-2S.

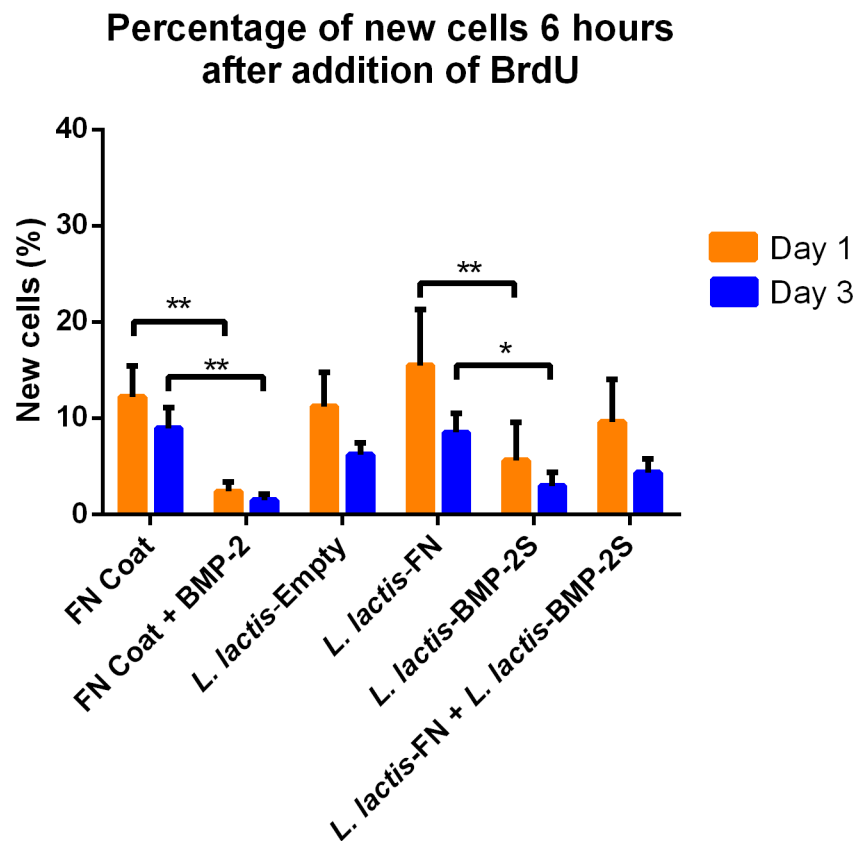


**Figure 5.5. Cell proliferation on inducible *L. lactis* clones.** Nisin was used at 10 ng/mL in all samples. Results are similar to those of the constitutive clones whereby *L. lactis*-BMP-2S shows similar results to that of the FN coat + BMP-2. A minimum of six images were analysed with three technical replicates per sample. Data is reported as the mean  $\pm$  SD and analysed with a two way ANOVA using a Bonferroni post-hoc test (data not normally distributed). Statistical significance levels are \* $p < 0.05$ , \*\* $p < 0.01$ .

The difference in cell proliferation could be explained by cell cycle dynamics. As described in the introduction of this chapter, differentiating cells must make a choice whether to self-renew or differentiate. Self-renewing cells will proceed through G1 to S phase, dictated by E2f proteins. On the contrary, differentiating cells will not leave G1 as retinoblastoma protein phosphorylation blocks S phase entry. Therefore, differentiating cells are unable to proliferate which may explain the lower proliferation rate on the FN-coated surface with 100 ng/mL BMP-2 added. *L. lactis*-BMP-2S also demonstrates a low proliferation rate, similar to that of the FN coat with added BMP-2. This could be due to the BMP-2 secreted by the bacteria effecting the mammalian cell population (Wen, Miyake et al. 2004, Xu, Peck et al. 2005).

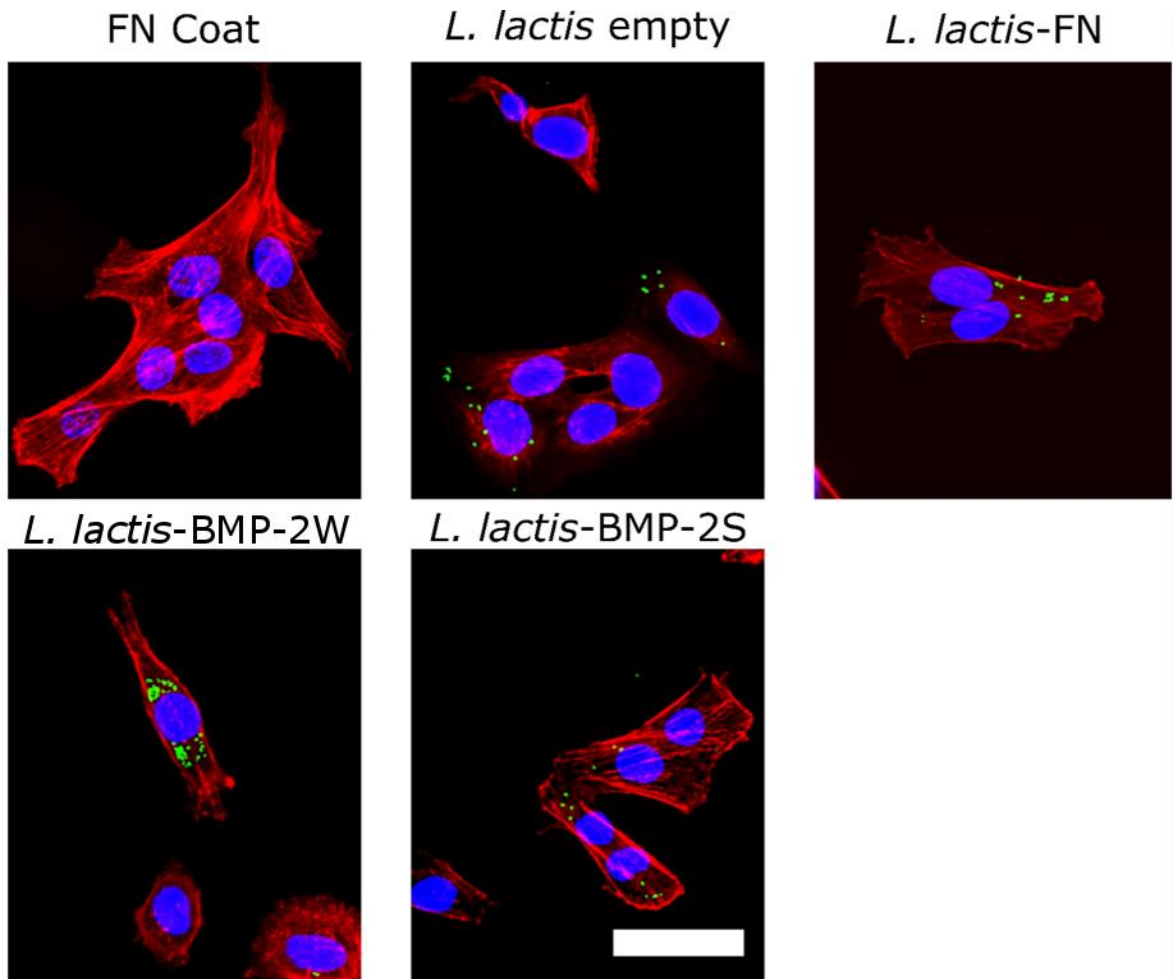
### 5.3.3 Cell-bacteria dynamics

The ability of a microbe to establish a niche within its host is an important parameter of its pathogenesis. Some pathogens can enter normally non-phagocytic host cells as this may be a requirement for their replication. Indeed, *L. lactis* are not pathogenic and therefore do not possess the mechanisms for invasion into non-phagocytic mammalian cells such as C2C12s and MSCs. However, the internalisation of particles is a constitutive property of most, if not all mammalian cells (Poussard, Decossas et al. 2015). Therefore, the potential of mammalian cells to internalise bacterial cells was studied. We postulated that the presence of FNIII<sub>7-10</sub> would lead to the internalisation of the bacteria due to the integrin endocytosis-exocytosis cycle. Integrins holding the cell to the surface will move rearwards as the cell migrates over a matrix. This means that the leading edge of the cell requires new receptors to anchor the cell to the surface; this is achieved by cycling integrins from the rear regions of the cell, and their subsequent transport in vesicular form to the leading edge of the cell for re-use (Bretscher 1984, Bretscher 1992).

To assess the localisation of bacteria, it was necessary to use a confocal microscope as this allows the user to isolate specific z-planes through a 3D structure. As the density of bacteria on normal co-cultured surfaces was high and made analysis of internalised bacteria extremely difficult, a new method to study internalisation was developed. Mammalian cells were first cultured on *L. lactis* using the same methods as reported previously, before trypsinisation and centrifugation; and then reseeding onto FN coated glass coverslips. The trypsinisation followed by centrifugation resulted in the removal of the bacteria from the mammalian cells. Reseeding these cells on a FN coat ensures that any bacteria present would

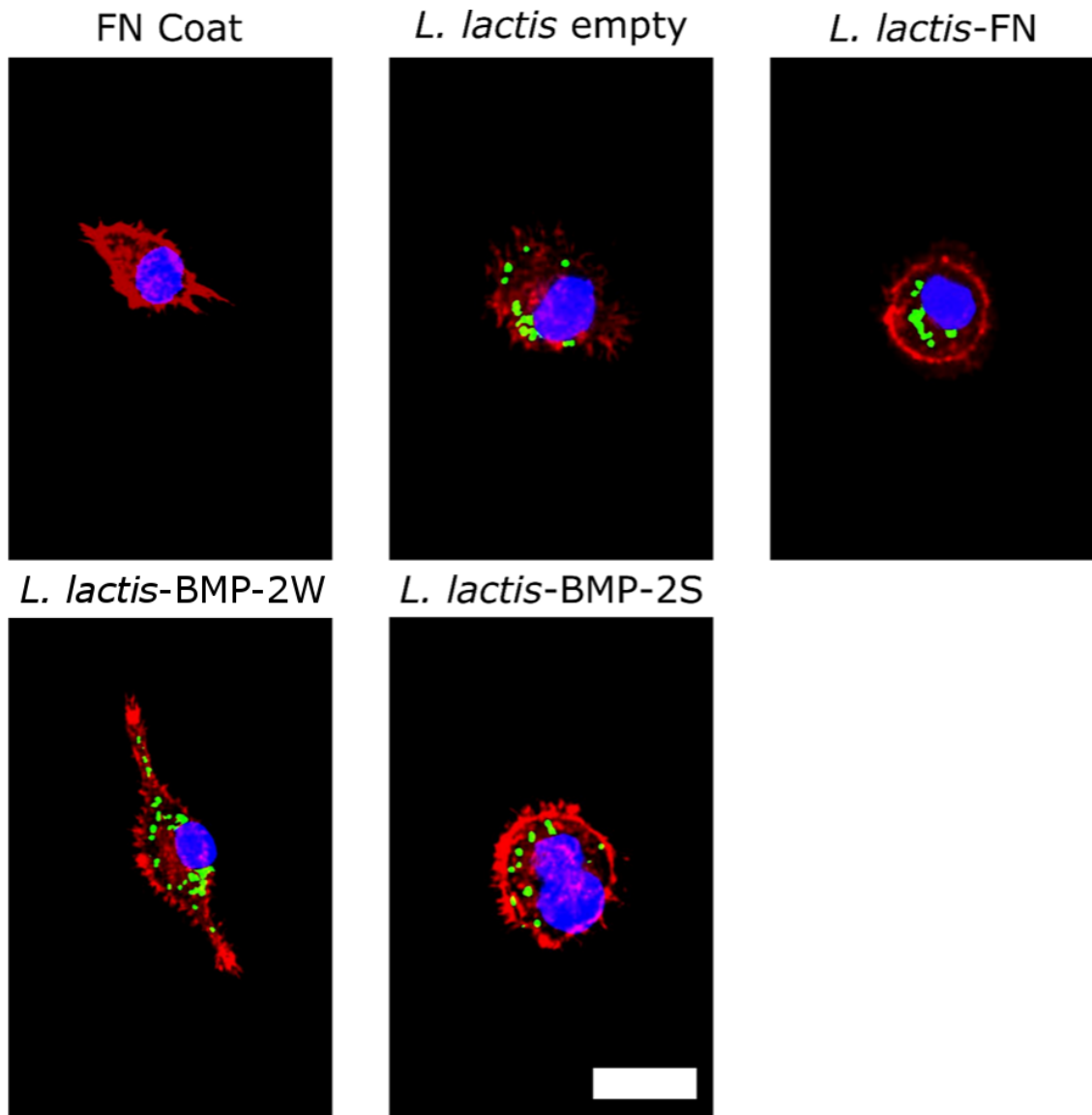
either be inside or stuck to the outside of the mammalian cell. The presence and localisation of these bacteria was determined by confocal microscopy.

Figure 5.6 highlights C2C12 cells imaged after being seeded on *L. lactis*-empty, FNIII<sub>7-10</sub>, BMP-2W and BMP-2S bacterial biofilms. To deduce their localisation, the co-localisation plugin on Volocity was used. Graphs detailing localisation can be seen in Figure 5.8.



**Figure 5.6. Bacterial internalisation by C2C12 murine myoblasts.** All mammalian cells were seen to engulf bacterial cells. *L. lactis* displaying a cell wall bound protein show a higher uptake than empty and secreted protein clones. Red = actin, blue = mammalian nuclei and green = bacterial cells. Scale bar is 100  $\mu\text{m}$ .

A complementary experiment with macrophages was also set up using the same method as described above. Figure 5.7 shows that all strains of bacteria were also engulfed. This is unsurprising as it is macrophages primary role in the body to engulf any foreign particles, including bacteria. Graphs detailing localisation can be seen in Figure 5.8.



**Figure 5.7. Bacterial internalisation by RAW macrophages.** All mammalian cells were seen to engulf bacterial cells. Red = actin, blue = nuclei and green = bacterial cells. Scale bar is 50  $\mu$ m.

Figure 5.8 shows quantitative data for the internalisation study. A direct trend can be observed whereby bacteria with cell wall bound proteins are internalised at higher rates. This trend can be seen in both the C2C12s (Figure 5.8 A) and macrophages (Figure 5.8 C). *L. lactis*-BMP-2W seem to be engulfed at a higher rate than that of *L. lactis*-FN. Furthermore, bacteria without cell wall bound proteins are still internalised, but at a much lower frequency. The number of bacteria internalised per cell in C2C12s is lower than that observed in macrophages. Additionally, all macrophages observed had internalised bacteria (Figure 5.8D) whereas C2C12s were seen to engulf bacteria with varying success rates. C2C12s were most likely to internalise *L. lactis*-BMP-2W, followed by *L. lactis*-FN as they were found in 75 % and 53 % of cells respectively. *L. lactis*-empty and *L. lactis*-BMP-2S showed very similar results to that of *L. lactis*-FN as 51 % of cells were found with bacteria internalised. However, the total number of *L. lactis*-FN and *L. lactis*-BMP-2S found in

C2C12 cells is drastically different with 20 and eight bacteria per cell respectively. This parameter explains that although the total amount of C2C12s with at least one bacteria is very similar, *L. lactis*-FN is more likely to be engulfed at higher rates. *L. lactis*-empty was found in the least amount of cells at 45 %.

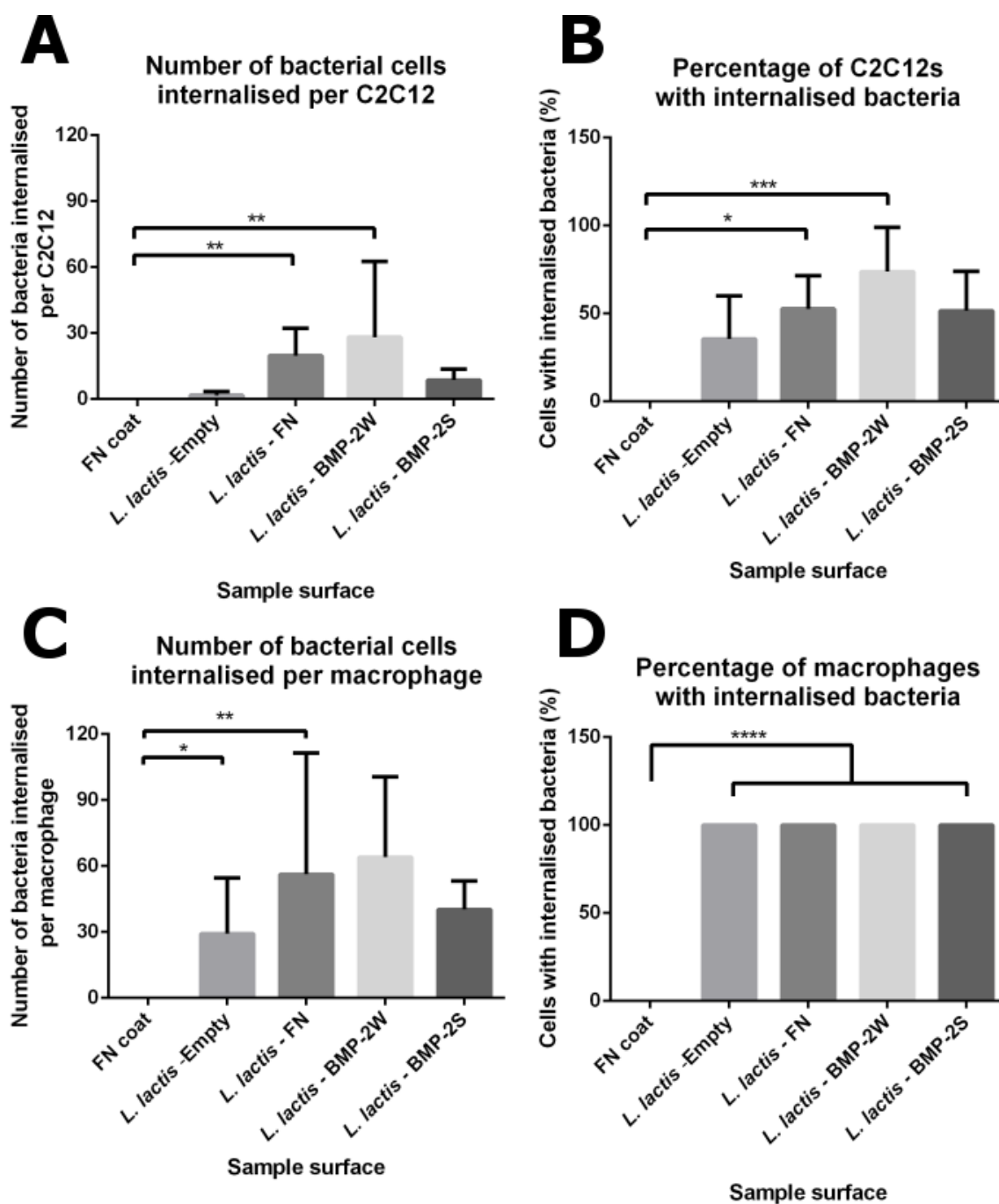


**Figure 5.8. Graphs detailing bacterial internalisation.** Graphs were constructed from 20 pictures per sample. A = number of bacterial cells internalised per C2C12, B = number of bacterial cells internalised per macrophage, C = the percentage of C2C12 cells with internalised bacteria and D = the percentage of macrophage cells with internalised bacteria. More bacteria were internalised in macrophages than C2C12s with bacteria displaying a cell wall bound protein being more likely to be internalised. All macrophages imaged had internalised bacteria whereas C2C12s displayed differing results. A minimum of 15 cells were tested and quantified per sample with three technical replicates completed. Data is presented as the mean  $\pm$  SD and analysed with a one way ANOVA using a Bonferroni post-hoc test (data not normally distributed). Statistical significance levels are \* $p < 0.05$ , \*\* $p < 0.01$ , \*\*\* $p < 0.001$  and \*\*\*\* $p < 0.0001$ .

## 5.4 Discussion

Cell adhesion and proliferation is essential for the construction of organs *in vitro*. Usually, a scaffold is functionalised with proteins to allow cell attachment which can direct cellular behaviour (Lendlein 2011, Ebara, Kotsuchibashi et al. 2014, Murphy, McDevitt et al. 2014). This material-cell interface is designed by the user and can be used to alter cells phenotype (Friess 1998, Hench and Polak 2002, Rosso, Marino et al. 2006, Oh, Brammer et al. 2009, Lendlein 2011). For example, the scaffolds used in our experiments are glass coverslips that are functionalised with genetically engineered bacteria expressing FNIII<sub>7-10</sub> and BMP-2 to control cell adhesion and differentiation.

It was found that this surface of *L. lactis* comprising the strains NZ9000 and NZ9020 can induce cell attachment through the FNIII<sub>7-10</sub> fragment in both a constitutive and inducible manner. Further to this, cell area is proportional to the amount of available protein which can be altered by the addition of different concentrations of inducer.

In terms of the BMP-2 clones, for both constitutive and inducible BMP-2, *L. lactis*-BMP-2S seems to show similar results to that of a FN-coated surface with 100 ng/mL BMP-2 added to the culture. Cell proliferation was studied in response to the addition of differentiation factors as differentiating cells do not proliferate at the same rate as those on normal FN coats (Wen, Miyake et al. 2004, Xu, Peck et al. 2005). The data shows that *L. lactis*-BMP-2S in both the constitutive and inducible forms inhibits higher cell proliferation rates showing that the BMP-2 from *L. lactis* could potentially be used as a long term successful dynamic differentiation platform for MSCs.

In addition to basic cell response, bacteria-mammalian cell dynamics were also evaluated. Mammalian cells have the machinery to internalise particles and is an inherent property of most, if not all mammalian cell types (Vannhieu and Isberg 1993, Poussard, Decossas et al. 2015). We found that C2C12 cells, as well as RAW macrophages internalise all forms of *L. lactis*. However, the rate of uptake is determined by whether the bacteria is displaying a cell wall bound protein. Interestingly, *L. lactis*-BMP-2W was internalised at higher rates than *L. lactis*-FN. We hypothesised that *L. lactis*-FN would be internalised at the highest rates due to the integrin endocytosis-exocytosis cycle. Furthermore, although *L. lactis*-BMP-2W was internalised at a higher rate, it does not alter the cells ability to proliferate like *L. lactis*-BMP-2S. This shows that although the cells are clearly interacting with *L. lactis*-BMP-2W, the BMP-2 does not stimulate the same cell response as *L. lactis*-BMP-2S.

The proteins displayed and expressed by *L. lactis* show biological function. *L. lactis*-FN can induce cell attachment whereas *L. lactis*-BMP-2S shows biological activity by preventing MSC proliferation at early time points (one and three days).

## 5.5 Conclusion

This chapter assessed the short-term interaction dynamics between constitutive and inducible *L. lactis* clones and mammalian cells. The results of this chapter suggest that the inducible system for both *L. lactis*-FN and *L. lactis*-BMP-2S are biologically active. This is in agreement with the western blot and fluorescence data shown in Chapter 4. In terms of the FNIII<sub>7-10</sub> expressing clones, the amount of nisin added to the system directly affects protein expression and that this in turn effects cell area. This is likely due to the fact that more RGD is available to the cells in the higher nisin cultures, and that this protein availability allows the cells to stretch further.

In terms of the BMP-2 expressing clones, *L. lactis*-BMP-2S shows osteogenic activity whereas *L. lactis*-BMP-2W seems to show no activity. Longer term cell differentiation studies will be shown in the next chapter.

# 6. Mammalian cell differentiation on BMP-2 expressing bacteria

## Summary

This chapter focusses on *L. lactis* clones and their ability to induce differentiation of MSCs. Mid (ALP activity) and long (OCN and von Kossa) term osteogenic markers were evaluated to ascertain the differentiation dynamics of different *L. lactis* clones. Both constitutive and inducible BMP-2 expressing clones were investigated *in vitro*. Lastly, constitutive NZ9000 BMP-2 producing clones were used in an *in vivo* mouse model to explore bone growth. *L. lactis* were incorporated into collagen sponges and the clone demonstrating the best osteogenic results *in vitro* were chosen for further experimentation *in vivo*. The results in this chapter demonstrate that *L. lactis*-BMP-2S can induce the differentiation of MSCs *in vitro* in both a constitutive and inducible fashion.

## 6.1 Introduction

MSCs are able to differentiate along the stromal lineages to give rise to osteoblasts, chondrocytes and adipocytes, typically through the application of chemical and physical cues (Pittenger, Mackay et al. 1999). More specifically, MSCs are sensitive to stiffness (Engler, Sen et al. 2006), cell tension through mechanotransduction (McBeath, Pirone et al. 2004), surface topography (Dalby, Gadegaard et al. 2007) and dimensionality (2D or 3D) (Oh, Brammer et al. 2009), these physical characteristics have the power to direct cellular fate. On the other hand, chemical stimuli, such as that of BMP-2 also have the ability to induce differentiation (Rahman, Akhtar et al. 2015).

Bone is a specialised form of connective tissue and is the main element of the skeletal system. The formation of bone is highly complex and a finely orchestrated process involving many of the physical and chemical stimuli mentioned above. BMPs play a major role in the regulation of osteoblast lineage specific differentiation, which later translates to bone formation. Since the discovery of BMPs in 1965, many authors have sought to find the importance of BMPs *in vivo* using transgenic animals. These loss-of-function experiments demonstrated a variety of bone related abnormalities during development (Urist 1997, Lechleider, Ryan et al. 2001, Zhao 2003). BMPs are therefore hugely important *in vivo* and demonstrate great therapeutic potential *in vitro* (Tamaki, Souchelnytskyi et al. 1998, Itoh, Itoh et al. 2000, Guicheux, Lemonnier et al. 2003, Afzal, Pratap et al. 2005, Ryoo, Lee et al. 2006, Bessa, Casal et al. 2008, Ulsamer, Ortuno et al. 2008).

The bone microenvironment mainly comprises MSCs, derived osteoblasts, osteoclasts, mineralised bone matrix and osteocytes (Chen, Deng et al. 2012). Osteogenesis can be separated into three distinct stages, migration and mitosis of MSCs, differentiation of MSCs and lastly, deposition of matrix (Gilbert 2000, Hoshiba, Kawazoe et al. 2009). During the differentiation stage, MSCs are the target of BMPs (Rahman, Akhtar et al. 2015). MSCs are therefore an important source of bone *in vivo* and show the greatest potential for recreating the bone microenvironment *in vitro*.

MSCs have been used for decades in the attempt to imitate the bone microenvironment with varying success (Osdoby and Caplan 1981, Sparks and Scott 1986, Anderson, Sahoo et al. 2016, Llopis-Hernandez, Cantini et al. 2016). It is currently postulated that the use of dynamic surfaces show the greatest potential to overcome problems with MSC culture (Ebara, Yamato et al. 2004, Todd, Scurr et al. 2009, Wirkner, Weis et al. 2011, Weis, Lee et al. 2013, Murphy, McDevitt et al. 2014, Roberts, Sahoo et al. 2016). The bone

microenvironment is constantly changing; therefore any synthetic material aiming to recapitulate this niche would need to be able to display a variety of behavioural cues. In terms of biochemical induced differentiation, the specific addition of supplements in a particular sequence is needed; the same will be needed for exact material control. We can expect to see a material that can be altered upon user defined conditions that relates material properties to gene activation, and thus has the power to control phenotype.

This work aims to demonstrate that bacterial biofilms formed by non-pathogenic *L. lactis* can be exploited to create an effective dynamic surface. They have the potential to be modified with a superfluity of proteins, displaying them either through cell wall bound or secreted expression that can influence cell behaviour. The use of constitutive and inducible plasmids with differing strength promoters allows for a variety of clones to be easily synthesised and tested. The user can tailor these microbial factories to express their protein of interest at desired concentrations in a spatiotemporal manner.

## **6.2 Materials and Methods**

### **6.2.1 Collagen sponges**

Collagen sponges with a 5 mm diameter were sterilised overnight in ethylene oxide and used in 96 well plates. Bacteria were grown on these using the same method as described for glass coverslips (section 2.2). MSCs were then seeded at 5000 cells/cm<sup>2</sup> under the same conditions used on glass coverslips (Section 2.5) and left to culture until the desired time point (one day for cell adhesion, 10 and 15 for ALP activity). For the positive control (100 ng BMP-2), BMP-2 was added after one day.

### **6.2.2 Cell adhesion to collagen sponges**

Sponges were fixed with 4 % formaldehyde for 15 minutes at 37 °C and then stained for actin with phalloidin (Invitrogen, UK) for one hour at 37 °C before mounting with DAPI (Vectashield, UK). These were viewed under a Nikon Eclipse Ti Confocal microscope fitted with a Scmos camera.

### **6.2.3 Alkaline phosphatase (ALP) assay**

Firstly, protein had to be extracted from the samples, cells were lysed by the addition of 50 mM Tris-HCl and sonicated for 20 seconds at 5 watts. To obtain protein content, a bicinchoninic acid (BCA) (Life Technologies, UK) was completed. For ALP activity, MUP (4-methylumbelliferyl phosphate) substrate was added. MUP substrate comprises: 500 µL 1M NaHCO<sub>3</sub>, 2 mL 5x Diethanolamine buffer, 7.5 mL water and 24 µL MUP stock. 5x diethanolamine buffer is 50 mM diethanolamine, 2.5 mg MgCl<sub>2</sub> in water, pH 9.5 and MUP stock is 83.3 mM MUP in 1x diethanolamine buffer.

The BCA was completed using the manufacturer's guidelines. Briefly, samples were incubated with the BCA working reagent at 37 °C for one hour. Then, the absorbance of the samples was measured at 562 nm using Infinite 200 PRO NanoQuant Plate Reader from Tecan. ALP concentration was measured through MUP fluorescence. Fluorescent readings were obtained by exciting the fluorophore at 360 nm and recording the fluorescence at 465 nm. mU ALP/mg protein was obtained by dividing ALP mU/µL by the protein content obtained in the BCA.

#### **6.2.4 Animals**

10 male mice (species Balb/c from Jackson Labs, USA) were used in the study, with two implants per mouse, to minimise animal usage. They were maintained in plastic cages in a room with a 12 h-day/night cycle and an ambient temperature of 21 °C, and were allowed ad libitum access to water and standard laboratory pellets. Animal selection and management, surgical protocol, and preparation followed the routines approved by the Georgia Tech Institutional Animal Care and Use Committee (IACUC).

#### **6.2.5 Surgical protocol**

The animals were generally anaesthetised with isoflurane anaesthesia. The surgical site was shaved and scrubbed with iodine. A vertical incision was made in the skin of the back. After flap reflection, a subcutaneous pocket was prepared by blunt dissection. Samples were implanted subcutaneously mid torso at the level of the panniculus carnosus. The incisions were closed with wound clips and mice were monitored daily until the wound clips were removed.

#### **6.2.6 Sponge implantation**

8 mm diameter sponges were sterilised in ethylene oxide overnight before the addition of bacteria. Bacteria were grown using the same method as used on glass coverslips. These were washed 2x in PBS before being implanted into the backs of mice. A small incision was made in the skin of the mice and the sponges, 1 on the left and 1 on the right were implanted subcutaneously, between the skin and muscle.

#### **6.2.7 Micro computed tomography ( $\mu$ CT)**

For  $\mu$ CT scanning, the region of implantation was scanned in anaesthetised, live mice using a VivaCT system (Scanco Medical, Wayne, PA, USA) at 145 mA intensity, 55 kVp energy, 376 ms integration time, and 12.5  $\mu$ m resolution). Bone structure was evaluated by contouring 2D slices to include only the collagen sponge. 3D  $\mu$ CT reconstructions were rendered and the ratio of bone volume to total volume was computed.

### **6.2.8 Implant removal and histology**

The implants were used for histological analysis. Sponges were removed from the mice after CO<sub>2</sub> asphyxiation and fixed in 4 % formalin overnight. All samples were then decalcified in 10 % (vol/vol) formic acid for two days, embedded in paraffin, and sectioned transversely at the top, middle and bottom of the sponge at a thickness of 5 µm. These were then rehydrated through a graded series of alcohol solutions. The sections were then stained with haematoxylin and eosin.

## 6.3 Results

### 6.3.1 Mesenchymal stem cell differentiation

#### Alkaline phosphatase activity

Alkaline phosphatase (ALP) catalyses the hydrolysis of phosphate esters (Sabokbar, Millett et al. 1994). Changes in ALP level and activity are associated with many biological states, including osteoblast activity. The precise mechanism of function is not understood, although it is believed to play a role in skeletal mineralisation and is therefore a marker of bone development (Siffert 1951, Orimo 2010).

Figures 6.1 and 6.2 show ALP activity of MSCs after 10 and 12 days respectively. High ALP activity can be seen in the positive controls (FN coat + osteogenic media and FN coat + 100 ng/mL BMP-2) when compared with the negative control (FN coat). ALP activity, was interestingly mostly equivalent to the FN coat in all *L. lactis* samples except *L. lactis*-BMP-2S, which was seen to be higher than the FN coat, with results very similar to that of a FN coat with the addition of BMP-2 at 100 ng/mL. This is true at both time points.

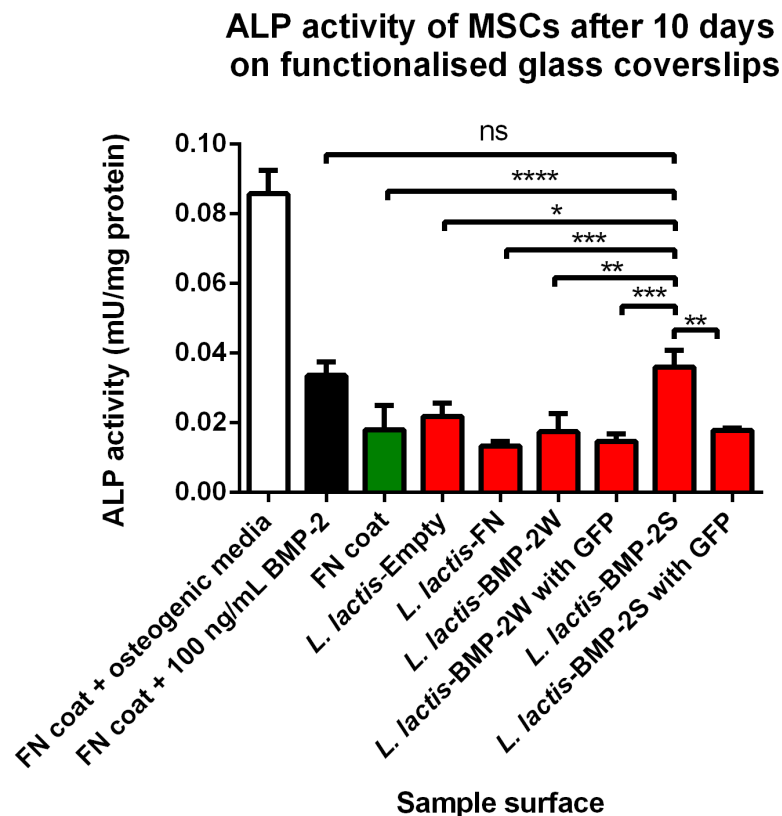


**Figure 6.1. ALP activity of MSCs after 10 days.** Cells were seeded over different *L. lactis* clones. ALP activity is highest in *L. lactis*-BMP-2S when compared with controls. Three technical replicates were completed per sample. Data is presented as the mean  $\pm$  SD and analysed with a one way ANOVA with a Tukey post hoc test. Statistical significance levels are \* $p < 0.05$ , \*\* $p < 0.01$ , \*\*\* $p < 0.001$  and \*\*\*\* $p < 0.0001$ .

## ALP activity of MSCs after 12 days on functionalised glass coverslips

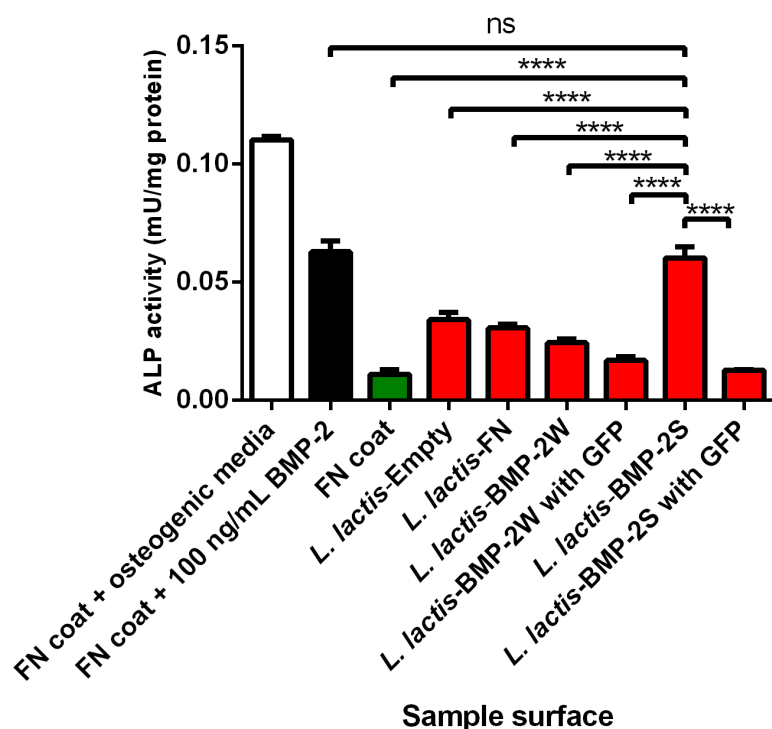


**Figure 6.2. ALP activity of MSCs after 12 days.** Cells were seeded over different *L. lactis* clones. ALP activity is highest in *L. lactis*-BMP-2S when compared with controls. Three technical replicates were completed per sample. Data is presented as the mean  $\pm$  SD and analysed with a one way ANOVA with a Tukey post-hoc test. Statistical significance levels are \*\*\*\*  $p < 0.0001$ .

This higher ALP activity could be due to the osteogenic potential of the secreted BMP-2 from *L. lactis*-BMP-2S. These results, compounded by the BrdU results from the previous chapter (Figures 5.4 and 5.5), show that out of our *L. lactis* clones, *L. lactis*-BMP-2S displays the highest potential for MSC osteoblastic differentiation.

For the long term experiments, only the differentiation characteristics of *L. lactis*-BMP-2S were explored as the other clones seem to show no osteoblastic potential.

Three different nisin induction profiles were designed to test the effectiveness of the inducible *L. lactis*-BMP-2S at different strengths. Figure 6.3A highlights the daily addition of nisin to the cultures and when the OCN and von Kossa experiments were completed. Figure 6.3B shows the amount of BMP-2 produced by NZ9020 in response to the nisin added shown in Figure 6.3A.

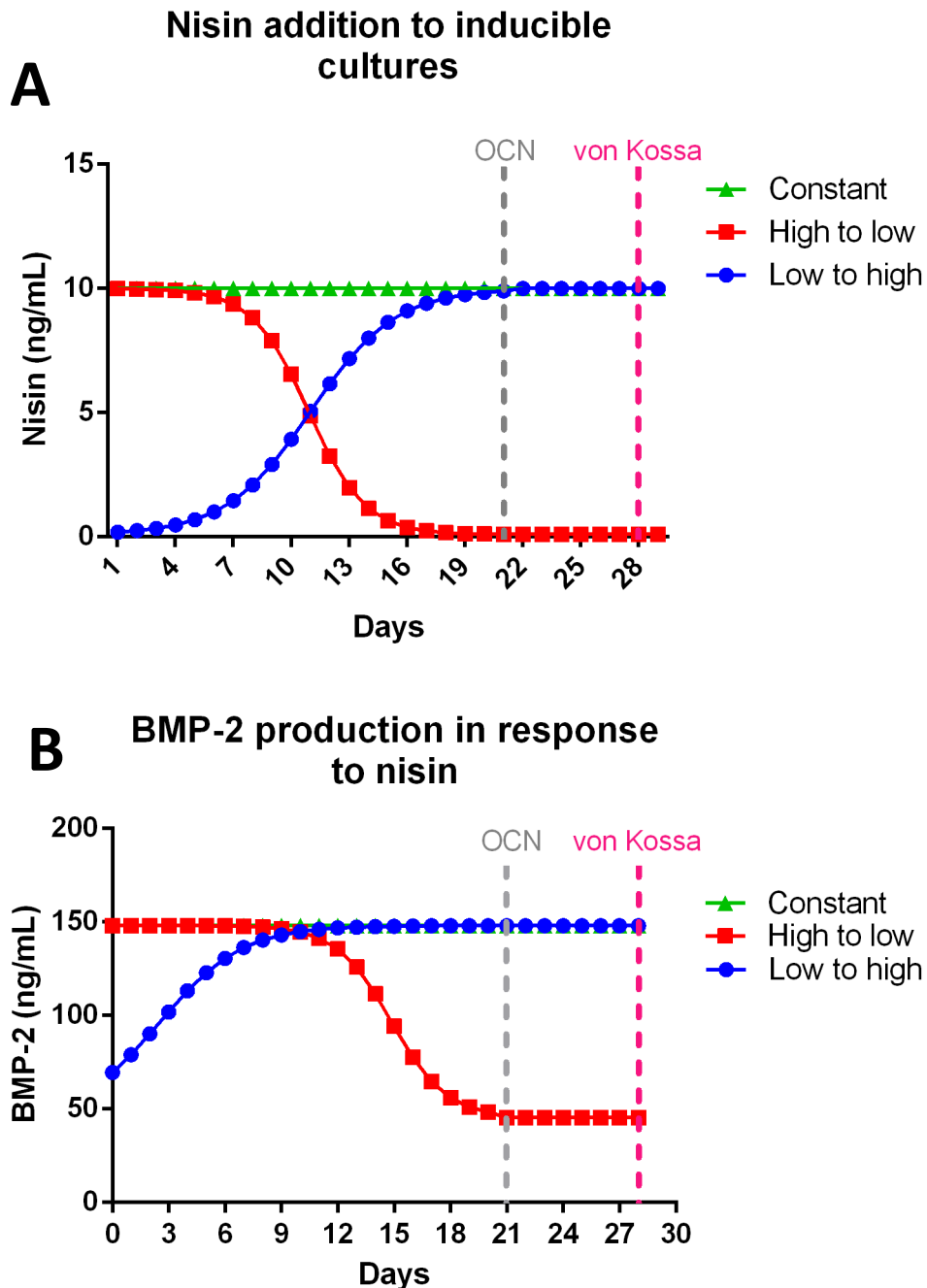


**Figure 6.3. Nisin and BMP-2 induction profiles.** (A) The inducible cultures were tailored to express BMP-2 and FNIII<sub>7-10</sub> at different rates throughout the course of the experiment to test the longevity and time dependency of BMP-2 towards osteogenic differentiation. Nisin was added daily to the cultures. (B) BMP-2 production in NZ9020 in response to nisin addition. Graph was completed using data taken from the ELISA (Figure 4.16). A continuous (green), high to low (red) and low to high (blue) induction profile was chosen to test BMP-2s osteogenic activity.

### Osteocalcin expression

The bone specific ECM protein OCN was used to determine MSC response to BMP-2 after 21 days. OCN is regularly used as a positive indicator of the onset of osteogenic commitment as it is expressed post-proliferatively by osteoblasts (Lian, Stewart et al. 1989, Rickard,

Kassem et al. 1996, Malaval, Liu et al. 1999, Kim, Yoo et al. 2005). OCN expression was seen to be present in all samples as shown in Figure 6.4, albeit, with varying amounts at day 21. Quantification of OCN (Figure 6.5) determined that their expression was higher in BMP-2 positive samples (added at 100 ng/mL and in the *L. lactis*-BMP-2S samples). OCN levels are consistently high between the FN coat +100 ng/mL BMP-2, constitutive *L. lactis*-BMP-2S and inducible *L. lactis*-BMP-2S at constant and high to low addition of nisin whilst OCN levels on the FN coat and constitutive *L. lactis*-FN are low.

Importantly, OCN expression was seen to be similar between the constitutive and inducible clones when nisin was added at a constant and high to low amount.

The results of OCN quantitation show clear differences in expression between a number of samples. For example, *L. lactis*-BMP-2S, in both its constitutive and inducible form shows a higher OCN expression than constitutive *L. lactis*-FN.

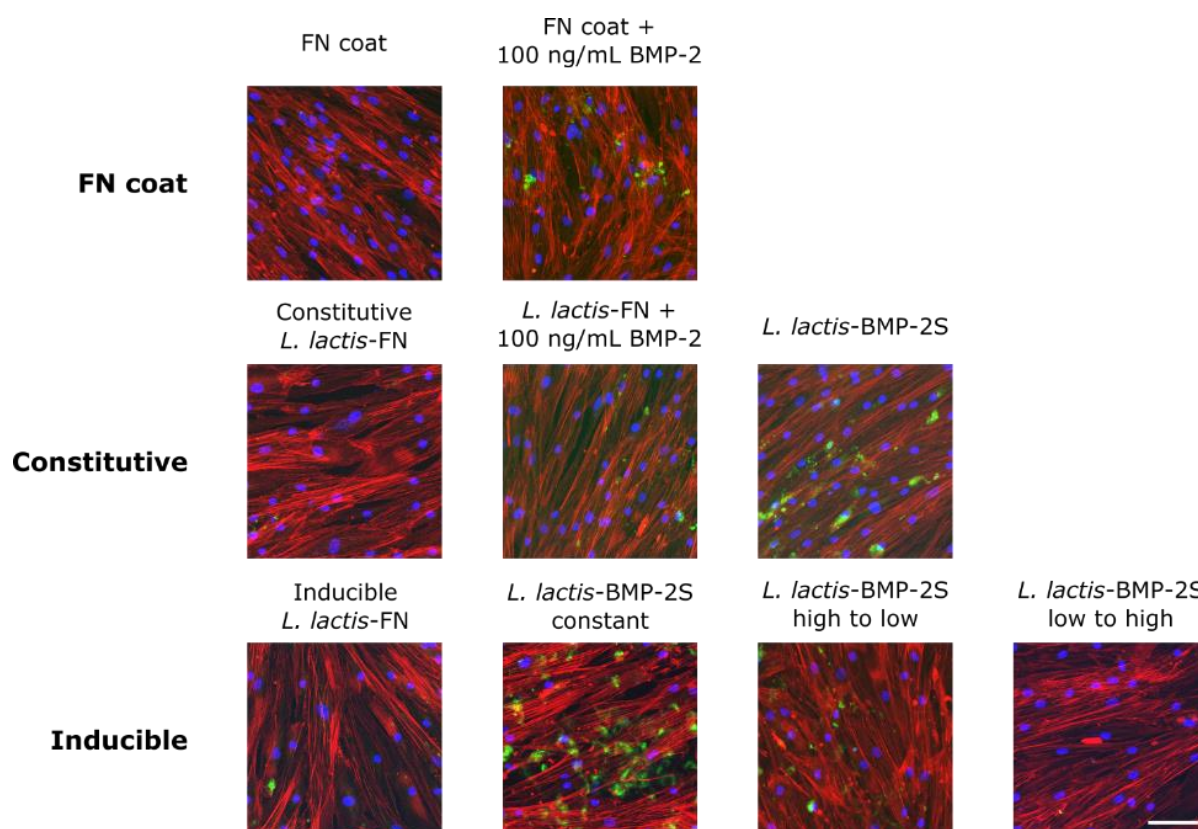


**Figure 6.4. Osteogenic differentiation of MSCs through osteocalcin.** MSCs were cultured for 21 days and immunostained for actin (red), osteocalcin (green) and nuclei (blue). The top row represents MSCs seeded on FN coats, the second row shows constitutive *L. lactis* clones. The third and fourth row represent MSCs seeded on *L. lactis*-BMP-2S with differing amounts of inducer and MSCs seeded over co-cultures of *L. lactis*-FN and *L. lactis*-BMP-2S with differing amounts of inducer respectively. Scale bar is 100  $\mu$ m.

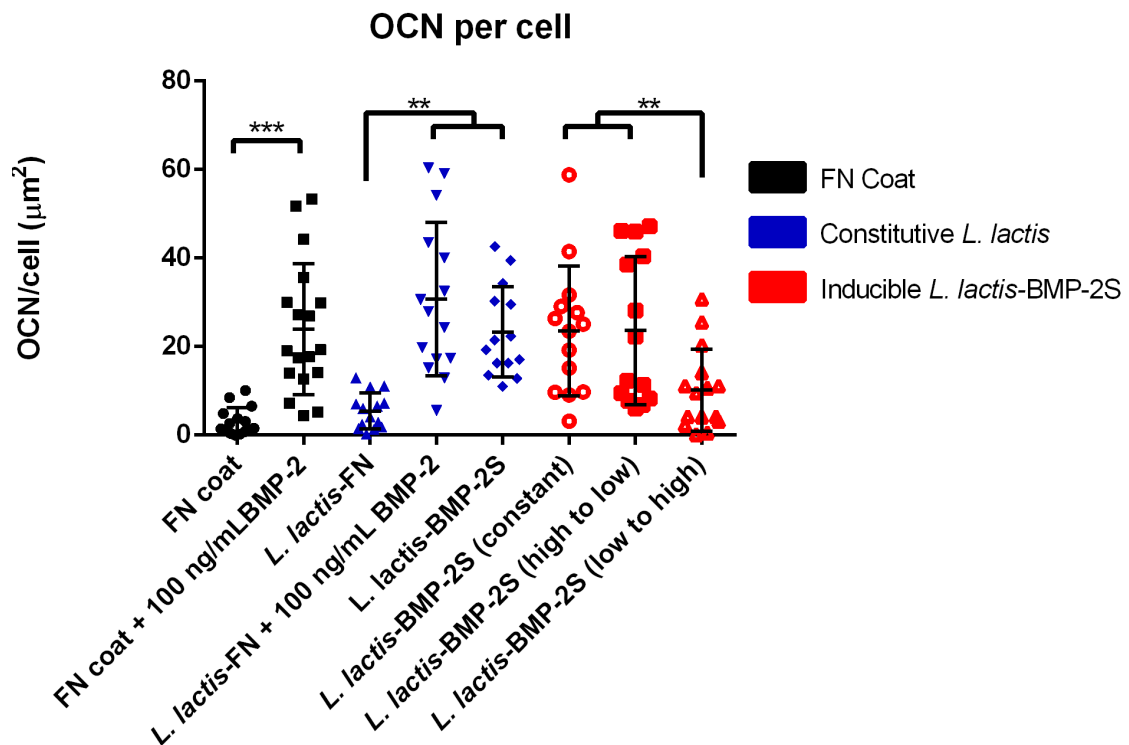


**Figure 6.5. Osteocalcin quantitation.** Graph shows integrated density corresponding to osteocalcin. OCN was found to be significantly higher in the samples with BMP-2 than in the samples without BMP-2. For the inducible clones, osteocalcin was seen to be higher in the sample sets where the inducer was highest at the start of the culture. A minimum of 400 cells from three technical replicates were used to analyse the samples. Data is presented at the mean  $\pm$  SD and analysed with a one way ANOVA with a Tukey post-hoc test. Significance levels are \*\* $p < 0.01$  and \*\*\* $p < 0.001$ .

### von Kossa staining

Osteoblasts deposit phosphate as a primary step of bone development and therefore this process is suggestive of terminal osteogenic differentiation. As can be seen from Figure 6.6A, phosphate deposition is distinctly higher (black deposits) in the samples with BMP-2 when compared to the negative control samples. Figure 6.6B shows a full coverslip as an example of the stain (*L. lactis*-BMP-2S high to low).

Quantification of phosphate deposition shown in Figure 6.7 again showed higher osteogenic markers in the BMP-2 positive samples. The positive control showed the highest differentiation with very comparable results between the BMP-2 positive sample sets. These results are complementary to the OCN results demonstrated above (Figures 6.4 and 6.5) with high OCN and von Kossa staining in the same samples.

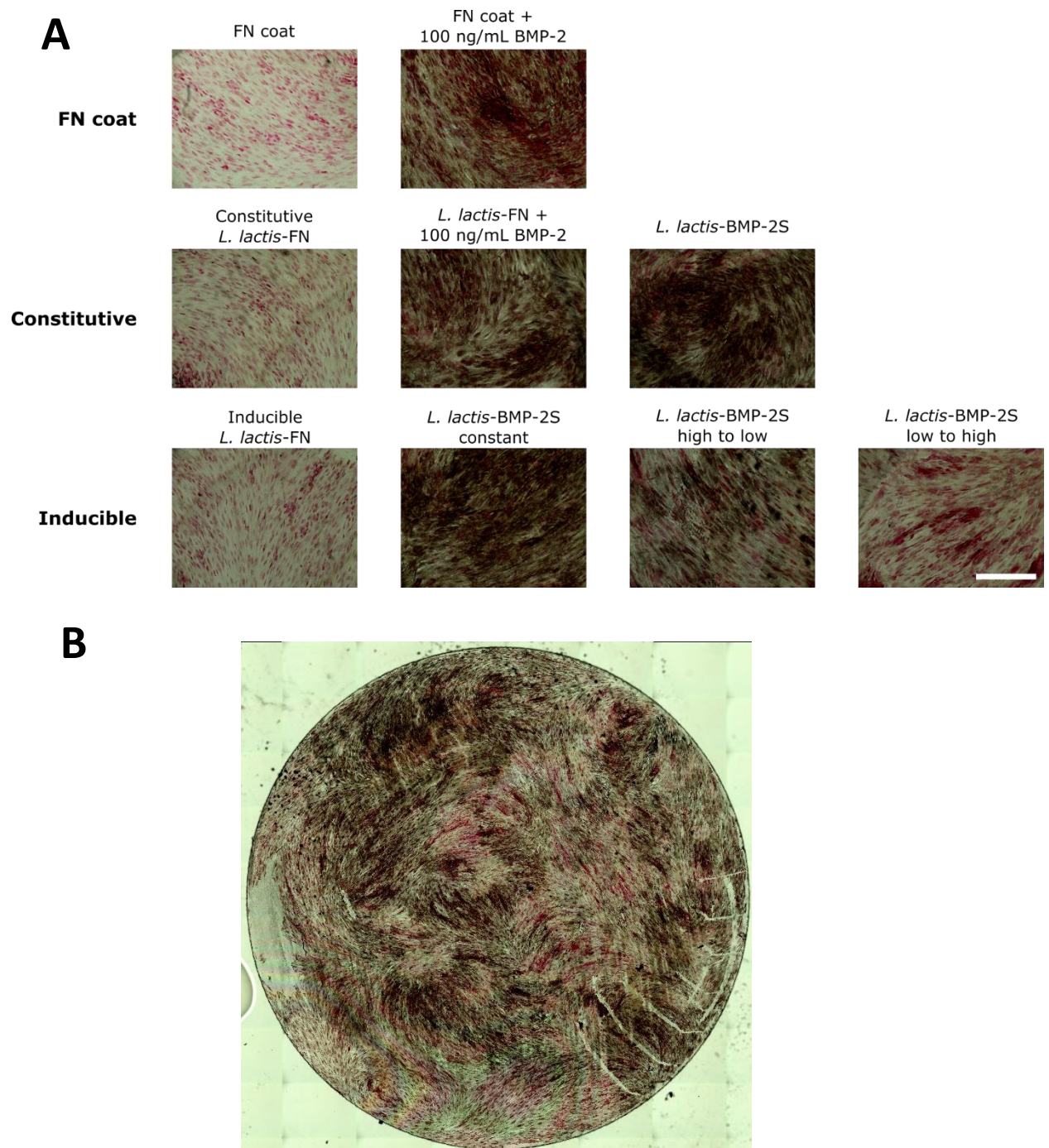


**Figure 6.6. Osteogenic differentiation of MSCs through von Kossa.** (A) Mineralisation (phosphate deposition) was assessed with a von Kossa staining on MSCs cultured after 28 days. Samples with BMP-2 showed much higher phosphate deposition than without BMP-2, as can be seen by the black deposits. The top row represents MSCs seeded on FN coats, the second row shows constitutive *L. lactis* clones. The third and fourth row represent MSCs seeded on *L. lactis*-BMP-2S with differing amounts of inducer and MSCs seeded over co-cultures of *L. lactis*-FN and *L. lactis*-BMP-2S with differing amounts of inducer respectively. Scale bar is 300  $\mu$ m. (B) Representative whole coverslip after von Kossa staining.

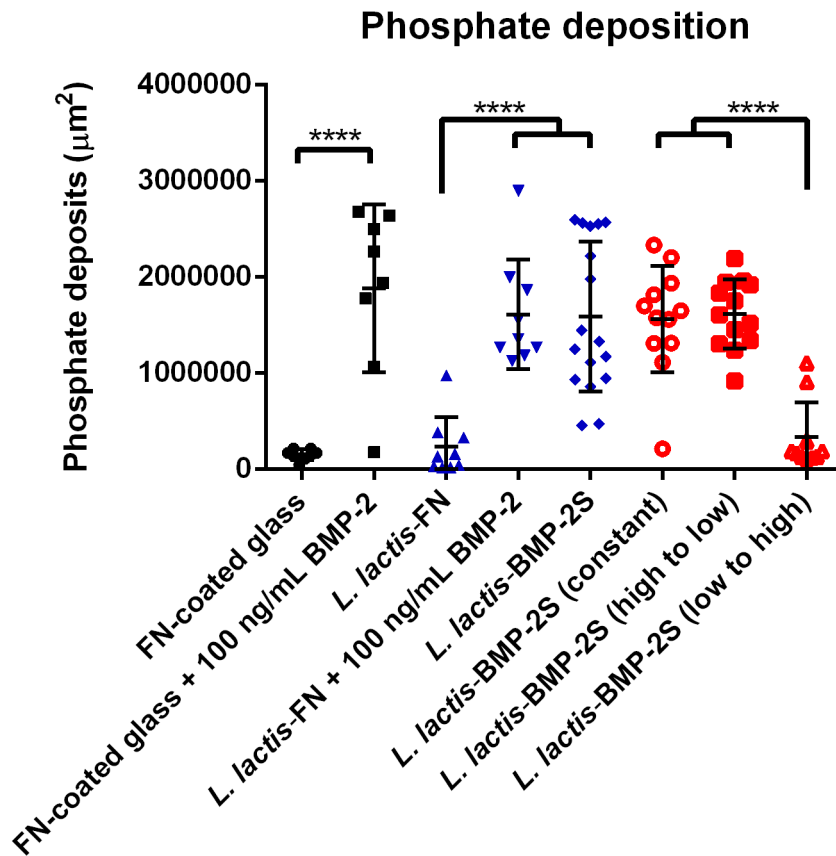


**Figure 6.7. Phosphate deposition quantitation.** Graph shows integrated density corresponding to phosphate deposition. von Kossa stains were found to be significantly higher in the samples with BMP-2 than in the samples without BMP-2. For the inducible clones, phosphate was seen to be higher in the sample sets where the inducer was highest at the start of the culture. A minimum of nine images were taken from three technical replicates. Data is presented as the mean  $\pm$  SD and analysed with a one way ANOVA with a Tukey post-hoc test. Significance levels are \*\*\*\*  $p < 0.0001$ .

Figure 6.8 shows OCN expression and phosphate deposition relative to the FN coated glass which is given value of '1'. On the constitutive clones, both *L. lactis*-FN + 100 ng/mL BMP-2 and *L. lactis*-BMP-2S show statistically significantly higher OCN and phosphate deposition with a mean fold change increase of 9 and 7 respectively in OCN and 10 and 9 in phosphate deposition. *L. lactis*-FN shows no difference and fold change remains close to '1'. Moreover, *L. lactis*-FN + 100 ng/mL BMP-2 and *L. lactis*-BMP-2S are not statistically different from each other, showing similar levels of differentiation.

In the inducible clones, constant and high to low addition of nisin showed statistically significantly more OCN and phosphate deposition than FN coated glass with very comparable fold change levels to those seen in the constitutive clones. On the contrary, low to high nisin addition resulted in statistically similar results to that of FN coated glass.

These results clearly show the differentiation potential of our *L. lactis*-BMP-2S in both a constitutive and inducible manner.

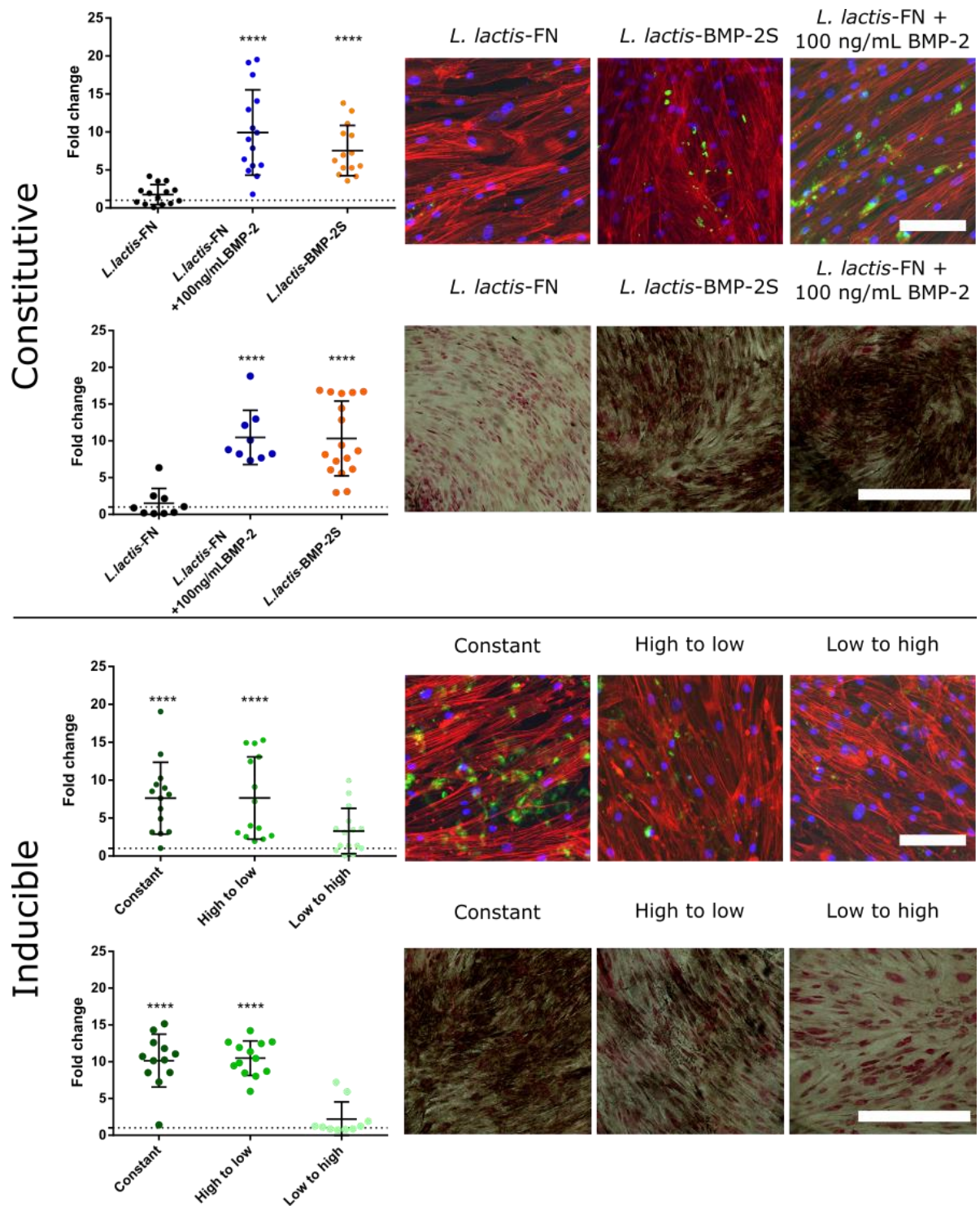


**Figure 6.8. Overall osteogenic differentiation.** Graphs detail fold changes for constitutive (top) and inducible *L. lactis* (bottom). Expression of OCN (above) and deposition of phosphate (below) was compared to that on FN coated glass (dotted line) and representative images are shown to the right. Data used here are the same as from Figures 6.5 and 6.7. Data is presented as the mean  $\pm$  SD and analysed with a one way ANOVA with a Tukey post-hoc test. Scale bar is 100  $\mu$ m for OCN and 300  $\mu$ m for von Kossa. Significance levels are \*\*\*\*  $p < 0.0001$ .

Altogether, the cell proliferation (Figures 5.4 and 5.5.), ALP (Figures 6.1 and 6.2.), OCN (Figures 6.4, 6.5 and 6.7.) and von Kossa (Figures 6.6, 6.7 and 6.8) confirm the ability of the living interface to induce MSC differentiation.

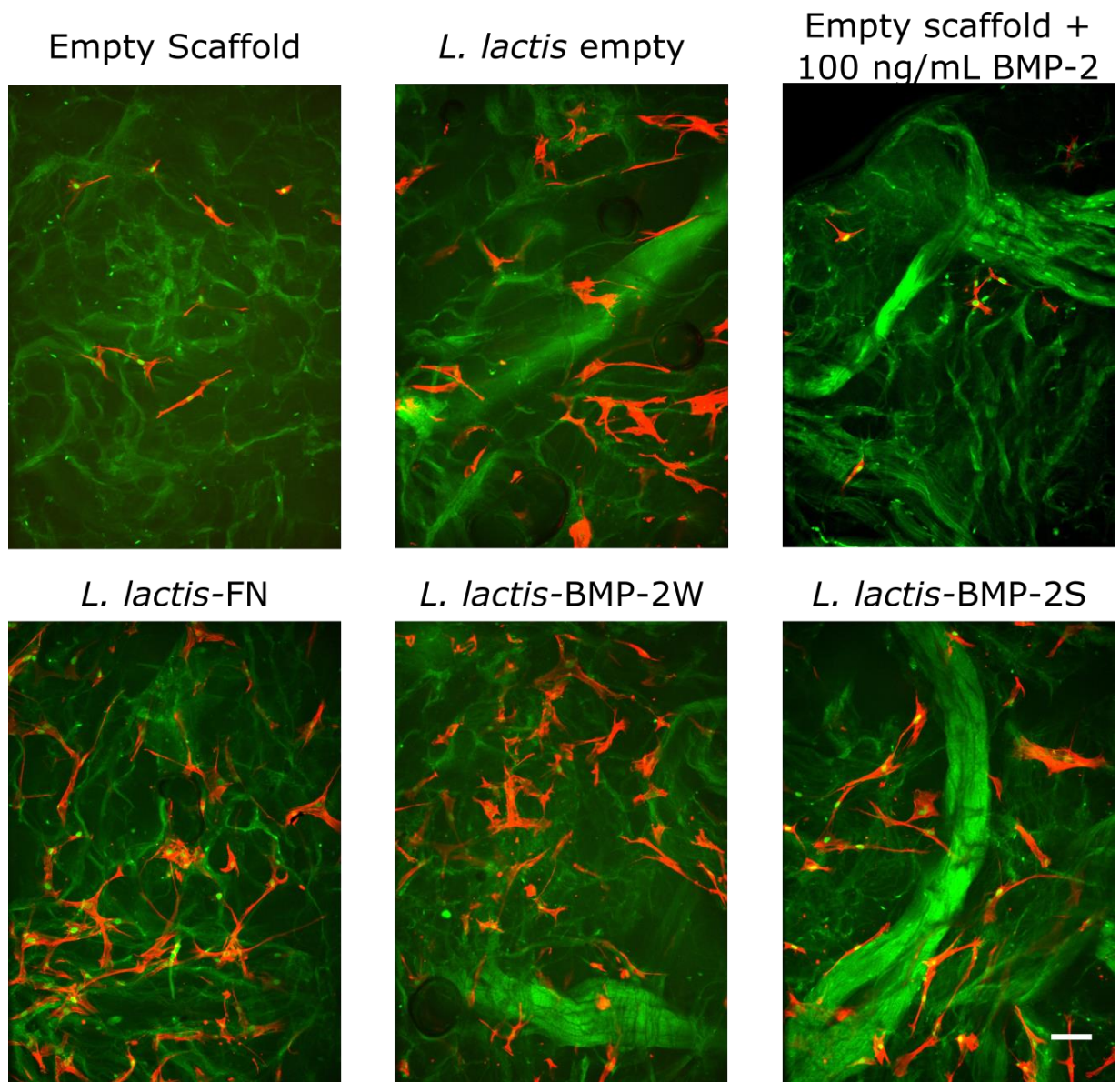
### 6.3.2 *In vivo* mouse study

The objective of this work was to evaluate the ability of biomaterial (collagen) scaffolds containing BMP-2 producing *L. lactis* to promote bone formation *in vivo* in an ectopic site. The model chosen was subcutaneous implantation as it is commonly used and an appropriate model to evaluate host responses to implanted biomaterials as well as the mineralisation capabilities of the therapy. The subcutaneous model also allows examination of the bacteria's capability to direct bone formation in an *in vivo* environment without contributions from host osteogenic cells. This implantation site provides a stringent, non-osseous environment to examine the inherent capacity of these bacteria to form bone tissue *in vivo* and gives important information on the inflammatory and immune response to these constructs (Friess 1998, Geiger, Li et al. 2003, Carstens, Chin et al. 2005, Lee, Kim et al. 2010).

Prior to the completion of the *in vivo* work, it was imperative to establish a sensible scaffold for the bacteria as the use of a glass coverslip would be detrimental to animal health. We chose to use the well characterised, absorbable collagen sponge (ACS) as it has high biocompatibility, is degradable and shows a suitable interaction with cells and other macromolecules (Friess 1998, Geiger, Li et al. 2003). Further to this, it has been used in conjunction with the delivery of BMP-2 to *in vivo* test sites (Carstens, Chin et al. 2005). ACS is used with BMP-2 as the protein acts optimally when combined with an adequate matrix. This matrix acts to prolong the residence time of the protein as well as acting as support for invading osteoprogenitor cells; the favourable influence of collagen on cellular infiltration in wound healing is well known (Kim, Lee et al. 2011). The efficacy and safety of the combination of the ACS and BMP-2 has been clearly proven in both animal and human trials (Nevins, Kirker-Head et al. 1996, Boyne, Marx et al. 1997, d'Aquino, De Rosa et al. 2009).

Cell adhesion to sponges was first explored. MSCs were seeded (5000 cells/cm<sup>3</sup>) over collagen sponges that had been pre-cultured with different strains of *L. lactis*. MSCs were cultured for one day before fixation and staining with DAPI and phalloidin. It is apparent from Figure 6.9 that cells have attached to all sponges with varying success. Scaffolds functionalised with bacteria seem to show a much higher cell attachment than without bacteria. Even scaffolds with *L. lactis*-empty were seen to harbour more cells than the non-bacterial samples. This is surprising as the collagen should induce cell adhesion. All cells display a stretched elongated morphology, indicative of their health and viability. Surprisingly, DAPI seemed to stain the collagen sponge as well as nuclei. This can be

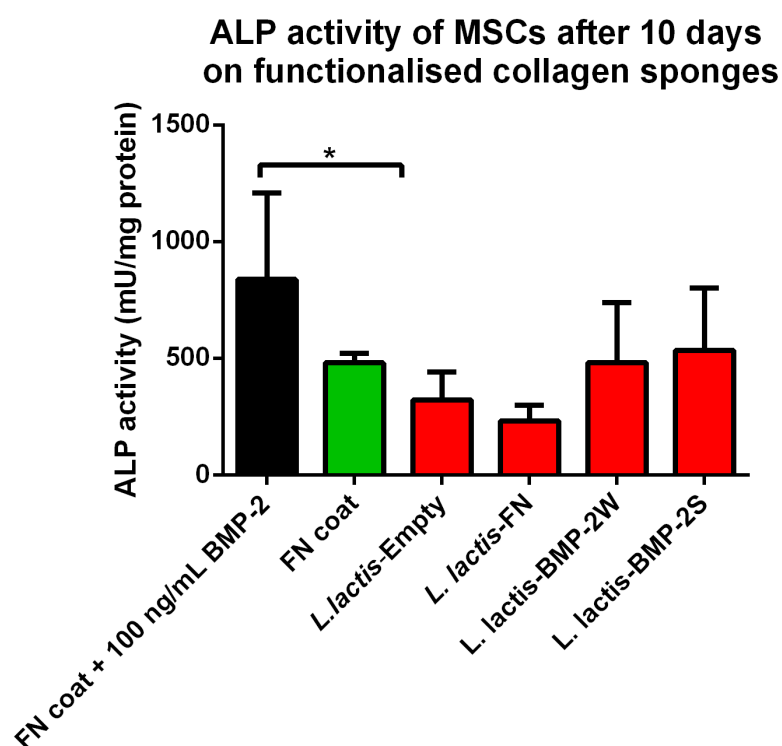
concluded by the fact that the sponge can be seen as green in the scaffolds without bacteria. Bacteria were present in the sponges as the medium (DMEM) could be seen to turn yellow, an indication of acidification by *L. lactis* NZ9000.



**Figure 6.9. MSC adhesion to functionalised collagen sponges after 1 day.** Cells were seeded over differently functionalised collagen sponges and MSCs can be seen to adhere all surfaces. Green = DAPI and red = actin. Scale bar = 100  $\mu$ m.

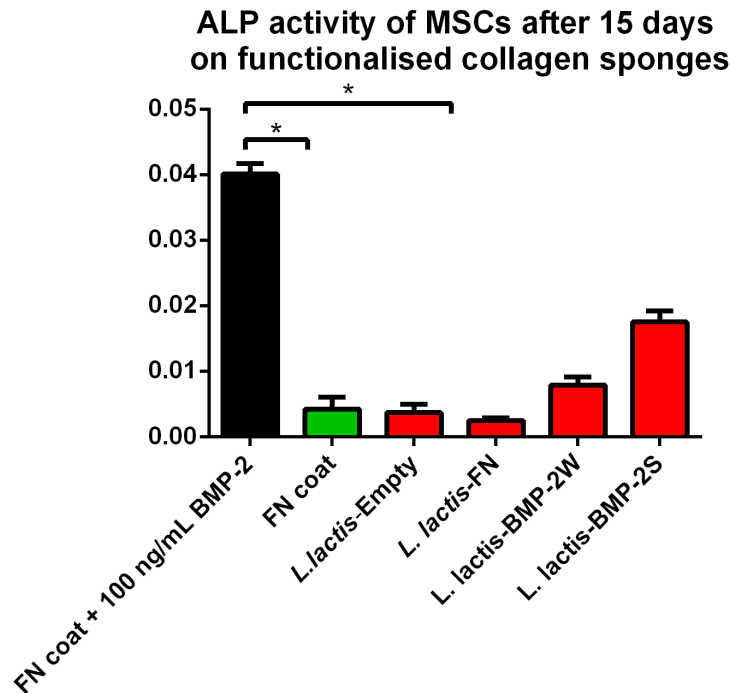
Figures 6.10 and 6.11 show activity of ALP in mU of ALP/mg protein on different functionalised collagen scaffolds. Cells were left to culture for 10 and 15 days before lysing and assaying for protein content and ALP activity.

Figure 6.10 shows ALP activity at day 10 in collagen sponges. It is clear that the samples with 100 ng/mL of BMP-2 added to the media (positive control) induced the highest amount of ALP activity, however, the negative control (no BMP-2), displayed a similar amount of ALP activity to that of our *L. lactis* displaying BMP-2 bacteria (albeit, slightly less than the secreted BMP-2). Further to this, our BMP-2 strains, both the membrane and secreted versions, produced higher amounts of ALP than our non BMP-2 expressing strains (not statistically different). The only statistically significant difference in the samples was between 100 ng/mL BMP-2 and *L. lactis*-FN.



**Figure 6.10. ALP activity of MSCs after 10 days on collagen sponges.** Cells were seeded over differently functionalised collagen sponges. ALP activity is highest in *L. lactis*-BMP-2S, however, is similar to the negative control. Three technical replicates were completed per sample. Data is presented as the mean  $\pm$  SD and analysed with a one way ANOVA with a Tukey post-hoc test. Statistical significance level is \* $p < 0.05$ .

Figure 6.11 highlights ALP activity at day 15 and shows that 100 ng/mL of BMP-2 (positive control) induced the highest amount of ALP activity. The next highest result is that of *L. lactis*-BMP-2S, which is the same result as for on glass coverslips shown in Figures 6.1 and 6.2. This confirms that the bacteria and mammalian cells behave in a similar way as to on the glass coverslips. This results demonstrates that *L. lactis*-BMP-2S has the ability to induce osteogenesis in a collagen sponge and was chosen as the *L. lactis* strain to continue the *in vivo* trial.



**Figure 6.11 ALP activity of MSCs after 15 days on collagen sponges.** Cells were seeded over differently functionalised collagen sponges. ALP activity is highest in *L. lactis*-BMP-2S. Three technical replicates were completed per sample. Data is presented as the mean  $\pm$  SD and analysed with a one way ANOVA with a Tukey post-hoc test. Statistical significance level is \* $p < 0.05$ .

### ***In vivo* study**

The preliminary *in vitro* study was used to ascertain which strain of *L. lactis* should be used *in vivo*. From the cell attachment and ALP studies, it was concluded that *L. lactis*-BMP-2S showed the best potential for bone production *in vivo*.

### **$\mu$ CT**

Mice were anaesthetised and imaged. Annex Figures 8.1 (two weeks) and 8.2 (four weeks) show reconstructed 2D images of the areas housing the collagen sponges and Tables 6.1 (two weeks) and 6.2 (four weeks) show the calculated bone volume ( $\text{mm}^3$ ). No mineralised bone was seen in any sample, including the positive control. Conventionally, a large amount of BMP-2 is used in these studies, with more than  $1 \mu\text{g/mL}$  being the normality. We used  $100 \text{ ng/mL}$  and are therefore at least at a 10 fold reduction in BMP-2 levels. This low dosage could explain the lack of bone formation in the sponges. This amount was chosen as it was the amount used in the *in vitro* controls. If the experiment were to be done again, a higher concentration positive control would be needed.

**Table 6.1. Calculated bone volume (mm<sup>3</sup>) in collagen sponges after two weeks.**

Scaffold	Empty scaffold	100 ng/mL BMP-2	<i>L. lactis</i> -empty	<i>L. lactis</i> -BMP-2S
1	0	0	0	0
2	0	0	0	0
3	0	0	0	0
4	0	0	0	0
5		0	0	0
6				0

**Table 6.2. Calculated bone volume (mm<sup>3</sup>) in collagen sponges after four weeks.**

Scaffold	Empty scaffold	100 ng/mL BMP-2	<i>L. lactis</i> -empty	<i>L. lactis</i> -BMP-2S
1	0	0	0	0
2	0	0	0	0
3	0	0	0	0
4	0	0	0	0
5		0	0	0
6				0

## **Histology**

The sponges were explanted from the mice and were stained with haematoxylin and eosin (H&E). Figure 6.14 shows H&E staining of 5 µm slices of the sponges. The light pink (detailed by the blue arrows) corresponds to regions of the sponge, the dark purple spots are cell nuclei and the lighter purple colour are the cell cytoplasm. It is apparent from the images that the sponges have been invaded by cells, including the middle of the sponge. The sponges have been vascularised as can be seen by the presence of a vein holding red blood cells (shown by green arrow). We expected an immune response from the animals due to the addition of the bacteria, with more white blood cells present in the bacterial samples, however, no differences in H&E staining were seen between the samples.

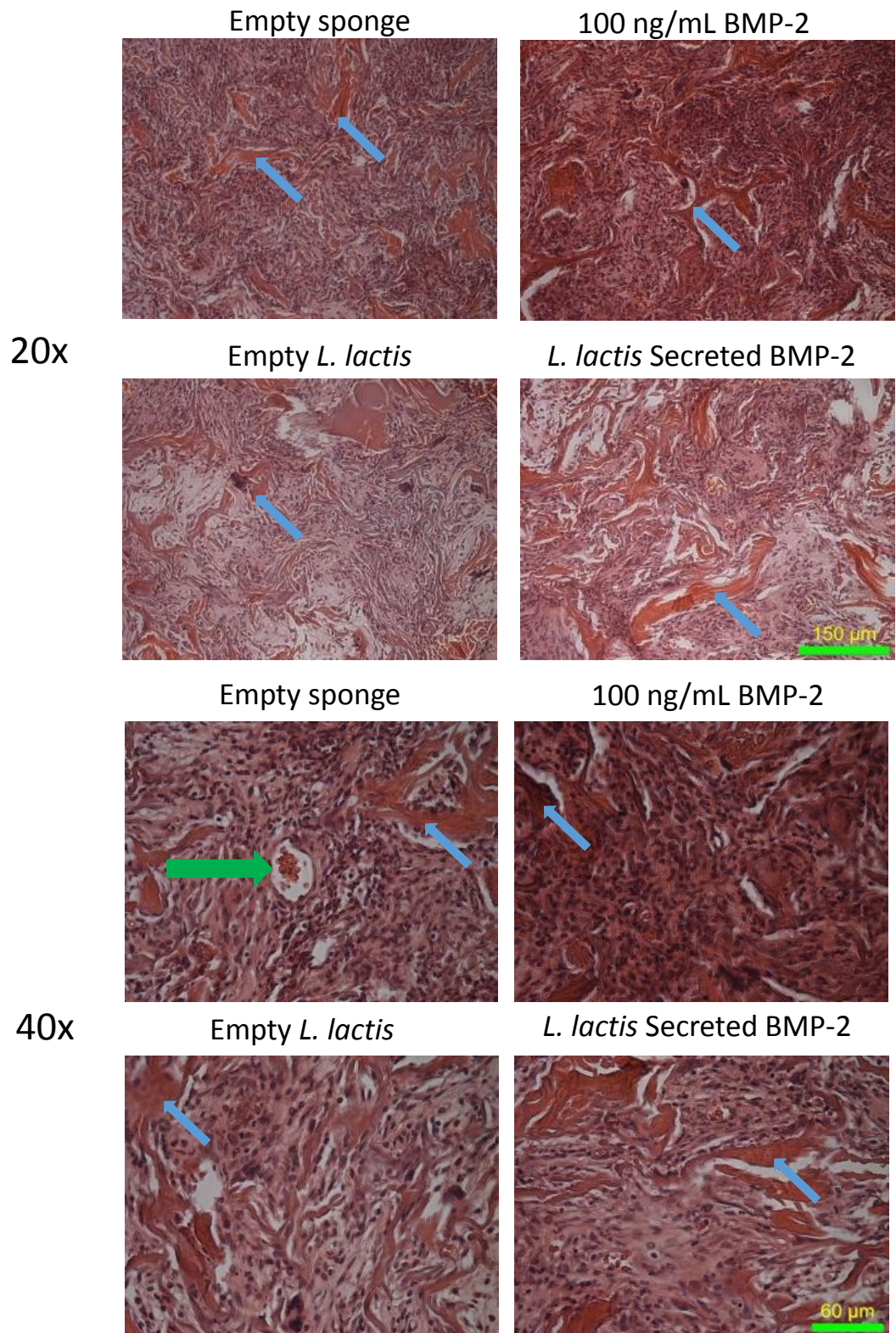


**Figure 6.12. Haematoxylin and eosin staining of sliced collagen sponges after four weeks.** Images were taken at 20x (top) and 40x (bottom) on empty sponge, sponges with 100 ng/mL BMP-2, sponges with *L. lactis*-empty and sponges with *L. lactis*-BMP-2S. Blue arrows show areas of collagen sponge and the green arrow shows a vascularised area.

## 6.4 Discussion

Engineering the cellular microenvironment to direct stem cell behaviour is of fundamental importance to biomedical applications. It is known that that cells interact with their environment, the ECM, through integrins and growth factor receptors resulting in biochemical signalling cascades. Collectively, these different signals dictate a plethora of responses already hardwired into the genes of the cell which control many cellular phenotypes, including differentiation.

This chapter highlights the osteogenic potential of *L. lactis*-BMP-2S at varying time points (10, 12, 21 and 28 days) and on different surfaces (PEA coated glass and ACS).

ALP activity of MSCs after 10 and 12 days (Figures 6.1 and 6.2) on differing constitutive *L. lactis* clones showed that *L. lactis*-BMP-2S demonstrated the best osteogenic potential as MSC ALP activity was almost identical to that of MSCs cultured on a FN coat with 100 ng/mL BMP-2 added to the medium. This was true at both 10 and 12 days. Therefore, *L. lactis*-BMP-2S shows the lowest proliferation rates at one and three days (Figures 5.4 and 5.5) on both constitutive and inducible clones, and highest ALP activity at day 10 and 12. The results for *L. lactis*-BMP-2S were most similar to our positive control, a FN coat with 100 ng/mL BMP-2 added to the medium. In contrast, *L. lactis*-FN, *L. lactis*-BMP-2W and *L. lactis*-BMP-2S and M-GFP showed high proliferation rates and low ALP activity, similar to that of a FN coat without BMP-2 added. These results suggested that *L. lactis*-BMP-2S showed the highest osteogenic potential which allowed us to select this clone for further study.

Upon selection of *L. lactis*-BMP-2S for long term differentiation studies, a 21 day OCN and 28 day von Kossa stain were completed. This was tested on both the constitutive and inducible clones. The OCN and von Kossa data validated *L. lactis*-BMP-2S' ability to induce differentiation of MSCs in both its constitutive and inducible forms. In its constitutive form, differentiation from both the OCN and von Kossa showed similar results to that of the positive control. The inducible form was tested at different strengths of inducer (profiles shown in Figure 6.3). Unsurprisingly, the constant expression with 10 ng/mL nisin showed high differentiation and low to high showing negligible differentiation. Surprisingly, high to low addition of nisin resulted in similar differentiation to that of constant addition. This data explains that nisin addition is needed at early time points in the experiment, as by day 19 nisin addition was at its maximum (10 ng/mL) in the low to high samples and insignificant differentiation was seen by 21 and 28 days. This details the importance the initial

cell/material interaction. This data supports the existing paradigm that cells react strongly to the initial stimuli. In the high to low sample, BMP-2 expression was relatively low by day 10 and the same level of differentiation was seen between this and the constantly high expressed BMP-2 samples.

These long-term (OCN and von Kossa), compounded by mid-term (ALP) and short-term (BrdU) differentiation results show that *L. lactis*-BMP-2S has strong osteogenic potential to direct the differentiation of MSCs to osteoblasts *in vitro*.

Next, the differentiation capabilities were examined in 3D collagen sponges before being trialled in an *in vivo* subcutaneous mouse model. NZ9000 bacteria were used in this model as they are capable of producing higher amounts of protein, and the mouse's vascular system would be able to remove any lactic acid produced by the bacteria, thus removing the biggest *in vitro* problem with the system (Eggleton and Evans 1930, Davies, Knibbs et al. 1970).

MSCs were found to adhere to all sponges as collagen proteins hold multiple cell adhesion motifs (Heino 2007, Taubenberger, Woodruff et al. 2010), regardless of *L. lactis* present. Interestingly, the presence of bacteria increased the adhesion of MSCs to the sponge when compared to the empty sponges. This was true of all *L. lactis* subtypes, and not only *L. lactis*-FN. A mid-term ALP activity assay was again utilised to ascertain the differentiation aptitude of *L. lactis* in these sponges. Once again, ALP activity was seen to be highest in the *L. lactis*-BMP-2S samples, however, the differences were not statistically significant. Nonetheless, the osteogenic capabilities shown in 2D and the fact that *L. lactis*-BMP-2S showed highest osteogenesis in the 3D model shows that it has some osteogenic potential and therefore this bacteria was chosen for *in vivo* tests.

A subcutaneous model was chosen to highlight the bacteria's capacity to direct ectopic bone formation in an *in vivo* environment, devoid of the host's osteogenic cells. *In vivo*  $\mu$ CT at two and four weeks showed no bone growth in any of our samples, including the positive control. This is likely due to the low amount of BMP-2 used in these samples. We decided to use BMP-2 at 100 ng/mL in the implanted sponges, the same as in the ALP experiment previous and in the *in vitro* models. However, it is reported that BMP-2 in collagen sponges is often up at the  $\mu$ g range, and is therefore at least a tenfold higher concentration than in our samples. However, the bacteria did not induce bone formation either and from the characterisation experiments, we expect 485 ng/mL of BMP-2 (Figure 4.3). This is clearly not the case in the 2D experiments as the bacteria samples are not fully saturated in the culture. For the 3D collagen sponge experiments, the bacteria are present in the sponge and

it is difficult to ascertain the number of bacteria present. In order to reach the  $\mu\text{g}$  range of secretion from our bacteria, we would need approximately 2 mL of saturated culture and would need a distinctly larger collagen sponge, however, it is difficult to directly assess the exact size of collagen sponge needed as it is impossible to measure the number of bacteria present in the sponge. The collagen sponges that were implanted were submersed in 1 mL of bacterial culture, however, it was apparent that there were considerable amounts of bacteria outside the sponge and therefore, there would not be 485 ng/mL BMP-2 present.

In addition to the  $\mu\text{CT}$ , a H&E stain was used to determine the presence of cellular differences between the functionalised sponges, however, no differences could be seen. We were looking for signs of osteoblasts and osteoclasts, as well as host immune cells to see if the bacteria were destroyed. After four weeks, no osteogenic cells, or host immune cells could be seen. However, it was apparent from the backs of the mice that sponges implanted with bacteria led to increased swelling of the area, when compared with the mice with sponges without bacteria. This was seen for the first week of the experiment, and soon dissipated. If repeated, blood tests would be taken from the mice within the first week to check for increased signs of infection. This could mean that the bacteria were engulfed and destroyed by the host's immune system within the first week of the trial, thus losing the source of the BMP-2, explaining the lack of differentiation. Although the 2D OCN and von Kossa inducible results (Figures 6.5, 6.7 and 6.8) detail the requirement for high BMP-2 concentrations needed at the beginning of the culture only, the lower amount of BMP-2 ( $< 1 \mu\text{g}$ ) may result in decreased differentiation in a non-osseous site. The high amount of BMP-2 needed, coupled with the likeliness of *L. lactis* death; could lead to the lack of bone growth *in vivo*.

Although the *in vivo* experiment did not proceed as planned, it is apparent that genetically engineered *L. lactis* secreting BMP-2 can indeed induce the osteogenic differentiation of MSCs, to a similar level to that of a FN coated coverslip with BMP-2 added to the media at 100 ng/mL *in vitro*. This result demonstrates that *L. lactis* can not only direct the attachment of MSCs through cell wall bound FNIII<sub>7-10</sub>, they also have the ability to change the phenotypical state of the cells seeded above through the osteogenic growth factor, BMP-2.

## 6.5 Conclusion

This chapter shows that *L. lactis*-BMP-2S can be used as a successful interface between a synthetic surface and MSCs to control their differentiation towards an osteoblastic fate to a similar extent as an FN coated substrate with 100 ng/mL BMP-2 added to the media. *L. lactis* can be modified to produce BMP-2 in a constitutive and inducible fashion, and that the BMP-2 is biologically active. Furthermore, differences in nisin addition emphasised the need for higher concentrations of BMP-2 towards the start of the experiment to allow for terminal differentiation of MSCs by 28 days. This result also demonstrates the power of our inducible system, in that we can allow cell growth to continue and upon user defined time points and concentrations, BMP-2 can be added to the system to induce the differentiation of the mammalian cells.

In addition, *L. lactis*-BMP-2S was used in an *in vivo* mouse model to explore subcutaneous ectopic bone formation. However, no bone growth was seen over four weeks. This is likely due to the fact that the bacteria were removed by the host's immune system and the low level of BMP-2 used.

This chapter has shown that genetically engineered *L. lactis* can be used to colonise a surface and that the differentiation cues supplied by growth factors can influence phenotypical decisions of stem cells.

# 7. Discussion and conclusion

## 7.1 Summary

The main findings from this work show that *in vitro*, genetically engineered *L. lactis* can direct the attachment and differentiation of MSCs. A schematic representation of the system can be seen in Figure 7.1. Both short and long term experimentation highlight that *L. lactis* secreted BMP-2 is biologically active and can induce the differentiation of MSCs to a similar level as achieved when exogenous BMP-2 is added to the culture. In addition, the system has also been made inducible, whereby the user can define the time and amount of protein to be expressed. The well characterised nisin controlled gene expression system (NICE) (Mierau and Kleerebezem 2005) was used with differing levels of inducer; protein expression and the level of MSC differentiation was seen to directly correlate with amount of inducer added.

However, findings from the *in vivo* model suggested that the system needs more development in order to transition to animal trials. A more robust positive control will need to be developed to allow for more accurate conclusions. A collagen sponge was implanted subcutaneously in the backs of mice, and ectopic bone formation was measured with micro-CT. No bone growth was seen over four weeks as we believe the bacteria were destroyed by the host's immune system. Moreover, this was only a pilot study and would need to be tested more vigorously in the future.

In summary, this thesis highlights the potential for non-pathogenic bacteria to be used as a substrate in the creation of dynamic surfaces for their use in regenerative medicine. Additionally, this system can be further modified, either in the production of other proteins or by the creation of other plasmids for controlled release in response to other inducers.

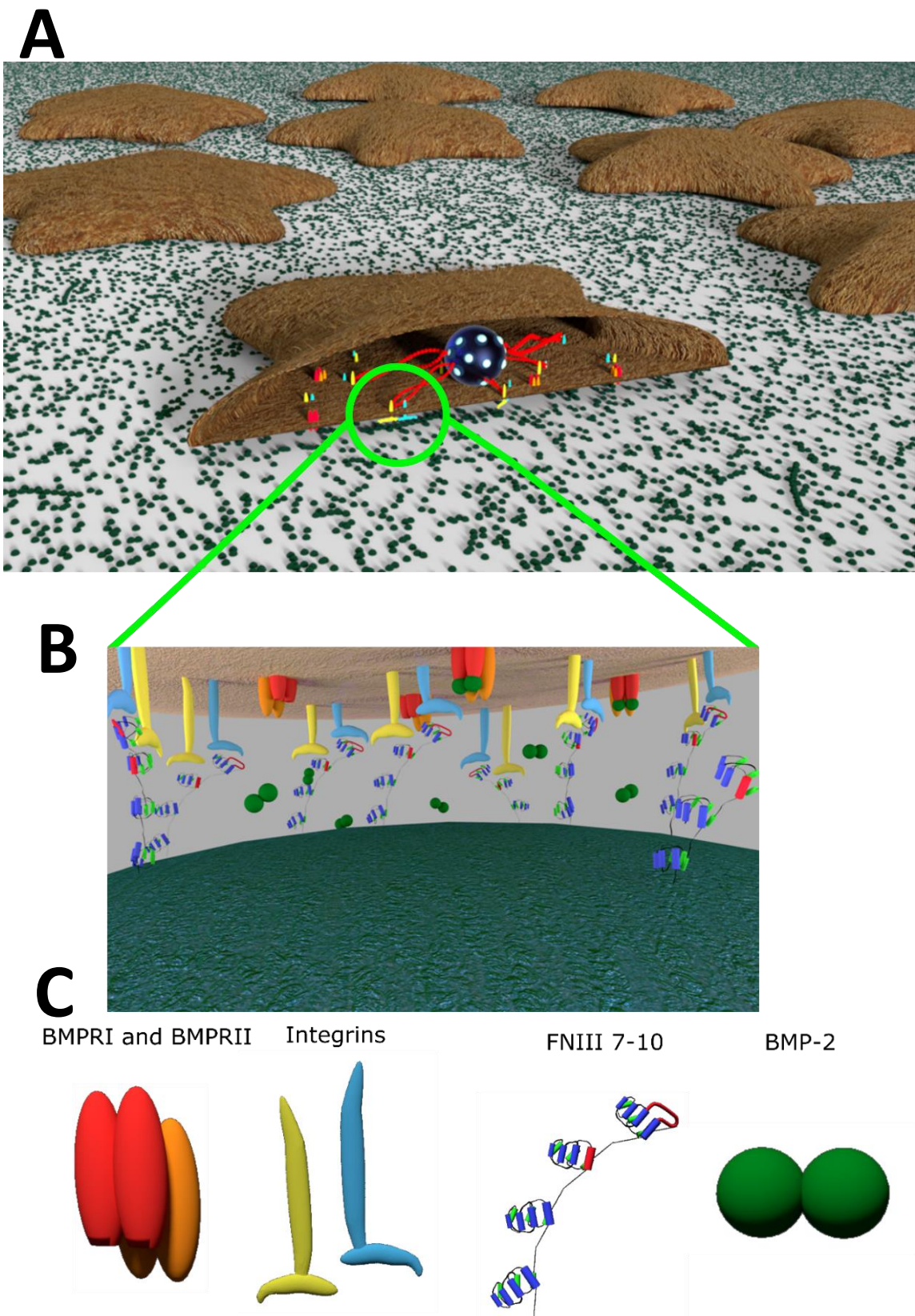


**Figure 7.1. 3D schematic representation of the interaction between *L. lactis* and MSCs.** (A) shows MSCs seeded on top of a monolayer of bacteria. (B) Shows a zoomed in representation of the area of interaction. (C) Shows from left to right, BMP receptors I and II, integrin subunits, FNIII<sub>7-10</sub> and BMP-2.

## 7.2 General discussion

Bacteria based therapeutics is a rapidly growing field, with non-pathogenic strains being used to fight an array of biomedical problems. Bacteria are already being used to fight cancer (Wang, Vuletic et al. 2017, Zheng, Nguyen et al. 2017), obesity (Chen, Guo et al. 2014) and various gastrointestinal diseases (Steidler, Wells et al. 1995, Schotte, Steidler et al. 2000). This thesis paves the way for advanced biofilm based therapeutics, as *L. lactis* secreting BMP-2 was found to be biologically active and can control the differentiation of MSCs. *L. lactis* has been modified to present and express FNIII<sub>7-10</sub> in a cell wall bound form and BMP-2 in a cell wall bound and secreted form. It was found that the cell wall bound FNIII<sub>7-10</sub> fragment could prompt cell adhesion in a variety of cell types including MSCs and C2C12s. The osteogenic growth factor BMP-2 was expressed in a cell wall bound and secreted form. The cell wall bound BMP-2 monomer did not show any biological activity. This is likely due to BMP-2 dimerisation being essential to bind to the BMP-2 receptor, in addition, it has been proven that modifying the C-terminal of BMP-2 (with SpaX in this work) renders the molecule inactive (Kashiwagi, Tsuji et al. 2009). In contrast, secreted BMP-2 showed good levels of biological activity with comparable levels of late term osteogenic markers to the positive control (FN coat with 100 ng/mL BMP-2 added to the medium).

This new work paves the way for advanced biofilm-driven cell therapies. Current stem cell culture systems fall far short of desired outcomes of enhanced growth and enhanced proliferation that can work in a bioreactor-like manner (Celiz, Smith et al. 2014). Furthermore, these culture systems are not dynamic and might be good either for growth (McMurray, Gadegaard et al. 2011) or for differentiation (McBeath, Pirone et al. 2004, Engler, Sen et al. 2006, Dalby, Gadegaard et al. 2007), but not for both. Dynamic culture systems have been developed but are limited typically to simple on/off states (Ebara, Yamato et al. 2004, Todd, Scurr et al. 2009, Wirkner, Weis et al. 2011, Lee, Garcia et al. 2015, Chaudhuri, Gu et al. 2016, Das, Gocheva et al. 2016). This work shows how simple biological cells such as *L. lactis* can be engineered to allow temporal expression of cell wall bound or secreted biologicals that can control MSC growth (FNIII<sub>7-10</sub>) and differentiation (BMP-2). It is easy to see how the complexity of this system can be tuned to express other proteins that could e.g. drive other phenotypes. Further, it is easy to see that as the system is compatible with 3D materials, adherent stem cell cultures, such as MSCs, can be scaled to 3D 'fermentation' type bioreactors for mass production of cells.

This thesis focuses on BMP-2 and osteogenic MSC differentiation as bone is the second most transplanted tissue after blood (Shegarfi and Reikeras 2009) and thus, there is a growing need for lab grown osteoblasts for cellular therapies. The ageing populations of many countries only exacerbates the problem as diseases such as osteoporosis are becoming more prevalent (Manolagas 2010). This work shows the osteogenic capabilities of genetically engineered bacteria in both 2D and 3D. Users can coat surfaces with or incorporate BMP-2 secreting *L. lactis* to induce highly efficient differentiation of MSCs to osteoblasts *in vitro*, with 3D systems such as hydrogels allowing bioreactor scale cell production. These cells can then be harvested for a variety of downstream applications, ranging from autologous or allogenic cell transplants or for the creation of lab grown bone (Burchardt 1983, Deans and Moseley 2000, Aggarwal and Pittenger 2005).

Using these simple biological cells, the system could be improved by creating an environment whereby BMP-2 compounded with other growth factors would assist in the creation of a bacterially expressed osteogenic ‘cocktail’. Bone morphogenetic protein-7 (BMP-7), platelet-derived growth factor (PDGF), and fibroblast growth factor (FGF-2) are all known osteogenic factors that in addition to BMP-2 could be engineered into the system to provide temporal controlled release and hence more efficient differentiation of MSCs (Mohan and Baylink 1991) in a manner that would be extremely different to using biomaterials approaches. It is exactly this flexibility that is the real benefit of this concept. There are already a wide variety of constitutive and inducible expression systems available for *L. lactis* and with these tools, one can create a plethora of on-off controlled systems to deliver the protein of interest at a desired time point and dose (Sanders, Venema et al. 1997, Siren, Salonen et al. 2009, Douillard, O’Connell-Motherway et al. 2011, Benbouziane, Ribelles et al. 2013, Mu, Montalban-Lopez et al. 2013). This would allow the creation of a highly dynamic interface with a wide range of temporal information delivered to stem cells.

### **7.3 Cell adhesion and proof of concept**

*L. lactis* MG1363 (it was later found that NZ9000 harbours roughly the equivalent amount of FNIII<sub>7-10</sub>) functionalised with the FN fragment FNIII<sub>7-10</sub> showed high viability counts at four weeks with different antibiotics and that bacteria displaying this FNIII<sub>7-10</sub> fragment can induce cell adhesion of a variety of cell types including MSCs. SEM, vinculin and integrin staining confirmed cell adhesion to *L. lactis*-FN. Most importantly, it was found that this interface of *L. lactis*-FN was able to sustain MSC differentiation for up to four weeks with

the addition of BMP-2 at 100 ng/mL to the samples. Bacteria were seen to be present in the mammalian-bacterial co-cultures at three weeks and are therefore still able to direct cell behaviour through the FNIII<sub>7-10</sub> fragment. OCN, OPN and von Kossa signalling was increased in the BMP-2 positive samples.

## **7.4 *L. lactis* characterisation**

The strain of *L. lactis* used was changed as MG1363 does not harbour the necessary genes (*NisK* and *NisR*) for inducible expression. The well characterised NZ9000 and its derivatives were used for the remainder of the work conducted in this thesis. *L. lactis* was modified to express cell wall bound and secreted forms of the osteogenic factor BMP-2. It was found that there are no commercial kits available for the detection of bacterially expressed BMP-2 (no glycosylation) and therefore the marker protein GFP was used as a reporter. Sequencing, western blot and fluorescence assays demonstrated the presence of BMP-2-GFP in the constitutive clones. For the inducible clones, a 6xHisTag was used and the cloning and presence of protein was confirmed by sequencing and western blots and ELISAs. Upon completion of the constitutive cloning, it was found that NZ9000 was detrimental to MSC viability after two weeks as the acidic conditions through lactic acid production began to kill the mammalian cells. Therefore, the lactate dehydrogenase knockout NZ9020 was used to complete long term mammalian cell culture. Plasmids harbouring BMP-2 and FNIII<sub>7-10</sub> were transferred to NZ9020 and mammalian cell viability was seen to be good at four weeks.

## **7.5 Initial mammalian cell studies**

MSC behaviour on the constitutive and inducible *L. lactis* clones was tested. It was found that the FNIII<sub>7-10</sub> fragment in both its constitutive and inducible forms were able to encourage MSC adhesion. It was also found that upon increased concentrations of nisin, cell spreading was seen to increase. This directly confirms the western blot data. Cell proliferation was also tested to see if the BMP-2 present could control cell cycle dynamics. It was found that the presence of BMP-2 slowed cell proliferation rates in both the positive control and in *L. lactis*-BMP-2S. This was the first sign that BMP-2 from *L. lactis*-BMP-2S was biologically active. Lastly, direct mammalian-bacterial cell dynamics were investigated. C2C12 murine myoblasts readily uptake all forms of *L. lactis*, albeit with different uptake rates. The presence of either protein, FNIII<sub>7-10</sub> or BMP-2W was shown to increase bacterial cell uptake.

## 7.6 *L. lactis* derived osteogenesis

The osteogenic potential of the *L. lactis* clones was first tested by their ability to induce ALP activity in MSCs. It was found that *L. lactis*-BMP-2S stimulated similar ALP levels to that found in the positive control. Moreover, ALP activity in *L. lactis*-FN and *L. lactis*-BMP-2W showed negligible ALP activity. This result, compounded by the low proliferation results highlighted *L. lactis*-BMP-2S as the best candidate for long term osteogenic differentiation. Next, long-term differentiation of MSCs on *L. lactis*-BMP-2S was tested. OCN and von Kossa staining showed higher osteogenic markers in the *L. lactis*-BMP-2S samples when compared with the negative controls. Additionally, the differentiation rates were seen to be similar to that of the positive control showing that *L. lactis*-BMP-2S can regulate MSC differentiation. In addition, the inducible results demonstrated the necessity of high nisin and therefore BMP-2 addition at the start of the experiment. This was concluded as differentiation rates as seen in the low to high nisin addition showed very little differentiation being similar to that of the negative control. Most interestingly, the high to low samples showed similar levels of differentiation as to that of constant addition. This shows that the behavioural cues driven by *L. lactis* are needed at the very beginning of the experiment and can begin to be decreased around day four.

The potential for *L. lactis* derived osteogenic differentiation was next tested in an *in vivo* subcutaneous mouse model, whereby ectopic bone formation was studied in absorbable collagen sponges implanted into the backs of mice. No bone formation was seen after four weeks in any sample, including the positive controls. This experiment will have to be modified in the future in order to come to more accurate conclusions for the potential of this technology.

## 7.7 Future work

Many aspects of this work would be interesting to extend and could provide many more insights into how *L. lactis* could be utilised to realise its therapeutic potential.

It would be exciting to investigate the *in vivo* models again as the pilot study did not achieve the desired results. The experiment would have to house a more adequate positive control to ascertain more accurate conclusions. In addition, many more variables would have to be tested. For example, blood tests at specified days after implantation would need to be

completed to determine the host's immune response to bacteria based implantation. It would also be interesting to remove the implants at different time points and explore cell types present to see if there was an increased immune response at early time points. This would also aid in the data to see if the bacteria were destroyed by the immune system.

Additionally, the use of other growth factors could assist in the creation of a bacterially expressed osteogenic 'cocktail'. Bone morphogenetic protein-7 (BMP-7), platelet-derived growth factor (PDGF), and fibroblast growth factor (FGF-2) are all known osteogenic factors that in addition to BMP-2 could provide unmet, efficient osteogenic differentiation of MSCs. These could be controlled in an inducible fashion, to tailor the dose and time dependency of the growth factors to maximise osteogenic potential. There are already a wide variety of constitutive and inducible expression systems available for *L. lactis*, the acid-inducible P170 promoter (Jorgensen, Vrang et al. 2014), a chloride inducible system (Sanders, Venema et al. 1997), a zinc regulated expression system (Mu, Montalban-Lopez et al. 2013), agmatine controlled expression (Linares, Alvarez-Sieiro et al. 2015) and thioredoxin gene fusion systems (Douillard, O'Connell-Motherway et al. 2011) amongst others. With these tools, the researcher can create a plethora of on-off controlled systems to deliver the protein of interest at a desired time point and dose. This would allow the creation of a highly dynamic interface with abounding informational cues for the cells seeded above.

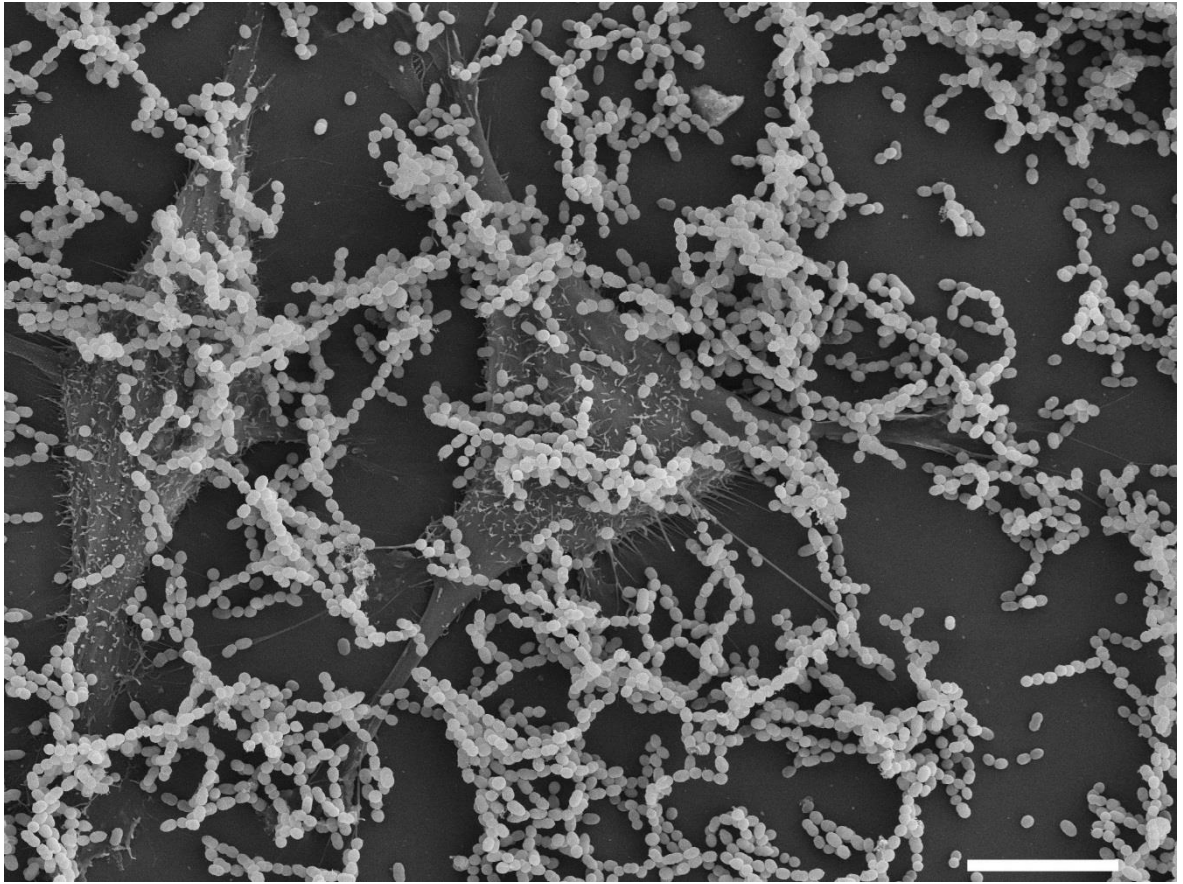
In addition to osteogenesis, many other therapeutic areas could be explored. For example, vascular endothelial growth factors (VEGFs) are diffusible mitogens with angiogenic properties. These growth factors support the development of blood vessels and wound healing and therefore, a bacteria expressing this growth factor would have a variety of properties.

## **7.8 General conclusion**

This thesis shows the regenerative potential of genetically engineered bacteria. The non-pathogenic bacteria, *Lactococcus lactis* has been modified to express a fragment of the mammalian cell adhesion peptide fibronectin as a cell wall bound protein. This has been shown to control cell adhesion. In addition, the system has been further modified to express, under dynamic temporal control, bone morphogenetic protein 2, a known osteoinducer to mesenchymal stem cells in a cell wall bound and secreted form. Whilst the cell wall bound BMP-2 exhibited no osteogenic effect, secreted BMP-2 showed good signs of biological activity, being comparable to 100 ng/mL of BMP-2. Short, mid and long-term tests all

showed the biological activity of secreted BMP-2, creating a new paradigm in surface engineering for regenerative medicine. The system can be further modified to produce a myriad of proteins in order to control a number of different therapeutic problems. Overall, this thesis has shown that genetically engineered bacteria can control the differentiation of mesenchymal stem cells.

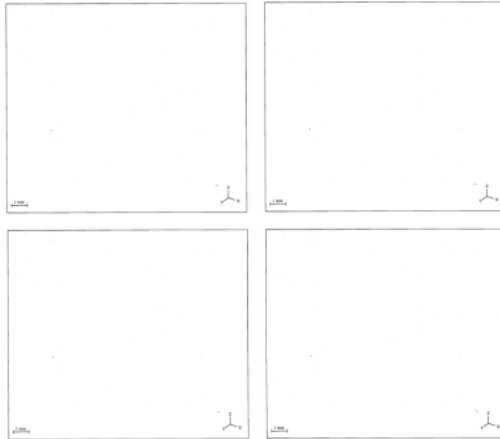
## 8. Annex



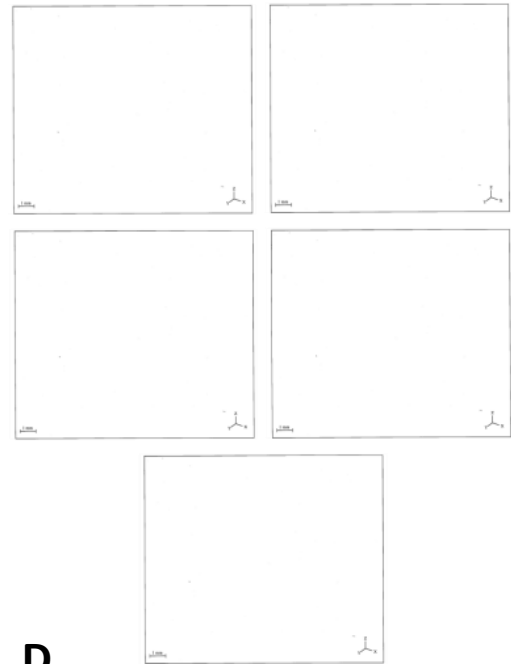
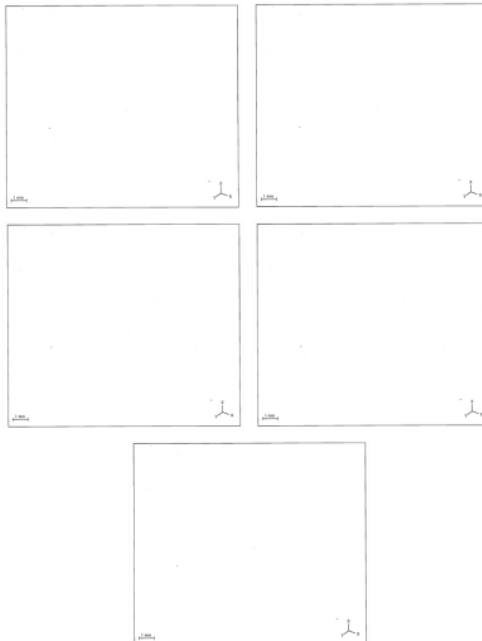
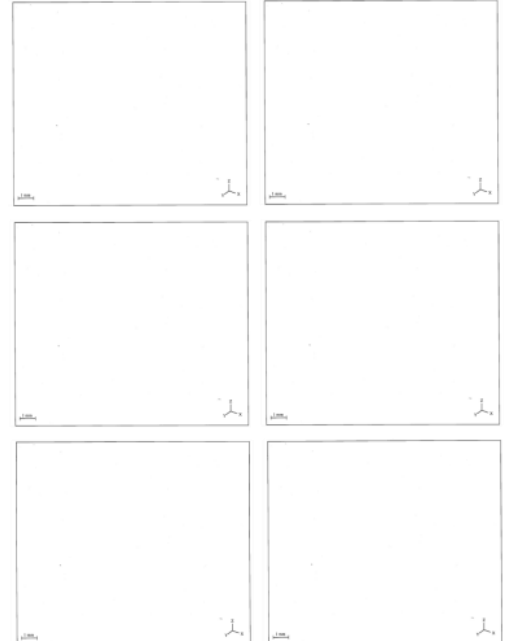
**Figure 8.1.** C2C12 murine myoblasts seeded over *L. lactis*-FN under alcian blue fixative for three hours

**A**

Micro CT of empty collagen sponges after 2 weeks

**B**

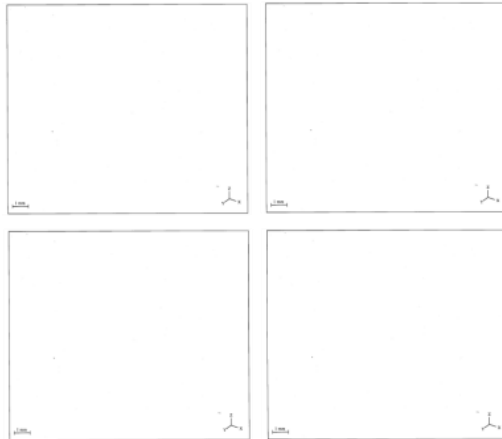
Micro CT of collagen sponges functionalised with 100 ng/mL BMP-2 after 2 weeks

**C**Micro CT of collagen sponges functionalised with empty *Lactococcus lactis* after 2 weeks**D**Micro CT of collagen sponges functionalised with BMP-2 secreting *Lactococcus lactis* after 2 weeks

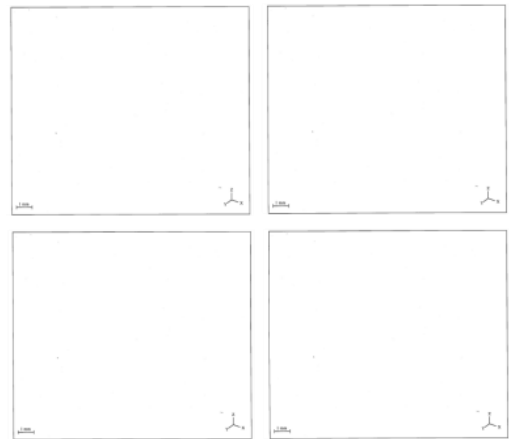
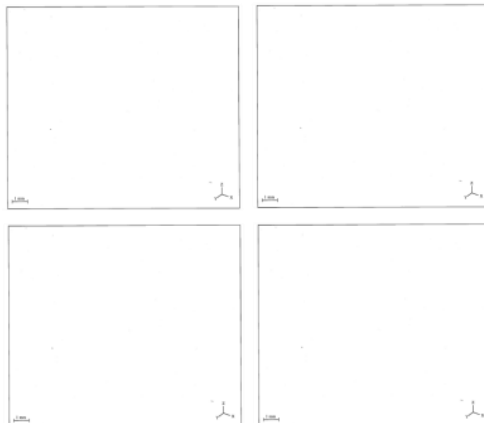
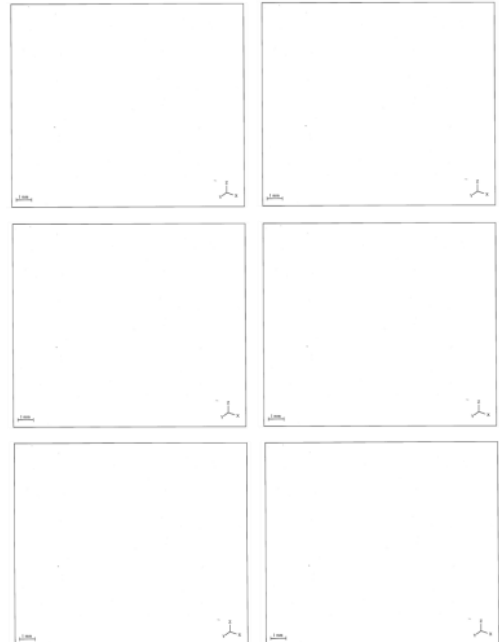
**Annex Figure 8.2.  $\mu$ CT images of functionalised collagen sponges after 2 weeks.** Live mice were imaged and regions containing the sponge were reconstructed in 3D. A = empty collagen sponges, B = sponges with 100 ng/mL BMP-2, C = sponges with *L. lactis*-empty and D = sponges with *L. lactis*-BMP-2S. No bone growth could be seen in any sample.

**A**

Micro CT of empty collagen sponges after 2 weeks

**B**

Micro CT of collagen sponges functionalised with 100 ng/mL BMP-2 after 2 weeks

**C**Micro CT of collagen sponges functionalised with empty *Lactococcus lactis* after 2 weeks**D**Micro CT of collagen sponges functionalised with BMP-2 secreting *Lactococcus lactis* after 2 weeks

**Annex Figure 8.3.  $\mu$ CT images of functionalised collagen sponges after 4 weeks.** Live mice were imaged and regions containing the sponge were reconstructed in 3D. A = empty collagen sponges, B = sponges with 100 ng/mL BMP-2, C = sponges with *L. lactis*-empty and D = sponges with *L. lactis*-BMP-2S. No bone growth could be seen in any sample.

## 9. References

Afzal, F., J. Pratap, K. Ito, Y. Ito, J. L. Stein, A. J. Van Winen, G. S. Stein, J. B. Lian and A. Javed (2005). "Smad function and intranuclear targeting share a Runx2 motif required for osteogenic lineage induction and BMP2 responsive transcription." Journal of Cellular Physiology **204**(1): 63-72.

Agarwal, R., C. Gonzalez-Garcia, B. Torstrick, R. E. Guldborg, M. Salmeron-Sanchez and A. J. Garcia (2015). "Simple coating with fibronectin fragment enhances stainless steel screw osseointegration in healthy and osteoporotic rats." Biomaterials **63**: 137-145.

Aggarwal, S. and M. F. Pittenger (2005). "Human mesenchymal stem cells modulate allogeneic immune cell responses." Blood **105**(4): 1815-1822.

Aikawa, R., I. Komuro, T. Yamazaki, Y. Zou, S. Kudoh, M. Tanaka, I. Shiojima, Y. Hiroi and Y. Yazaki (1997). "Oxidative stress activates extracellular signal-regulated kinases through Src and Ras in cultured cardiac myocytes of neonatal rats." J Clin Invest **100**(7): 1813-1821.

Alahari, S. K., P. J. Reddig and R. L. Juliano (2002). "Biological aspects of signal transduction by cell adhesion receptors." International Review of Cytology - a Survey of Cell Biology, Vol 220 **220**: 145-184.

Allendorph, G. P., W. W. Vale and S. Choe (2006). "Structure of the ternary signaling complex of a TGF-beta superfamily member." Proceedings of the National Academy of Sciences of the United States of America **103**(20): 7643-7648.

Alvarez-Buylla, A., B. Seri and F. Doetsch (2002). "Identification of neural stem cells in the adult vertebrate brain." Brain Res Bull **57**(6): 751-758.

An, Y. H. and R. J. Friedman (1998). "Concise review of mechanisms of bacterial adhesion to biomaterial surfaces." J Biomed Mater Res **43**(3): 338-348.

Anderson, H. J., J. K. Sahoo, R. V. Ulijn and M. J. Dalby (2016). "Mesenchymal Stem Cell Fate: Applying Biomaterials for Control of Stem Cell Behavior." Front Bioeng Biotechnol **4**: 38.

Aouadi, M., B. Binetruy, L. Caron, Y. Le Marchand-Brustel and F. Bost (2006). "Role of MAPKs in development and differentiation: lessons from knockout mice." Biochimie **88**(9): 1091-1098.

Aplin, A. E. and R. L. Juliano (1999). "Integrin and cytoskeletal regulation of growth factor signaling to the MAP kinase pathway." J Cell Sci **112 ( Pt 5)**: 695-706.

Arioli, S., D. Zambelli, S. Guglielmetti, I. De Noni, M. B. Pedersen, P. D. Pedersen, F. Dal Bello and D. Mora (2013). "Increasing the heme-dependent respiratory efficiency of *Lactococcus lactis* by inhibition of lactate dehydrogenase." Appl Environ Microbiol **79**(1): 376-380.

Arvidson, K., B. M. Abdallah, L. A. Applegate, N. Baldini, E. Cenni, E. Gomez-Barrena, D. Granchi, M. Kassem, Y. T. Konttinen, K. Mustafa, D. P. Pioletti, T. Sillat and A. Finne-Wstrand (2011). "Bone regeneration and stem cells." J Cell Mol Med **15**(4): 718-746.

Aumailley, M. and B. Gayraud (1998). "Structure and biological activity of the extracellular matrix." Journal of Molecular Medicine-Jmm **76**(3-4): 253-265.

Aumailley, M., M. Gurrath, G. Muller, J. Calvete, R. Timpl and H. Kessler (1991). "Arg-Gly-Asp Constrained within Cyclic Pentapeptides - Strong and Selective Inhibitors of Cell-Adhesion to Vitronectin and Laminin Fragment-P1." Febs Letters **291**(1): 50-54.

Avery, O. T., C. M. Macleod and M. McCarty (1944). "Studies on the Chemical Nature of the Substance Inducing Transformation of Pneumococcal Types : Induction of Transformation by a Desoxyribonucleic Acid Fraction Isolated from Pneumococcus Type Iii." J Exp Med **79**(2): 137-158.

Bai, X. C., D. Lu, J. Bai, H. Zheng, Z. Y. Ke, X. M. Li and S. Q. Luo (2004). "Oxidative stress inhibits osteoblastic differentiation of bone cells by ERK and NF-kappaB." Biochem Biophys Res Commun **314**(1): 197-207.

Bandyopadhyay, A., K. Tsuji, K. Cox, B. D. Harfe, V. Rosen and C. J. Tabin (2006). "Genetic analysis of the roles of BMP2, BMP4, and BMP7 in limb patterning and skeletogenesis." PLoS Genet **2**(12): e216.

Bayoudh, S., A. Othmane, L. Mora and H. Ben Ouada (2009). "Assessing bacterial adhesion using DLVO and XDLVO theories and the jet impingement technique." Colloids Surf B Biointerfaces **73**(1): 1-9.

Becker, A. J., C. E. Mc and J. E. Till (1963). "Cytological demonstration of the clonal nature of spleen colonies derived from transplanted mouse marrow cells." Nature **197**: 452-454.

Benayahu, D., Y. Kletter, D. Zipori and S. Wientroub (1989). "Bone marrow-derived stromal cell line expressing osteoblastic phenotype in vitro and osteogenic capacity in vivo." J Cell Physiol **140**(1): 1-7.

Benbouziane, B., P. Ribelles, C. Aubry, R. Martin, P. Kharrat, A. Riazi, P. Langella and L. G. Bermudez-Humaran (2013). "Development of a Stress-Inducible Controlled Expression (SICE) system in Lactococcus lactis for the production and delivery of therapeutic molecules at mucosal surfaces." J Biotechnol **168**(2): 120-129.

Benoit, D. S., M. C. Tripodi, J. O. Blanchette, S. J. Langer, L. A. Leinwand and K. S. Anseth (2007). "Integrin-linked kinase production prevents anoikis in human mesenchymal stem cells." J Biomed Mater Res A **81**(2): 259-268.

Benoit, D. S. W., M. P. Schwartz, A. R. Durney and K. S. Anseth (2008). "Small functional groups for controlled differentiation of hydrogel-encapsulated human mesenchymal stem cells." Nature Materials **7**(10): 816-823.

- Bessa, P. C., M. Casal and R. L. Reis (2008). "Bone morphogenetic proteins in tissue engineering: the road from the laboratory to the clinic, part I (basic concepts)." J Tissue Eng Regen Med **2**(1): 1-13.
- Bessho, K., Y. Konishi, S. Kaihara, K. Fujimura, Y. Okubo and T. Iizuka (2000). "Bone induction by Escherichia coli -derived recombinant human bone morphogenetic protein-2 compared with Chinese hamster ovary cell-derived recombinant human bone morphogenetic protein-2." Br J Oral Maxillofac Surg **38**(6): 645-649.
- Bianco, P. and P. G. Robey (2001). "Stem cells in tissue engineering." Nature **414**(6859): 118-121.
- Bissell, M. J. and D. Radisky (2001). "Putting tumours in context." Nature Reviews Cancer **1**(1): 46-54.
- Block, H., B. Maertens, A. Spriestersbach, N. Brinker, J. Kubicek, R. Fabis, J. Labahn and F. Schafer (2009). "Immobilized-metal affinity chromatography (IMAC): a review." Methods Enzymol **463**: 439-473.
- Bolotin, A., P. Wincker, S. Mauger, O. Jaillon, K. Malarme, J. Weissenbach, S. D. Ehrlich and A. Sorokin (2001). "The complete genome sequence of the lactic acid bacterium Lactococcus lactis ssp lactis IL1403." Genome Research **11**(5): 731-753.
- Bonde, M. T., M. Pedersen, M. S. Klausen, S. I. Jensen, T. Wulff, S. Harrison, A. T. Nielsen, M. J. Herrgard and M. O. Sommer (2016). "Predictable tuning of protein expression in bacteria." Nat Methods **13**(3): 233-236.
- Bongers, R. S., M. H. Hoefnagel, M. J. Starrenburg, M. A. Siemerink, J. G. Arends, J. Hugenholtz and M. Kleerebezem (2003). "IS981-mediated adaptive evolution recovers lactate production by IdhB transcription activation in a lactate dehydrogenase-deficient strain of Lactococcus lactis." J Bacteriol **185**(15): 4499-4507.
- Boyer, H. W. and D. Roulland-Dussoix (1969). "A complementation analysis of the restriction and modification of DNA in Escherichia coli." J Mol Biol **41**(3): 459-472.
- Boyne, P. J., R. E. Marx, M. Nevins, G. Triplett, E. Lazaro, L. C. Lilly, M. Alder and P. Nummikoski (1997). "A feasibility study evaluating rhBMP-2/absorbable collagen sponge for maxillary sinus floor augmentation." Int J Periodontics Restorative Dent **17**(1): 11-25.
- Bretscher, M. S. (1984). "Endocytosis: relation to capping and cell locomotion." Science **224**(4650): 681-686.
- Bretscher, M. S. (1992). "Circulating integrins: alpha 5 beta 1, alpha 6 beta 4 and Mac-1, but not alpha 3 beta 1, alpha 4 beta 1 or LFA-1." EMBO J **11**(2): 405-410.

- Bryksin, A. V. and I. Matsumura (2010). "Overlap extension PCR cloning: a simple and reliable way to create recombinant plasmids." Biotechniques **48**(6): 463-465.
- Budirahardja, Y. and P. Gonczy (2009). "Coupling the cell cycle to development." Development **136**(17): 2861-2872.
- Burchall, J. J. (1973). "Mechanism of action of trimethoprim-sulfamethoxazole. II." J Infect Dis **128**: Suppl: 437-441.
- Burchardt, H. (1983). "The biology of bone graft repair." Clin Orthop Relat Res(174): 28-42.
- Burmolle, M., J. S. Webb, D. Rao, L. H. Hansen, S. J. Sorensen and S. Kjelleberg (2006). "Enhanced biofilm formation and increased resistance to antimicrobial agents and bacterial invasion are caused by synergistic interactions in multispecies biofilms." Applied and Environmental Microbiology **72**(6): 3916-3923.
- Caina, J. A., N. Solis and S. J. Cordwell (2014). "Beyond gene expression: The impact of protein post-translational modifications in bacteria." Journal of Proteomics **97**: 265-286.
- Calderwood, D. A. (2004). "Integrin activation." J Cell Sci **117**(Pt 5): 657-666.
- Campagnoli, C., I. A. Roberts, S. Kumar, P. R. Bennett, I. Bellantuono and N. M. Fisk (2001). "Identification of mesenchymal stem/progenitor cells in human first-trimester fetal blood, liver, and bone marrow." Blood **98**(8): 2396-2402.
- Campbellplatt, G. (1994). "Fermented Foods - a World Perspective." Food Research International **27**(3): 253-257.
- Cano-Garrido, O., J. Seras-Franzoso and E. Garcia-Fruitos (2015). "Lactic acid bacteria: reviewing the potential of a promising delivery live vector for biomedical purposes." Microbial Cell Factories **14**.
- Cargnello, M. and P. P. Roux (2011). "Activation and function of the MAPKs and their substrates, the MAPK-activated protein kinases." Microbiol Mol Biol Rev **75**(1): 50-83.
- Carreira, A. C., F. H. Lojudice, E. Halcsik, R. D. Navarro, M. C. Sogayar and J. M. Granjeiro (2014). "Bone Morphogenetic Proteins Facts, Challenges, and Future Perspectives." Journal of Dental Research **93**(4): 335-345.
- Carstens, M. H., M. Chin and X. J. Li (2005). "In situ osteogenesis: regeneration of 10-cm mandibular defect in porcine model using recombinant human bone morphogenetic protein-2 (rhBMP-2) and Helistat absorbable collagen sponge." J Craniofac Surg **16**(6): 1033-1042.

- Case, L. B., M. A. Baird, G. Shtengel, S. L. Campbell, H. F. Hess, M. W. Davidson and C. M. Waterman (2015). "Molecular mechanism of vinculin activation and nanoscale spatial organization in focal adhesions." Nat Cell Biol **17**(7): 880-892.
- Celiz, A. D., J. G. Smith, R. Langer, D. G. Anderson, D. A. Winkler, D. A. Barrett, M. C. Davies, L. E. Young, C. Denning and M. R. Alexander (2014). "Materials for stem cell factories of the future." Nat Mater **13**(6): 570-579.
- Chamberlain, G., J. Fox, B. Ashton and J. Middleton (2007). "Concise review: Mesenchymal stem cells: Their phenotype, differentiation capacity, immunological features, and potential for homing." Stem Cells **25**(11): 2739-2749.
- Chang, J., W. Sonoyama, Z. Wang, Q. M. Jin, C. F. Zhang, P. H. Krebsbach, W. Giannobile, S. T. Shi and C. Y. Wang (2007). "Noncanonical Wnt-4 signaling enhances bone regeneration of mesenchymal stem cells in craniofacial defects through activation of p38 MAPK." Journal of Biological Chemistry **282**(42): 30938-30948.
- Chaudhuri, O., L. Gu, D. Klumpers, M. Darnell, S. A. Bencherif, J. C. Weaver, N. Huebsch, H. P. Lee, E. Lippens, G. N. Duda and D. J. Mooney (2016). "Hydrogels with tunable stress relaxation regulate stem cell fate and activity." Nat Mater **15**(3): 326-334.
- Chen, G. Q., C. X. Deng and Y. P. Li (2012). "TGF-beta and BMP Signaling in Osteoblast Differentiation and Bone Formation." International Journal of Biological Sciences **8**(2): 272-288.
- Chen, R. and J. A. Hunt (2007). "Biomimetic materials processing for tissue-engineering processes." Journal of Materials Chemistry **17**(38): 3974-3979.
- Chen, Z., L. Guo, Y. Zhang, R. L. Walzem, J. S. Pendergast, R. L. Printz, L. C. Morris, E. Matafonova, X. Stien, L. Kang, D. Coulon, O. P. McGuinness, K. D. Niswender and S. S. Davies (2014). "Incorporation of therapeutically modified bacteria into gut microbiota inhibits obesity." J Clin Invest **124**(8): 3391-3406.
- Chong, J. L., P. L. Wenzel, M. T. Saenz-Robles, V. Nair, A. Ferrey, J. P. Hagan, Y. M. Gomez, N. Sharma, H. Z. Chen, M. Ouseph, S. H. Wang, P. Trikha, B. Culp, L. Mezache, D. J. Winton, O. J. Sansom, D. Chen, R. Bremner, P. G. Cantalupo, M. L. Robinson, J. M. Pipas and G. Leone (2009). "E2f1-3 switch from activators in progenitor cells to repressors in differentiating cells." Nature **462**(7275): 930-934.
- Chong, L. (2001). "Molecular cloning - A laboratory manual, 3rd edition." Science **292**(5516): 446-446.
- Cocaign-Bousquet, M., C. Garrigues, P. Loubiere and N. D. Lindley (1996). "Physiology of pyruvate metabolism in *Lactococcus lactis*." Antonie Van Leeuwenhoek **70**(2-4): 253-267.

- Cordonnier, T., J. Sohier, P. Rosset and P. Layrolle (2011). "Biomimetic Materials for Bone Tissue Engineering - State of the Art and Future Trends." Advanced Engineering Materials **13**(5): B135-B150.
- Corliss, J. O. (1975). "Three centuries of protozoology: a brief tribute to its founding father, A. van Leeuwenhoek of Delft." J Protozool **22**(1): 3-7.
- Crespo, P., N. Xu, W. F. Simonds and J. S. Gutkind (1994). "Ras-dependent activation of MAP kinase pathway mediated by G-protein beta gamma subunits." Nature **369**(6479): 418-420.
- d'Aquino, R., A. De Rosa, V. Lanza, V. Tirino, L. Laino, A. Graziano, V. Desiderio, G. Laino and G. Papaccio (2009). "Human mandible bone defect repair by the grafting of dental pulp stem/progenitor cells and collagen sponge biocomplexes." Eur Cell Mater **18**: 75-83.
- Dalby, M. J., N. Gadegaard, R. Tare, A. Andar, M. O. Riehle, P. Herzyk, C. D. W. Wilkinson and R. O. C. Oreffo (2007). "The control of human mesenchymal cell differentiation using nanoscale symmetry and disorder." Nature Materials **6**(12): 997-1003.
- Das, R. K., V. Gocheva, R. Hammink, O. F. Zouani and A. E. Rowan (2016). "Stress-stiffening-mediated stem-cell commitment switch in soft responsive hydrogels." Nat Mater **15**(3): 318-325.
- Davies, C. T., A. V. Knibbs and J. Musgrove (1970). "The rate of lactic acid removal in relation to different baselines of recovery exercise." Int Z Angew Physiol **28**(3): 155-161.
- de Vos, W. M. (1999). "Gene expression systems for lactic acid bacteria." Current Opinion in Microbiology **2**(3): 289-295.
- De Vuyst, L. and E. J. Vandamme (1992). "Influence of the carbon source on nisin production in *Lactococcus lactis* subsp. *lactis* batch fermentations." J Gen Microbiol **138**(3): 571-578.
- de Wert, G. and C. Mummery (2003). "Human embryonic stem cells: research, ethics and policy." Hum Reprod **18**(4): 672-682.
- Deans, R. J. and A. B. Moseley (2000). "Mesenchymal stem cells: biology and potential clinical uses." Exp Hematol **28**(8): 875-884.
- Debruijn, F. J. and J. R. Lupski (1984). "The Use of Transposon Tn5 Mutagenesis in the Rapid Generation of Correlated Physical and Genetic Maps of DNA Segments Cloned into Multicopy Plasmids - a Review." Gene **27**(2): 131-149.
- del Rio, A., R. Perez-Jimenez, R. Liu, P. Roca-Cusachs, J. M. Fernandez and M. P. Sheetz (2009). "Stretching single talin rod molecules activates vinculin binding." Science **323**(5914): 638-641.

- DeLano, W. L. (2009). "PyMOL molecular viewer: Updates and refinements." Abstracts of Papers of the American Chemical Society **238**.
- deRuyter, P. G. G. A., O. P. Kuipers, M. M. Beerthuyzen, I. vanAlenBoerrigter and W. M. deVos (1996). "Functional analysis of promoters in the nisin gene cluster of *Lactococcus lactis*." Journal of Bacteriology **178**(12): 3434-3439.
- Derynck, R. and Y. E. Zhang (2003). "Smad-dependent and Smad-independent pathways in TGF-beta family signalling." Nature **425**(6958): 577-584.
- Deutscher, J. (2008). "The mechanisms of carbon catabolite repression in bacteria." Curr Opin Microbiol **11**(2): 87-93.
- Dhowre, H. S., S. Rajput, N. A. Russell and M. Zelzer (2015). "Responsive cell-material interfaces." Nanomedicine (Lond) **10**(5): 849-871.
- Ding, Z., Z. Fan, X. Huang, Q. Lu, W. Xu and D. L. Kaplan (2016). "Silk-Hydroxyapatite Nanoscale Scaffolds with Programmable Growth Factor Delivery for Bone Repair." ACS Appl Mater Interfaces **8**(37): 24463-24470.
- Docheva, D., D. Padula, C. Popov, W. Mutschler, H. Clausen-Schaumann and M. Schieker (2008). "Researching into the cellular shape, volume and elasticity of mesenchymal stem cells, osteoblasts and osteosarcoma cells by atomic force microscopy." Journal of Cellular and Molecular Medicine **12**(2): 537-552.
- Dominici, M., K. Le Blanc, I. Mueller, I. Slaper-Cortenbach, F. Marini, D. Krause, R. Deans, A. Keating, D. Prockop and E. Horwitz (2006). "Minimal criteria for defining multipotent mesenchymal stromal cells. The International Society for Cellular Therapy position statement." Cytotherapy **8**(4): 315-317.
- Douillard, F. P., M. O'Connell-Motherway, C. Cambillau and D. van Sinderen (2011). "Expanding the molecular toolbox for *Lactococcus lactis*: construction of an inducible thioredoxin gene fusion expression system." Microb Cell Fact **10**: 66.
- Dsouza, S. E., M. H. Ginsberg and E. F. Plow (1991). "Arginyl-Glycyl-Aspartic Acid (Rgd) - a Cell-Adhesion Motif." Trends in Biochemical Sciences **16**(7): 246-250.
- Duscher, D., J. Barrera, V. W. Wong, Z. N. Maan, A. J. Whittam, M. Januszyk and G. C. Gurtner (2016). "Stem Cells in Wound Healing: The Future of Regenerative Medicine? A Mini-Review." Gerontology **62**(2): 216-225.
- Ebara, M., Y. Kotsuchibashi, R. Narain, N. Idota, Y. J. Kim, J. M. Hoffman, K. Uto and T. Aoyagi (2014). "Smart Biomaterials." Smart Biomaterials: 1-373.

- Ebara, M., M. Yamato, T. Aoyagi, A. Kikuchi, K. Sakai and T. Okano (2004). "Temperature-responsive cell culture surfaces enable "on-off" affinity control between cell integrins and RGD ligands." Biomacromolecules **5**(2): 505-510.
- Ebara, M., M. Yamato, T. Aoyagi, A. Kikuchi, K. Sakai and T. Okano (2008). "A novel approach to observing synergy effects of PHSRN on integrin-RGD binding using intelligent surfaces." Advanced Materials **20**(16): 3034-3038.
- Efstathiou, J. D. and L. L. McKay (1976). "Plasmids in Streptococcus-Lactis - Evidence That Lactose Metabolism and Proteinase Activity Are Plasmid Linked." Applied and Environmental Microbiology **32**(1): 38-44.
- Efstathiou, J. D. and L. L. McKay (1977). "Inorganic salts resistance associated with a lactose-fermenting plasmid in Streptococcus lactis." J Bacteriol **130**(1): 257-265.
- Eggleton, M. G. and C. L. Evans (1930). "Lactic acid formation and removal with change of blood reaction." J Physiol **70**(3): 261-268.
- Ehrlich, P. J. and L. E. Lanyon (2002). "Mechanical strain and bone cell function: a review." Osteoporos Int **13**(9): 688-700.
- Engelhardt, J. F. (2001). "Stem cell niches in the mouse airway." Am J Respir Cell Mol Biol **24**(6): 649-652.
- Engler, A. J., S. Sen, H. L. Sweeney and D. E. Discher (2006). "Matrix elasticity directs stem cell lineage specification." Cell **126**(4): 677-689.
- Erlandsen, S. L., C. J. Kristich, G. M. Dunny and C. L. Wells (2004). "High-resolution visualization of the microbial glycocalyx with low-voltage scanning electron microscopy: dependence on cationic dyes." J Histochem Cytochem **52**(11): 1427-1435.
- Escos, A., A. Risco, D. Alsina-Beauchamp and A. Cuenda (2016). "p38gamma and p38delta Mitogen Activated Protein Kinases (MAPKs), New Stars in the MAPK Galaxy." Front Cell Dev Biol **4**: 31.
- Evans, D. G., R. P. Silver, D. J. Evans, Jr., D. G. Chase and S. L. Gorbach (1975). "Plasmid-controlled colonization factor associated with virulence in Escherichia coli enterotoxigenic for humans." Infect Immun **12**(3): 656-667.
- Evans, M. J. and M. H. Kaufman (1981). "Establishment in culture of pluripotential cells from mouse embryos." Nature **292**(5819): 154-156.
- Ferris, M. J., G. Muyzer and D. M. Ward (1996). "Denaturing gradient gel electrophoresis profiles of 16S rRNA-defined populations inhabiting a hot spring microbial mat community." Appl Environ Microbiol **62**(2): 340-346.

- Filipak, M., D. N. Estervig, C. Y. Tzen, P. Minoo, B. J. Hoerl, P. B. Maercklein, M. A. Zschunke, M. Edens and R. E. Scott (1989). "Integrated control of proliferation and differentiation of mesenchymal stem cells." Environ Health Perspect **80**: 117-125.
- Fincham, V. J., M. James, M. C. Frame and S. J. Winder (2000). "Active ERK/MAP kinase is targeted to newly forming cell-matrix adhesions by integrin engagement and v-Src." EMBO J **19**(12): 2911-2923.
- Francis, D. M. and R. Page (2010). "Strategies to optimize protein expression in E. coli." Curr Protoc Protein Sci **Chapter 5**: Unit 5 24 21-29.
- Friedenstein, A. J., U. F. Deriglasova, N. N. Kulagina, A. F. Panasuk, S. F. Rudakowa, E. A. Luria and I. A. Ruadkow (1974). "Precursors for fibroblasts in different populations of hematopoietic cells as detected by the in vitro colony assay method." Exp Hematol **2**(2): 83-92.
- Friedenstein, A. J., K. V. Petrakova, A. I. Kurolesova and G. P. Frolova (1968). "Heterotopic of bone marrow. Analysis of precursor cells for osteogenic and hematopoietic tissues." Transplantation **6**(2): 230-247.
- Friedland, J. C., M. H. Lee and D. Boettiger (2009). "Mechanically activated integrin switch controls alpha5beta1 function." Science **323**(5914): 642-644.
- Friess, W. (1998). "Collagen--biomaterial for drug delivery." Eur J Pharm Biopharm **45**(2): 113-136.
- Frisch, S. M. and H. Francis (1994). "Disruption of Epithelial Cell-Matrix Interactions Induces Apoptosis." Journal of Cell Biology **124**(4): 619-626.
- Frisch, S. M. and E. Ruoslahti (1997). "Integrins and anoikis." Current Opinion in Cell Biology **9**(5): 701-706.
- Frisch, S. M. and R. A. Screaton (2001). "Anoikis mechanisms." Current Opinion in Cell Biology **13**(5): 555-562.
- Froon, A. H. M., M. A. Dentener, J. W. M. Greve, G. Ramsay and W. A. Buurman (1995). "Lipopolysaccharide Toxicity-Regulating Proteins in Bacteremia." Journal of Infectious Diseases **171**(5): 1250-1257.
- Fuchs, E. (2009). "The Tortoise and the Hair: Slow-Cycling Cells in the Stem Cell Race." Cell **137**(5): 811-819.
- Garcia, A. J., M. D. Vega and D. Boettiger (1999). "Modulation of cell proliferation and differentiation through substrate-dependent changes in fibronectin conformation." Molecular Biology of the Cell **10**(3): 785-798.

- Gaspar, P., A. R. Neves, M. J. Gasson, C. A. Shearman and H. Santos (2011). "High Yields of 2,3-Butanediol and Mannitol in *Lactococcus lactis* through Engineering of NAD(+) Cofactor Recycling." *Applied and Environmental Microbiology* **77**(19): 6826-6835.
- Ge, C. X., G. Z. Xiao, D. Jiang, Q. Yang, N. E. Hatch, H. Roca and R. T. Franceschi (2009). "Identification and Functional Characterization of ERK/MAPK Phosphorylation Sites in the Runx2 Transcription Factor." *Journal of Biological Chemistry* **284**(47): 32533-32543.
- Geigenmuller, U. and K. H. Nierhaus (1986). "Tetracycline Can Inhibit Transfer-Rna Binding to the Ribosomal P-Site as Well as to the a-Site." *European Journal of Biochemistry* **161**(3): 723-726.
- Geiger, M., R. H. Li and W. Friess (2003). "Collagen sponges for bone regeneration with rhBMP-2." *Adv Drug Deliv Rev* **55**(12): 1613-1629.
- Giancotti, F. G. (2000). "Complexity and specificity of integrin signalling." *Nature Cell Biology* **2**(1): E13-E14.
- Giancotti, F. G. and E. Ruoslahti (1999). "Transduction - Integrin signaling." *Science* **285**(5430): 1028-1032.
- Giaouris, E., M. P. Chapot-Chartier and R. Briandet (2009). "Surface physicochemical analysis of natural *Lactococcus lactis* strains reveals the existence of hydrophobic and low charged strains with altered adhesive properties." *Int J Food Microbiol* **131**(1): 2-9.
- Gibson, D. G., L. Young, R. Y. Chuang, J. C. Venter, C. A. Hutchison and H. O. Smith (2009). "Enzymatic assembly of DNA molecules up to several hundred kilobases." *Nature Methods* **6**(5): 343-U341.
- Gilbert, S. (2000). "Osteogenesis: The Development of Bones." *Developmental Biology* **6th Edition**.
- Godon, J. J., K. Jury, C. A. Shearman and M. J. Gasson (1994). "The *Lactococcus lactis* sex-factor aggregation gene *cluA*." *Mol Microbiol* **12**(4): 655-663.
- Gold, L. (1988). "Posttranscriptional regulatory mechanisms in *Escherichia coli*." *Annu Rev Biochem* **57**: 199-233.
- Greenblatt, M. B., J. H. Shim, W. G. Zou, D. Sitara, M. Schweitzer, D. Hu, S. Lotinun, Y. Sano, R. Baron, J. M. Park, S. Arthur, M. Xie, M. D. Schneider, B. Zhai, S. Gygi, R. Davis and L. H. Glimcher (2010). "The p38 MAPK pathway is essential for skeletogenesis and bone homeostasis in mice." *Journal of Clinical Investigation* **120**(7): 2457-2473.
- Grinnell, F. (1986). "Focal adhesion sites and the removal of substratum-bound fibronectin." *J Cell Biol* **103**(6 Pt 2): 2697-2706.

- Gronthos, S., S. E. Graves, S. Ohta and P. J. Simmons (1994). "The STRO-1+ fraction of adult human bone marrow contains the osteogenic precursors." Blood **84**(12): 4164-4173.
- Guicheux, J., J. Lemonnier, C. Ghayor, A. Suzuki, G. Palmer and J. Caverzasio (2003). "Activation of p38 mitogen-activated protein kinase and c-Jun-NH2-terminal kinase by BMP-2 and their implication in the stimulation of osteoblastic cell differentiation." Journal of Bone and Mineral Research **18**(11): 2060-2068.
- Guilak, F., D. M. Cohen, B. T. Estes, J. M. Gimble, W. Liedtke and C. S. Chen (2009). "Control of stem cell fate by physical interactions with the extracellular matrix." Cell Stem Cell **5**(1): 17-26.
- Gulot, E., P. Georges, A. Brun, M. P. Fontaine-Aupart, M. N. Bellon-Fontaine and R. Briandet (2002). "Heterogeneity of diffusion inside microbial biofilms determined by fluorescence correlation spectroscopy under two-photon excitation." Photochem Photobiol **75**(6): 570-578.
- Gunnewijk, M. G. W. and B. Poolman (2000). "Phosphorylation state of HPr determines the level of expression and the extent of phosphorylation of the lactose transport protein of *Streptococcus thermophilus*." Journal of Biological Chemistry **275**(44): 34073-34079.
- Guo, W. J. and F. G. Giancotti (2004). "Integrin signalling during tumour progression." Nature Reviews Molecular Cell Biology **5**(10): 816-826.
- Habimana, O., C. Le Goff, V. Juillard, M. N. Bellon-Fontaine, G. Buist, S. Kulakauskas and R. Briandet (2007). "Positive role of cell wall anchored proteinase PrtP in adhesion of lactococci." Bmc Microbiology **7**.
- Habimana, O., M. Meyrand, T. Meylheuc, S. Kulakauskas and R. Briandet (2009). "Genetic features of resident biofilms determine attachment of *Listeria monocytogenes*." Appl Environ Microbiol **75**(24): 7814-7821.
- Hanks, S. K. and T. R. Polte (1997). "Signaling through focal adhesion kinase." Bioessays **19**(2): 137-145.
- Hanson, M. L., J. A. Hixon, W. Li, B. K. Felber, M. R. Anver, C. A. Stewart, B. M. Janelins, S. K. Datta, W. Shen, M. H. McLean and S. K. Durum (2014). "Oral delivery of IL-27 recombinant bacteria attenuates immune colitis in mice." Gastroenterology **146**(1): 210-221 e213.
- Hay, J. J., A. Rodrigo-Navarro, K. Hassi, V. Moulisova, M. J. Dalby and M. Salmeron-Sanchez (2016). "Living biointerfaces based on non-pathogenic bacteria support stem cell differentiation." Sci Rep **6**: 21809.
- Hayman, E. G. and E. Ruoslahti (1979). "Distribution of Fetal Bovine Serum Fibronectin and Endogenous Rat-Cell Fibronectin in Extracellular Matrix." Journal of Cell Biology **83**(1): 255-259.

Hazen, T. C., E. A. Dubinsky, T. Z. DeSantis, G. L. Andersen, Y. M. Piceno, N. Singh, J. K. Jansson, A. Probst, S. E. Borglin, J. L. Fortney, W. T. Stringfellow, M. Bill, M. E. Conrad, L. M. Tom, K. L. Chavarria, T. R. Alusi, R. Lamendella, D. C. Joyner, C. Spier, J. Baelum, M. Auer, M. L. Zemla, R. Chakraborty, E. L. Sonnenthal, P. D'Haeseleer, H. Y. Holman, S. Osman, Z. Lu, J. D. Van Nostrand, Y. Deng, J. Zhou and O. U. Mason (2010). "Deep-sea oil plume enriches indigenous oil-degrading bacteria." Science **330**(6001): 204-208.

Heino, J. (2007). "The collagen family members as cell adhesion proteins." Bioessays **29**(10): 1001-1010.

Hench, L. L. and J. M. Polak (2002). "Third-generation biomedical materials." Science **295**(5557): 1014-+.

Hindley, C. and A. Philpott (2012). "Co-ordination of cell cycle and differentiation in the developing nervous system." Biochem J **444**(3): 375-382.

Hitchings, G. H. (1973). "Mechanism of action of trimethoprim-sulfamethoxazole. I." J Infect Dis **128**: Suppl:433-436 p.

Hochuli, E., W. Bannwarth, H. Dobeli, R. Gentz and D. Stuber (1988). "Genetic Approach to Facilitate Purification of Recombinant Proteins with a Novel Metal Chelate Adsorbent." Bio-Technology **6**(11): 1321-1325.

Hoshiba, T., N. Kawazoe, T. Tateishi and G. Chen (2009). "Development of stepwise osteogenesis-mimicking matrices for the regulation of mesenchymal stem cell functions." J Biol Chem **284**(45): 31164-31173.

Hu, E. D., J. B. Kim, P. Sarraf and B. M. Spiegelman (1996). "Inhibition of adipogenesis through MAP kinase-mediated phosphorylation of PPAR gamma." Science **274**(5295): 2100-2103.

Humphreys, J. M., A. T. Pinal, R. Akella, H. He and E. J. Goldsmith (2013). "Precisely ordered phosphorylation reactions in the p38 mitogen-activated protein (MAP) kinase cascade." J Biol Chem **288**(32): 23322-23330.

Humphries, J. D., P. Wang, C. Streuli, B. Geiger, M. J. Humphries and C. Ballestrem (2007). "Vinculin controls focal adhesion formation by direct interactions with talin and actin." J Cell Biol **179**(5): 1043-1057.

Huston, A. L., B. B. Krieger-Brockett and J. W. Deming (2000). "Remarkably low temperature optima for extracellular enzyme activity from Arctic bacteria and sea ice." Environ Microbiol **2**(4): 383-388.

Hynes, R. O. (2002). "Integrins: Bidirectional, allosteric signaling machines." Cell **110**(6): 673-687.

- Hynes, R. O. (2009). "The extracellular matrix: not just pretty fibrils." Science **326**(5957): 1216-1219.
- Inman, G. J., F. J. Nicolas and C. S. Hill (2002). "Nucleocytoplasmic shuttling of Smads 2, 3, and 4 permits sensing of TGF-beta receptor activity." Molecular Cell **10**(2): 283-294.
- Itoh, S., F. Itoh, M. J. Goumans and P. ten Dijke (2000). "Signaling of transforming growth factor-beta family members through Smad proteins." European Journal of Biochemistry **267**(24): 6954-6967.
- Johnson, D. G., J. K. Schwarz, W. D. Cress and J. R. Nevins (1993). "Expression of transcription factor E2F1 induces quiescent cells to enter S phase." Nature **365**(6444): 349-352.
- Jorgensen, C. M., A. Vrang and S. M. Madsen (2014). "Recombinant protein expression in Lactococcus lactis using the P170 expression system." Fems Microbiology Letters **351**(2): 170-178.
- Kanchanawong, P., G. Shtengel, A. M. Pasapera, E. B. Ramko, M. W. Davidson, H. F. Hess and C. M. Waterman (2010). "Nanoscale architecture of integrin-based cell adhesions." Nature **468**(7323): 580-584.
- Kanno, T., T. Takahashi, T. Tsujisawa, W. Ariyoshi and T. Nishihara (2007). "Mechanical stress-mediated Runx2 activation is dependent on Ras/ERK1/2 MAPK signaling in Osteoblasts." Journal of Cellular Biochemistry **101**(5): 1266-1277.
- Kao, S., R. K. Jaiswal, W. Kolch and G. E. Landreth (2001). "Identification of the mechanisms regulating the differential activation of the mapk cascade by epidermal growth factor and nerve growth factor in PC12 cells." J Biol Chem **276**(21): 18169-18177.
- Kashiwagi, K., T. Tsuji and K. Shiba (2009). "Directional BMP-2 for functionalization of titanium surfaces." Biomaterials **30**(6): 1166-1175.
- Katagiri, T., A. Yamaguchi, M. Komaki, E. Abe, N. Takahashi, T. Ikeda, V. Rosen, J. M. Wozney, A. Fujisawashera and A. Suda (1995). "Bone Morphogenetic Protein-2 Converts the Differentiation Pathway of C2c12 Myoblasts into the Osteoblast Lineage (Vol 127, Pg 1755, 1994)." Journal of Cell Biology **128**(4): U8-U8.
- Khetan, S., M. Guvendiren, W. R. Legant, D. M. Cohen, C. S. Chen and J. A. Burdick (2013). "Degradation-mediated cellular traction directs stem cell fate in covalently crosslinked three-dimensional hydrogels." Nature Materials **12**(5): 458-465.
- Kilian, K. A., B. Bugarija, B. T. Lahn and M. Mrksich (2010). "Geometric cues for directing the differentiation of mesenchymal stem cells." Proceedings of the National Academy of Sciences of the United States of America **107**(11): 4872-4877.

Kim, D. H., K. H. Yoo, K. S. Choi, J. Choi, S. Y. Choi, S. E. Yang, Y. S. Yang, H. J. Im, K. H. Kim, H. L. Jung, K. W. Sung and H. H. Koo (2005). "Gene expression profile of cytokine and growth factor during differentiation of bone marrow-derived mesenchymal stem cell." Cytokine **31**(2): 119-126.

Kim, I. S., E. N. Lee, T. H. Cho, Y. M. Song, S. J. Hwang, J. H. Oh, E. K. Park, T. Y. Koo and Y. K. Seo (2011). "Promising efficacy of Escherichia coli recombinant human bone morphogenetic protein-2 in collagen sponge for ectopic and orthotopic bone formation and comparison with mammalian cell recombinant human bone morphogenetic protein-2." Tissue Eng Part A **17**(3-4): 337-348.

Knoepfler, P. S. (2009). "Deconstructing stem cell tumorigenicity: a roadmap to safe regenerative medicine." Stem Cells **27**(5): 1050-1056.

Koch, W. J., B. E. Hawes, L. F. Allen and R. J. Lefkowitz (1994). "Direct evidence that Gi-coupled receptor stimulation of mitogen-activated protein kinase is mediated by G beta gamma activation of p21ras." Proc Natl Acad Sci U S A **91**(26): 12706-12710.

Kole, R., A. R. Krainer and S. Altman (2012). "RNA therapeutics: beyond RNA interference and antisense oligonucleotides." Nat Rev Drug Discov **11**(2): 125-140.

Komori, T., H. Yagi, S. Nomura, A. Yamaguchi, K. Sasaki, K. Deguchi, Y. Shimizu, R. T. Bronson, Y. H. Gao, M. Inada, M. Sato, R. Okamoto, Y. Kitamura, S. Yoshiki and T. Kishimoto (1997). "Targeted disruption of Cbfa1 results in a complete lack of bone formation owing to maturational arrest of osteoblasts." Cell **89**(5): 755-764.

Kooreman, N. G. and J. C. Wu (2010). "Tumorigenicity of pluripotent stem cells: biological insights from molecular imaging." J R Soc Interface **7 Suppl 6**: S753-763.

Kuipers, O. P., P. G. G. A. de Ruyter, M. Kleerebezem and W. M. de Vos (1998). "Quorum sensing-controlled gene expression in lactic acid bacteria." Journal of Biotechnology **64**(1): 15-21.

Kumar, S. and V. Weaver (2009). "Mechanics, malignancy, and metastasis: The force journey of a tumor cell." Cancer and Metastasis Reviews **28**(1-2): 113-127.

Labrie, S. J., J. E. Samson and S. Moineau (2010). "Bacteriophage resistance mechanisms." Nat Rev Microbiol **8**(5): 317-327.

Laddy, D. J. and D. B. Weiner (2006). "From plasmids to protection: a review of DNA vaccines against infectious diseases." Int Rev Immunol **25**(3-4): 99-123.

Landete, J. M., S. Langa, C. Revilla, A. Margolles, M. Medina and J. L. Arques (2015). "Use of anaerobic green fluorescent protein versus green fluorescent protein as reporter in lactic acid bacteria." Applied Microbiology and Biotechnology **99**(16): 6865-6877.

- Lane, N. (2015). "The unseen world: reflections on Leeuwenhoek (1677) 'Concerning little animals'." Philosophical Transactions of the Royal Society B-Biological Sciences **370**(1666).
- Lange, C. and F. Calegari (2010). "Cdks and cyclins link G1 length and differentiation of embryonic, neural and hematopoietic stem cells." Cell Cycle **9**(10): 1893-1900.
- Lathrop, B., K. Thomas and L. Glaser (1985). "Control of myogenic differentiation by fibroblast growth factor is mediated by position in the G1 phase of the cell cycle." J Cell Biol **101**(6): 2194-2198.
- Le Loir, Y., V. Azevedo, S. C. Oliveira, D. A. Freitas, A. Miyoshi, L. G. Bermudez-Humaran, S. Nouaille, L. A. Ribeiro, S. Leclercq, J. E. Gabriel, V. D. Guimaraes, M. N. Oliveira, C. Charlier, M. Gautier and P. Langella (2005). "Protein secretion in *Lactococcus lactis* : an efficient way to increase the overall heterologous protein production." Microb Cell Fact **4**(1): 2.
- Lechleider, R. J., J. L. Ryan, L. Garrett, C. Eng, C. Deng, A. Wynshaw-Boris and A. B. Roberts (2001). "Targeted mutagenesis of Smad1 reveals an essential role in chorioallantoic fusion." Dev Biol **240**(1): 157-167.
- Lederberg, J. and E. M. Lederberg (1952). "Replica plating and indirect selection of bacterial mutants." J Bacteriol **63**(3): 399-406.
- Lee, J., A. A. Abdeen, D. Zhang and K. A. Kilian (2013). "Directing stem cell fate on hydrogel substrates by controlling cell geometry, matrix mechanics and adhesion ligand composition." Biomaterials **34**(33): 8140-8148.
- Lee, J. H., C. S. Kim, K. H. Choi, U. W. Jung, J. H. Yun, S. H. Choi and K. S. Cho (2010). "The induction of bone formation in rat calvarial defects and subcutaneous tissues by recombinant human BMP-2, produced in *Escherichia coli*." Biomaterials **31**(13): 3512-3519.
- Lee, T. T., J. R. Garcia, J. I. Paez, A. Singh, E. A. Phelps, S. Weis, Z. Shafiq, A. Shekaran, A. Del Campo and A. J. Garcia (2015). "Light-triggered in vivo activation of adhesive peptides regulates cell adhesion, inflammation and vascularization of biomaterials." Nat Mater **14**(3): 352-360.
- Lenas, P., F. P. Luyten, M. Doblare, E. Nicodemou-Lena and A. E. Lanzara (2011). "Modularity in developmental biology and artificial organs: a missing concept in tissue engineering." Artif Organs **35**(6): 656-662.
- Lendlein, A. (2011). "Smart Biomaterials." International Journal of Artificial Organs **34**(8): 607-607.
- Li, L. and H. Clevers (2010). "Coexistence of quiescent and active adult stem cells in mammals." Science **327**(5965): 542-545.

- Lian, J., C. Stewart, E. Puchacz, S. Mackowiak, V. Shalhoub, D. Collart, G. Zambetti and G. Stein (1989). "Structure of the rat osteocalcin gene and regulation of vitamin D-dependent expression." Proc Natl Acad Sci U S A **86**(4): 1143-1147.
- Lin, G. L. and K. D. Hankenson (2011). "Integration of BMP, Wnt, and notch signaling pathways in osteoblast differentiation." J Cell Biochem **112**(12): 3491-3501.
- Linares, D. M., P. Alvarez-Sieiro, B. del Rio, V. Ladero, B. Redruello, M. C. Martin, M. Fernandez and M. A. Alvarez (2015). "Implementation of the agmatine-controlled expression system for inducible gene expression in *Lactococcus lactis*." Microb Cell Fact **14**: 208.
- Liu, X. H., I. O. Smith and P. X. Ma (2009). "Biomimetic Nanophase Materials to Promote New Tissue Formation for Tissue-Engineering Applications." Biological Interactions on Materials Surfaces: Understanding and Controlling Protein, Cell, and Tissue Responses: 283-296.
- Llopis-Hernandez, V., M. Cantini, C. Gonzalez-Garcia, Z. A. Cheng, J. L. Yang, P. M. Tsimbouri, A. J. Garcia, M. J. Dalby and M. Salmeron-Sanchez (2016). "Material-driven fibronectin assembly for high-efficiency presentation of growth factors." Science Advances **2**(8).
- Luesink, E. J., R. E. M. A. van Herpen, B. P. Grossiord, O. P. Kuipers and W. M. de Vos (1998). "Transcriptional activation of the glycolytic *las* operon and catabolite repression of the *gal* operon in *Lactococcus lactis* are mediated by the catabolite control protein CcpA." Molecular Microbiology **30**(4): 789-798.
- Luo, B. H. and T. A. Springer (2006). "Integrin structures and conformational signaling." Curr Opin Cell Biol **18**(5): 579-586.
- Lutolf, M. P. and J. A. Hubbell (2005). "Synthetic biomaterials as instructive extracellular microenvironments for morphogenesis in tissue engineering." Nature Biotechnology **23**(1): 47-55.
- Ma, P. X. (2008). "Biomimetic materials for tissue engineering." Advanced Drug Delivery Reviews **60**(2): 184-198.
- Maestroni, G. J. M. (2001). "The immunotherapeutic potential of melatonin." Expert Opinion on Investigational Drugs **10**(3): 467-476.
- Makarenkova, H. P., M. P. Hoffman, A. Beenken, A. V. Eliseenkova, R. Meech, C. Tsau, V. N. Patel, R. A. Lang and M. Mohammadi (2009). "Differential interactions of FGFs with heparan sulfate control gradient formation and branching morphogenesis." Sci Signal **2**(88): ra55.
- Malaval, L., F. Liu, P. Roche and J. E. Aubin (1999). "Kinetics of osteoprogenitor proliferation and osteoblast differentiation in vitro." J Cell Biochem **74**(4): 616-627.

- Manolagas, S. C. (2010). "From estrogen-centric to aging and oxidative stress: a revised perspective of the pathogenesis of osteoporosis." Endocr Rev **31**(3): 266-300.
- Mao, Y. and J. E. Schwarzbauer (2005). "Fibronectin fibrillogenesis, a cell-mediated matrix assembly process." Matrix Biol **24**(6): 389-399.
- Margulis, L. and D. Bermudes (1985). "Symbiosis as a mechanism of evolution: status of cell symbiosis theory." Symbiosis **1**: 101-124.
- Massague, J., J. Seoane and D. Wotton (2005). "Smad transcription factors." Genes Dev **19**(23): 2783-2810.
- Mazmanian, S. K., I. T. Hung and O. Schneewind (2001). "Sortase-catalysed anchoring of surface proteins to the cell wall of Staphylococcus aureus." Molecular Microbiology **40**(5): 1049-1057.
- McBeath, R., D. M. Pirone, C. M. Nelson, K. Bhadriraju and C. S. Chen (2004). "Cell shape, cytoskeletal tension, and RhoA regulate stem cell lineage commitment." Developmental Cell **6**(4): 483-495.
- McMurray, R. J., N. Gadegaard, P. M. Tsimbouri, K. V. Burgess, L. E. McNamara, R. Tare, K. Murawski, E. Kingham, R. O. C. Oreffo and M. J. Dalby (2011). "Nanoscale surfaces for the long-term maintenance of mesenchymal stem cell phenotype and multipotency." Nature Materials **10**(8): 637-644.
- Mendez-Ferrer, S., T. V. Michurina, F. Ferraro, A. R. Mazloom, B. D. Macarthur, S. A. Lira, D. T. Scadden, A. Ma'ayan, G. N. Enikolopov and P. S. Frenette (2010). "Mesenchymal and haematopoietic stem cells form a unique bone marrow niche." Nature **466**(7308): 829-834.
- Mercier, C., C. Durrieu, R. Briandet, E. Domakova, J. Tremblay, G. Buist and S. Kulakauskas (2002). "Positive role of peptidoglycan breaks in lactococcal biofilm formation." Molecular Microbiology **46**(1): 235-243.
- Mierau, I. and M. Kleerebezem (2005). "10 years of the nisin-controlled gene expression system (NICE) in Lactococcus lactis." Appl Microbiol Biotechnol **68**(6): 705-717.
- Mierau, I., K. Olieman, J. Mond and E. J. Smid (2005). "Optimization of the Lactococcus lactis nisin-controlled gene expression system NICE for industrial applications." Microbial Cell Factories **4**.
- Miranti, C. K. and J. S. Brugge (2002). "Sensing the environment: a historical perspective on integrin signal transduction." Nat Cell Biol **4**(4): E83-90.
- Mitra, S. K., D. A. Hanson and D. D. Schlaepfer (2005). "Focal adhesion kinase: in command and control of cell motility." Nat Rev Mol Cell Biol **6**(1): 56-68.

- Miyazono, K., Y. Kamiya and M. Morikawa (2010). "Bone morphogenetic protein receptors and signal transduction." J Biochem **147**(1): 35-51.
- Mohan, S. and D. J. Baylink (1991). "Bone growth factors." Clin Orthop Relat Res(263): 30-48.
- Moon, J. J., M. S. Hahn, I. Kim, B. A. Nsiah and J. L. West (2009). "Micropatterning of poly(ethylene glycol) diacrylate hydrogels with biomolecules to regulate and guide endothelial morphogenesis." Tissue Eng Part A **15**(3): 579-585.
- Moustakas, A., S. Souchelnytskyi and C. H. Heldin (2001). "Smad regulation in TGF-beta signal transduction." Journal of Cell Science **114**(24): 4359-4369.
- Mouw, J. K., Guanqing Ou, and Valerie M. Weaver. "Extracellular matrix assembly: a multiscale deconstruction." Nature Reviews Molecular Cell Biology. (2014).
- Mu, D. D., M. Montalban-Lopez, Y. Masuda and O. P. Kuipers (2013). "Zirex: a Novel Zinc-Regulated Expression System for Lactococcus lactis." Applied and Environmental Microbiology **79**(14): 4503-4508.
- Murphy, W. L., T. C. McDevitt and A. J. Engler (2014). "Materials as stem cell regulators." Nature Materials **13**(6): 547-557.
- Muzzarelli, R. A., M. El Mehtedi, C. Bottegoni and A. Gigante (2016). "Physical properties imparted by genipin to chitosan for tissue regeneration with human stem cells: A review." Int J Biol Macromol **93**(Pt B): 1366-1381.
- Nagae, M., S. Re, E. Mihara, T. Nogi, Y. Sugita and J. Takagi (2012). "Crystal structure of alpha5beta1 integrin ectodomain: atomic details of the fibronectin receptor." J Cell Biol **197**(1): 131-140.
- Nagai, T., M. Urushihara, Y. Kinoshita, J. Ariunbold, S. Kondo and S. Kagami (2016). "Extracellular Signal Regulated Kinase-1/2 and-5 Signaling Pathways Via Renin Angiotensin System Activation Play Differential Regulatory Roles in Progressive Glomerulonephritis." Nephrology Dialysis Transplantation **31**: 49-49.
- Nevins, M., C. Kirker-Head, M. Nevins, J. A. Wozney, R. Palmer and D. Graham (1996). "Bone formation in the goat maxillary sinus induced by absorbable collagen sponge implants impregnated with recombinant human bone morphogenetic protein-2." Int J Periodontics Restorative Dent **16**(1): 8-19.
- Nikukar, H., S. Reid, P. M. Tsimbouri, M. O. Riehle, A. S. G. Curtis and M. J. Dalby (2013). "Osteogenesis of Mesenchymal Stem Cells by Nanoscale Mechanotransduction." Acs Nano **7**(3): 2758-2767.

- Nishiyama, K., M. Sugiyama and T. Mukai (2016). "Adhesion Properties of Lactic Acid Bacteria on Intestinal Mucin." Microorganisms **4**(3).
- Nobes, C. D. and A. Hall (1995). "Rho, Rac and Cdc42 Gtpases - Regulators of Actin Structures, Cell-Adhesion and Motility." Biochemical Society Transactions **23**(3): 456-459.
- O'Sullivan D, J. and T. R. Klaenhammer (1993). "Rapid Mini-Prep Isolation of High-Quality Plasmid DNA from Lactococcus and Lactobacillus spp." Appl Environ Microbiol **59**(8): 2730-2733.
- Oh, S., K. S. Brammer, Y. S. Li, D. Teng, A. J. Engler, S. Chien and S. Jin (2009). "Stem cell fate dictated solely by altered nanotube dimension." Proc Natl Acad Sci U S A **106**(7): 2130-2135.
- Orimo, H. (2010). "The mechanism of mineralization and the role of alkaline phosphatase in health and disease." J Nippon Med Sch **77**(1): 4-12.
- Osdoby, P. and A. I. Caplan (1981). "Characterization of a bone-specific alkaline phosphatase in chick limb mesenchymal cell cultures." Dev Biol **86**(1): 136-146.
- Owen, M. and A. J. Friedenstein (1988). "Stromal stem cells: marrow-derived osteogenic precursors." Ciba Found Symp **136**: 42-60.
- Papadimitropoulos, A., E. Piccinini, S. Brachat, A. Braccini, D. Wendt, A. Barbero, C. Jacobi and I. Martin (2014). "Expansion of Human Mesenchymal Stromal Cells from Fresh Bone Marrow in a 3D Scaffold-Based System under Direct Perfusion." Plos One **9**(7).
- Park, J. T. and J. L. Strominger (1957). "Mode of Action of Penicillin - Biochemical Basis for the Mechanism of Action of Penicillin and for Its Selective Toxicity." Science **125**(3238): 99-101.
- Petersen, L. K. and R. S. Stowers (2011). "A Gateway MultiSite recombination cloning toolkit." PLoS One **6**(9): e24531.
- Phelps, E. A., N. Landazuri, P. M. Thule, W. R. Taylor and A. J. Garcia (2010). "Bioartificial matrices for therapeutic vascularization." Proc Natl Acad Sci U S A **107**(8): 3323-3328.
- Pierschbacher, M. D. and E. Ruoslahti (1984). "Cell Attachment Activity of Fibronectin Can Be Duplicated by Small Synthetic Fragments of the Molecule." Nature **309**(5963): 30-33.
- Piltti, K. M., D. L. Haus, E. Do, H. Perez, A. J. Anderson and B. J. Cummings (2011). "Computer-aided 2D and 3D quantification of human stem cell fate from in vitro samples using Volocity high performance image analysis software." Stem Cell Res **7**(3): 256-263.
- Pittenger, M. F. (2008). "Mesenchymal stem cells from adult bone marrow." Methods Mol Biol **449**: 27-44.

- Pittenger, M. F., A. M. Mackay, S. C. Beck, R. K. Jaiswal, R. Douglas, J. D. Mosca, M. A. Moorman, D. W. Simonetti, S. Craig and D. R. Marshak (1999). "Multilineage potential of adult human mesenchymal stem cells." Science **284**(5411): 143-147.
- Plotnikov, A., E. Zehorai, S. Procaccia and R. Seger (2011). "The MAPK cascades: signaling components, nuclear roles and mechanisms of nuclear translocation." Biochim Biophys Acta **1813**(9): 1619-1633.
- Poussard, S., M. Decossas, O. Le Bihan, S. Mornet, G. Naudin and O. Lambert (2015). "Internalization and fate of silica nanoparticles in C2C12 skeletal muscle cells: evidence of a beneficial effect on myoblast fusion." Int J Nanomedicine **10**: 1479-1492.
- Raborn, J. and B. H. Luo (2012). "Mutagenesis studies of the beta I domain metal ion binding sites on integrin alphaVbeta3 ligand binding affinity." J Cell Biochem **113**(4): 1190-1197.
- Rahman, M. S., N. Akhtar, H. M. Jamil, R. S. Banik and S. M. Asaduzzaman (2015). "TGF-beta/BMP signaling and other molecular events: regulation of osteoblastogenesis and bone formation." Bone Research **3**.
- Ramsay, A. G., J. F. Marshall and I. R. Hart (2007). "Integrin trafficking and its role in cancer metastasis." Cancer and Metastasis Reviews **26**(3-4): 567-578.
- Rao, S. M., G. M. Ugale and S. B. Warad (2013). "Bone morphogenetic proteins: periodontal regeneration." N Am J Med Sci **5**(3): 161-168.
- Ratner, B. D. and S. J. Bryant (2004). "Biomaterials: Where we have been and where we are going." Annual Review of Biomedical Engineering **6**: 41-75.
- Reizer, J., C. Hoischen, F. Titgemeyer, C. Rivolta, R. Rabus, J. Stulke, D. Karamata, M. H. Saier and W. Hillen (1998). "A novel protein kinase that controls carbon catabolite repression in bacteria." Molecular Microbiology **27**(6): 1157-1169.
- Rezaiki, L., B. Cesselin, Y. Yamamoto, K. Vido, E. van West, P. Gaudu and A. Gruss (2004). "Respiration metabolism reduces oxidative and acid stress to improve long-term survival of *Lactococcus lactis*." Mol Microbiol **53**(5): 1331-1342.
- Rickard, D. J., M. Kassem, T. E. Hefferan, G. Sarkar, T. C. Spelsberg and B. L. Riggs (1996). "Isolation and characterization of osteoblast precursor cells from human bone marrow." J Bone Miner Res **11**(3): 312-324.
- Rico, P., C. Gonzalez-Garcia, T. A. Petrie, A. J. Garcia and M. Salmeron-Sanchez (2010). "Molecular assembly and biological activity of a recombinant fragment of fibronectin (FNIII7-10) on poly(ethyl acrylate)." Colloids and Surfaces B-Biointerfaces **78**(2): 310-316.

Ridley, A. J. and A. Hall (1992). "The Small Gtp-Binding Protein Rho Regulates the Assembly of Focal Adhesions and Actin Stress Fibers in Response to Growth-Factors." Cell **70**(3): 389-399.

Ritchey, T. W. and H. W. Seely, Jr. (1976). "Distribution of cytochrome-like respiration in streptococci." J Gen Microbiol **93**(2): 195-203.

Roberts, J. N., J. K. Sahoo, L. E. McNamara, K. V. Burgess, J. Yang, E. V. Alakpa, H. J. Anderson, J. Hay, L. A. Turner, S. J. Yarwood, M. Zelzer, R. O. Oreffo, R. V. Ulijn and M. J. Dalby (2016). "Dynamic Surfaces for the Study of Mesenchymal Stem Cell Growth through Adhesion Regulation." ACS Nano **10**(7): 6667-6679.

Rodrigo-Navarro, A., P. Rico, A. Saadeddin, A. J. Garcia and M. Salmeron-Sanchez (2014). "Living biointerfaces based on non-pathogenic bacteria to direct cell differentiation." Scientific Reports **4**.

Rodriguez-Carballo, E., B. Gamez and F. Ventura (2016). "p38 MAPK Signaling in Osteoblast Differentiation." Front Cell Dev Biol **4**: 40.

Rosso, F., G. Marino, A. Giordano, M. Barbarisi, D. Parmeggiani and A. Barbarisi (2006). "Smart materials as scaffolds for tissue engineering (vol 203, pg 468, 2006)." Journal of Cellular Physiology **209**(3): 1054-1054.

Rueda, F., O. Cano-Garrido, U. Mamat, K. Wilke, J. Seras-Franzoso, E. Garcia-Fruitos and A. Villaverde (2014). "Production of functional inclusion bodies in endotoxin-free Escherichia coli." Applied Microbiology and Biotechnology **98**(22): 9229-9238.

Ryoo, H. M., M. H. Lee and Y. J. Kim (2006). "Critical molecular switches involved in BMP-2-induced osteogenic differentiation of mesenchymal cells." Gene **366**(1): 51-57.

Saadeddin, A., A. Rodrigo-Navarro, V. Monedero, P. Rico, D. Moratal, M. L. Gonzalez-Martin, D. Navarro, A. J. Garcia and M. Salmeron-Sanchez (2013). "Functional Living Biointerphases." Advanced Healthcare Materials **2**(9): 1213-1218.

Sabate, R., N. S. de Groot and S. Ventura (2010). "Protein folding and aggregation in bacteria." Cell Mol Life Sci **67**(16): 2695-2715.

Sabokbar, A., P. J. Millett, B. Myer and N. Rushton (1994). "A rapid, quantitative assay for measuring alkaline phosphatase activity in osteoblastic cells in vitro." Bone Miner **27**(1): 57-67.

Sagan, L. (1967). "On the origin of mitosing cells." J Theor Biol **14**(3): 255-274.

Saha, K., Y. Mei, C. M. Reisterer, N. K. Pyzocha, J. Yang, J. Muffat, M. C. Davies, M. R. Alexander, R. Langer, D. G. Anderson and R. Jaenisch (2011). "Surface-engineered substrates for improved human pluripotent stem cell culture under fully defined

- conditions." Proceedings of the National Academy of Sciences of the United States of America **108**(46): 18714-18719.
- Salmeron-Sanchez, M. and M. J. Dalby (2016). "Synergistic growth factor microenvironments." Chemical Communications **52**(91): 13327-13336.
- Salmeron-Sanchez, M., P. Rico, D. Moratal, T. T. Lee, J. E. Schwarzbauer and A. J. Garcia (2011). "Role of material-driven fibronectin fibrillogenesis in cell differentiation." Biomaterials **32**(8): 2099-2105.
- Sambrook, D. W. R. a. J. (2001). Molecular cloning: a laboratory manual, Cold Spring Harbor.
- Sanders, J. W., G. Venema and J. Kok (1997). "A chloride-inducible gene expression cassette and its use in induced lysis of *Lactococcus lactis*." Applied and Environmental Microbiology **63**(12): 4877-4882.
- Sawitzke, J. A., L. C. Thomason, N. Costantino, M. Bubunencko, S. Datta and D. L. Court (2007). "Recombineering: in vivo genetic engineering in *E. coli*, *S. enterica*, and beyond." Methods Enzymol **421**: 171-199.
- Schiller, H. B. and R. Fassler (2013). "Mechanosensitivity and compositional dynamics of cell-matrix adhesions." Embo Reports **14**(6): 509-519.
- Schindelin, J., I. Arganda-Carreras, E. Frise, V. Kaynig, M. Longair, T. Pietzsch, S. Preibisch, C. Rueden, S. Saalfeld, B. Schmid, J. Y. Tinevez, D. J. White, V. Hartenstein, K. Eliceiri, P. Tomancak and A. Cardona (2012). "Fiji: an open-source platform for biological-image analysis." Nature Methods **9**(7): 676-682.
- Schleifer, K. H. and W. Ludwig (1996). "Phylogeny of the genus *Lactobacillus* and related genera." Systematic and Applied Microbiology **18**(4): 461-467.
- Schmoekel, H., J. C. Schense, F. E. Weber, K. W. Gratz, D. Gnagi, R. Muller and J. A. Hubbell (2004). "Bone healing in the rat and dog with nonglycosylated BMP-2 demonstrating low solubility in fibrin matrices." J Orthop Res **22**(2): 376-381.
- Schotte, L., L. Steidler, J. Vandekerckhove and E. Remaut (2000). "Secretion of biologically active murine interleukin-10 by *Lactococcus lactis*." Enzyme and Microbial Technology **27**(10): 761-765.
- Scott, J. E. (1995). "Extracellular-Matrix, Supramolecular Organization and Shape." Journal of Anatomy **187**: 259-269.
- Seger, R. and E. G. Krebs (1995). "The MAPK signaling cascade." FASEB J **9**(9): 726-735.
- Shegarfi, H. and O. Reikeras (2009). "Review article: bone transplantation and immune response." J Orthop Surg (Hong Kong) **17**(2): 206-211.

- Shi, Y. and J. Massague (2003). "Mechanisms of TGF-beta signaling from cell membrane to the nucleus." Cell **113**(6): 685-700.
- Shih, Y. R., K. F. Tseng, H. Y. Lai, C. H. Lin and O. K. Lee (2011). "Matrix stiffness regulation of integrin-mediated mechanotransduction during osteogenic differentiation of human mesenchymal stem cells." J Bone Miner Res **26**(4): 730-738.
- Shin, H., S. Jo and A. G. Mikos (2003). "Biomimetic materials for tissue engineering." Biomaterials **24**(24): 4353-4364.
- Sieg, D. J., C. R. Hauck and D. D. Schlaepfer (1999). "Required role of focal adhesion kinase (FAK) for integrin-stimulated cell migration." J Cell Sci **112 ( Pt 16)**: 2677-2691.
- Siffert, R. S. (1951). "The Role of Alkaline Phosphatase in Osteogenesis." Journal of Experimental Medicine **93**(5): 415-&.
- Sijpesteijn, A. K. (1970). "Induction of cytochrome formation and stimulation of oxidative dissimilation by hemin in *Streptococcus lactis* and *Leuconostoc mesenteroides*." Antonie Van Leeuwenhoek **36**(3): 335-348.
- Silva, A. K., C. Richard, M. Bessodes, D. Scherman and O. W. Merten (2009). "Growth factor delivery approaches in hydrogels." Biomacromolecules **10**(1): 9-18.
- Singh, P., C. Carraher and J. E. Schwarzbauer (2010). "Assembly of fibronectin extracellular matrix." Annu Rev Cell Dev Biol **26**: 397-419.
- Siren, N., K. Salonen, M. Leisola and A. Nyssola (2009). "A new salt inducible expression system for *Lactococcus lactis*." Biochemical Engineering Journal **48**(1): 132-135.
- Sopory, S., S. M. Nelsen, C. Degnin, C. Wong and J. L. Christian (2006). "Regulation of bone morphogenetic protein-4 activity by sequence elements within the prodomain." J Biol Chem **281**(45): 34021-34031.
- Sparks, R. L. and R. E. Scott (1986). "Transforming Growth-Factor Type-Beta Is a Specific Inhibitor of 3t3-T Mesenchymal Stem-Cell Differentiation." Experimental Cell Research **165**(2): 345-352.
- Stahl, M., G. Molin, A. Persson, S. Ahrne and S. Stahl (1990). "Restriction Endonuclease Patterns and Multivariate-Analysis as a Classification Tool for *Lactobacillus* Spp." International Journal of Systematic Bacteriology **40**(2): 189-193.
- Steidler, L., J. Viaene, W. Fiers and E. Remaut (1998). "Functional display of a heterologous protein on the surface of *Lactococcus lactis* by means of the cell wall anchor of *Staphylococcus aureus* protein A." Applied and Environmental Microbiology **64**(1): 342-345.

- Steidler, L., J. M. Wells, A. Raeymaekers, J. Vandekerckhove, W. Fiers and E. Remaut (1995). "Secretion of biologically active murine interleukin-2 by *Lactococcus lactis* subsp. *lactis*." Appl Environ Microbiol **61**(4): 1627-1629.
- Stein, G. S., J. B. Lian and T. A. Owen (1990). "Relationship of cell growth to the regulation of tissue-specific gene expression during osteoblast differentiation." FASEB J **4**(13): 3111-3123.
- Stentz, R., K. Jury, T. Eaton, M. Parker, A. Narbad, M. Gasson and C. Shearman (2004). "Controlled expression of CluA in *Lactococcus lactis* and its role in conjugation." Microbiology **150**(Pt 8): 2503-2512.
- Sternlicht, M. D. and Z. Werb (2001). "How matrix metalloproteinases regulate cell behavior." Annual Review of Cell and Developmental Biology **17**: 463-516.
- Stevens, M. M. and J. H. George (2005). "Exploring and engineering the cell surface interface." Science **310**(5751): 1135-1138.
- Takagi, J. (2007). "Structural basis for ligand recognition by integrins." Curr Opin Cell Biol **19**(5): 557-564.
- Takahashi, K. and S. Yamanaka (2006). "Induction of pluripotent stem cells from mouse embryonic and adult fibroblast cultures by defined factors." Cell **126**(4): 663-676.
- Tamaki, K., S. Souchelnytskyi, S. Itoh, A. Nakao, K. Sampath, C. H. Heldin and P. ten Dijke (1998). "Intracellular signaling of osteogenic protein-1 through Smad5 activation." J Cell Physiol **177**(2): 355-363.
- Tan, K., K. Zheng, D. Li, H. Lu, S. Wang and X. Sun (2017). "Impact of adipose tissue or umbilical cord derived mesenchymal stem cells on the immunogenicity of human cord blood derived endothelial progenitor cells." PLoS One **12**(5): e0178624.
- Taub, M. (1990). "The Use of Defined Media in Cell and Tissue-Culture." Toxicology in Vitro **4**(3): 213-225.
- Taubenberger, A. V., M. A. Woodruff, H. Bai, D. J. Muller and D. W. Hutmacher (2010). "The effect of unlocking RGD-motifs in collagen I on pre-osteoblast adhesion and differentiation." Biomaterials **31**(10): 2827-2835.
- Terpe, K. (2003). "Overview of tag protein fusions: from molecular and biochemical fundamentals to commercial systems." Appl Microbiol Biotechnol **60**(5): 523-533.
- Terzaghi, B. E. and W. E. Sandine (1975). "Improved medium for lactic streptococci and their bacteriophages." Appl Microbiol **29**(6): 807-813.

- Thomas, T. D., D. C. Ellwood and V. M. C. Longyear (1979). "Change from Homo-Fermentation to Heterolactic Fermentation by *Streptococcus-Lactis* Resulting from Glucose Limitation in Anaerobic Chemostat Cultures." Journal of Bacteriology **138**(1): 109-117.
- Thomson, J. A., J. Itskovitz-Eldor, S. S. Shapiro, M. A. Waknitz, J. J. Swiergiel, V. S. Marshall and J. M. Jones (1998). "Embryonic stem cell lines derived from human blastocysts." Science **282**(5391): 1145-1147.
- Todd, S. J., D. J. Scurr, J. E. Gough, M. R. Alexander and R. V. Ulijn (2009). "Enzyme-activated RGD ligands on functionalized poly(ethylene glycol) monolayers: surface analysis and cellular response." Langmuir **25**(13): 7533-7539.
- Tollefsbol, T. O. (2007). "Techniques for analysis of biological aging." Methods Mol Biol **371**: 1-7.
- Tsien, R. Y. (1998). "The green fluorescent protein." Annual Review of Biochemistry **67**: 509-544.
- Ulsamer, A., M. J. Ortuno, S. Ruiz, A. R. G. Susperregui, N. Osses, J. L. Rosa and F. Ventura (2008). "BMP-2 induces osterix expression through up-regulation of Dlx5 and its phosphorylation by p38." Journal of Biological Chemistry **283**(7): 3816-3826.
- Urist, M. R. (1965). "Bone: formation by autoinduction." Science **150**(3698): 893-899.
- Urist, M. R. (1997). "Bone morphogenetic protein: the molecularization of skeletal system development." J Bone Miner Res **12**(3): 343-346.
- Valdramidou, D., M. J. Humphries and A. P. Mould (2008). "Distinct roles of beta1 metal ion-dependent adhesion site (MIDAS), adjacent to MIDAS (ADMIDAS), and ligand-associated metal-binding site (LIMBS) cation-binding sites in ligand recognition by integrin alpha2beta1." J Biol Chem **283**(47): 32704-32714.
- van de Watering, F. C., J. J. van den Beucken, S. P. van der Woning, A. Briest, A. Eek, H. Qureshi, L. Winnubst, O. C. Boerman and J. A. Jansen (2012). "Non-glycosylated BMP-2 can induce ectopic bone formation at lower concentrations compared to glycosylated BMP-2." J Control Release **159**(1): 69-77.
- Van Oss, C. J. (2002). "Use of the combined Lifshitz-van der Waals and Lewis acid-base approaches in determining the apolar and polar contributions to surface and interfacial tensions and free energies." Journal of Adhesion Science and Technology **16**(6): 669-677.
- van Oss, C. J., W. Wu and R. F. Giese (1998). "Lifshitz-van der Waals, Lewis acid-base and electrostatic interactions in adhesion in aqueous media." First International Congress on Adhesion Science and Technology - Invited Papers: 49-61.

- Vanasseldonk, M., G. Rutten, M. Oteman, R. J. Siezen, W. M. Devos and G. Simons (1990). "Cloning of Usp45, a Gene Encoding a Secreted Protein from Lactococcus-Lactis Subsp Lactis Mg1363." Gene **95**(1): 155-160.
- Vannhieu, G. T. and R. R. Isberg (1993). "Bacterial Internalization Mediated by Beta-1 Chain Integrins Is Determined by Ligand Affinity and Receptor Density." Embo Journal **12**(5): 1887-1895.
- Velica, P. and C. M. Bunce (2011). "A quick, simple and unbiased method to quantify C2C12 myogenic differentiation." Muscle Nerve **44**(3): 366-370.
- Vert, M., Y. Doi, K. H. Hellwich, M. Hess, P. Hodge, P. Kubisa, M. Rinaudo and F. Schue (2012). "Terminology for biorelated polymers and applications (IUPAC Recommendations 2012)." Pure and Applied Chemistry **84**(2): 377-408.
- von Kriegsheim, A., D. Baiocchi, M. Birtwistle, D. Sumpton, W. Bienvenut, N. Morrice, K. Yamada, A. Lamond, G. Kalna, R. Orton, D. Gilbert and W. Kolch (2009). "Cell fate decisions are specified by the dynamic ERK interactome." Nat Cell Biol **11**(12): 1458-1464.
- Wainwright, M., N. C. Wickramasinghe, J. V. Narlikar, P. Rajaratnam and J. Perkins (2004). "Bacteria in the stratosphere-confirmation of viable but non-cultureable forms." Instruments, Methods, and Missions for Astrobiology Vii **5163**: 218-221.
- Wallner, E. I., Q. W. Yang, D. R. Peterson, J. Wada and Y. S. Kanwar (1998). "Relevance of extracellular matrix, its receptors, and cell adhesion molecules in mammalian nephrogenesis." American Journal of Physiology-Renal Physiology **275**(4): F467-F477.
- Wang, L., I. Vuletic, D. Deng, W. Crielaard, Z. Xie, K. Zhou, J. Zhang, H. Sun, Q. Ren and C. Guo (2017). "Bifidobacterium breve as a delivery vector of IL-24 gene therapy for head and neck squamous cell carcinoma in vivo." Gene Ther.
- Wang, W., G. Fu and B. H. Luo (2010). "Dissociation of the alpha-subunit Calf-2 domain and the beta-subunit I-EGF4 domain in integrin activation and signaling." Biochemistry **49**(47): 10158-10165.
- Ward, D. F., R. M. Salaszyk, R. F. Klees, J. Backiel, P. Agius, K. Bennett, A. Boskey and G. E. Plopper (2007). "Mechanical strain enhances extracellular matrix-induced gene focusing and promotes osteogenic differentiation of human mesenchymal stem cells through an extracellular-related kinase-dependent pathway." Stem Cells and Development **16**(3): 467-479.
- Warner, J. B. and J. S. Lolkema (2003). "CcpA-dependent carbon catabolite repression in bacteria." Microbiology and Molecular Biology Reviews **67**(4): 475-+.
- Watanabe, M., N. Masuyama, M. Fukuda and E. Nishida (2000). "Regulation of intracellular dynamics of Smad4 by its leucine-rich nuclear export signal." EMBO Rep **1**(2): 176-182.

Waterfield, N. R., R. W. F. Lepage, P. W. Wilson and J. M. Wells (1995). "The Isolation of Lactococcal Promoters and Their Use in Investigating Bacterial Luciferase Synthesis in Lactococcus-Lactis." Gene **165**(1): 9-15.

Watt, F. M. and B. L. M. Hogan (2000). "Out of Eden: Stem cells and their niches." Science **287**(5457): 1427-1430.

Watt, K. I., R. Judson, P. Medlow, K. Reid, T. B. Kurth, J. G. Burniston, A. Ratkevicius, C. De Bari and H. Wackerhage (2010). "Yap is a novel regulator of C2C12 myogenesis." Biochemical and Biophysical Research Communications **393**(4): 619-624.

Weis, S., T. T. Lee, A. del Campo and A. J. Garcia (2013). "Dynamic cell-adhesive microenvironments and their effect on myogenic differentiation." Acta Biomater **9**(9): 8059-8066.

Wen, X. Z., S. Miyake, Y. Akiyama and Y. Yuasa (2004). "BMP-2 modulates the proliferation and differentiation of normal and cancerous gastric cells." Biochem Biophys Res Commun **316**(1): 100-106.

White, C. A. and J. F. Kennedy (1979). "Microbial Technology - Current State, Future-Prospects - Bull,at, Ellwood,Dc, Ratledge,C." Futures **11**(6): 524-525.

Williams, D. F. (2008). "On the mechanisms of biocompatibility." Biomaterials **29**(20): 2941-2953.

Wilson, R. C. and J. A. Doudna (2013). "Molecular mechanisms of RNA interference." Annu Rev Biophys **42**: 217-239.

Wirkner, M., S. Weis, V. San Miguel, M. Alvarez, R. A. Gropeanu, M. Salierno, A. Sartoris, R. E. Unger, C. J. Kirkpatrick and A. del Campo (2011). "Photoactivatable caged cyclic RGD peptide for triggering integrin binding and cell adhesion to surfaces." Chembiochem **12**(17): 2623-2629.

Wolfenson, H., I. Lavelin and B. Geiger (2013). "Dynamic Regulation of the Structure and Functions of Integrin Adhesions." Developmental Cell **24**(5): 447-458.

Xia, Y., C. Makris, B. Su, E. Li, J. Yang, G. R. Nemerow and M. Karin (2000). "MEK kinase 1 is critically required for c-Jun N-terminal kinase activation by proinflammatory stimuli and growth factor-induced cell migration." Proc Natl Acad Sci U S A **97**(10): 5243-5248.

Xiao, Z., N. Watson, C. Rodriguez and H. F. Lodish (2001). "Nucleocytoplasmic shuttling of Smad1 conferred by its nuclear localization and nuclear export signals." J Biol Chem **276**(42): 39404-39410.

Xie, T. (2008). Germline stem cell niches. StemBook. Cambridge (MA).

Xiong, J. P., T. Stehle, R. Zhang, A. Joachimiak, M. Frech, S. L. Goodman and M. A. Arnaout (2002). "Crystal structure of the extracellular segment of integrin alpha Vbeta3 in complex with an Arg-Gly-Asp ligand." Science **296**(5565): 151-155.

Xu, R. H., R. M. Peck, D. S. Li, X. Feng, T. Ludwig and J. A. Thomson (2005). "Basic FGF and suppression of BMP signaling sustain undifferentiated proliferation of human ES cells." Nat Methods **2**(3): 185-190.

Xu, R. Q. and Q. S. Q. Li (2008). "Protocol: Streamline cloning of genes into binary vectors in *Agrobacterium* via the Gateway (R) TOPO vector system." Plant Methods **4**.

Xu, X., Q. Wang, Y. Long, R. Zhang, X. Wei, M. Xing, H. Gu and X. Xie (2013). "Stress-mediated p38 activation promotes somatic cell reprogramming." Cell Res **23**(1): 131-141.

Yang, G. B., G. H. Yuan, X. Y. Li, P. X. Liu, Z. Chen and M. W. Fan (2014). "BMP-2 Induction of Dlx3 Expression Is Mediated by p38/Smad5 Signaling Pathway in Osteoblastic MC3T3-E1 Cells." Journal of Cellular Physiology **229**(7): 943-954.

Yang, J. L., L. E. McNamara, N. Gadegaard, E. V. Alakpa, K. V. Burgess, R. M. D. Meek and M. J. Dalby (2014). "Nanotopographical Induction of Osteogenesis through Adhesion, Bone Morphogenic Protein Cosignaling, and Regulation of MicroRNAs." Acs Nano **8**(10): 9941-9953.

Yim, E. K. F., E. M. Darling, K. Kulangara, F. Guilak and K. W. Leong (2010). "Nanotopography-induced changes in focal adhesions, cytoskeletal organization, and mechanical properties of human mesenchymal stem cells." Biomaterials **31**(6): 1299-1306.

Yin, T. and L. Li (2006). "The stem cell niches in bone." J Clin Invest **116**(5): 1195-1201.

Yousefi, A. M., P. F. James, R. Akbarzadeh, A. Subramanian, C. Flavin and H. Oudadesse (2016). "Prospect of Stem Cells in Bone Tissue Engineering: A Review." Stem Cells Int **2016**: 6180487.

Zaidi, A. H., P. J. Bakkes, B. P. Krom, H. C. van der Mei and A. J. M. Driessen (2011). "Cholate-Stimulated Biofilm Formation by *Lactococcus lactis* Cells." Applied and Environmental Microbiology **77**(8): 2602-2610.

Zelzer, M., D. J. Scurr, M. R. Alexander and R. V. Ulijn (2012). "Development and validation of a fluorescence method to follow the build-up of short peptide sequences on solid 2D surfaces." ACS Appl Mater Interfaces **4**(1): 53-58.

Zhang, J., W. Zhi, M. Tan, X. Chen, X. Li and L. Deng (2010). "[An experimental study on rabbit bone marrow mesenchymal stem cells double-labeled by PKH26 and 5-bromo-2'-deoxyuridine in vitro and application in cardiac patch]." Zhongguo Xiu Fu Chong Jian Wai Ke Za Zhi **24**(7): 828-833.

Zhang, P., Y. Q. Wu, Z. L. Jiang, L. Y. Jiang and B. Fang (2012). "Osteogenic response of mesenchymal stem cells to continuous mechanical strain is dependent on ERK1/2-Runx2 signaling." International Journal of Molecular Medicine **29**(6): 1083-1089.

Zhang, S. G. (2003). "Fabrication of novel biomaterials through molecular self-assembly." Nature Biotechnology **21**(10): 1171-1178.

Zhao, G. Q. (2003). "Consequences of knocking out BMP signaling in the mouse." Genesis **35**(1): 43-56.

Zheng, J. H., V. H. Nguyen, S. N. Jiang, S. H. Park, W. Tan, S. H. Hong, M. G. Shin, I. J. Chung, Y. Hong, H. S. Bom, H. E. Choy, S. E. Lee, J. H. Rhee and J. J. Min (2017). "Two-step enhanced cancer immunotherapy with engineered Salmonella typhimurium secreting heterologous flagellin." Sci Transl Med **9**(376).

Zheng, W. F., W. Zhang and X. Y. Jiang (2010). "Biomimetic Collagen Nanofibrous Materials for Bone Tissue Engineering." Advanced Engineering Materials **12**(9): B451-B466.

Zheng, X. Y., H. Baker, W. S. Hancock, F. Fawaz, M. McCaman and E. Pungor (2006). "Proteomic analysis for the assessment of different lots of fetal bovine serum as a raw material for cell culture. Part IV. Application of proteomics to the manufacture of biological drugs." Biotechnology Progress **22**(5): 1294-1300.

Zisch, A. H., M. Ehrbar, J. Hubbell, G. Raeber, C. Schnell and B. Walpoth (2006). "Biomimetic materials for injectable tissue engineering: studies of acute, lasting and unexpected angiogenesis response." Faseb Journal **20**(4): A20-A21.

Zomer, A. L., G. Buist, R. Larsen, J. Kok and O. P. Kuipers (2007). "Time-resolved determination of the CcpA regulon of Lactococcus lactis subsp. cremoris MG1363." J Bacteriol **189**(4): 1366-1381.

Zuk, P. A., M. Zhu, P. Ashjian, D. A. De Ugarte, J. I. Huang, H. Mizuno, Z. C. Alfonso, J. K. Fraser, P. Benhaim and M. H. Hedrick (2002). "Human adipose tissue is a source of multipotent stem cells." Mol Biol Cell **13**(12): 4279-4295.